



IFM-GEOMAR

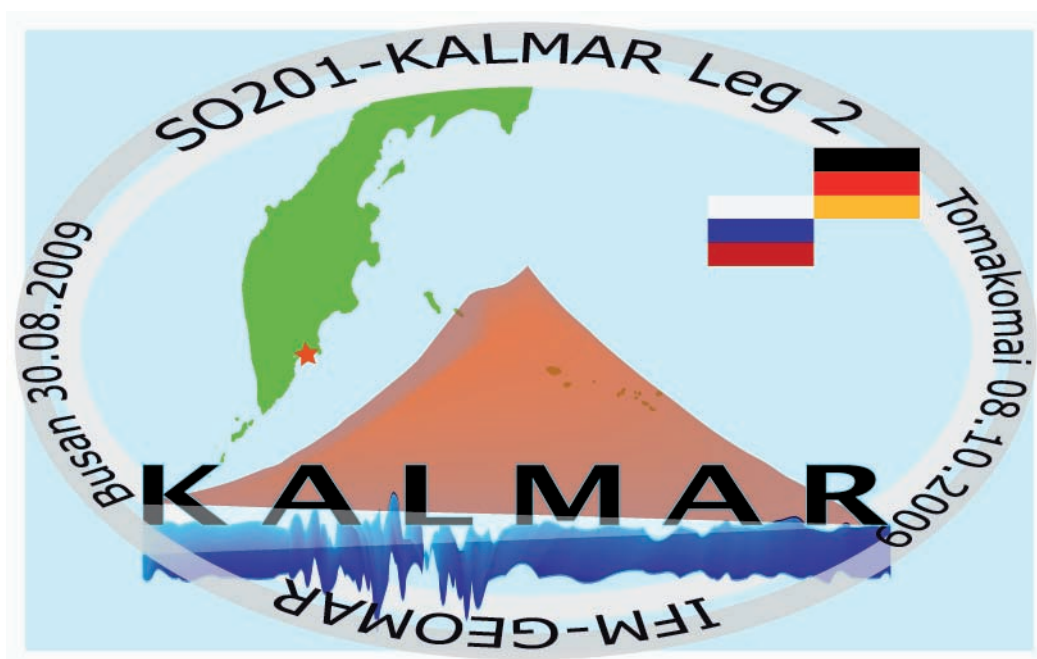
Leibniz-Institut für Meereswissenschaften
an der Universität Kiel

**FS Sonne Fahrtbericht / Cruise Report
SO201-2**

KALMAR:

Kurile-Kamchatka and **A**leutian **M**arginal Sea-Island Arc Systems:
Geodynamic and Climate Interaction in Space and Time

Busan/Korea – Tomakomai/Japan
30.08. - 08.10.2009



Berichte aus dem Leibniz-Institut
für Meereswissenschaften an der
Christian-Albrechts-Universität zu Kiel

Nr. 35
Dezember 2009



IFM-GEOMAR

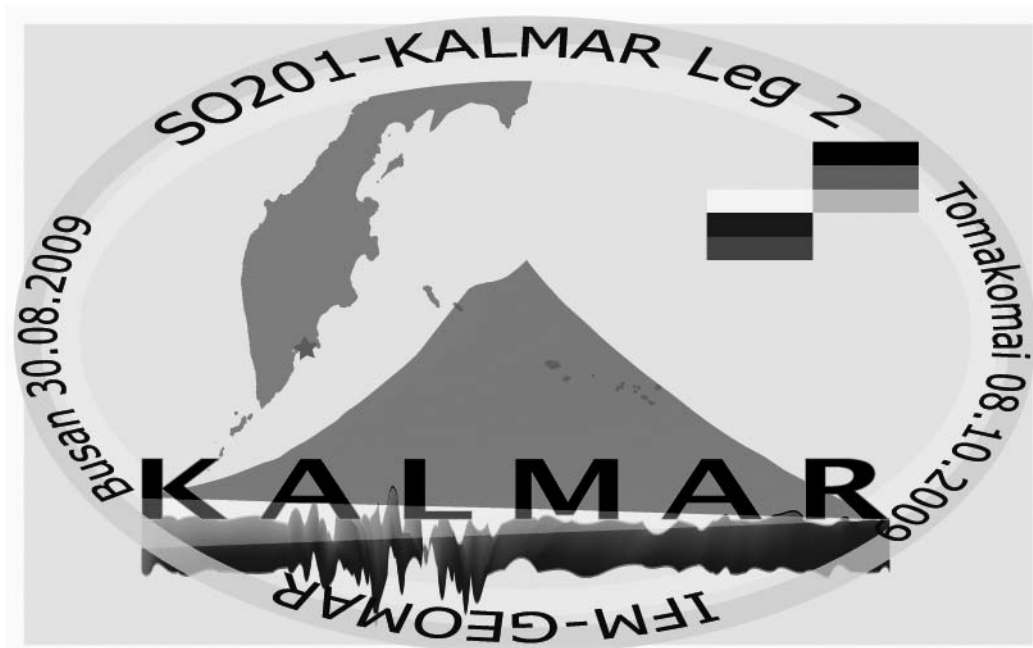
Leibniz-Institut für Meereswissenschaften
an der Universität Kiel

FS Sonne Fahrtbericht / Cruise Report SO201-2

KALMAR:

Kurile-Kamchatka and **A**leutian **M**ARginal Sea-Island Arc Systems:
Geodynamic and Climate Interaction in Space and Time

Busan/Korea – Tomakomai/Japan
30.08. - 08.10.2009



Berichte aus dem Leibniz-Institut
für Meereswissenschaften an der
Christian-Albrechts-Universität zu Kiel

Nr. 35

Dezember 2009

ISSN Nr.: 1614-6298



IFM-GEOMAR

Leibniz-Institut für Meereswissenschaften
an der Universität Kiel

Das Leibniz-Institut für Meereswissenschaften
ist ein Institut der Wissenschaftsgemeinschaft
Gottfried Wilhelm Leibniz (WGL)

The Leibniz-Institute of Marine Sciences is a
member of the Leibniz Association
(Wissenschaftsgemeinschaft Gottfried
Wilhelm Leibniz).

Herausgeber / Editor:

Wolf-Christian Dullo, Boris Baranov, and Christel van den Bogaard

IFM-GEOMAR Report

ISSN Nr.: 1614-6298

Leibniz-Institut für Meereswissenschaften / Leibniz Institute of Marine Sciences

IFM-GEOMAR
Dienstgebäude Westufer / West Shore Building
Düsternbrooker Weg 20
D-24105 Kiel
Germany

Leibniz-Institut für Meereswissenschaften / Leibniz Institute of Marine Sciences

IFM-GEOMAR
Dienstgebäude Ostufer / East Shore Building
Wischhofstr. 1-3
D-24148 Kiel
Germany

Tel.: ++49 431 600-0
Fax: ++49 431 600-2805
www.ifm-geomar.de

ACKNOWLEDGEMENTS

We would like to thank the Russian and German Ministeries for the possibility to carry out the scientific cruise SO201-KALMAR Leg 2 KALMAR in the frame of scientific-technical Programme as agreed on the WTZ-Protocoll of the 10th WTZ - Working Group Meeting (February 7th 2006 as project Nr. 19).

The SO201-KALMAR Leg 2 project is funded by the « Bundesministerium für Bildung und Forschung » (BMBF) project award to Prof. Wolf-Christian Dullo (head project, ship's time), Dr. Christoph Gaedicke (subproject 1), Prof. Kaj Hoernle (subproject 3), Prof. Ralf Tiedemann and PD Dr. Dirk Nürnberg (subproject 4), and by a Grant of the Russian Foundation of Basic Researches (RFFI N05-08-00017, RFFI 07-05-00807-a) and the Russian Academy of Sciences (Grants of Programme #17).

We thank the Federal Agency for Science and Innovations of Russia for granting permission to work within their territorial waters.

We would also like to thank Captain Meyer and the crew of the R/V SONNE. Their hard and dedicated work, their high level of experience and willingness to help, created a pleasant working atmosphere on board that contributed to the success of the SO201-KALMAR Leg 2 cruise.

CONTENTS

Acknowledgements

1.	INTRODUCTION (<i>C. Dullo, B. Baranov</i>)	7
2.	PARTICIPANTS	10
	2.1. SHIP'S CREW	10
	2.2. PRINCIPAL INVESTIGATORS	10
	2.3. SHIPBOARD SCIENTIFIC PARTY	10
	2.4. INSTITUTIONS	11
3.	MAJOR OBJECTIVES AND BACKGROUND	13
	3.1. HYDROGRAPHY OF THE STUDY AREAS (<i>C. Dullo, S. Shapovalov</i>)	13
	3.2. HEAT FLOW MEASUREMENTS (<i>G. Delisle, M. Zeibig</i>)	14
	3.3. GEODYNAMICS AND VOLCANOLOGY	
	(<i>M. Portnyagin, G. Yogodzinski, B. Baranov, R. Werner</i>)	15
	3.3.1. Meiji Seamount	
	and subduction-related tectonics at the Kamchatka trench	16
	3.3.2. Komandorsky Basin and related fracture zones	17
	3.3.3. Volcanologists' Massif and Piip Volcano	19
	3.3.4. Shirshov Ridge	20
	3.4. PALEOCEANOGRAPHY (<i>R. Tiedemann, D. Nürnberg</i>)	21
4.	CRUISE NARRATIVE (<i>C. Dullo, B. Baranov, G. Yogodzinski, C. v. d. Bogaard</i>)	25
5.	OPERATIONS AND PRELIMINARY RESULT	36
	5.1. CTD-PROFILING AND ROSETTE (<i>C. Dullo, S. Shapovalov</i>)	36
	5.1.1. Preliminary results of hydrographic measurements	36
	5.1.2. Fluorometer (<i>B. Glückselig</i>)	40
	5.2. PLANKTON (<i>S. Korsun, B. Glückselig</i>)	41
	5.2.1. Oceanographic setting	41
	5.2.2. Methods	41
	5.2.3. Results	41
	5.2.4. Preliminary conclusions	42
	5.3. HYDROACOUSTIC MEASUREMENTS (<i>B. Baranov, R. Werner, L. Max,</i>	
	<i>J. Riethdorf</i>)	44
	5.3.1. SIMRAD EM120 swath bathymetry – methods	44
	5.3.1.1. Data Acquisition	44
	5.3.1.2. Data Processing	44
	5.3.2. Sedimentacoustics: ATLAS PARASOUND (<i>L. Max</i>)	45
	5.3.2.1. First results	46
	5.4. HEAT FLOW (<i>G. Delisle, M. Zeibig</i>)	49
	5.4.1. Site selection	49
	5.4.2. First results	50
	5.5. DREDGE OPERATIONS (<i>M. Portnyagin, G. Yogodzinski, R. Werner,</i>	
	<i>B. Baranov</i>)	53
	5.5.1. Rock Sampling - Methods	53
	5.5.2. Volcanology	54
	5.5.2.1 Meiji Seamount	55
	5.5.2.2. Komandorsky Basin and fracture zones	57
	5.5.2.3. Volcanologists' Massif and Piip Volcano	60
	5.5.2.4. Shirshov Ridge	61
	5.6. SEDIMENT SAMPLING (<i>D. Nürnberg, R. Tiedemann</i>)	67
	5.6.1. Multicorer	67
	5.6.2. Gravity corer and piston corer	68
	5.6.2.1. Sampling scheme of sediment cores	70
	5.6.2.2. Shipboard core logging	72

5.6.2.2.1.	Magnetic susceptibility data (<i>L. Max / R. Tiedemann</i>) ..	72
5.6.2.2.2.	Color scan (<i>J. Riethdorf / D. Nürnberg</i>)	72
5.6.2.2.3.	Humidity (<i>S. Gorbarenko / A. Derkachev</i>)	73
5.6.3.	Results and Discussion.....	74
5.6.3.1.	Sediment Facies	74
5.6.3.2.	Magnetic susceptibility	79
5.6.3.3.	Tephra layers in the NW-Pacific and Bering Sea	79
6.	SUMMARY	84
7.	REFERENCES	86

APPENDICES

I	Overview Station Map	A 1
II	Stationlist	A 5
III	Sampling Summary Dredges.....	A 17
IV	Rock Description Dredges.....	A 21
V	Summary Sediment Sampling	A 55
VI	Core Description	A 59
VII	Core Photograph	A 111
VIII	Magnetic Susceptibility Records.....	A 121
IX	Color Reflectance Values.....	A 127

1. INTRODUCTION

(C. Dullo, B. Baranov)

The R/V SONNE cruise SO201 Leg 2 (http://kalmar.ifm-geomar.de/?Marine_expeditions:SO201_Leg_2) is one of three marine expeditions carried out within the framework of the German-Russian KALMAR project which is funded by German ministry of Education and Research (BMBF) and the Russian Ministry of Education and Science. SO201-KALMAR Leg 2 comprises several multidisciplinary investigations in the NW-Pacific and the Bering Sea. The function of the complex and climate governing geosystem "Kurile-Kamchatka-Arc with the adjacent areas in the NW-Pacific and the Bering Sea" will be investigated with geophysical, volcanological and geochemical research methods, because here, like nowhere else on earth the interaction between asthenosphere, lithosphere, hydrosphere, atmosphere, and biosphere is so distinct. The effects of the geodynamic and physical processes on the distribution and cycling of matter, water mass formation and circulation, climate and natural hazards will be investigated in a broad and integrative geoscientific approach. The cruise SONNE-KALMAR is an integrative part of the amphibic project within the German-Russian research co-operation "KALMAR - Kurile-Kamchatka and Aleutian MARGinal sea-island arc systems: geodynamic and climate interaction in space and time". Two main research subjects form the scientific backbone of the cruise.

The first objective focuses on the geodynamic and volcanological-magmatic development of the Kurile-Kamchatka island arc system and the Kamchatka Aleutian Islands Triple-Junction. In the western part of the Aleutian Arc, in the Komandorsky-Fracture zone E of Kamchatka, the subducting plate is disintegrated into four larger segments, which converge in an orthogonal direction with increasing speed from N to S below the overriding plate. These segments are separated by transform faults which split into splay faults at their western end (Gaedicke et al. 2000). Pull apart basins start to form parallel to the transform faults exhibiting heat flow values between 150 – 200 mW/m² (Baranov et al. 1991, Smirnov and Sugrobov 1979, 1980). The Bering- and Steller-Transform Faults can be traced below Kamchatka down to a depth of 20 – 40 km (Davaille and Lees 2004). The Kamchatka Cape Peninsula, W of the Kamchatka Aleutian Islands Triple-Junction, is characterized by a complex fault system, which is dominated by transform faults and normal faults creating blocks of different uplift rates (Freitag et al. 2001). North of the Triple-Junction the subduction related volcanisms ceased about 10 Ma ago (Levin et al. 2002). According to Levin et al. (2002), the subducting plate was disrupted during two phases (between 5-10 Ma ago and about 2 Ma ago) and does not exist any more.

Very little is known about the composition of the mantle and the oceanic crust as well as of the seamounts including their ages in the area of the Kamchatka Aleutian Islands Triple-Junction. The best studied site is the Volcanologists' Massif located between the Bering- and the Alpha Fracture Zone (Tsvetkov 1990, Volynets et al. 1992, Yogodzinsky et al. 1994), which structurally belongs to the Komandorsky Basin. The main part of the massif consists of intermediate K basalts, basaltic andesites and andesites, which exhibit higher ratios of radiogenic Sr isotopes and which are enriched in K, Ba and Sr values in contrast to MORB. The oldest rocks of the Volcanologists' Massif show very similar trace element and isotope signatures like those rocks cropping out in the volcanoes on Kamchatka in the prolongation of the Alpha Fracture Zone (Portnyagin et al. 2005a), indicating similar conditions of magma formation. The top of the Volcanologist's Massif is characterized by the young (< 0.5 Ma) and hydrothermally active Piip volcano, which consists of special magnesium rich andesites ("Piip type"). These andesites may represent melts originated from the subducting Pacific plate re-equilibrated with the mantle (Yogodzinsky et al. 1994, 2001). Therefore, one of the major targets is to collect new samples from this massif, since no more material exists in any laboratory today (G. Yogodzinsky and B. Baranov, personal communication) to apply new geochemical methods on fluid inclusions to study the fluid regime and the magma formation.

The proper Komandorsky Basin is interpreted as a spreading center, which ceased in Miocene times (Baranov et al. 1991). The DSDP drilling site 191 recovered the only sample of the basement till now. This sample has similar geochemical signatures like the rocks of the older part of the Volcanologists' Massif (Yogodzinsky et al. 1995) and has been dated as 9.3 ± 0.8 Ma old (Seliverstov 1998). In order to reconstruct the age of the basin and the composition of the underlying mantle, it is necessary to retrieve more samples from the NW-SE trending fracture zones including the young volcanoes resting on top of these structures. Such sample material will also allow to evaluate the importance of Pacific mantle material in the formation of the highly active volcanoes of central Kamchatka (Portnyagin et al. 2005a).

The Shirshov Ridge is a structural high running in N-S direction, about which very little is known. It separates the Komandorsky Basin in the West from the Aleutian Basin in the East. The formation of this ridge may be related to Miocene spreading activities in the Komandorsky Basin (Baranov et al. 1991). The few geochemical data from the ridge derived from amphibolites indicate a metamorphosis of a subduction environment (Silantiev et al. 1985). Originally these rocks may represent Ti-rich gabbros or basalts from a MOR or from a back arc setting. In the South of the Shirshov Ridge some lavas with island arc signatures of probably Late Oligocene age have been reported by Cooper et al. (1976).

The Meiji-Seamount is the northernmost seamount of the hotspot spur of the Hawaii-Emperor-Seamount chain, having an age of probably > 85 Ma. The only existing basement rocks from this seamount were gained during DSDP Leg 19. These are basalts with MORB like trace element and isotope signatures (Keller et al. 2000, Regelous et al. 2003).

These data indicate that the Hawaii-Hotspot was at a MOR in Cretaceous time and that large volumes of depleted mantle material played a role during the magma formation. By dredge sampling we want to get samples from the Meiji Seamount as well as from the Komandorsky Block in order to reconstruct the Mesozoic history of this globally unique hotspot spur including the rift related magmatism as well as to reconstruct the input into the Kurile-Kamchatka subduction system.

The second objective focuses on paleoceanographic investigations concentrating on the sediments along the eastern continental slope of Kamchatka, in the Komandorsky Basin, and on the Shirshov Ridge in order to explore paleoclimate archives to better understand the subpolar water mass transfer and the oceanographic and climatic development in the subarctic NW-Pacific. Studies on the dynamics of the east Kamchatka current, which regulates the export of water masses from the Bering Sea into the N Pacific and hence influences the formation of intermediate-water masses, sea ice cover, nutrient distribution, productivity, and ventilation, will contribute to our understanding of the atmospheric and oceanic teleconnections between the Atlantic and Pacific.

Comparisons of Late Pleistocene and Holocene temperature changes within the near surface water masses between the NW-Pacific and the N-Atlantic resulted in a new hypothesis, the "Atlantic-Pacific seesaw" (Kiefer et al. 2001, Kim et al. 2004, Kiefer and Kienast, 2005). This Atlantic-Pacific pattern of opposite temperature variations dominates the last 60 kyr on millennial timescales. Modelling results of Saenko et al. (2004) support the hypothesis of the "Atlantic-Pacific seesaw" and they postulate a mechanistic connection between the two regions driven by salinity variations, which couples both regions through the thermohaline circulation. A different model relates the Holocene Atlantic-Pacific dipole to the atmospheric teleconnection between the Arctic Oscillation/N-Atlantic Oscillation and the Pacific N-American Oscillation (Kim et al. 2004). The envisaged coring sites may provide high resolution sedimentary records to contribute to the question which of these different mechanisms is the driving force behind the "Atlantic-Pacific seesaw".

The marginal seas of the NW-Pacific, the Bering Sea and the Sea of Ochotsk, are important sources for the formation of intermediate water masses and therefore play an important role for the ventilation of the whole N Pacific Ocean, like the Labrador sea acts for the N-Atlantic. Stable carbon isotopes ($\delta^{13}\text{C}$) from epibenthic foraminifera derived from Detroit Seamount indicate an increased production of N-Pacific intermediate water (Keigwin 1998), which formed in both marginal seas during isotope stages 5 – 3, while the Bering Sea

was the major source during the last glacial in contrast to the Holocene, during which the Sea of Ochotsk is the predominant origin for intermediate water (Tanaka and Takahashi 2005). Since these results contradict results of our working group derived from cores from the Sea of Ochotsk (Lembke et al. in prep, Abelmann et al. in prep), new cores from the envisaged sites may shed light on this question, where the major sources for intermediate water mass formation are located.

The distribution of ice masses in the eastern part of Sibiria and around the Bering Sea during the Last Glacial Maximum is discussed controversially (St. John and Krissek 1999, Dyke et al. 2002; Brigham-Grette and Gualtieri 2004). It is completely unknown how the development of the ice sheets on Kamchatka and the dynamics of the East Kamchatka current including the export of ice from the Bering Sea and the sea ice distribution within the Sea of Ochotsk matches with the Atlantic-Pacific temperature pattern. Meltwater input from these areas into the subarctic Pacific impact on the water masses and their circulation as well as on the biological production (Nakatsuka et al. 1995) and therefore influencing the global pattern. The western part of the Bering Sea with its shelf areas off Kamchatka is one of the most productive regions of the global ocean today (Mordasova et al. 1995). This high productivity of $2.2 - 3.4 \text{ g C m}^{-2}\text{d}^{-1}$ is documented in these sediments by high opal contents (20 – 40%: Lisitsin 1959). Studies of Pleistocene sediment cores from the Sea of Ochotsk showed that variations in sea ice formation, ocean circulation and even atmospheric circulation impact on marine productivity (Nürnberg and Tiedemann 2004) due to nutrient transport in intermediate and bottom water masses as well as atmospheric input (Tsuda et al. 2003, Sarmiento et al. 2004).

2. PARTICIPANTS

2.1. SHIP'S CREW

Meyer, Oliver	Master	Globke, Valerie	Apprentice
Aden, Nils Arne	Chief Mate	Tiemann, Frank	Chief Cook
Linnenbecker, Matthias	2nd Mate	Kapitanski, Misha	2nd Cook
Büchele, Heinz-Ulrich	2nd Mate	Pohl, Andreas	Ch. Steward
Walther, Anke	Surgeon	Royo, Luis	2nd Steward
Rex, Andreas	Chief Engineer	Steep, Maik	2nd Steward
Klinder, Klaus-Dieter	2nd Engineer	Mucke, Hans-Peter	Boatswain
Hermesmeyer, Dieter	Techn. Watch Off.	Fricke, Ingo	A.B.
Rieper, Uwe	Electrician	Stängl, Günter	A.B.
Angermann, Rudolf	Chief Electrician	Dehne, Dirk	A.B.
Borchert, Wolfgang	System Manager	Kraft, Jürgen	A.B.
Ehmer, Andreas	System Manager	Dolief, Joachim	A.B.
Rosemeyer, Rainer	Fitter	Eidam, Oliver	Apprentice
Blohm, Volker	Motorman	Peplow, Michael	Apprentice
Henning, Tim	Motorman		

2.2. PRINCIPAL INVESTIGATORS FOR SO201 LEG2 KALMAR

Head project:	Dullo, Wolf-Christian	IFM-GEOMAR
	Baranov, Boris	Shirshov Inst.
Sub-project 2:	Gaedicke, Christoph	BGR Hannover
Sub-project 3:	Hoernle, Kaj	IFM-GEOMAR
Sub-project 4:	Tiedemann, Ralf	AWI-Bremerhaven
	Nürnberg, Dirk	IFM-GEOMAR
	Abelmann, Andrea	AWI-Bremerhaven

2.3. SHIPBOARD SCIENTIFIC PARTY *(in alphabetical order)*

Baranov, Boris (Chief Scientist)	Geophysist	IO RAS / Moscow
Delisle, Georg	Geophysist	BGR / Hannover
Derkachev, Alexander	Geologist	POI FEB RAS / Vladivostok
Dullo, Wolf-Christian (Chief Scientist)	Geologist	IFM-GEOMAR / Kiel
Glückselig, Birgit	Technician	AWI / Bremerhaven
Gorbarenko, Sergey	Geologist	POI FEB RAS / Vladivostok
Gottschalk, Julia	Student	AWI / Bremerhaven
Invanova, Elena	Geologist	IO RAS / Moscow
Kawohl, Helmut	Technician	Marinetechnik
Korsun, Sergey	Geologist	IO RAS / Moscow
Maicher, Doris	Geologist	IFM-GEOMAR
Max, Lars Wolfgang	Ph.D.. Student	AWI / Bremerhaven
Mironov, Nikita	Geologist	GEOGHI RAS / Moscow
Nürnberg, Dirk	Geologist	IFM-GEOMAR / Kiel
Portnyagin, Maxim	Geologist	IFM-GEOMAR / Kiel
Riethdorf, Jan-Rainer	Ph.D. Student	IFM-GEOMAR / Kiel
Saveliev, Dmitry	Geologist	IVS FEB RAS / Petropavlovsk

Shadrin, Konstantin	Observer	Vladivostok
Shapovalov, Sergey	Geologist	IO RAS / Moscow
Tiedmann, Ralf	Geologist	AWI / Bremerhaven
Tsukanov, Nikolay	Geologist	IO RAS / Moscow
Van den Bogaard, Christel	Geologist	IFM-GEOMAR / Kiel
Werner, Reinhard	Geologist	IFM-GEOMAR / Kiel
Yogodzinski, Gene	Geologist	Univ. South Carolina
Zeibig, Michael	Technician	BGR / Hannover



The SO201 Leg 2 Shipboard Scientific Party

2.4. INSTITUTIONS *(in alphabetical order)*

AWI / Bremerhaven	Alfred-Wegener-Institut für Polar- und Meeresforschung Columbusstrasse 27568 Bremerhaven Germany (http://www.awi.de)
BGR / Hannover	Bundesanstalt für Geowissenschaften und Rohstoffe (BGR) Stilleweg 2 D-30655 Hannover Germany

	http://www.bgr.bund.de
GEOKHI RAS / Moscow	V.I. Vernadsky Institute of Geochemistry and Analytical Chemistry RAS Kosygin St. 19 119991 Moscow Russia http://www.geokhi.ru
IFM-GEOMAR / Kiel	Leibniz Institut für Meereswissenschaften Wischhofstr. 1-3 24148 Kiel Germany http://www.ifm-geomar.de
IO RAS / Moscow	Center for Coordination of Oceanic Research RAS P.P. Shirshov Institute of Oceanology RAS Nakhimovsky Prospekt 36 117997 Moscow Russia http://www.ocean.ru
IVS FEB RAS / Petropavlovsk	Institute of Volcanology and Seismology FEB RAS Boulevard Piypa 9 683006 Petropavlovsk-Kamchatsky Russia http://www.kscnet.ru
POI FEB RAS / Vladivostok	Pacific Oceanological Institute FEB RAS Baltiyskaya Street 43 690041 Vladivostok Russia http://www.poi.dvo.ru
Marinetechnik	Am Kreuzkamp 27 31311 Uetze OT. Hänigsen Germany
University of South Carolina	Dept. of Geological Sciences University of South Carolina 701 Sumter St., EWSC617 Columbia, SC 29208 USA http://www.geol.sc.edu

3. MAJOR OBJECTIVES AND BACKGROUND OF SO201 LEG2 KALMAR

3.1. HYDROGRAPHY OF THE STUDY AREAS (C. Dullo, S. Shapovalov)

The hydrography of the study areas is determined by the surface circulation and the water mass distribution in the North Pacific.

The surface hydrography of the subarctic North Pacific is characterized by a counterclockwise regime of the involved currents. The Subarctic Current flows from W to E almost along the latitude of 40° N. Off the American continent it divides into the southward flowing California Current and into the northward flowing Alaska Current. The Alaska Current develops into the Alaskan Stream running along the Aleutian Islands from E to W. Waters exiting the Bering Sea through the Kamchatka Strait merge with the Alaskan Stream to form the East Kamchatka Current, flowing in a southward direction and later mixing with waters coming from the Sea of Okhotsk to form the still southward flowing Oyashio Current. Somewhere around 40° N off Japan the Oyashio converges with the Kuroshio Current to constitute the Subarctic Current (Fig. 3.1). This simple current regime is more complex, since it involves two separate gyres, the Alaskan Gyre and the Western subarctic Gyre, and the Northwestern Subtropical Gyre and the Northeastern subtropical Gyre respectively (Favorite et al. 1976, Roden et al. 1982).

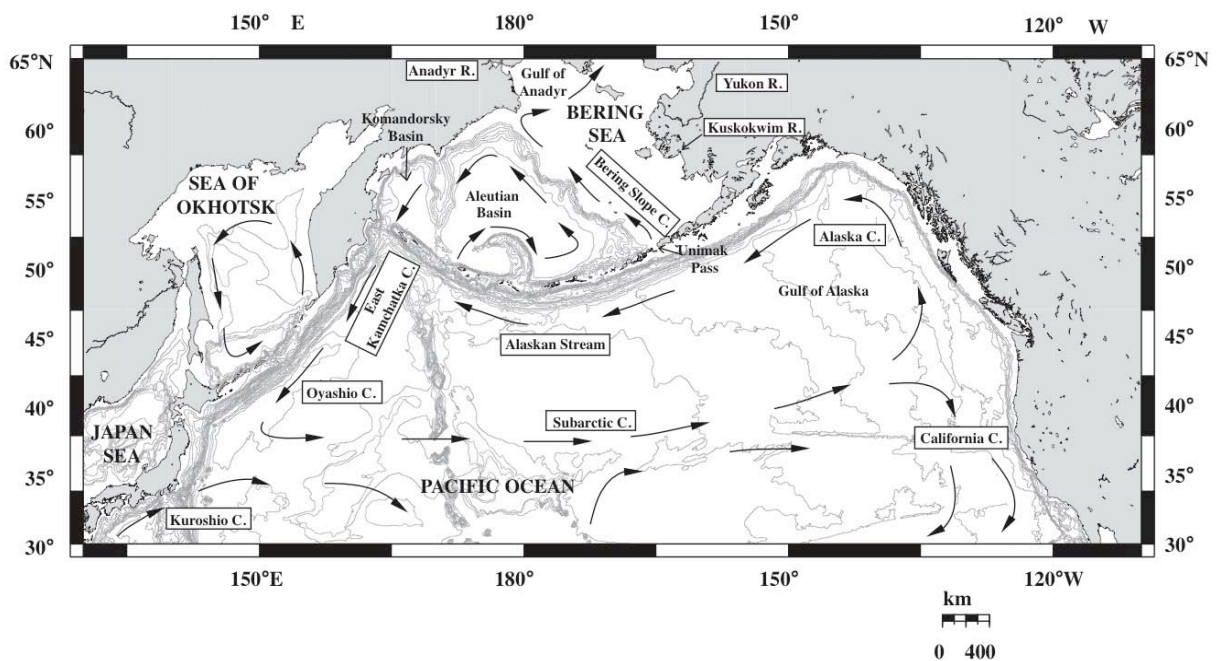


Fig. 3.1.: Surface circulation pattern in the North Pacific and the Bering Sea. Redrawn from Aizawa et al. (2005).

The Alaska Coastal Current Waters that follow the Alaskan coastline, enter into the Bering Sea through the Unimak Pass (Stabeno et al. 1995). These waters initially travel northeastwards close to the Aleutian Islands, continuing northwestwards across the shallow eastern shelf before exiting through the Bering Strait. According to Stabeno et al. (1999), parts of the Alaskan Stream enter the Bering Sea through many of the 14 major passes, especially the deep central and western passes (Kamchatka 4420 m, Near 2000 m, Amchitka 1155 m) and some several shallower passes (Buldir 640 m, Amukta 430 m, Unimak Passes < 80 m). Waters mainly entering the Bering Sea through the Amchitka Strait form the eastward flowing Aleutian North Slope Current, which turns northwestward across the shelf break as a slightly modified current, the Bering Slope Current. Some of these off-

slope waters eventually flow northwards along the Siberian coast to form a western boundary current, which enters the Gulf of Anadyr and passes into the Chukchi Sea through the Bering Strait. Some of the Alaskan Stream waters pass into the Aleutian Basin through the Near Strait. These northward flowing waters combine with west flowing waters from the Bering Slope Current to form a western boundary current, the Kamchatka Current (Stabeno et al. 1994), which then flows southwards along the Kamchatka Peninsula in the western part of the Komandorsky Basin. This current exits the Bering Sea through the deep Kamchatka Strait and merges with the Alaskan Stream waters to form the East Kamchatka Current.

The vertical structure of the water mass distribution is characterized by the upper mixed layer, by a cold intermediate layer of low salinity water, a warmer intermediate layer, and a deep water from surface to bottom (Moroz and Bogdanov 2007; Takahashi 2005). A very strong thermocline in concert with a distinct halocline separates the surface mixed water from the cold intermediate water. This water is formed in the Bering Sea during winter time. The Bering Sea is a source region for the Western Subarctic Pacific Water (WSPW), which plays a major role in the circulation of the western subarctic Pacific. The Western Subarctic Pacific Water is characterized by a marked stratification with cold upper layers in winter and a remarkable dichothermal layer around 100 m depth during summer (Ohtani et al. 1972).

Beneath the cold low-salinity WSPW lies a mesothermal layer which is a major feature of the waters off Kamchatka. This layer consists of warm (~3.5–3.8°C) water at a depth range between 200 - 600 m. The source of the mesothermal water in the western Sub-Arctic Gyre and the Alaskan Stream is the warm and saline water of the Kuroshio located south and east of Japan (Endoh et al. 2004; Yasuda 2004). Below the mesothermal layer there is the domain of the North Pacific Deep Water (NPDW). Properties of the water in the Pacific are set by their very distant sources in the Antarctic and the North Atlantic, with modification through diapycnal processes, oxygen consumption as well as nutrient regeneration, and by the complicated basin geometry (Tsuchiya and Talley 1996).

Tidal currents and eddies can play a significant role in the formation of the water mass structure in the Bering Sea and in the region off Kamchatka side by side with stream currents. Strong tidal currents mix the water column from the top to the bottom over the shallow sills in the passes of the Aleutian Archipelago (Stabeno et al. 2005; Moroz and Bogdanov 2007). The Aleutian eddies also may play a substantial role in the transport of warm Alaskan Stream water westward to Kamchatka (Rogachev et al. 2007).

3.2. HEAT FLOW MEASUREMENTS (*G. Delisle, M. Zeibig*)

Oceanic crust is subducted south of the Kamchatka-Aleutian-Islands-Triple Junction (at about 55°30'N) at right angle below the Kamchatka Peninsula. A roughly NNE-SSW trending, more than 6 km deep trench zone delineates the eastern boundary of a well developed fore-arc ridge. The southeast trending Emperor Seamount Chain rests on top of the subducting oceanic plate. The Meiji Seamount complex forms currently the front complex which is on the verge of entering the trench zone prior to subduction. The heat flow distribution along the east coast of Kamchatka including the Meiji Seamount had been extensively surveyed in the 1970s (Smirnov and Sugrobov 1979, 1980; Sugrobov and Yanovsky 1993). These measurements show a moderate positive geothermal anomaly on the north-western flank of the Meiji Seamount and positive as well as negative anomalies along the fore-arc ridge as well as in the trench area. The presence of a pronounced positive geothermal anomaly in old oceanic crust is unexpected. The variable geothermal heat flow in the trench and fore-arc areas points to complex heat transfer processes at depth. With our investigation we aimed to concentrate on this aspect.

3.3. GEODYNAMICS AND VOLCANOLOGY (M. Portnyagin, G. Yogodzinski, B. Baranov, R. Werner)

Project SO201 Leg 2 KALMAR included investigations of volcanic and tectonic structures and dredging of basement rocks in the NW Pacific and Bering Sea, the areas adjacent to the Kamchatka-Aleutian Arc junction and located within three lithospheric plates of different provenance and evolution (Pacific, Okhotsk and North American Plates) (Fig. 3.3.1). The geological studies during the SO201 Leg 2 targeted on four major regions: (1) Meiji Seamount on the Pacific Plate, (2) Komandorsky Basin, (3) Volcanologists' Massif and Piip Volcano, and (4) Shirshov Ridge in the Bering Sea. None of the areas were previously mapped with multi-beam echo-sounding system. Data on the basement rock compositions from these areas are sparse or even not available yet crucial for the elucidation of the evolution of the North Pacific-Kamchatka-Aleutian realm. Geological, volcanological, petrological, geochemical and geochronological analyses subsequent to the cruise are aimed to provide principle information on:

- the origin, age and composition of the Hawaiian hotspot volcanism during the Late Cretaceous time;
- the origin of Komandorsky Basin, its mantle and crust composition;
- the origin and evolution of recent volcanism in the Western Aleutian Arc;
- the origin of Shirshov Ridge;
- the composition of oceanic crust subducting beneath Kamchatka.

The integration of these results with existing data as well as with the data obtained during on-land and marine (SO201 Leg 1b) investigations within the KALMAR project will contribute to better understanding of the geodynamic evolution of the NW Pacific Ocean, its convergent margins and marginal seas.

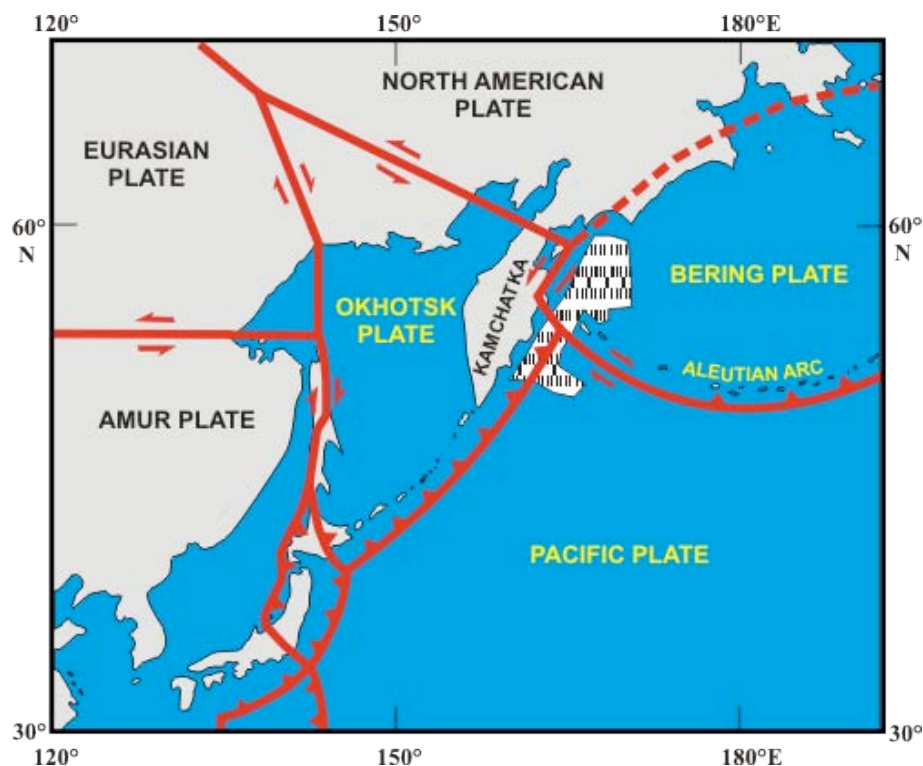


Fig. 3.3.1.: Recent plate boundaries of the northwestern Pacific and location of the study area (hatched). Lines with teeth indicate subduction zones, lines with arrows mark strike-slip zones; dashed line mark suggested plate boundary.

3.3.1 Meiji Seamount and subduction-related tectonics at the Kamchatka trench

The Hawaiian-Emperor Seamount Chain, produced during the passage of the Pacific Plate over the Hawaiian hotspot, extends for 5800 km from the presently most active Island of Hawaii and Loihi Seamount (the present location of the hotspot) northwest to the Meiji Seamount seaward of the Kamchatka-Aleutian arc junction. Meiji is presumably the oldest seamount in the Emperor Chain, preserved on the ocean floor, with the inferred age of more than 81 Ma (Duncan and Keller 2004) (Fig. 3.3.2). Despite the extensive data set on the modern Hawaiian plume magmatism, geochemical and age data are still scarce for the submarine part of the hotspot track, particularly for its oldest part. These data are however crucial for elucidating the compositional and thermal evolution of the Hawaiian mantle plume and for paleotectonic reconstructions of the Pacific Ocean in the Late Cretaceous-Early Cenozoic.

Presently available information on the age and composition of the northern Emperor Seamounts is based on results of the DSDP and ODP investigations which recovered basement rocks from Meiji, Detroit and Suiko Seamounts (Keller et al. 2000; Duncan and Keller 2004; Regelous et al. 2001; Huang et al. 2004; Frey et al. 2005). These data have significantly changed previous views on the compositional range of the Hawaiian plume magmas and were used to demonstrate significant southward motion of the hotspot during the Late Cretaceous (Tarduno et al. 2003). Reliable age data were obtained for Detroit (76 Ma at ODP Site 1203, 81 Ma at ODP Site 884) and Suiko Seamount (61 Ma at ODP Site 433). An important result from geochemical investigations of the Meiji and Detroit Seamounts was a discovery of rocks with relatively depleted trace element and isotopic compositions, which were interpreted to result from the location of the Hawaiian plume on young and thus thin oceanic lithosphere in the late Cretaceous (Huang et al. 2005; Keller et al. 2000; Regelous et al. 2003). The models proposed to explain the MORB-like composition of the late-Cretaceous Hawaiian rocks favored either entrainment of the depleted upper mantle by an upwelling mantle plume near an oceanic ridge (Keller et al. 2000) or involvement of a depleted plume component due to enhanced melting beneath thin lithosphere (Huang et al. 2005; Regelous et al. 2003).

The most western part of the Meiji Seamount enters the Kurile-Kamchatka Trench at a velocity of ca. 9 cm/year. The trench-facing slope of the seamount has a prominent structural pattern, which is different from the normal oceanic plate to the south (formed in a mid-ocean-ridge setting), and consists of a series of blocks subsided step-by-step toward the trench and separated from each other by normal faults. It is widely accepted that normal faults on an oceanic plate approaching a subduction zone originate due to plate bending at its outer rise (e.g. Ranero et al. 2003). In the case of the Meiji Seamount, the amplitude of vertical movement along the normal faults is however unusually large and reaches several hundreds of meters, which is probably related to different mechanical behavior of a thickened crust beneath the Meiji Seamount. It was also suggested that the lowest and nearest to the Kamchatka trench block has started to split from the oceanic slope to accrete on the island-arc slope (Seliverstov 1998). The presence of the high-amplitude normal faults makes it possible to sample the Meiji basement rocks by dredging. Whereas the basement is not accessible without drilling further east from the trench due to 1-1.5 km-thick sediments covering the Meiji Seamount (Seliverstov 1998).

Investigations during the Leg 2 of the KALMAR SO201 project targeted at sampling the western flank of the Meiji Seamount where basement rocks could be exposed on the seafloor at the fault-related scarps. This study is anticipated to have implications for the evolution of the Hawaiian hotspot volcanism in the Cretaceous and also is relevant to a better understanding of the subduction input into the Kamchatka arc system and its influence on the compositional variability of erupted magmas, periodicity of volcanism and turn-over of climate-relevant volatiles in the subduction zone. The studies during SO201-2 included also a multi-beam mapping of the seafloor at the Kamchatka trench offshore Kronotsky Peninsula and at the trench-facing slope of the Meiji Seamount in order to investigate the normal

faulting at the seamount and mechanisms of its subduction and/or accretion at the Kamchatkan convergent margin.

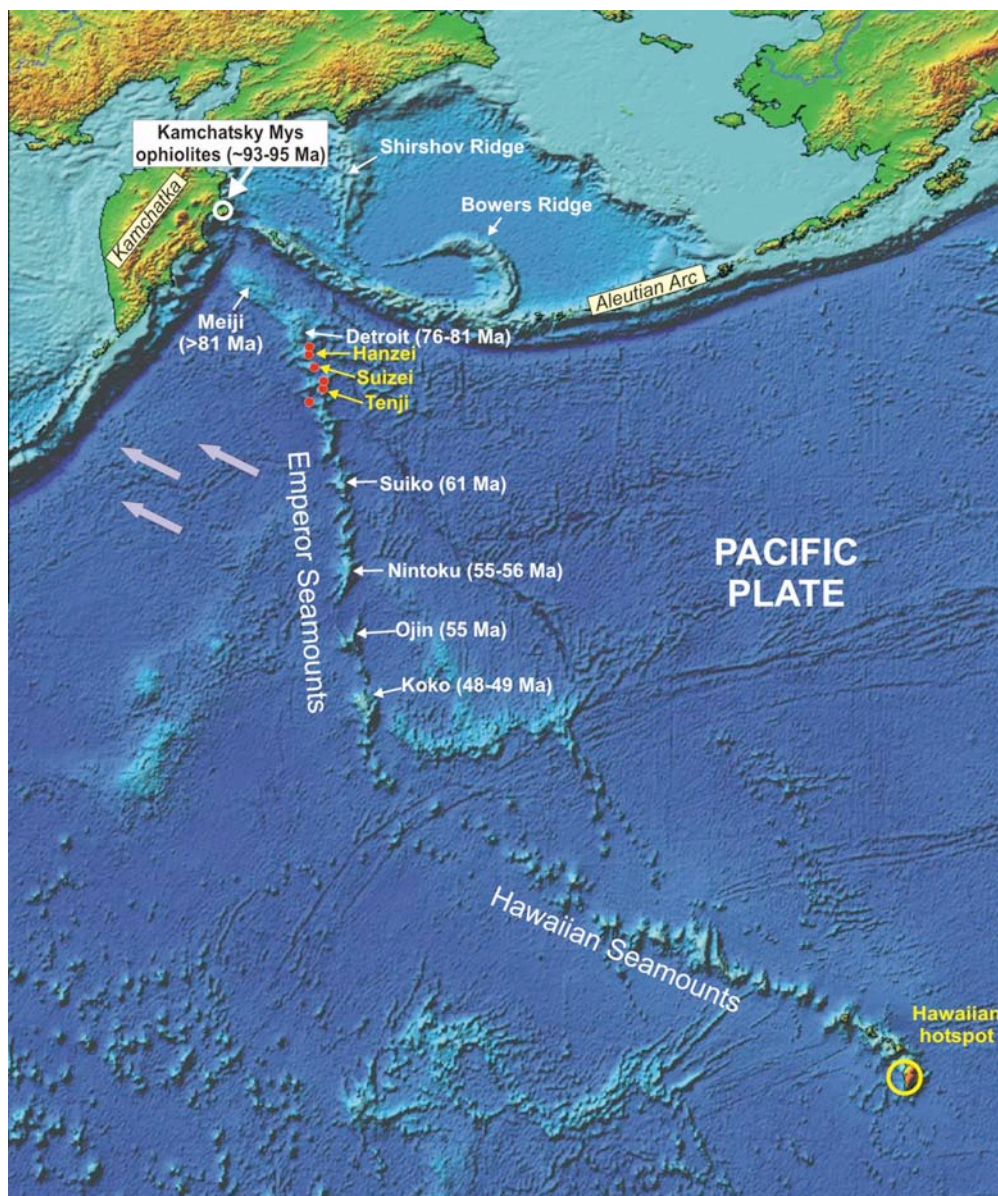


Figure 3.3.2.: The Hawaiian-Emperor Seamount Chain produced by passage of the Pacific Plate over the Hawaiian hotspot since the Cretaceous. Red dots indicate sites at the Emperor Seamounts dredged during the SO201 Leg 1b KALMAR cruise. Seamount ages are from Duncan and Keller (2004).

3.3.2. Komandorsky Basin and related fracture zones

The Komandorsky Basin is located in the western part of the Bering Sea (Fig. 3.3.3). It is bound on the south by the Komandorsky segment of the Aleutian Arc and on the east by the Shirshov Ridge. Magnetic lineations and heat flow data indicate that the main part of the Komandorsky Basin originated in the Oligocene-Miocene due to sea-floor spreading which continued until recently in the western and southern parts of the basin (Valyashko et al. 1993; Baranov et al. 1991). Basement basalts were recovered during DSDP Leg 19 at Site 191 in the eastern part of the Komandorsky Basin. These basalts have MORB-type

compositional affinities and absolute ages of approximately 30 Ma, as determined by conventional K-Ar dating of whole-rock and plagioclase-separate samples (Stewart et al. 1973). The Komandorsky Basin floor is a plain of active sedimentation, deepening slightly east-southward from 3500 m to 3900 m. Within the basin, sediment veils the rough surface of the acoustic basement. The average sedimentary thickness in the central basin is 1 to 1.5 km, increasing up to 3 km or more in depressions confined to the continental rise along the western border of the basin.

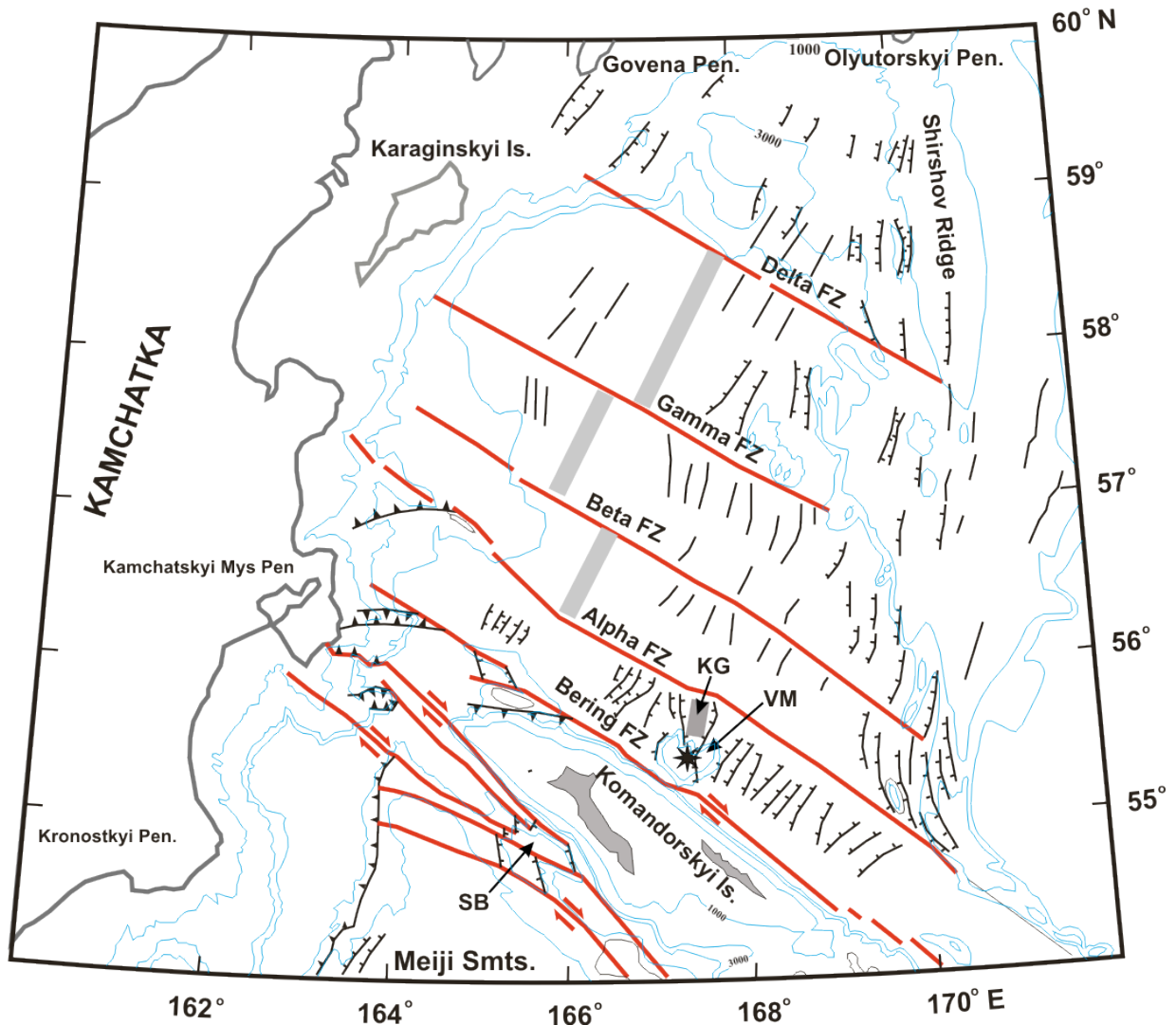


Fig. 3.3.3.: Structural pattern of the Komandorsky Basin (Baranov et al. 1991; Seliverstov 1996; Gaedicke et al. 2000, simplified). Red lines mark fracture zones, thick grey lines indicate spreading axes including the Komandor Graben (KG). Lines with sticks and triangles show normal and reverse faults, correspondently. Thin lines indicate basement highs. Abbreviations: VM – Vulkanologists' Massif, SB – Steller Basin.

The most peculiar feature of the Komandorsky Basin basement structure is the occurrence of the NW-SE – striking fracture zones (FZ) that can be traced from the continental slope of the Kamchatka Peninsula to the Shishov Ridge. From the south to the north, the following fracture zones can be distinguished: Alpha, Beta, Gamma and Delta (Fig. 3.3.3). These fracture zones coincide with chains of linear highs or scarps of basement.

Along some segments, the highs are flanked by depressions filled with up to 2 km-thick sediments. The fracture zones are mostly buried under sediments with exception of the northwestern segment of the Alpha FZ which is expressed on the seafloor as a 600 to 700 m high ridge, and the western part of the Gamma FZ, where its small part forms an isolated seamount.

The Komandorsky Basin basement comprises a number of north-striking tilted blocks. The blocks in the western and eastern parts of the basin are faced to its central part, in a pattern resembling that of a slow spreading ridge. Based on the structural fabric of the basin basement (Baranov et al. 1991) and the distribution of magnetic lineations (Valyashko et al. 1993), several spreading/extension axes were distinguished. These axes are shifted to each other along the NW-SE-trending fracture zones. All axes except the southern one are covered by sediments. The southernmost spreading centre is manifested in bottom relief as the Komandor Graben hosting the Vulkanologists' Massif and active Piip Volcano.

Studies conducted during the SO201 Leg 2 were aimed at mapping and sampling of the Komandorsky Basin basement at uplifted segments of fracture zones in order to obtain material to refine the age and composition of the Komandorsky crust as well as the mantle composition unmodified by subduction-related processes. Geochemical investigations of the oceanic-type Kommandorsky Basin crust, formed away from the active subduction zone, should provide direct insights into the composition of the upper mantle feeding volcanoes in Kamchatka and the Western Aleutian Arc. This study will allow us to test the hypothesis that enriched plume mantle, that has been detected beneath some Kamchatka volcanoes in KALMAR Block A and the KOMEX project, is flowing northward through a slab-window beneath the Western Aleutian Arc and possibly contributes to the Kamchatkan volcanism (e.g. Portnyagin et al. 2005).

Transtensional structures are common features for the eastern, trailing parts of the Komandorsky fracture zone system. The most prominent of the structures is the Steller Basin located on the Aleutian trench (Fig. 3.3.3). This basin has rhomb-like outlines and represents a pull-apart basin originated between dextral strike-slip faults. It is suggested, that some blocks located inside the fault system are slices of oceanic crust that had been accreted to the Komandorsky Islands, by collision and shearing along the front of the western Aleutian arc (Seliverstov 1987). One of such blocks forms the southeastern margin of the Steller Basin. In order to test the hypothesis, dredging has been planned at one of the tectonic blocks on the northern side of the Aleutian trench during the SO201 Leg 2.

3.3.3 Volcanologists' Massif and Piip Volcano

The Volcanologists' Massif is located ca. 50 km north of Medny Island between Alpha and Bering FZ and occupies the axial part of the Komandor Graben, which is interpreted to be the southernmost spreading center of the Komandorsky Basin (Baranov et al. 1991). The massif has a complex structure and can be subdivided into three parts: eastern, northwestern and central. The first two parts of the massif are NE-striking asymmetric ridges and are confined to the sides of this structure. Their steeper slopes are of normal fault origin and are represented by a series of scarps facing each other. Piip Volcano occupies the central part and consists of three merged volcanic cones with crater depressions, forming a N-S-elongated volcanic edifice rising up to within approximately 350 m of the sea surface. Hydrothermal activity was found on the northern and southern cones. The most recent eruption of Piip volcano was suggested to take place just a few hundred years ago on the basis of tephra-chronological evidence (Seliverstov et al. 1995).

The petrology and geochemistry of lavas from Piip Volcano and the underlying rocks of the Volcanologists' Massif were studied by Yogodzinski et al. (1994). Their results indicate that Piip Volcano is composed primarily of crystal-rich, hornblende and plagioclase-bearing andesite and dacite, which define a medium-K, calc-alkaline series from 58% to 68% SiO₂ and 1.5% to 4.0% MgO. More mafic lavas from Piip were collected in only a single dredge of a satellite vent, at a depth of 2100-2400 meters on the northwestern flank of the volcano. This dredge recovered magnesian andesite, with 56% to 58% SiO₂ and approximately 6%

MgO and 5% FeO*. These andesites are sparsely phyrlic and contain microphenocrysts of forsteritic olivine (FO88-91), which, combined with high whole-rock Mg#s (>0.68), imply a composition for these lavas sufficiently primitive to have been equilibrated with mantle olivine. These primitive andesites have geochemical features that have lead some to conclude that they are an important end-member among Aleutian lavas resulting from a relatively large proportion of eclogite or pyroxenite melt in their source (Yogodzinski et al. 1995; Kelemen et al. 2003).

Trace element patterns of Piip lavas show enrichments and depletions that are broadly similar to island arc lavas worldwide, but Pb, Sr and Nd isotopic compositions that are close to those of normal MORB. The depleted isotopic compositions of the Piip lavas are attributed to their genesis in a dominantly transform setting where the rate of subduction is low and where there is apparently no sediment subducted into the source of the melts beneath the volcano (Yogodzinski et al. 1994). Rocks of the underlying Volcanologists' Massif are generally more mafic than at Piip Volcano, including andesites, basaltic andesites and basalts. Basalts are somewhat variable in composition and include relatively high titanium varieties that have flat or slightly depleted rare-earth element patterns and are in general transitional between island arc basalt and depleted MORB-type basalt geochemistry.

The investigations at the Volcanologists' Massif during SO201-2 cruise included detailed geomorphological mapping of the entire massif and dredging of structural units of different ages within the volcanic complex. The goals of the study are (1) development of an overall model of the geodynamic evolution of the Volcanologists' Massif and Piip Seamount, and (2) testing a number of petrogenetic models on the origin of active volcanism in the Western Aleutian Arc.

3.3.4. Shirshov Ridge

The Shirshov Ridge strikes in N-S direction and extends for about 700 km, separating the Aleutian and Komandorsky Basins over its entire length. The Olyutorskyi Ridge of the Koryakskyi Highland is its northern on-land continuation. In the south, as it approaches the Aleutian Arc, the Shirshov Ridge narrows sharply and changes its strike to the northwest. At the depth of 3800 m it almost joins the Bowers Ridge.

Shirshov Ridge is an asymmetric feature. Its western slope is more gentle, in contrast to the eastern one, and is covered by 2-3 km thick sediments (Rabinowitz and Cooper 1977). The western slope and the summit of the Shirshov Ridge comprise a series of scarps 200 to 1000 m high facing mainly the Komandorsky Basin. The scarps divide the ridge into a number of N-S-striking blocks, which subside step by step towards the basin floor. The subsided blocks can be traced under the bottom of the basin for several tens of kilometers from the base of the ridge, which is morphologically manifested in the bottom relief. Judging from the eastward tilt of the blocks, their western sides are bounded by east-dipping listric faults. This is shown by the structure of the sedimentary layers and by the occurrence of asymmetric depressions (grabens) at the base of the scarps. These grabens are filled with more than 1.5 km thick sediments. It has been proposed that normal faults on the western slope of the ridge and its summit are related to extensional tectonics in the Komandorsky Basin (Baranov et al. 1991).

Various magmatic and metamorphic rocks were recovered on the Shirshov Ridge during Leg 29 expedition of Russian research vessel of R/V Dmitrii Mendeleev in 1982. Among these rocks only amphibolites dredged from the western slope of the ridge were studied for petrography and geochemistry (Silantiev et al. 1985). The amphibolites were shown to originate after cumulative gabbro and volcanogenic sediments originally formed in back arc spreading center. Metamorphic conditions were characterized by moderate temperature (450-500°C), high pressure (6-8 kbar) and isochemical trends of the metamorphism.

Since the tectonic structure and basement composition of the Shirshov Ridge are poorly investigated, there exists a variety of ideas about the origin of the ridge and its place in the structure of the region. According to different concepts, the ridge is proposed to be an extinct island arc (Kienle 1971; Scholl et al. 1975), an intra-oceanic rise accreted onto the active

Eurasian margin (Ben-Avraham and Cooper 1981; Savostin et al. 1986) or a part of the Hawaiian hotspot track preserved in the Bering Sea (Steinberger and Gaina 2007), a stacking zone, compensating for the spreading in the Komandorsky Basin (Bogdanov and Neprochnov 1984) and, finally, an oceanic plateau accreted onto western Aleutian Arc and then split due to the spreading in the Komandorsky Basin (Baranov et al. 1991).

The studies carried out during the SO201-2 expedition were aimed at mapping of some parts of the Shirshov Ridge and dredging its basement with the goal to shed further light on the structure, origin and evolution of the prominent tectonic structure in the Bering Sea. The studies were complimentary to those carried out during SO201 Leg1b KALMAR cruise which succeeded at dredging in-situ rocks from a submarine ridge connecting Shirshov and Bowers Ridges.

3.4. PALEOCEANOGRAPHY (*R. Tiedemann, D. Nürnberg*)

Our paleoceanographic studies aim to reconstruct the late Pleistocene and Holocene oceanographic and climatic evolution of the subarctic NW-Pacific and of NE Siberia as they respond to and modulate the effects of major climatic events, such as expansions of sea ice and polar ice sheets, the effectivity of the biological pump, and the formation of intermediate to deep water. We intend to investigate what role the physical and biological processes in this region play in the global climate system on decadal to orbital timescales. Since only a few high-quality Pleistocene paleoceanographic records exist from the open Pacific and the northwestern Bering Sea, it is not well understood what changes occurred in the subarctic NW-Pacific realm during the deglaciation and the last glacial period, when large reorganizations in meridional overturning occurred in the North Atlantic. Recent progress in understanding Pleistocene changes in the North Pacific oceanography suffers from stratigraphic uncertainties and restricted application of paleoceanographic tools for various reasons: (1) Increased carbonate dissolution below ca. 2500 m water depth prevents the use of common paleoceanographic proxies and stratigraphic techniques that are based on carbonate tests from foraminifers, e.g. oxygen isotope ($\delta^{18}\text{O}$) stratigraphy and AMS- ^{14}C -dating. (2) The reconstruction of climate processes that operate on decadal to millennial timescales requires sediment archives with high sedimentation rates of 10-100 cm/kyr. Accordingly, the establishment of high-resolution carbonate-based proxy records is limited to a few seamounts in the NW-Pacific, the Bering Sea and the continental margin of Kamchatka. The continental slopes along eastern Kamchatka and on Shirshov Ridge in the Bering Sea provide unique and hitherto unknown climate archives, which will allow to further decipher the timing and effects of decadal/centennial to orbital scale climate changes. Hence, a major task of cruise SO201-2 was to discover high-resolution sedimentary archives with the Parasound system and to retrieve sediment records from such archives by using multicorer and piston corer techniques.

In order to better understand the climatically relevant causal effects between oceanic, terrestrial, cryogenic and atmospheric processes and their effects on the late Pleistocene to Holocene climatic evolution in the western subarctic Pacific and in NE Siberia, we will apply a suite of state-of-the-art paleoceanographic proxies to reconstruct climate and ocean variables, which can be included in numerical climate models. Our studies will focus on the following topics:

Stratification of the upper water column and its effects on nutrient concentration, marine productivity, oceanic/atmospheric gas exchange during the past.

Today, the upper water column in the N-Pacific and the Bering Sea is marked by a permanent halocline, a salinity-driven density gradient in the upper 300 m, which also marks

the maximum depth of wind-driven winter mixing (Levitus and Boyer, 1994). This halocline acts as a barrier for exchange of heat, gas and nutrients between the atmosphere and the deep ocean interior. Winter mixing transports nutrients from the subsurface into the euphotic zone and triggers a diatom-dominated bloom during spring until early summer, when the euphotic zone deepens and the mixed layer shoals. During late summer and autumn, when most of the nutrients are consumed (especially silicate), a secondary biogenic bloom occurs, which is typically dominated by coccolithophores and foraminifers (Ohkouchi et al. 1999; Pagani et al. 2002). Whether this pattern of stratification persisted or changed during the millennial climate oscillations of the last glacial interval and over the course of the last termination will be examined by a multi-proxy approach. Any significant change in N-Pacific stratification has the potential to influence biogenic productivity and the oceanic release of CO₂ into the atmosphere. The few existing paleoceanographic records are suggestive but not conclusive.

Formation and ventilation of NW-Pacific intermediate water during the late Pleistocene

From paleoceanographic evidence, it is hypothesized that the formation and ventilation of North Pacific Intermediate Water (NPIW) was higher in the past (e.g. Keigwin and Jones 1990; Keigwin 1998; Ahagon et al. 2003, Matsumoto et al. 2002). Gorbarenko (1996) suggested that the intermediate water formation in the NW-Pacific (including the Sea of Okhotsk and the Bering Sea) was intensified during the last glaciation. Tanaka and Takahashi (2005) suggested that the source regions of NPIW shifted from the Bering Sea to the Sea of Okhotsk after the last glacial maximum. Kiefer et al. (2001) proposed that the ocean circulation in the North Atlantic and North Pacific were out of phase. When the Atlantic meridional overturning circulation is strong, the formation of NPIW was weak and vice versa. However, none of these reconstructions is based on sediment records from water depths shallower than 2000 m. Accordingly, one of our paleoceanographic goals during cruise SO201-2 was to recover an intermediate water transect of high resolution sediment records from 500 – 2000 m water depth to reconstruct changes in intermediate water circulation and to verify the existing and partly intriguing hypotheses. Any change in intermediate water production would imply a significant change in freshwater and/or salt supply to the N-Pacific, which should have also effected upper ocean stratification.

Another feature at intermediate water levels is the widespread occurrence of laminated sediments during the last deglaciation along the continental margins of the N-Pacific (Gulf of California, Gulf of Alaska, eastern Bering Sea, Japanese Margin), thereby suggesting low-oxygen contents at intermediate water depth of the N-Pacific (van Geen et al. 2003; McKay et al. 2004; Cook et al. 2005; Narita et al. 2002). However, there is yet no consensus about the mechanism of this phenomenon. Although the basin-wide reduction in oxygen contents within the oxygen minimum zone (OMZ) suggests a basin-wide change in ocean chemistry (Cook et al. 2005). Accordingly, another target of cruise SO201 Leg 2 was to retrieve high-resolution sediment records from the OMZ depth (300 – 1000 m) to prove whether this phenomenon is also typical for the western N-Pacific margin and to assess the underlying mechanisms, including changes in biogenic productivity.

NW-Pacific sea surface temperature patterns and meridional temperature gradients during the Holocene and the late Pleistocene

Kim et al. (2004) investigated the spatial and temporal sea surface temperature (SST) variability in the North Pacific and North Atlantic for the middle to late Holocene and the teleconnections between the two oceans. Their studies were based on a set of Holocene North Pacific (only one record from the NW-Pacific) and North Atlantic alkenone-derived SST in combination with simulations of a coupled atmosphere–ocean general circulation model. Their analyses suggest a sea surface temperature seesaw pattern between the N-Pacific and the N-Atlantic on centennial time scales, which may indicate fundamental inter-oceanic

teleconnections during the Holocene. The authors hypothesized that the seesaw pattern is connected to an atmospheric circulation field that comprises the elements of the decadal Pacific North American oscillation (PNA) and the North Atlantic Oscillation (NAO) in opposite phases. This contrasting SST-pattern obviously occurred also during the millennial-scale climate fluctuations of the last glacial interval (Kiefer and Kienast 2005). However, the database and the stratigraphic constraints are weak and require further investigation. We hope that the sediment records retrieved during the SO201-2 expedition will allow high-resolution temperature reconstruction to verify this hypothesis.

Changes in sea ice distribution, iceberg transport, and meltwater flux in the NW-Pacific and the Bering Sea

The knowledge of sea ice distribution and variability is a key parameter for understanding changes in intermediate water formation and upper ocean stratification in the Bering Sea and the NW-Pacific. Sea ice formation drives densification of the mixed layer via brine rejection and thus promotes overturning circulation. In contrast, sea ice melting is a mechanism for producing enhanced stratification by lowering sea surface salinities. Today, the formation and distribution of winter sea ice in the western Bering Sea is restricted to the northern and northwestern shelf areas and did not expand into the Kommandorsky Basin. Whether the Kommandorsky Basin was seasonally ice-free or perennially ice-covered during the last ice age is unknown. Studies on diatom assemblages in sediment records from the eastern basin of the Bering Sea suggest that sea-ice coverage extended to the central Aleutian Basin during the last glacial maximum (Tanaka and Takahashi 2005). Evidence of better-ventilated glacial NPIW also suggests that sea ice formation and brine rejection processes continued probably at greater rates than today (Keigwin 1998). An expansion of sea ice coverage into the open Bering Sea, followed by melting, would have likely caused extended water column stratification in that area. Our planned studies on diatom assemblages and the distribution of ice-rafted debris are thought to provide not only basic insights into this issue, but also into the glaciation history of Kamchatka.

Improvement of chronostratigraphy

AMS-¹⁴C-dating on high resolution records spanning the last 50,000 years faces the problem that the paleo-¹⁴C reservoir ages of surface waters are poorly known and possibly highly variable in this region (reservoir ages for surface water range from 700 to 1500 yr; Keigwin 1998, Sarnthein et al. 2004). A precise age model is essential to understand the millennial-scale pattern of climate variability in the N-Pacific and the phase relationship between North Atlantic and North Pacific climate change. Since the duration of millennial scale events is shorter than a few 1000 years, an inaccuracy in dating of 700 years can lead to fatal misinterpretations of N-Pacific climate change and its role in a global context. Therefore, we plan narrow spaced 14 datings on high-resolution sediment records to define the top and base of ¹⁴C-plateaus for which an age calibrated tie to the time scale of the Greenland ice core record GISP2 exists (Hughen et al. 2004). Since such analyses need sufficient amounts of foraminiferal tests, we performed double-coring at distinct core locations to guarantee enough material. In addition, paleomagnetic intensity records will be established on selected sediment cores, since such records provide an excellent tool for correlating the marine and lake sediment records between Kamchatka and the NW-Pacific on millennial to sub-millennial time scales. In addition, the frequent occurrence of ash layers within the NW-Pacific realm offers an excellent potential to significantly improve the dating and interpretation of marine sequences.

In summary, our paleoceanographic research will focus on the following topics:

- Reconstruction of the Pleistocene to Holocene climatic evolution of NE Siberia and the oceanography of the subarctic NW-Pacific and its marginal seas.
- Assessing continent-ocean-atmosphere climate linkages: glaciation history of Kamchatka.
- Paleoceanographic reconstruction of processes that play a key role in ocean-atmosphere interactions and feedbacks (sea ice, stratification), ocean circulation (e.g., melt water events), and marine productivity (nutrient cycle).
- Testing the hypothesis of a sea surface temperature seesaw pattern between the N-Pacific and the N-Atlantic.
- Effects of the E-Kamchatka/Oyashio current system on the oceanic regime in the subarctic NW-Pacific, and on the climate of Kamchatka and of Japan: Comparison to the N-Atlantic analog – the E-Greenland Current.
- Importance of the Bering Sea as a glacial source of well-ventilated intermediate waters in comparison to the Sea of Okhotsk – Did the western Bering Sea experience dysoxic conditions at intermediate water levels during the deglaciation?

4. CRUISE NARRATIVE

(C. Dullo, B. Baranov, G. Yogodzinski, C. v. d. Bogaard)

On 6. September, the scientific work on-station began at 5:45 AM, ship time, which is 10 hours different from Germany. We were taking a hydro-acoustic section from 51°03.0' N, 157°53.5' E to 50°13.0'N, 159°39.5' E. This location is approximately 150 miles south of Petropavlovsk, Kamchatsky. This is the first echo-sound mapping of the Kurile-Kamchatka subduction zone, where the Pacific oceanic plate is subducted beneath the Siberian-Eurasian plate at a rate of up to 79 mm/year.

Several members of the scientific crew of the R/V SONNE cruise SO201 Leg 2 arrived in Busan, South Korea on morning of 28. August at 7:35 AM (Fig. 4.1.). After the transfer from the airport to the hotel, driving through rush-hour traffic in Busan, one of the most lively port cities of SE Asia, we arrived at the ship on Pier 1.

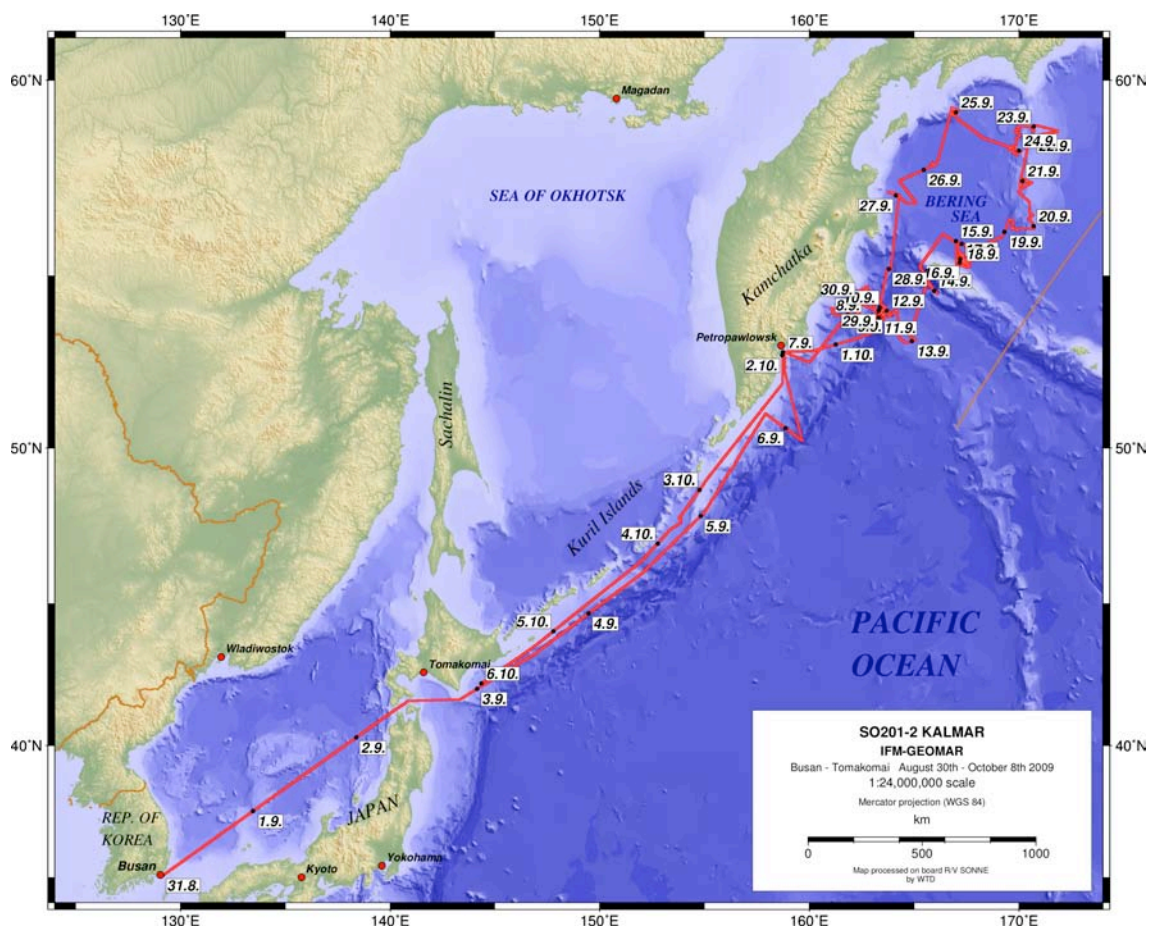


Fig. 4.1.: Cruise track for SO201 Leg2 (map processed onboard RV SONNE by WTD).

The previous expedition group was unloading their equipment, laboring in 30°C heat and high humidity. Our early arrival allowed us to take control of some of the heavy equipment used during the previous cruise. On the following day, most of the remaining participants from Germany, Russia and the US arrived, and together with the help of the crew, we loaded five containers of scientific equipment and supplies aboard the ship. Some of the containers were unloaded while the ship was still in the port. The skies were overcast, so it was not as hot as on the previous day. Our official embarkation was planned for Sunday at 9:00 AM.

On August 31, all hands were aboard and we left the harbor at 8:30 AM. The skies were still cloudy and the water in the port showed small, white-capped waves, predicting strong wind and waves at sea. A typhoon which had formed southeast of Japan and had wind velocities up to 80 knots, was felt even in Busan. The center of the typhoon drifted out of our

path to the north and northeast, but the resulting strong winds and waves tested our sea legs early. By evening time the storm had slowed, and all participants were able to enjoy the great food of our excellent cook on board.



Fig. 4.2.: All container on board.

The following days were used to organize our sea-going laboratories, and to prepare the heavy coring, dredging and heat-flow measurement equipment, which we will use to carry out research under the KALMAR-Project (Kurile-Kamchatka and Aleutian MARGinal sea-island arc systems: geodynamic and climate interaction in space and time). One of the goals of this multifaceted project is to understand the relationships between the compositions of seamounts and the dynamics of the oceanic crust and upper mantle in the area where the Aleutian Island chain meets the Kurile-Kamchatka arc. By collecting rock samples from volcanic and tectonic structures, and by measuring heat flow through the oceanic crust, we will investigate the origin and evolution of the Aleutian-Kamchatka junction and its vicinity. This project will also contribute to an improved understanding of the geologic processes that underlie volcanic catastrophes in the North-West Pacific, and the effects of the volcanism in Kamchatka (the most volcanically active subduction zone on earth) on climate changes during the Holocene. An additional goal of the project is to reconstruct the oceanographic and climatic records of the sub-arctic NW Pacific and NE Siberia, and to understand their role in the global climate system. Specifically, this project will allow us to investigate the relationships between the different air masses of the region, such as the Siberian high and the Aleutian low (Pacific/N-American Oscillation) and the Azore system and Greenland deep (Arctic Oscillation/North Atlantic Oscillation). We will also investigate the dynamics of the North Pacific medium water (in between waters, not deep and not shallow), which are important to the renewal of the water masses in the Pacific and to nutrient cycles in the global oceans.

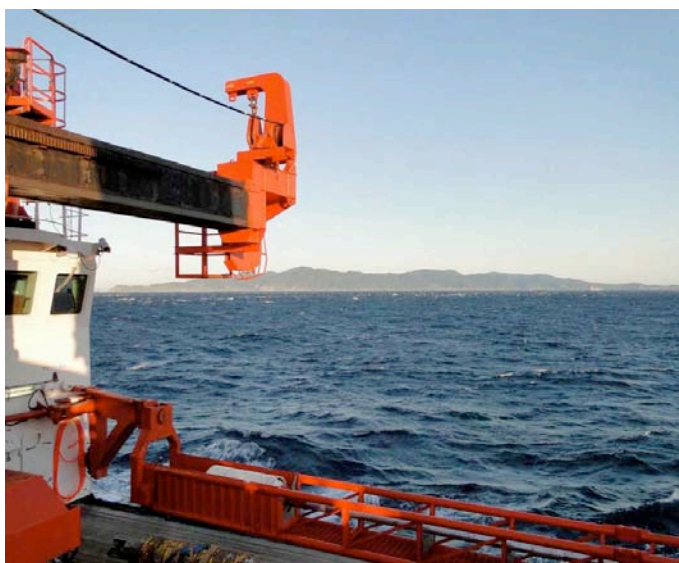


Fig. 4.3.: SONNE entering the Tsugaru-Kaikyo Straits.

continued mostly to the north, along the Kurile Islands chains until September 6th, when we

After crossing the Sea of Japan, we reached the Tsugaru-Kaikyo Straits in the evening of September 2nd. This strait, or ocean pass, is underlain by the worlds longest railway-tunnel, which connects the island of Hokkaido with the main Japanese island of Honshu. As we passed through the straits, we observed a spectacular coastal landscape and experienced greatly increased wind velocities due to the effects of the narrow pass between the islands. The topic of the day on September 3 was switching the ship's air condition system from cooling to heating. The cooler air and the surface ocean temperatures of the North Pacific lead quickly to our first whale sightings. Our path

turned east and began hydro-acoustic soundings of the Kurile-Kamchatka trench.

September 7th we planned to pick up colleagues from Petropavlovsk while staying outside the Avachinsky Bay. Once our crew was complete with 24 scientists and 1 Russian naval observer, we started with the ground touching work of the cruise.

Picking up our colleagues from Petropavlovsk and Vladivostok to embark on the R/V Sonne, we were right on time at location 52°50.7N 158°44.2E on September 7th. We had calculated some waiting time for their final arrival, and indeed we needed it. At 16:15 a relatively large vessel appeared from the lifting fog and came along our starboard side, allowing our colleagues to jump aboard the *Sonne*. There was a hearty greeting, which was followed quickly by an excellent dinner, making up for the long hours of waiting, both for the crew on board and the new arrivals.

After a transit of 16 hours we arrived at our first station at 08:45 ship time, at 53°55,14N 161°49,83E. Here we made CTD (conductivity, temperature, density) and oxygen concentration measurements. Surface water temperatures here of 11.5°C reflect the summer warming. These surface water temperatures drop to a minimum of 1.58°C at a depth of 108 m. We reached the constant thermocline with 3.74°C at 43 m depth. The extended depth range of oxygen depletion in this area, from 380 m to 1143 m at a concentration below 0.31 ml/l, was remarkable. We ended our work at the first station with a multi-net station.

With the acoustic profile from the first CTD station, we calibrated the hydroacoustic data recorders and our mapping of the ocean floor was begun. After recording its first data on September 6th, the Parasound system suddenly failed. This is the system that we use to map the thickness of sediment cover and the geometry of sediment layers in the first few tens of meters on the ocean floor. A complete restart of the system and re-installation of the software did not remove the failure. The electronics experts aboard the *Sonne* eventually discovered a defect in one of the data-transfer cables of the system. With the failure corrected, we quickly began recording Parasound data again. In the first working area, on the Shatsky Rise and on the continental slope east of Kamchatka, the ocean floor showed a rough topography, resulting from intensive shear and deformation, caused by the interaction of tectonic plates. Similar structural features were seen on land during fieldwork done in 2007 and 2008 in the Kumroch range and the Kronotsky peninsula on Kamchatka. We encountered equivalent structures on ocean crust, east of the Kamchatka continental shelf. The search for a promising core location was difficult. Thanks to our PhD students, who received excellent training in the Parasound system prior to this cruise, we eventually found



Fig. 4.4.: Core from the continental slope off Kamtchatka with turbidites.

an appropriate spot. The core system (Kolbenlot) from the Marinetechnik-Kawohl company worked without failure and we quickly completed three very successful Multicorer stations. The sediments were in some areas highly dewatered, so the corer did not penetrate deep into the sediments. The multicorer was only successful, after we began to run the corer with higher speeds towards the ocean bottom. Besides the somewhat dewatered sediments, sandy turbidites and foraminiferal sands made the deep penetration of the core difficult.

Almost on the latitude of Kiel (54°N) but at 163°20'E, we made our first dredging at Meiji

Seamount, which is exposed by faulting in water depths from 3000-6000 m. This seamount is the most northerly, and therefore most likely the oldest volcano in the Hawaiian-Emperor Seamount chain. These seamounts are eroded and subsided volcanic islands that were initially formed over the Hawaiian hotspot. As time passed, they moved with the Pacific Plate to their current position east of Kamchatka. The first dredging at Meiji Seamount recovered a variety of sedimentary and volcanic rocks from nearly 6000 m water depths. On Thursday morning September 10th we measured the heat-flow for the first time near this spot.



Fig. 4.5.: The „hard-ground“ Heat flow sonar system back on deck.

Starting early on September 9 we began to observe the weather development. A new typhoon, which had formed in the warm Pacific waters east of Japan, was moving to the NE and on a course to merge with a deep, low-pressure system over Sakhalin Island which was already at 988 mbar. On Thursday the typhoon was reduced to a deep, low-pressure cell, and it began to merge with the low over Sachalin. During September 10th the air pressure fell at a rate 1 mb per hour for much of the day, and we recorded wind speeds of more than 30 kts. Due to the sustained winds and resulting strong waves, we were forced to stop our work at 20:00 shipboard time. In the early hours of

September 11, Friday, the air pressure sank to 980 mbar, but the winds slowed, allowing us to begin our hydroacoustic mapping again, this time at a reduced speed of 8 kts, due to the rough conditions. This gave us reasonably good results, which allowed us to locate two additional stations for dredging.

The first dredge after the storm was a complete success. Besides volcanic sediments, this dredge contained large quantities of pillow basalt fragments, produced by submarine volcanism during the growth of the volcano. These lavas are surely the best samples that have ever been collected from the volcanic basement of Meiji Seamount. These samples will give us insights into the early history of the Hawaiian mantle plume, and they will contribute to the reconstruction of the development of the Pacific oceanic crust in the time period from 85-90 million ago. Another dredge some 7 nautical miles further to the northeast, brought only a small number of rocks aboard, which were determined to be mostly ice-rafted debris.



Fig. 4.6.: Successful dredge.

In the early Saturday morning hours, additional measurements of heat flow through the ocean floor were carried out. These results confirmed the trend of the data collected by Russian scientists in the 1970's. They saw strong positive and negative anomalies in the heat distribution in a relatively small area. We interpret our new findings as clear sign for water circulation in the tectonically broken oceanic crust of the western part of the seamount study area. More heat-flow measurements at Meiji Seamount were done on September 13th, thus completing this program.

The warmth of the Sun only occasionally reached the ship's deck this week. The cumulative sunshine was well below 5 hours. Aside from the grey weather, all on board are doing well.

We have enjoyed blue, cloudless skies and mild breezes for almost five days, thanks to the strong high-pressure system of 1028 mbar that has been nearly stationary over the western Bering Sea. After the blustery conditions of last week and earlier this week, the calm conditions are a welcome experience. At lunchtime it is so warm in the sun that it is hard to believe that we are in an arctic-marginal ocean.

At the start of the week we worked on a seafloor structure southwest of Bering Island that was interpreted as a possible slice of oceanic crust that had been accreted to the Komandorsky Island block, by collision and shearing along the front of the western Aleutian arc. Two dredge stations on the flanks of this structure produced mostly sandstones similar to those seen on the Bering Island during the fieldwork there in 2008. These results indicate that this structure is unlikely to be a block of oceanic crust, but is more likely a fragment of Aleutian Island arc crust, which has been sheared and transported by strike-slip faulting along the western Aleutian fore-arc.

In the morning hours of September 15th, at 05:30 we crossed the Aleutian trench, which is the oblique shear zone that marks the boundary between the Pacific and North American Plates in the northwest Pacific. Passing the southwest of the tip of Bering Island at a distance of 12 nautical miles, the wind hit us first from SE, but then shifted slowly to the NW, as a result of a passing low-pressure system. The ocean waves continued from SE as the wind direction changed, resulting in a chaotic sea. The mapping of the seafloor was difficult under these circumstances, because the ship's movement over rough seas produced air under the ship which impaired the operation of the sonar systems. Under these conditions, the ship was able to work only at reduced speeds and while driving in certain directions. The wind slowly abated toward the evening hours. On September 16 in the morning the skies had cleared but the rough seas calmed slowly through the day.

Through the afternoon of September 18th the ship's work was concentrated on mapping and sampling of the Volcanologist Massif and Piip Seamount, which are located on the sea floor northeast of the Komandorsky Islands. This young volcanic complex, which is

hydrothermally active and shows signs of recent volcanism, extends from ocean depths of 4000 meters, up to within less than 350 meters from the sea surface at its summit. The

Volcanologists' Massif and Piip Seamount constitute the largest active volcanic complex in the western Aleutian arc. The diameter of their

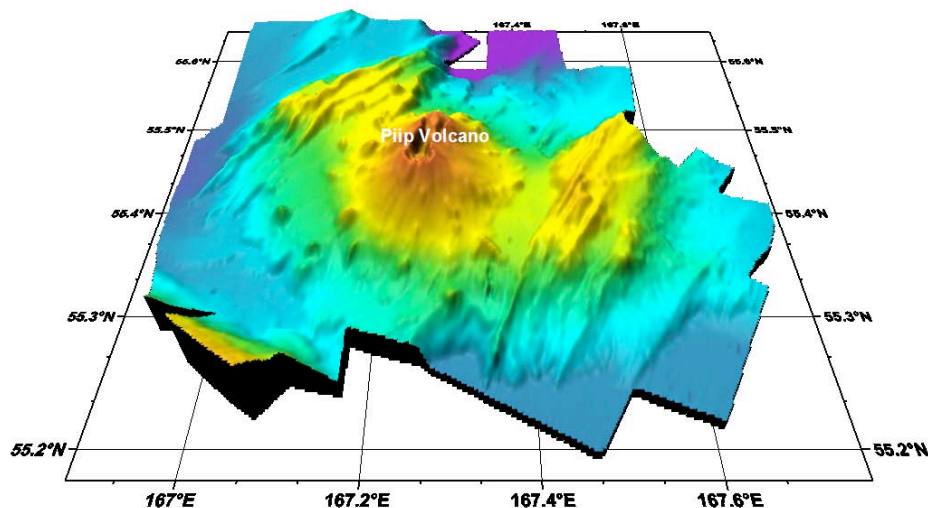


Fig. 4.7.: 3D view of Volcanologist Massiv mapped with a multi-beam sonar system.

structure is 30 nautical miles and it encompasses an area of more than 2500 km². This makes it nearly 22-times the size of Kiel (118 km²), 1/6 the size of Schleswig-Holstein, or 2.4 times the area of Moscow (1081 km²). For the first time, this area was mapped completely during our cruise by a modern, multi-beam sonar system. This mapping clearly shows north-

trending structural features, which are interpreted to be normal faults produced by right-lateral shearing to form a structural depression (graben) by 'pull-apart' tectonics between the Bering Shear Zone to the south, and the Alpha Shear Zone to the north. The young and active Piip Seamount lies at the center of this structural depression.

Dredging of the Volcanologist' Massif was aimed at sampling structural units of different ages within the volcanic complex. In total we carried out 11 dredges, 10 of them were successful. These dredges recovered a variety of volcanic rocks, including plagioclase-bearing and aphyric basalts from the basement rocks upon-which Piip Seamount is built, as well as olivine-bearing basalts and andesites from the flanks of the volcano and from satellite cones that occur on all of its sides.

At a locality close to the main edifice of Piip Seamount, the dredge recovered a large quantity of fresh dacitic pumice. Most of the rocks recovered in dredges at the Volcanologists' Massif are unaltered pillow lavas with well-preserved quenched rims, which

are excellent for geochemical investigations.

Olive-green, magnesium-rich olivine crystals in many of these samples, indicate that they have primitive compositions, similar to magmas derived from the mantle. Previous studies have indicated that some Piip lavas are an important primitive end-member among Aleutian arc lavas. The samples that we have recovered on this cruise will provide an outstanding opportunity to expand and test this idea. Laboratory studies will eventually reveal the age and origin of lavas produced by this important volcanic complex. In combination with results from geomorphology and tectonic studies, an overall model of the geodynamic evolution of the Volcanologists' Massif and Piip Seamount will be developed.



Fig. 4.8.: *Pillow lava from Piip volcano.*

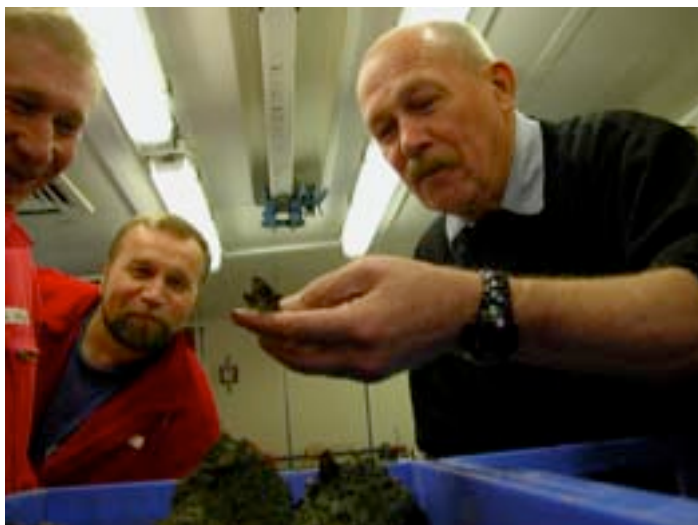


Fig. 4.9.: *Critical evaluation of teconized samples*

On Friday evening, September 19, we departed for work on Shirshov Ridge, a NS-trending ridge of uncertain age and origin on the floor of the western Bering Sea. On Saturday morning on a deep plain ahead of the ridge, we carried out hydrographic measurements followed by a multi-core station and a piston core. On September 20th, Sunday, more core locations followed in different water depth on the Shirshov Ridge.

Important technical problems, such as a malfunctioning winch brake and various cable and wire connections on electronic equipment, were quickly repaired by the very capable ship's crew this week. All of them we thank heartily.

During the fourth week our work concentrated in the region of the Shirshov Ridge, a structural high that separates the Komandorsky Basin to the west, from the Aleutian Basin and the Bering Shelf to the east.

The hydrographic analyses show a uniformly rapid decrease in the summer-surface-water warming, presently still at temperatures of 11.5 °C. At water depths of 50 m, we measured the winter minimum water temperature of 0.65° C. The northern stations on both sides of the ridge show a thicker mass of winter water, that goes down to depths of 200 m at the thermocline and halocline. Below this, the water temperature increases slightly and reaches a value of 3.8°C at 350 m depths, and then continuously decreasing below this to 1.47°C at 3800 m. The salinity is 33.25 PSU above the halocline and reaches 34.69 PSU in the bottom water. The surface water in the north is more ventilated, oxygen reduction beginning at water depths of 200 m, in contrast to the hydrographic measurements at the southern end of ridge shows a decrease in the oxygen content beginning at 160 m. At depth the oxygen minimum zone is reached throughout the area at 1300 m. Below this depth, a weak, but continuous increase is seen. Below 3400 m in Komandorsky Basin these reach values of 2 ml/l.



Fig. 4.10.: *Partly laminated core from N'Shirshov-Ridge*

Along the N-S transect over the Shirshov-Ridge we used our piston corer to sample up to 20 meters of undisturbed marine sediments which contain a high-resolution record of sedimentation and sea floor and water column conditions. Some of the cores from the shallow stations in the north show unclear laminations, resulting from the minor oxygen content and high productivity in this area. Numerous volcanic ash layers (tephra) in these sediments can be accurately dated and will provide time markers for us. The ash layers will also allow us to correlate the record of volcanism in our cores with volcanic sections studied on land in Kamchatka and in the lake sediments that were studied in 2007 and 2008.

So far we have recovered 155 meters core. Double coring at the same station was successfully carried out on this cruise. High resolution measurements done on board, like magnetic susceptibility and color scanning, show an excellent correspondence of the parallel cores. The doubling of the cores provides us with enough sediment to carry out our extensive analytical procedures in the lab, that will allow us to reconstruct the environmental parameters of the past for these locations. From these sedimentary cores we will reconstruct the



Fig. 4.11.: *Successful recovery of the coreliner from the piston corer*

climate history for the last 300,000 years of this oceanic region, which was previously not well explored.

Dredging operations from 21st to 17th September also focused on Shirshov Ridge, which follows a north-south trend and continues on shore to the north at the Olyutorsky Peninsula. Detailed hydro-acoustic mapping shows displacement of the ridge axis along northwest and southeast-striking faults. The faults follow parallel to the direction of the major fault in the Komandorsky Basin. In the center of the structural high of the Shirshov Ridge, a tilted block was mapped over several kilometers. The margin of this block is a steep escarpment, indicating a pull-apart tectonic connection with the opening and widening of the basin. The parasound measurements show that this escarpment continues in the subsurface, into the youngest sediment layers, reflecting the still ongoing tectonic activity on this structure. In general, the morphology of the ocean floor in the steeper topographic regions shows a structure that is controlled by pull-apart tectonics. The geological structure of the Shirshov Ridge is complex, as indicated by the rocks recovered in our dredges. These can be separated into three groups: 1) Andesites and tuffs showing similarities to island arc rocks, 2) chert and basalts that represent oceanic crust and 3) metamorphic rocks, seen over quite a distance.

Late Friday night (September 25) and in the early hours of Saturday we departed for working area 3, which lies in the central part of the Komandorsky Basin in water depths of 3500 m and greater. Here we mapped a small northwest-trending ridge which reached 500 m above the local abyssal sea floor. The direction of the ridge follows the pattern of the Komandorsky Basin and belongs to the regional Gamma Fault Zone. The rocks recovered by dredging here were fragments of pillow lavas, similar to those formed at oceanic ridges. Geochemical analyses of these rocks will give us information on the composition of the underlying mantle and the age of the Komandorsky Basin. As in the first week of the cruise, the steering device of the multi-net failed again. This time we had given up on the idea of using it further, when due to the enormous efforts of Rudi Angermann, who managed to bring even this totally drowned device back to life, we were able to take a section at the northernmost Shirshov Ridge. When on Thursday (September 24th) the CTD-winch failed (this is also the winch used by the multi-net), we were impressed that it was possible to deploy both devices on the larger deep-sea winch, after only some short preparations including the addition of weights to the devices. Again, we can only acknowledge our debt of gratitude to the highly capable electricians and engineers aboard Sonne - well done! The captain and crew are tireless in their actions to support our scientific mission - we thank each of them heartily.



Fig. 4.12.: Sawing of a sample from the dredge.



Fig. 4.13.: The multi-net driven at night.

The weather was again mostly nice to us week. The sky was only partly clouded and the sun shone on-and-off, with a few rain showers and more than one rainbow. The wind blew only lightly. We felt the effects of passing lows only in the form of higher waves from the southeast. On Saturday afternoon the wind began to rise as the barometer dropped, but work continued. As-of Sunday afternoon, high winds and generally poor weather conditions have forced a stop to scientific operations, and the ship stands in place with its bow the wind.

The stormy weather that forced us to hold station with the ship's bow in the wind last Sunday, the 27th of September, prevented us from continuing our activities for several hours. On Monday the bottom of the low-pressure system at 976 mbar was centered over the Komandorsky Islands, so we decided to leave the Bering Sea and return along the back side of the low to working area B, which includes the continental slope of Kamchatka and the plate boundary area where Meiji Seamount is being subducted.



Fig. 4.14.: *Holding station in bad weather.*

that this structure was most likely a tilted fragment of subducting oceanic crust that had accreted to the inner trench wall. We dredged the eastern flank of this ridge with the aim of collecting rocks from the accreted oceanic crust, but the dredge only brought up ice-rafted 'dropstone' material. Subsequently we continued our work at the Meiji

Seamount, the oldest preserved volcano of the Hawaiian-Emperor-Seamount chain. Samples from this seamount will give us new insights into the history of the Hawaii-hotspot, but also information about the input into the Kamchatka-Aleutian subduction system. Two further dredges at the NW-Flank of the Meiji Seamount were meant to enlarge our sample set taken at the beginning of the cruise. Dredging of this area produced mostly sedimentary rocks which provide information about inputs to the Kamchatka subduction system. While mapping the continental margin of the Meiji area at the beginning of our cruise, we had already observed a seafloor geomorphology caused by

We continued with the station work in the night from Monday (September 28) to Tuesday, completing the hydro-acoustic mapping of the deep sea trench between the NW-Flank of the Meiji Seamount and the continental slope of Kamchatka. In the deep sea trench we mapped a ridge-like structure in 6000 m water depth, about 20 km long and about 500 m high. We concluded



Fig. 4.15.: *The last dredge from Meiji-Seamount*

active subduction and accretion of tectonic blocks. After careful rereading of the previously mapped areas, we reasoned that small pockets of sediment would likely be found in graben-like, down-faulted structures, where sedimentation rates would be high and preservation good. The newly chosen mapping route was a



Fig. 4.16.: *Sampling the last meters of core*

the Aleutian Low – Siberian High influence on local and global climate. With the Multinet successfully repaired, we were able to repeat and finish data collection previously attempted at the cruise's first station. This part of the scientific program was thus successfully completed, despite technical problems with the equipment. The last station work for the ship was the completion of the echosound mapping. When this work was done, we left for Petropavlovsk.

success. The position was close to land, less than 25 nautical miles to the coast. As the skies cleared, the mountains of the Kronotsky-Peninsula, which rise more than 1000 m in the vicinity to the coast, were well within sight. A multicorer and a pistoncorer were successfully deployed into sediments accumulated over a down-faulted block in water depths of ~1400 m. Opening of the core liner showed immediately that more than 5 m of Holocene sediment had been recovered. This is a relatively long core for just the Holocene time period, so we anticipate that it may hold a record of decadal resolution which will contribute significantly to the understanding of



Fig. 4. 17.: *The morning view of Veluchinsky Volcano, close to Petropavlovsk*

On October 2nd in the early morning at 06:00 ship-board time, we arrived on station to disembark our Russian colleagues, who will travel home via Petropavlovsk, Kamchatka. In contrast to our previous visit at beginning of the cruise, the skies on this morning were clear, and revealed an impressive view of several volcanoes in the morning sun. Radio contact with the port did not bring response. Only phone contact with the ship's agent indicated that disembarkation would commence in the afternoon, but events proceeded faster than anticipated, when the boat to pick up our colleagues arrived at 11:00. We bade our friends a hearty but wistful farewell. We did our work together at sea very well. This experience deepened our already well established contacts and gave us hope for continued collaboration on future projects.

We were passing the Kurile Islands while transiting to Japan. Packing of the valuable samples has started and the writing of our cruise report is underway. Despite some uncomfortable weather conditions (we are now headed toward another storm) our cruise has been successful in all areas and has given us excellent samples. We head homeward with a good harvest.



Fig. 4.18.: Farewell to our friends and colleagues as they depart.

Last but not least, we acknowledge the great efforts of the ship's crew which have made our scientific success possible. For this we express our warmest thanks to EVERYBODY!!!

5. OPERATIONS AND PRELIMINARY RESULT

5.1. CTD-PROFILING AND ROSETTE (C. Dullo, S. Shapovalov)

A SBE 911 plus CTD profiler was used at 6 stations in conjunction with a Sea Bird SBE 32 carousel water sampler to study the vertical variability of temperature, salinity, and oxygen, and to obtain water samples over the water profile. The system consists of a CTD sensor unit (temperature, conductivity, pressure), an oxygen sensor, and a Rosette with twenty four 10 l Niskin-bottles. Further, a mobile fluoroprobe was installed to monitor the chlorophyll a content in the upper water column. The registration of the hydrographic parameters was performed from sea surface down to sea bottom and vice versa. Depending on the regional hydrography, sea water samples were taken between the surface and at maximum water depth of 4500 m immediately after recovery for the following purposes:

- 1 glass bottle (25 ml) for the analyses of stable carbon isotopes of total dissolved CO₂
- 1 glass bottle (25 ml) for the analyses of stable oxygen isotopes of seawater
- 1 PE bottle (100 ml) for the analyses of trace elements and calcium isotopes
- 1 PE bottle (20ml) for the analyses of stable Sr isotopes

To prevent any biological activity, the water samples for $\delta^{13}\text{C}$ and total CO₂ were poisoned with 1 ml saturated HgCl solution and stored at 4°C.

5.1.1. Preliminary results of hydrographic measurements

Hydrographic measurements of temperature, salinity, and oxygen collected during the SO201-2 cruise in the NW Pacific and the Bering Sea were used to characterize the distribution of temperature, salinity, typical water masses, and their spatial variability in the region. The position of the stations responds to the original aim of the project, and some valuable information on the water column can be extracted. The hydrographic stations were carried out in three regions: two stations offshore the Kamchatka Peninsula in the area B, one station in the southern part of the Komandorsky Basin in the area 7, and 3 stations crossing the northern part of the Shirshov Ridge in an E W direction in area E including the northern part of the Komandorsky Basin (Fig. 5.1.1.).

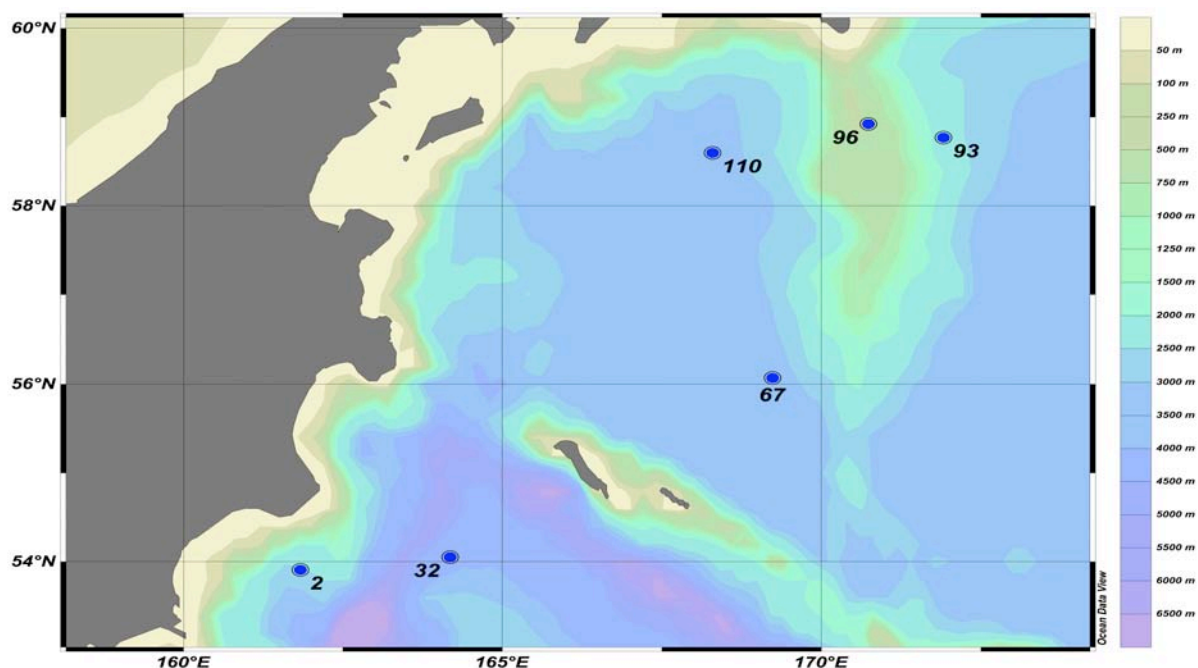


Fig. 5.1.1.: Location of hydrographic stations during R/V SONNE cruise SO201-2.

The general pattern in all stations shows a rapid decrease in sea surface temperature within the upper 50 m of the water column followed by a slight increase below 150 m and 210 m respectively down to 200 and 290 m which marks the constant thermocline. Below, temperature decreases reaching values around 1.47°C in the deepest station (SO201-2-32CTD: 4282 m) off Kamchatka (Fig. 5.1.2.). Salinity in contrast, increases rapidly in the sea surface water of the upper 50 m, followed by slightly constant values down to 150 m and 210 m, respectively. The distinct increase below marks the halocline, which parallels the thermocline. Highest salinity values within the deep water were recorded around 34.69 PSU off Kamchatka (SO201-2-32CTD: 4282 m). The deeper position of the thermocline and the halocline shown in figure 5.1.2. is observed in the northern stations (93, 96, 110) of the Komandorsky Basin running over the Shrishov-Ridge, while the shallower thermocline and halocline occurs in the southern Komandorsky Basin (Station 67) and in the stations off Kamchatka (2, 32: Fig. 5.1.1.). This regional feature is also seen in the cross section of Figure 5.1.3.

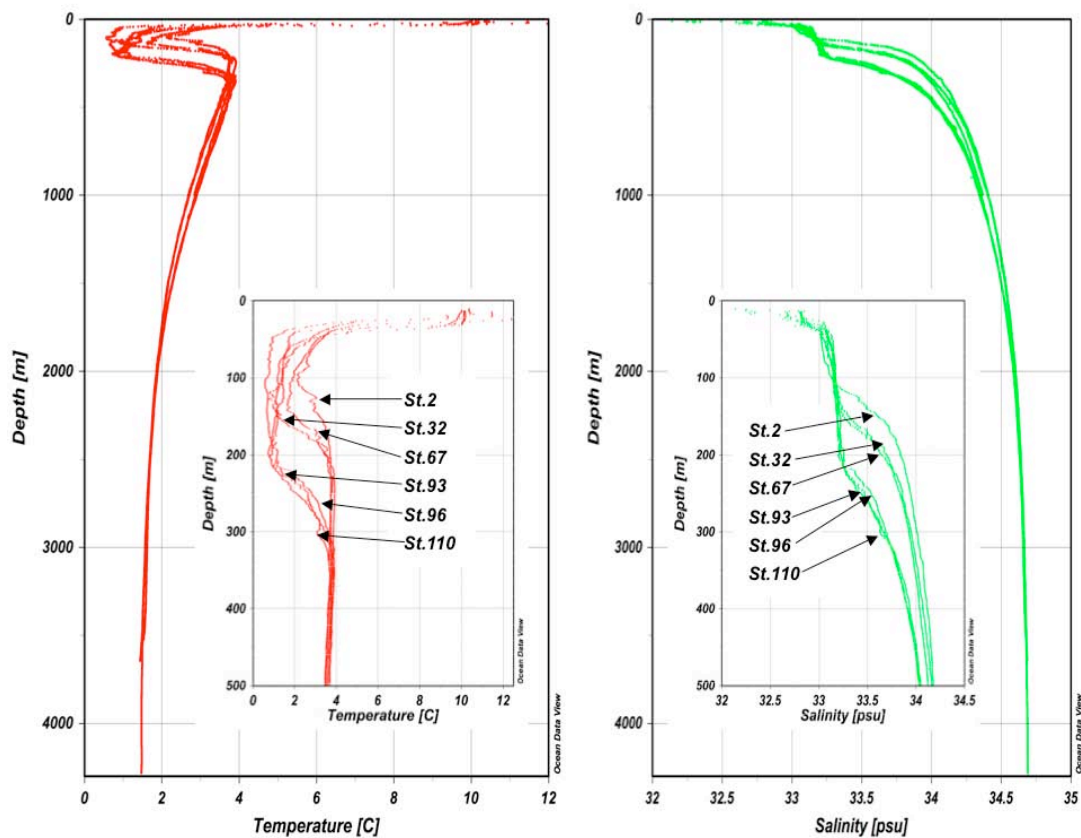


Fig. 5.1.2.: Temperature and salinity profiles. The insets display the upper 500 m enlarged.

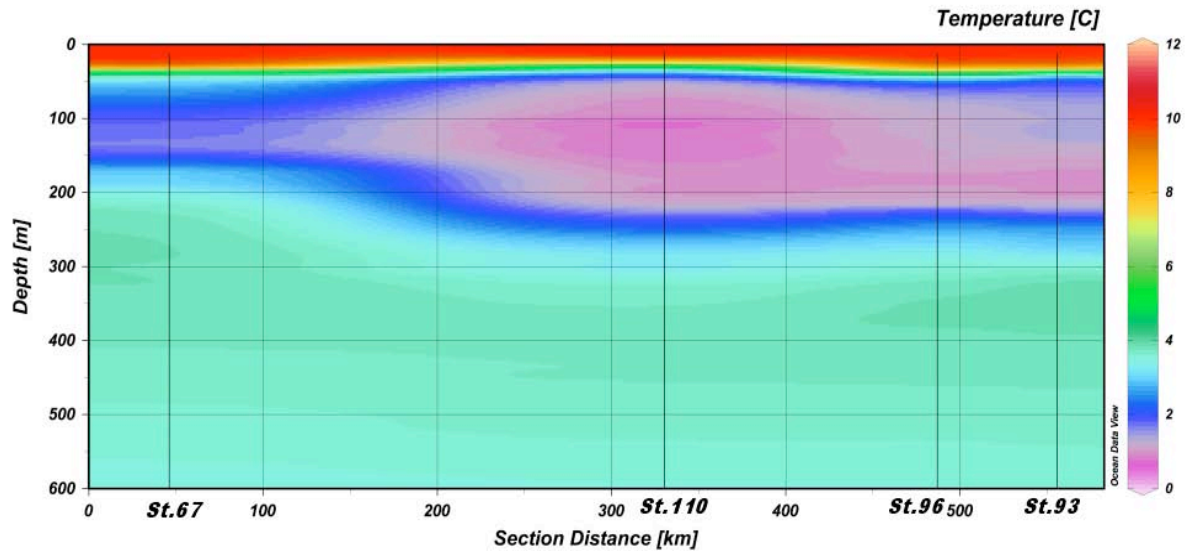


Fig. 5.1.3.: Section within the Commander Basin showing the temperature minimum.

The high temperatures and low salinity values of the uppermost, and almost homogenous 20 m we ascribe the seasonal effect of the summer warming and in relation to this to higher rates of precipitation, runoff, and ice-melting. The pronounced cooling in the sea surface water masses reflect winter water, which is the source for WSPW. Coldest temperatures were recorded in station SO201-2-110 at 109 m showing 0.57°C. The winterwater mainly forms in the northern Bering Sea, which is nicely seen in Figure 5.1.3. The Stations 93, 96, and 110 are characterized by a distinct T-minimum which is less pronounced in station 67 due to advection of Pacific Water mainly through the Near Strait and less through the Kamchatka Strait (Takahashi 2005). The signature of the winterwater within the two Pacific stations (2, 32) originate from the advection of Bering Sea Water through the Kamchatka Strait. Fig. 5.1.4. summarizes the observed watermasses.

Since we had no onboard calibration of the oxygen values, we used only the data in a qualitative way. The Pacific stations and the station in the southern Commander Basin showed a rapid decrease in oxygen already below 280 – 300 m, while the sections in the northern Bering Sea had better ventilated upper water masses down to 380 m. Generally the oxygen minimum zone was extended down to 1200 m.

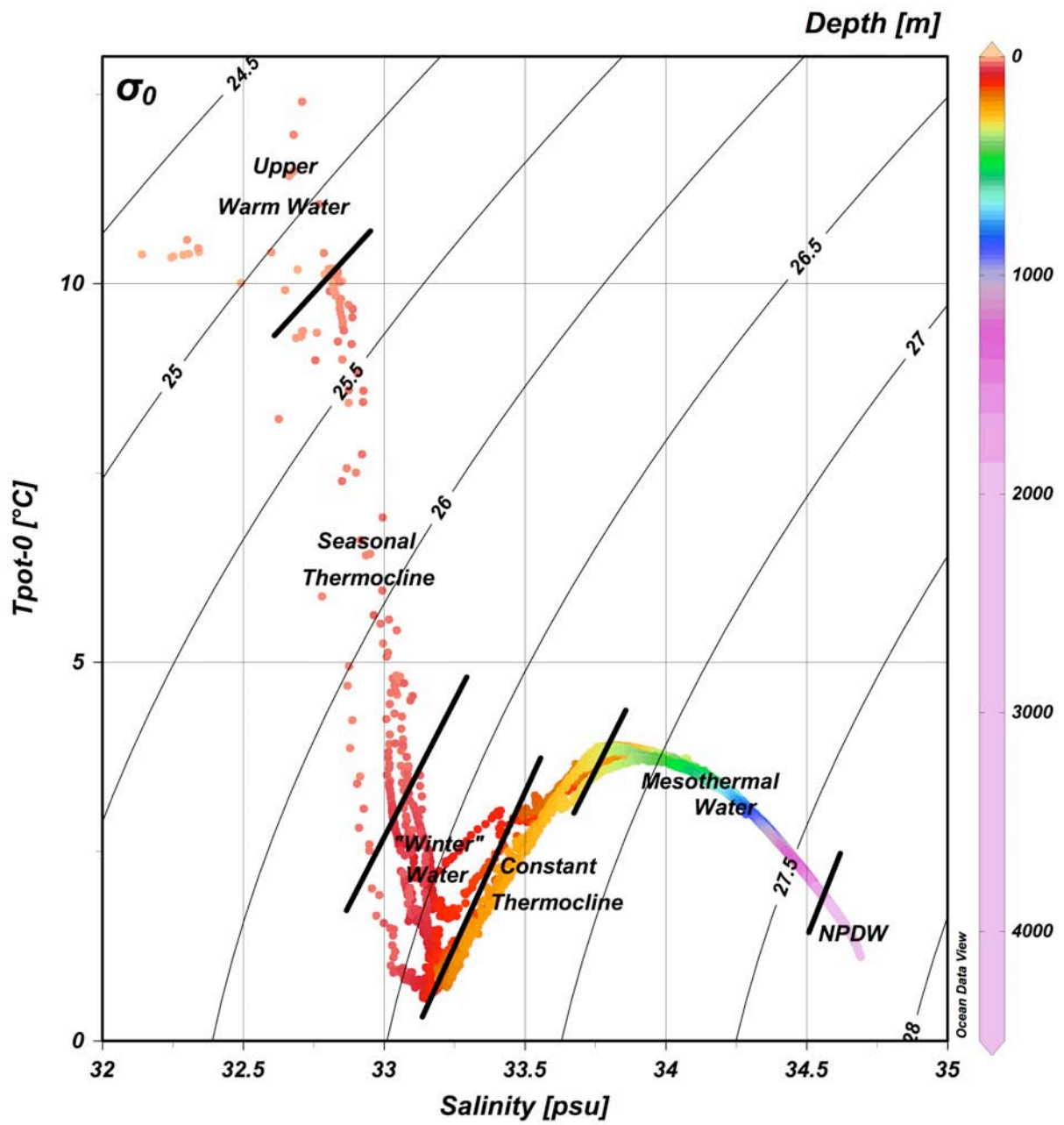


Fig. 5.1.4.: T-S plot showing the different water masses.

5.1.2 Fluorometer (*B. Glückselig*)

The distribution of chlorophyll *a* concentrations within the water column was measured with a BackScat Fluorometer (Model: 1101.1 MP/Chla/MO/2R) to assess changes in biological productivity. The fluorometer was attached to the CTD and lowered to 1000 m water depth at the first station (SO201-2-2) and to 500 m water depth at the following stations (SO201-2-4, -31, -66, -92, -96, -109) and provided a continuous, vertical profile of chlorophyll *a* concentrations for these depth intervals. The maximum depth of profiling has been adjusted to 500 m due to time constraints and because chlorophyll *a* concentrations did not change below 100 m water depth. The chlorophyll *a* profiles are shown in Fig. 5.1.5.

Maxima in chlorophyll *a* concentrations ranged between 38 and 68 $\mu\text{g/l}$ and marked the uppermost warm surface layer above the seasonal thermocline, which regionally varied from 12 to 50 m water depth. Below the seasonal thermocline, chlorophyll *a* concentrations decreased to 3-5 $\mu\text{m/l}$ at 100 m water depth and remained at this low level down to 500 or 1000 m water depth. A special feature occurs at stations SO201-2-4 (continental margin of Kamtchatka, area B) and SO201-2-92 (northwestern Shirshov Ridge, area E), where the chlorophyll maximum extended to about 15-20 m below the seasonal thermocline into a layer that is characterized by a small zone of high oxygen concentrations.

The highest chlorophyll *a* concentrations (phytoplankton productivity) were registered at station SO201-2-31 (Meiji Seamount) and at stations SO201-2-96 and SO201-2-109 (northern and northwestern Shirshov Ridge) with values of 60 $\mu\text{g/l}$, 66 $\mu\text{g/l}$, and 68 $\mu\text{g/l}$, respectively. At other locations, chlorophyll *a* concentrations were ca. 20 $\mu\text{g/l}$ lower.

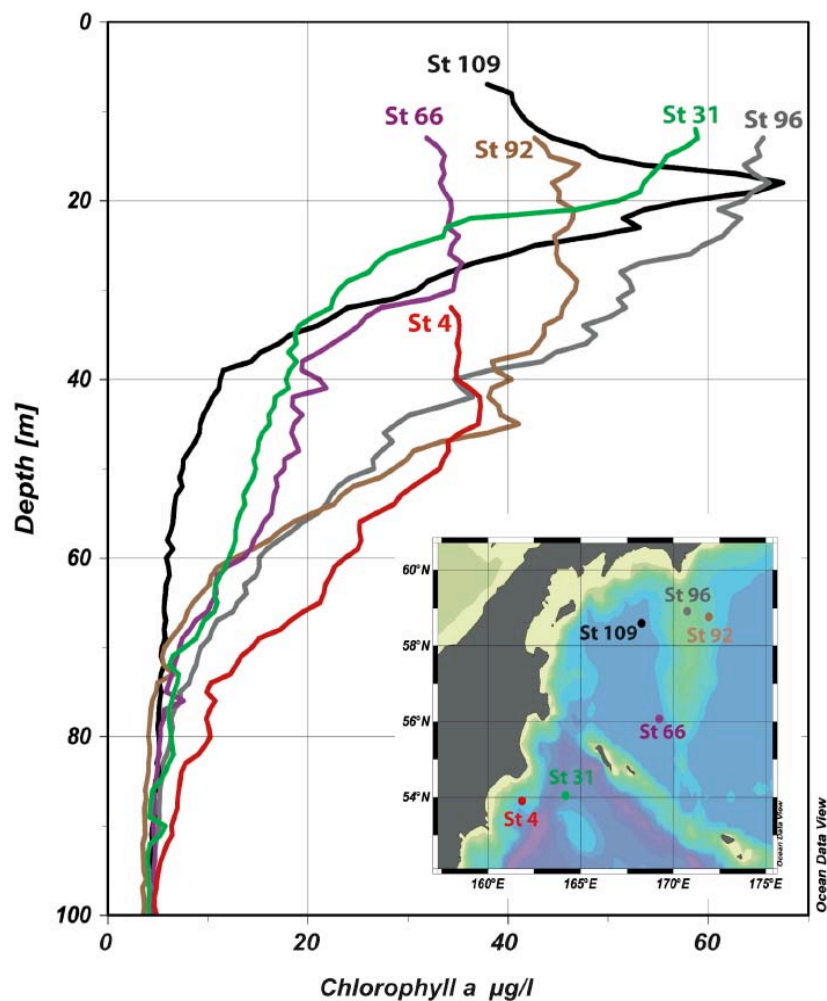


Fig. 5.1.5.: Vertical profiles of chlorophyll-concentrations at stations SO201-2-4, -31, -66, -92, -96, -109

5.2 PLANKTON (*S. Korsun, B. Glückselig*)

Screening of unfixed filtrate, on one hand, provides express environmental information and, on the other hand, reveals delicate planktonic organisms that will disintegrate in preserved samples.

5.2.1. Oceanographic setting

The Multinet was deployed at three stations in the central Bering Sea and at one station in the NW Pacific (see Fig. 5.1.1.). Based on vertical CTD profiles (see Chapter 5.1.) the structure of the water column at the time of collection (late September 2009) was as follows:

- from 0 to 22 or (depending on the area) to 32 m water depth, the seasonally warmed layer, $t \sim 10^\circ\text{C}$, $S \sim 32.5\text{‰}$;
- 30-60 m, the seasonal thermocline;
- 60-220 m, the winter water, $t = 1^\circ\text{C}$, $S = 33.2\text{‰}$;
- 220-320 m, the permanent halocline;
- 320 m to the bottom, the intermediate water. The oceanographic characteristics changed gradually with increasing water depth:

mwd	t [$^\circ\text{C}$]	S [‰]
320	3.8	33.8
1000	2.9	34.3
3000	1.6	34.7

The upper part of this water mass is oxygen depleted. The rosette recorded concentrations of c. 0.2 ml/l in the center of the oxygen minimum zone (OMZ) at a depth of c. 1000 m (Chapter 5.1.).

Chl *a* concentration estimated from fluorometry (see Chapter 5.1.2.) was relatively high within the seasonally warmed layer with peak values just above the seasonal thermocline and then declined asymptotically downwards.

5.2.2. Methods

The Multinet has an opening of 50x50 cm, a mesh size of 55 μm , and is towed at 0.3 m/sec. Unfortunately, seawater flooded the electronic switching unit through a leak in the sealing gasket during the very first deployment. Later on, however, the unit was repaired and we successfully used the multinet during the second half of the cruise.

The vessel kept its position dynamically at stations. The Multinet was towed vertically from 1000 m water depth or, when the sea was shallower than 1000 m, from c. 50 m above the seafloor. A Multinet deployment followed that of the rosette, and we used the CTD profiles to set up the plankton sampling intervals so that these intervals would reflect major features of water column stratification, primarily the permanent halocline. The nets were switched at the following depth levels: 500 m, 200 or 300 m (depending on the depth of the permanent halocline), 150 m, and 50 m.

The plankton samples were stored at 4 $^\circ\text{C}$ for several hours before being fixed with formaldehyde. Several milliliters of unfixed filtrate was pipetted out from the bottom of sample bottles and examined under a dissecting microscope at magnification x16 in incident light. Observed taxa were subjectively assigned an abundance grade – rare, common, abundant (Table 5.2.1.). Smaller organisms such as ciliates and small dinoflagellates, which were present in the samples but were discernable only by use of a compound microscope, are not listed in the table. As the samples were examined several hours after collection, the predatory crustaceans, where abundant, had possibly diminished the number of the copepods.

5.2.3. Results

Diatoms and dinoflagellates were not numerous and were restricted to upper water layers.

There were some dinoflagellate cysts.

Radiolarians occurred largely in the intermediate water. While the pterodarians always dwell in deeper waters, many polycystines inhabit the photic zone. It is probably known from the literature (unavailable onboard) whether polycystines in this region are confined to the intermediate water seasonally or permanently.

Planktonic foraminifers demonstrated an obvious trend. Live specimens were highly abundant in the surface waters, and their numbers steadily decreased downwards, whereas the empty shells conversely became more and more numerous in deeper layers.

Gelatinous plankton (comb jellies and hydromedusae) occurred essentially in the intermediate water.

Copepods were common in all intervals. The large *Calanus cf. hyperboreus* adults were also recognized easily on underwater video (a camera mounted to the multicorer) throughout at least 1000 m water depth. The predatory amphipod *Themisto*, which preys on copepods, did not penetrate into the intermediate water and thus was possibly deterred by oxygen deficiency.

The pteropod *Limacina helicina* occurred throughout the sampled range but always at low density.

Larvae were scarce at all depths, which was no surprise at the end of the vegetation period.

5.2.4. Preliminary conclusions

Planktonic consumers were rather diverse and abundant throughout the sampled 1000-m range and the community showed no signs of deprivation due to oxygen deficiency in the intermediate water.

Of planktonic groups that are retained by the Multinet and are employed in paleoceanographic research, namely diatoms, dinoflagellates, polycystine radiolarians, foraminifers and pteropods, only foraminifers were abundant in the central Bering Sea at the end of the vegetation period (late September) 2009.

deployment #	water depth [m]	interval [m]	94				97				111				129			
			0-50	50-150	150-200	200-500	500-1000	0-50	50-150	150-200	200-500	500-1000	0-50	50-150	150-200	200-500	500-1000	
Bacillariophyta	x	xx																
Dinoflagellata	x	x																
Dinoflagellata cysts																		
Radiolaria-Polycystina		x																
Radiolaria-Phaeodaria		x																
Foraminifera live	xxx	xx																
Foraminifera dead	xx	xx																
Ctenophora																		
Trachymedusae: <i>Crossota brunnea</i>																		
Polychaeta (adult)																		
Polychaeta (nectochaetae)																		
<i>Calanus cf. hyperboreus</i>	xx	xx																
other Copepoda	xxx	xx																
<i>Themisto</i>	xx																	
Euphausiacea																		
Ostracoda?																		
Gastropoda (veliger)																		
<i>Limacina helicina</i>	x																	
other Pteropoda																		
Bivalvia (juvenile)																		
Brachiopoda (larvae)																		
Chaetognatha	xxx	xxx																
Tunicata/Appendicularia																		
eggs																		

x	rare
xx	common
xxx	abundant

mesh size 55 µm
opening 0.5x0.5 m
tow at 0.3 m/sec

Tab. 5.2.1.: Plankton: semiquantitative screening of multinet tows, Bering Sea and NW Pacific, late September 2009

5.3 HYDROACOUSTIC MEASUREMENTS (*B. Baranov, R. Werner, L. Max, J. Riethdorf*)

5.3.1. SIMRAD EM120 swath bathymetry – methods

5.3.1.1. Data Acquisition

Since June 2001 the R/V SONNE has been equipped with a SIMRAD EM120 multi-beam echo sounder system (Kongsberg) for continuous mapping of the seafloor. The SIMRAD EM120 system consists of several units. A transmitter/receiver transducer array is fixed in a mills cross below the keel of the vessel. A preamplifier unit contains the preamplifiers for the received signals. The transceiver unit contains the transmitter and receiver electronics and processors for beam-forming and control of all parameters with respect to gain, ping rate and transmit angles. The system has serial interfaces for vessel motion sensors, such as roll, pitch and heave, external clock and vessel position. The system also includes a SUN-workstation as an operator station. The operator station processes the collected data, applying all corrections, displays the results and logs the data to internal or external disks. The EM120 system has an interface to a sound speed sensor, which is installed near by the transducers.

The SIMRAD EM120 system uses a frequency of about 12 kHz with a whole angular coverage sector of up to 150° (75° per port/starboard side). When one ping is sent, the transmitting signal is formed into 191 beams by the transducer unit through the hydrophones. The beam spacing can be defined in equidistant or equiangular modes or in a mix of both. The ping-rate depends on the water depth and the runtime of the signal through the water column. The variation of angular coverage sector and beam pointing angles was set automatically. This optimized the number of usable beams.

During a survey the transmitter fan is split into individual sectors with independent active steering according to vessel roll, pitch and yaw. This forces all soundings on a line perpendicular to the survey line and enables a continuous sampling with a complete coverage. Pitch and roll movements within ±10 degrees are automatically compensated by the software. Thus, the SIMRAD EM120 system can map the seafloor with a swath width about up to six times the water depth. The geometric resolution depends on the water depth and the used angular coverage sector and is less than 10 m at depths of 2,000 - 3,000 m.

The accuracy of the depth data obtained from the system is usually critically dependent upon weather conditions and the use of a correct sound speed profile. During SO201-2 sound profiles have been recorded after reaching the working area, ensuring the use of the correct sound velocity on this cruise.

5.3.1.2. Data Processing

The collected data were processed onboard with the EM120 coverage software. The post-processing was done on two other workstations by the accessory Neptune software. The Neptune software converted the raw data in 9 different files which contains information about position, status, depth, sound velocity and other parameters and are stored in a SIMRAD binary format.

The data cleaning procedure was accomplished by the Neptune software. The first step was to assign the correct navigational positions to the data without map projections. The second step was the depth corrections, for which a depth threshold was defined to eliminate erratic data points. In the third part of post-processing statistical corrections were applied. Therefore, a multitude of statistical functions are available in a so called BinStat window where the data are treated by calculating grid cells with an operator-chosen range in x and y direction. Each kind of treatment is stored as rule and has an undo option. For the calculation the three outermost beams (1 - 3 and 188 - 191) were not considered. Also a noise factor, filtering and a standard deviation were applied to the calculated grid. All this work was done by the system operators of RV SONNE. After the post-processing the data have been exported in an ASCII x,y,z file format with header information and it was transferred to another workstation where assembling, girding and contouring with the GMT software

(Wessel and Smith 1995) were done.

All maps presented in this report are created by W. Borchert and A. Ehmer (RF Forschungsschiffahrt GmbH, scientific and technical department [WTD]) onboard RV SONNE (except of Figs. 5.1.1., 5.4.4., 5.5.1., 5.6.5.).

5.3.2. Sedimentacoustics: ATLAS PARASOUND (L. Max)

The ATLAS PARASOUND sub-bottom profiler acts as a low-frequency sediment echosounder and as high-frequency narrow-beam sounder to determine the water depth. It uses the parametric effect, which produces additional frequencies through nonlinear acoustic interaction of finite amplitude waves. If two sound waves of similar frequencies (18 kHz and e.g. 22 kHz) are emitted simultaneously, a signal of the difference frequency (e.g. 4 kHz) is generated for sufficiently high primary amplitudes. The new component is travelling within the emission cone of the original high frequency waves, which are limited to an angle of only 4.5° for the equipment used. The resulting footprint size of 7 % of the water depth is much smaller than for conventional systems and both vertical and lateral resolution is significantly improved (Fig.1).

The ATLAS PARASOUND system is permanently installed on R/V SONNE. The hull-mounted transducer array has 128 elements on an area of 1 m^2 . It requires up to 70 kW of electric power due to the low degree of efficiency of the parametric effect.

The PARASOUND sub-bottom profiler on R/V SONNE is equipped with the digital data acquisition software from ATLAS Hydrographic, which is subdivided in ATLAS Parastore and ATLAS Hydromap Control. ATLAS Parastore allows the buffering, transfer and storage as well as the visualization of the digital seismograms at very high repetition rates. ATLAS Hydromap Control is responsible for user defined modifications of the system (e.g. pulse rate or interval) and also supports the operator in running the system properly.

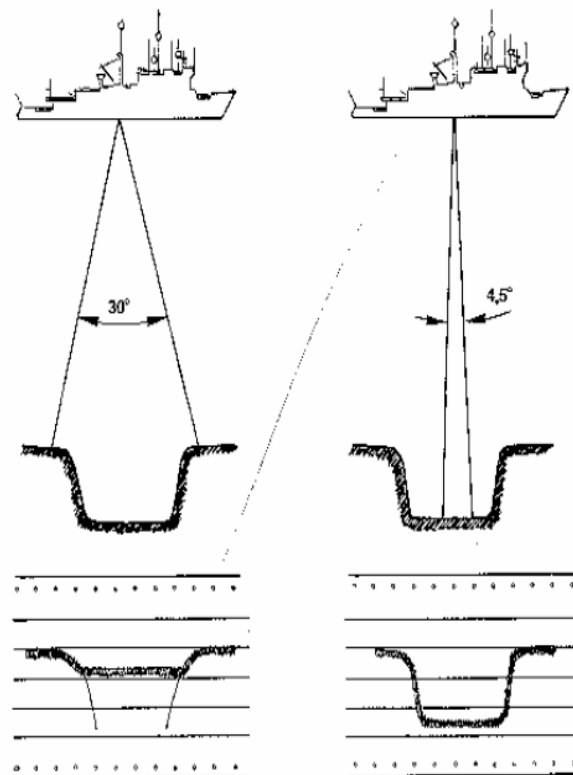


Fig. 5.3.1.: The extremely narrowed beam of the ATLAS PARASOUND of 4.5° compared with a conventional echosounder system and an angle of 30° . The ATLAS PARASOUND even resolves small-scale bottom structures and has a deeper penetration into the seafloor

(ATLAS Hydrographic).

5.3.2.1. First results

The PARASOUND system was the major tool to recover high-resolution sediment archives and to detect suitable core locations during cruise SO201 Leg 2. Figs. 5.3.2.-5.3.4. provide a summary of sub-bottom profiles for all core locations. Fig.5.3.2. and 5.3.3. show the core locations of areas B and D. Area B was subdivided by the deep-sea trench into the eastern Kamchatka continental margin and the Meiji Seamount region. Area D represents our northernmost core locations at the Kamchatka continental margin. The PARASOUND records from the continental margin indicate rough seafloor topography and suitable core sites were only found on top of ridge structures or in small-scale depressions filled with sediments (Fig. 5.3.2. a-d and Fig.5.3.3. a-b). In contrast, huge packages of well-layered sediments exist at the Meiji Seamount, which cover vast areas and indicate a typical pelagic deposition pattern (Fig. 5.3.2. e).

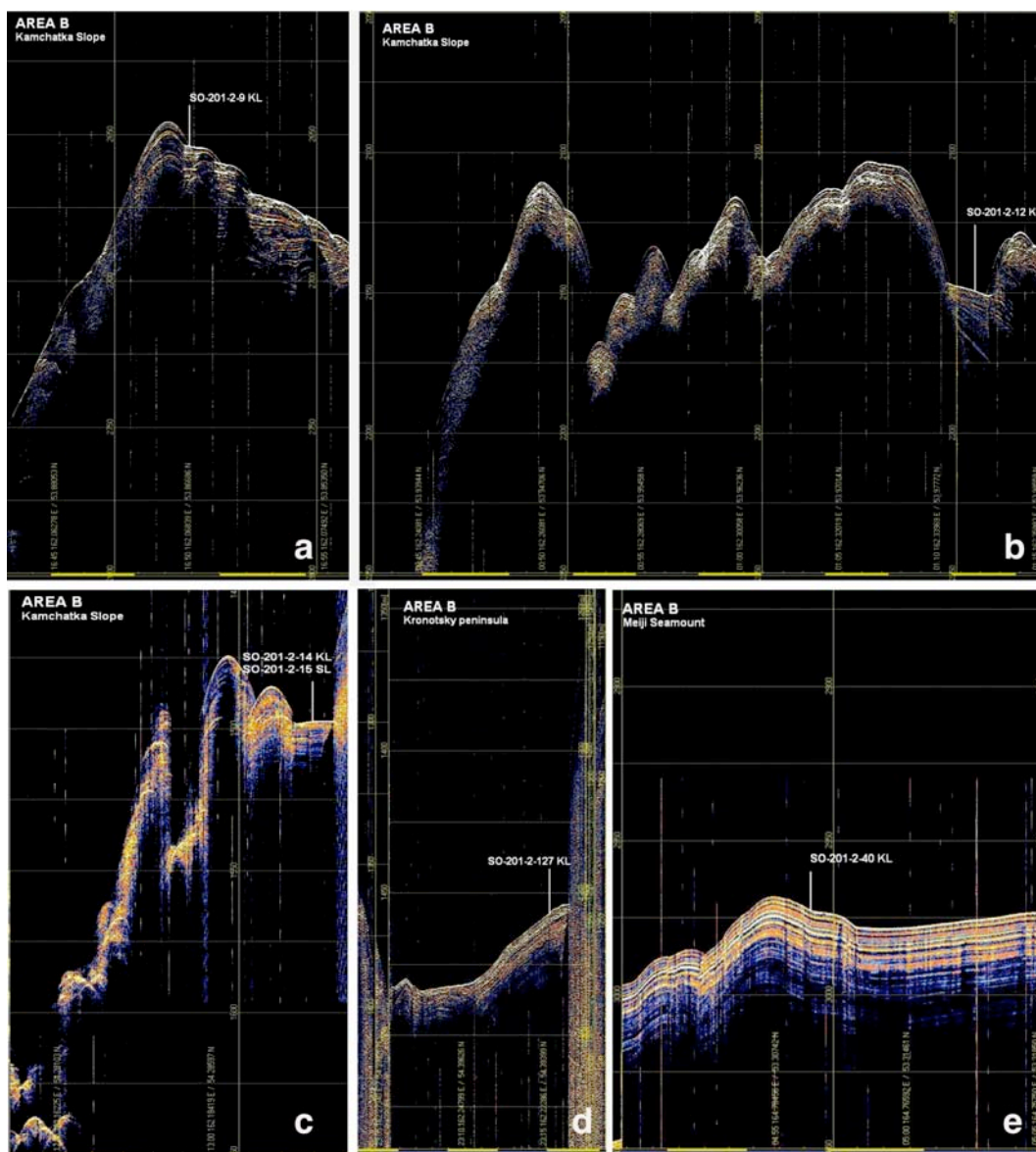


Fig. 5.3.2.: (a-d) Area B. Summary of PARASOUND profiles from core sites at the Kamchatka continental margin and (e) the core site at the Meiji Seamount (vertical white lines). Note the deeper seismic penetration (>25m) at the Meiji Seamount compared with the low penetration (<25m) at the continental margin.

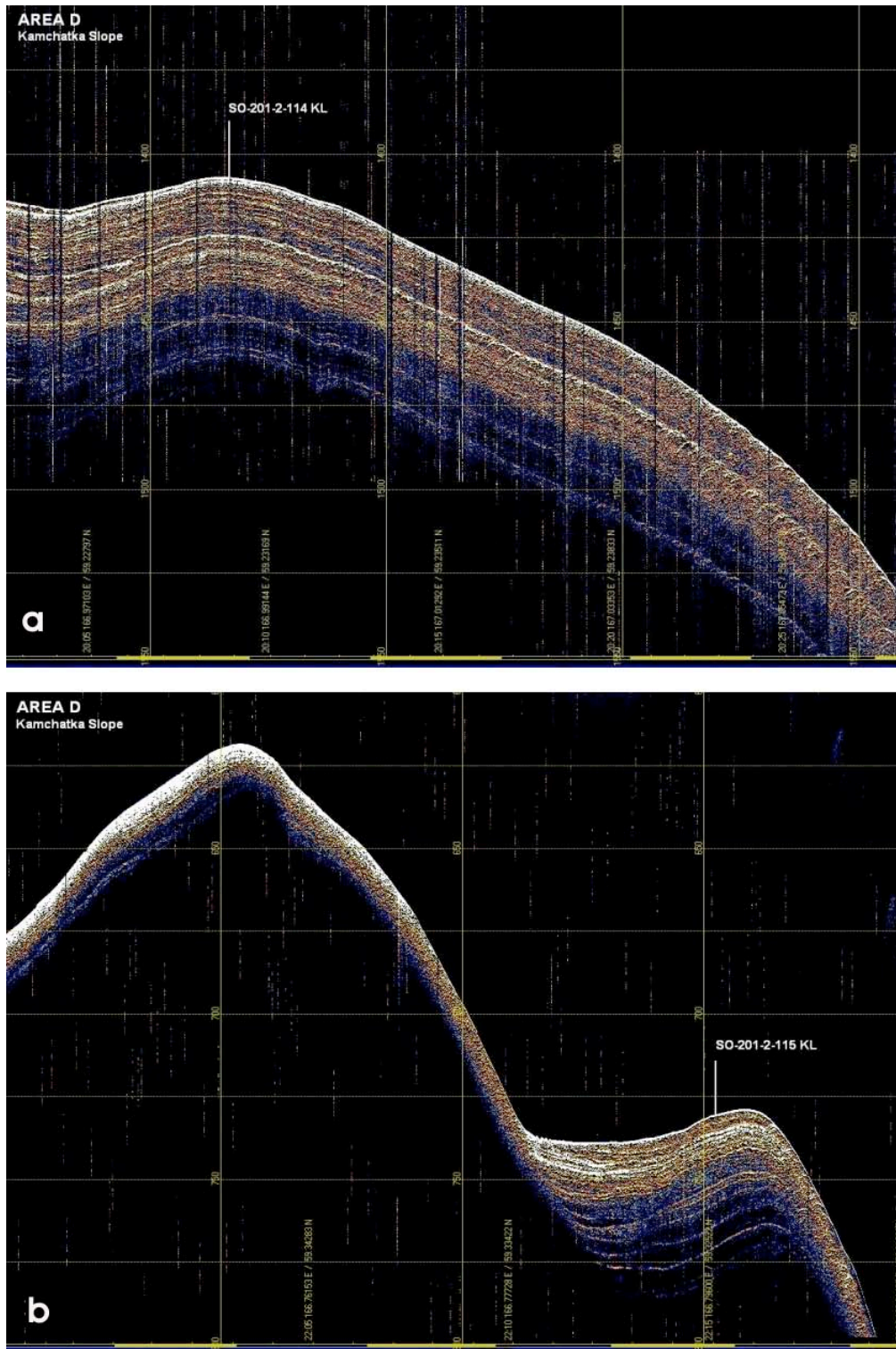


Fig. 5.3.3.: (a-b) Area D. Summary of PARASOUND profiles from core sites (vertical white lines) at the northwestern Kamchatka continental margin.

Area E is located at the Shirshov Ridge and shows, similar to the Meiji Seamount, thick and well-defined sediment layers (Fig. 5.3.4. a-d). Another core site is given in Fig. 5.3.4. e, which is located in the Kommandorsky Basin. The well-developed sediment layers at this deep-sea site (>3900m water depth) are also typical for pelagic conditions.

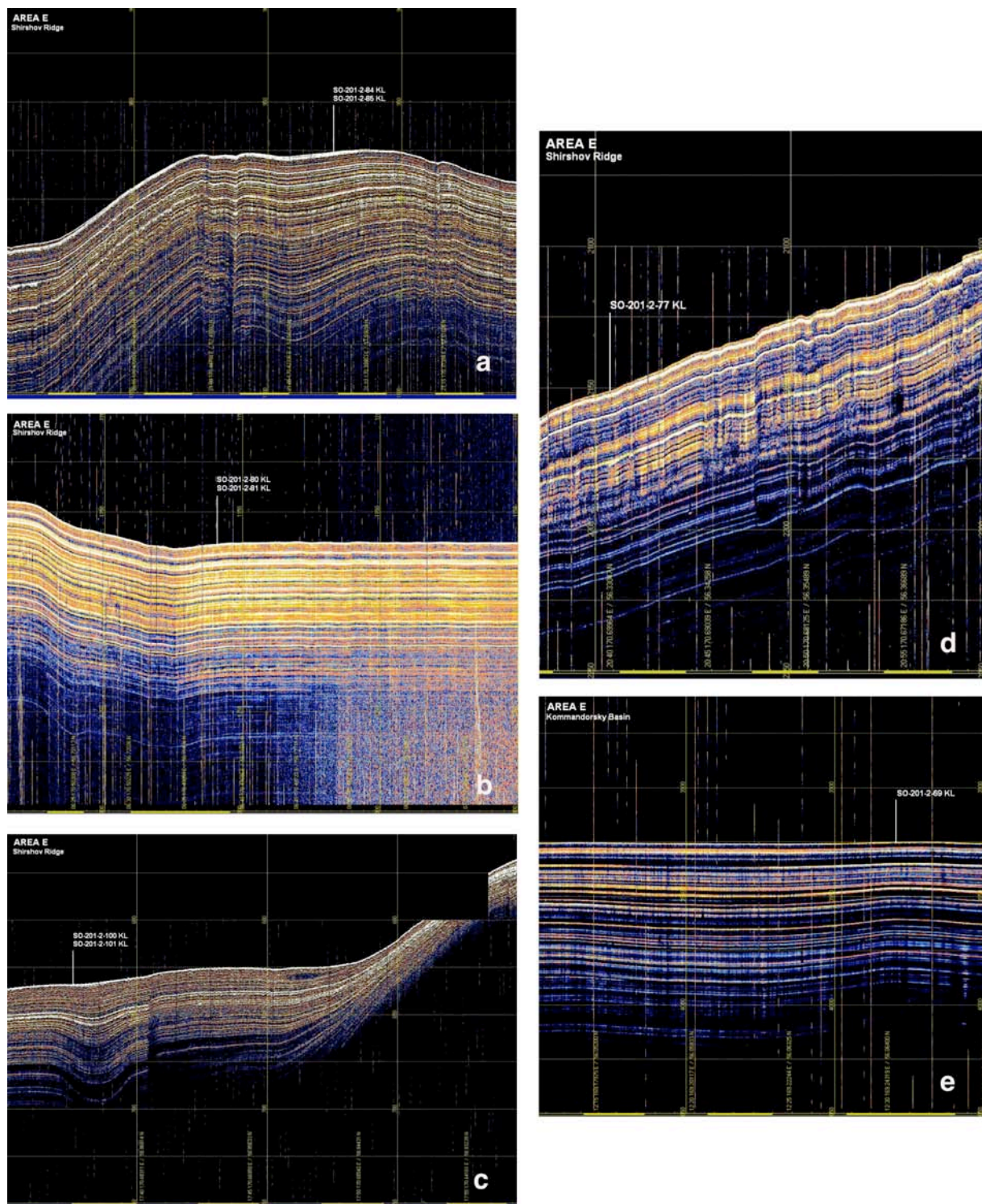


Fig. 5.3.4.: (a-d) PARASOUND profiles and core locations (vertical white lines) at Shirshov Ridge and the Kommandorsky Basin (Area E, Fig. e). All profiles show thick and well-stratified sediment sequences with penetration depths of more than 50 m.

5.4. HEAT FLOW (G. Delisle, M. Zeibig)

Equipment: BGR employs currently two different types of marine heat flow probes – a conventional probe, built after the so-called violin-bow concept and a second probe, specially designed for employment in hard ground situations. As it turned out, the sediments adjacent to the east of Kamchatka Peninsula along the eastern flank of the trench are characterized by rather hard top sediments, which excluded the use of the conventional type marine heat flow probe. For this reason the BGR-“hard ground” heat flow probe turned out to be an indispensable instrument during this cruise.

The “hard ground” heat flow probe features a 2.2 m long sensor rod made of steel with a diameter of 2 cm mounted along the long axis of a cage and held in position by a special mechanism to prevent bending during penetration of hard ground sediments. The necessary force to press the sensor rod into the sediments is provided by a cylinder, which houses lead plates with a total weight of 600 kg and an electronic unit within a pressure vessel with a total weight of additional 144 kg. The purpose of the electronic unit housed in the pressure vessel is to control the data transfer and the measurements. All measured data are transferred via cable in real time online to a laptop PC on board.

All measured data are recorded, stored, digitized and monitored by so-called “intelligent sensor modules” (ISM) installed in the pressure vessel. This technology relies on immediate digitization and downloads of measured values in the memory and enables us to improve the accuracy of measurement to $\sim 0.002\text{K}$. All recorded values are sent to an analogue-multiplexer and then to a 16bit-A/D-converter. The high accuracy and linearity during A/D-transformation is achieved by the application of the sigma delta method. To further improve the accuracy of the measurements, an arithmetic mean of 20 consecutive measurements per sensor is formed and then accepted as one single measured value.

All specific modules, which control the configuration, linearization and scaling data in the ISM-module, are stored in an EPROM. Storage and display of the measured data is done via a special computer code, stored on PC.

To achieve optimum thermistor calibration, the heat flow probe is stopped slightly above the seafloor on the down trip. After a time period of typically less than 2 minutes, thermal stabilization within $\sim 0.001\text{K}$ is obtained at all thermistors. It is assumed that the thermistors measure identical seawater temperatures. Recalibration of all thermistors is achieved by using one thermistor as the master sensor, whose measured value is used to calibrate the data measured by the other thermistors.

Following this procedure, the probe is lowered with a velocity of 0.3 m s^{-1} , until penetration of the seafloor by the sensor rod is achieved. The thermal gradient in the sediments is measured continuously for a time period of typically 8 minutes. After this period, the frictional heat component caused by the penetration of the rod into the sediments has decayed to negligible values. Thereafter, a constant electric current is sent through the heating wire for the measurement of the in-situ thermal conductivity (λ). The temperature increase in the metallic rod is inversely proportional to the in-situ thermal conductivity of the adjacent sediments. We have measured the linear T-increase after initial heat-up of the assemblage and will derive λ from this curve.

A patent has been issued for this particular design.

5.4.1. Site selection

Permission to carry out heat flow measurements were restricted by Russian authorities to areas, designated as Area 13 and 14. These areas cover the north-eastern flank and parts of the central portion of the Meiji Seamount. It was therefore attempted to define points of measurement along a profile extending upslope from the lower flank to the near top of the Meiji Seamount. The key intention of this profile was to determine the variability of heat flow in this area. The site selection had to be carried out with limited prior knowledge of the hardness of the sea floor sediments at the sites, since due to time constraints no prior gravity or piston core experiments were carried out at identical positions. However the obvious

relative hardness of the recovered sediments by the first piston core stations (KL9, KL12, KL14), together with estimates based on the Parasound images did cause us to deploy the BGR-hard ground heat flow probe. Later on, the deployment of the conventional heat flow probe of BGR would have been possible in the softer surface sediments on top of the Meiji Seamount. However, to save ship's time, any equipment change was avoided.

5.4.2. First results

Four heat flow measurements were carried out in Area 13 (north-western flank of Meiji Seamount), where we have measured consistently highly linear temperature gradients (Fig. 5.4.1.). This result implies a priori a high data quality achieved by the employed equipment. At all four data points we have measured high temperature gradients (and therefore high heat flow in excess of 100 mW/m²) - implying the presence of a regional positive heat flow anomaly.

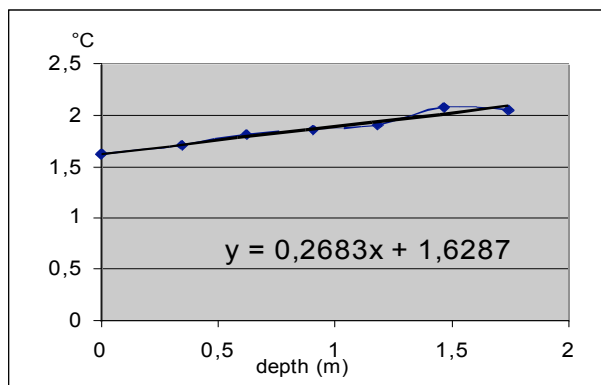


Fig. 5.4.1.: Thermal gradient determined at position 53° 52'; 163° 48'.

In contrast, the three measurements in Area 14 have consistently shown a slight and systematic deviation of the measured subsurface temperatures from linearity (Fig. 5.4.2.).

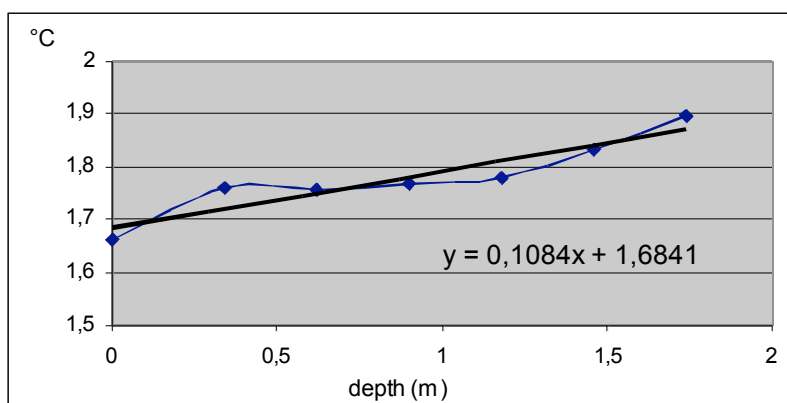


Fig. 5.4.2.: Typical measurement in Area 14: Slight deviations of temperature points from linearity were observed at all three stations.

In principle several potential processes can be listed as cause for this deviation: a) erosional/depositional processes, b) periodic fluctuations of sea floor temperatures throughout the year, or c) near surface sediment compaction upon impact of the instrument on the seafloor. Erosional /depositional processes influencing only modestly the near surface temperature distribution can be considered as unlikely. Due to the shallow penetration of the

observed temperature fluctuation any periodic fluctuation of sea floor temperatures would have to be short-periodic (days/weeks), which represents alike an unlike scenario. The last aspect is considered to be the most likely cause for the observed sinusoidal deviation from linearity. The deviation was only observed in relatively soft sediments (Area 14 vs. Area 13). It is plausible that the impact upon harder sediments in Area 13 was insufficient to initiate vertical mass movement associated with compaction.

Irrespective of this point, all three data points in Area 14 show considerably lower temperature gradients (and therefore lower heat flow) as the four data points in Area 13. (Compaction by instrument impact tends to artificially slightly increase the temperature gradient and heat flow, as the sediment temperatures thereafter raise over a shorter distance.)

Approximate heat flow values were calculated with an assumed uniform thermal conductivity value of $0.9 \text{ Wm}^{-1}\text{K}^{-1}$. In-situ thermal conductivity values were measured at all stations with the conventional heating experiment. The results will be evaluated in a second step after return to BGR. The heating experiment was regularly performed for a time period of 8 minutes.

Table 5.4.1. shows a summary of the measured heat flow values (based on an approximation of λ) gained during the cruise.

Station	T-gradient (K/m)	Thermal conductivity (W/mK)	Water depth (m)	Heat flow (mW/m ²)	Area	Lat. N	Long. E
HF17	0.131	0.9	5285	118.7	13	54°	163° 20'
HF25	0.112	0.9	4994	101	13	54° 5'	163° 37'
HF27	0.187	0.9	5471	168.4	13	54° 9.4'	163° 36.6'
HF29	0.268	0.9	3891	241.5	13	53° 52'	163° 48'
HF34	0.108	0.9	2996	97.5	14	53° 15.45'	164° 17.5'
HF36	0.058	0.9	3223	52.4	14	53° 7.16'	164° 34.4'
HF38	0.066	0.9	3205	60.1	14	53° 11.3'	165° 5.48'

Table 5.4.1.: Summary of measured heat flow values.

Fig. 5.4.3. shows the measured heat flow values in Area 13 in context with the geologic situation. By chance three of the four points of measurement were placed at what appears to be in positions near major faults according to detailed seafloor mapping by the SIMRAD E 120 system of RV SONNE. Notably, the three highest heat flow values were measured near fault positions, while the lowest value was obtained in a ridge position away from faults.

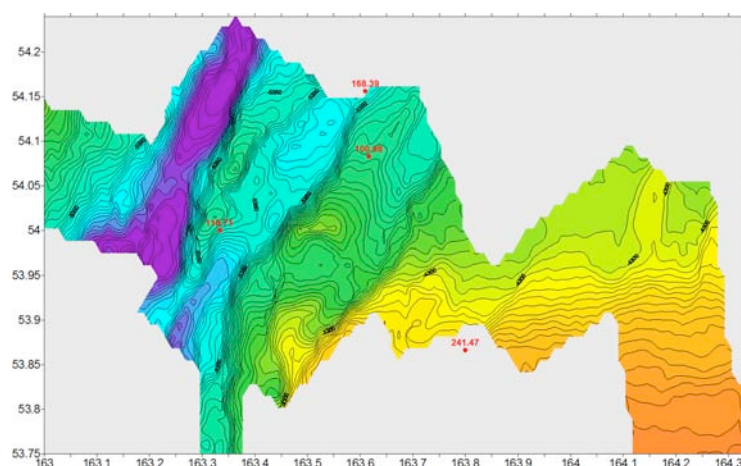


Fig. 5.4.3.: Measured heat flow values in Area 13.

This result can be considered to be an indication that the observed high heat flow is caused by fault-controlled upward migrating fluid flow.

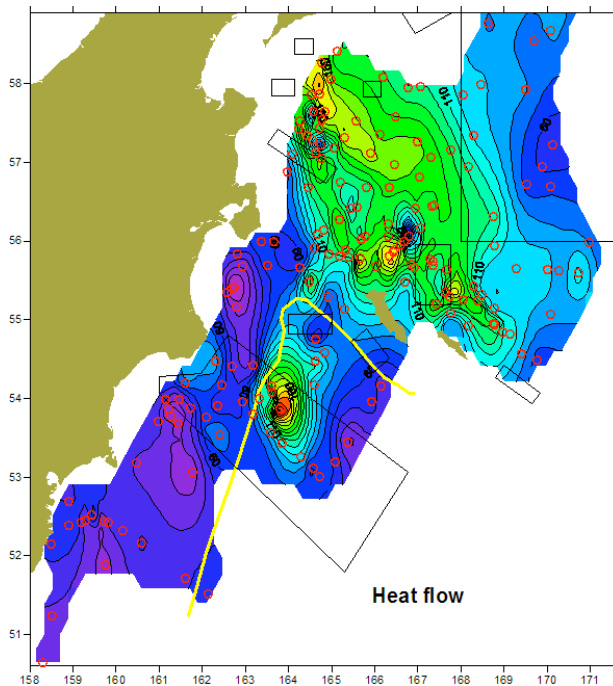


Fig. 5.4.4.: *Heat flow distribution offshore Kamchatka.*

This aspect will be further studied with the help of a numerical model on conductive/convective heat transport in the area of investigation.

Fig. 5.4.4. shows the heat flow distribution in the whole area with the inclusion of our measurements. Our 4 data points of Area 13 define the major positive heat flow anomaly around 54°N, 163° 30' E, while our three measurements in Area 14 are located on the eastern flank of this anomaly: They are positioned within the area of steady decline of heat flow towards the centre of the Meiji Seamount. It appears that high heat flow is concentrated along the north-western flank of the seamount.

The shape of the anomaly is not necessarily indicative of a shallow emplaced magma body as cause of the anomaly. A preferable interpretation of the observed heat flow distribution is given by the assumption of fluid circulation in highly fractured rock within the descending limb of the Meiji Seamount, associated with convective upward transport of heat from depth.

5.5. DREDGE OPERATIONS (*M. Portnyagin, G. Yogodzinski, R. Werner, B. Baranov*)

5.5.1. Rock Sampling - Methods

Rock sampling on SO201 Leg 2 was carried out using chain bag dredges. Chain bag dredges are similar to large steel buckets with a chain bag attached to their bottom and steel teeth at their openings, which are dragged along the ocean floor by the ship or the ship's winch.

Selection of Dredge Sites

Sites for detailed SIMRAD EM120 mapping and dredging were chosen on the basis of a number of existing datasets. These include:

1. Predicted bathymetry, derived from gravity data and ship depth soundings (Smith and Sandwell 1997), as well as GEBCO data sets.
2. Bathymetry data and maps, provided by B. Baranov and N.I. Seliverstov.
3. Single-channel seismic profiles provided by B. Baranov, N.I. Seliverstov, and N. Tsukanov.
4. Published monographs and papers (see, for example, chapter 3.3.).

Shipboard Procedure

Once onboard, a selection of the rocks recovered by the dredge were cleaned in fresh water and cut using a rock saw. The rocks were then examined with a hand lens and microscope, and grouped according to all aspects of their lithology, including the primary mineralogy and degree of alteration / weathering, and/or the presence of Mn encrustations. The immediate aim of these observations is to determine whether material suitable for geochemistry and radiometric age dating had been recovered. Suitable samples have an unweathered and unaltered groundmass, empty vesicles, glassy rims (ideally), and fresh phenocryst minerals. If suitable samples are present, the ship moves to the next station. If they are not, then the importance of obtaining samples from the station is weighed against considerations of the available time. In general, a second, nearby dredge is necessary in only very few cases.

Fresh blocks of representative samples were then cut for thin section and microprobe preparation, geochemistry. Additional trimming of the sample is sometimes necessary to remove Mn crusts and alteration products and/or to extract fresh glass in cases when it is present. Each of these sub-samples, together with any remaining bulk sample, was described, labeled, and finally sealed in plastic bags for transportation to IFM-GEOMAR or cooperating institutions.

Shore Based Analyses

Magmatic rocks sampled by the R/V SONNE from the ocean floor will be analyzed using a variety of different geochemical methods. The ages of whole rocks and minerals will be determined by $^{40}\text{Ar}/^{39}\text{Ar}$ laser dating. Major element geochemistry by X-ray fluorescence (XRF) and electron microprobe (EMP) will constrain magma chamber processes within the crust, and also yield information on the average depth of melting, temperature and source composition to a first approximation. Phenocryst assemblages and compositions are used to quantify magma evolution, e.g. differentiation, accumulation and wall rock assimilation. Petrologic studies of the volcanic rocks also help to constrain the conditions under which the melts formed (e.g., melting depths and temperatures). Further analytical efforts concentrate on methods that constrain deep seated mantle processes. For example, trace element data by inductively coupled plasma mass spectrometry (ICP-MS) may help to define the degree of mantle melting and to characterize the chemical composition of the source. Long-lived radiogenic isotopic ratios by Thermal Ionization Mass Spectrometry (TIMS) and Multi-Collector ICP-MS such as $^{87}\text{Sr}/^{86}\text{Sr}$, $^{143}\text{Nd}/^{144}\text{Nd}$, $^{206}\text{Pb}/^{204}\text{Pb}$, $^{207}\text{Pb}/^{204}\text{Pb}$, $^{208}\text{Pb}/^{204}\text{Pb}$, and $^{187}\text{Hf}/^{188}\text{Hf}$ are independent of the melting process and reflect the long term evolution of a

source region and thus serve as tracers to identify mantle and recycled crust sources. Additionally, morphological studies and volcanological analyses of the dredged rocks will be used to constrain eruption processes, eruption environment and evolution of the volcanoes. Through integration of the various geochemical parameters, the morphological and volcanological data, and the age data the origin and evolution of the sampled structures can be reconstructed.

Non-magmatic rocks and Mn-Fe oxides yielded by dredging are transferred to co-operating specialists for further shore based analyses.

5.5.2. Volcanology

Results of dredging, which was primarily focused on sampling basement rocks from four areas described in Section 3.3, are presented in Figure 5.5.1 and Appendix III and IV. In total,

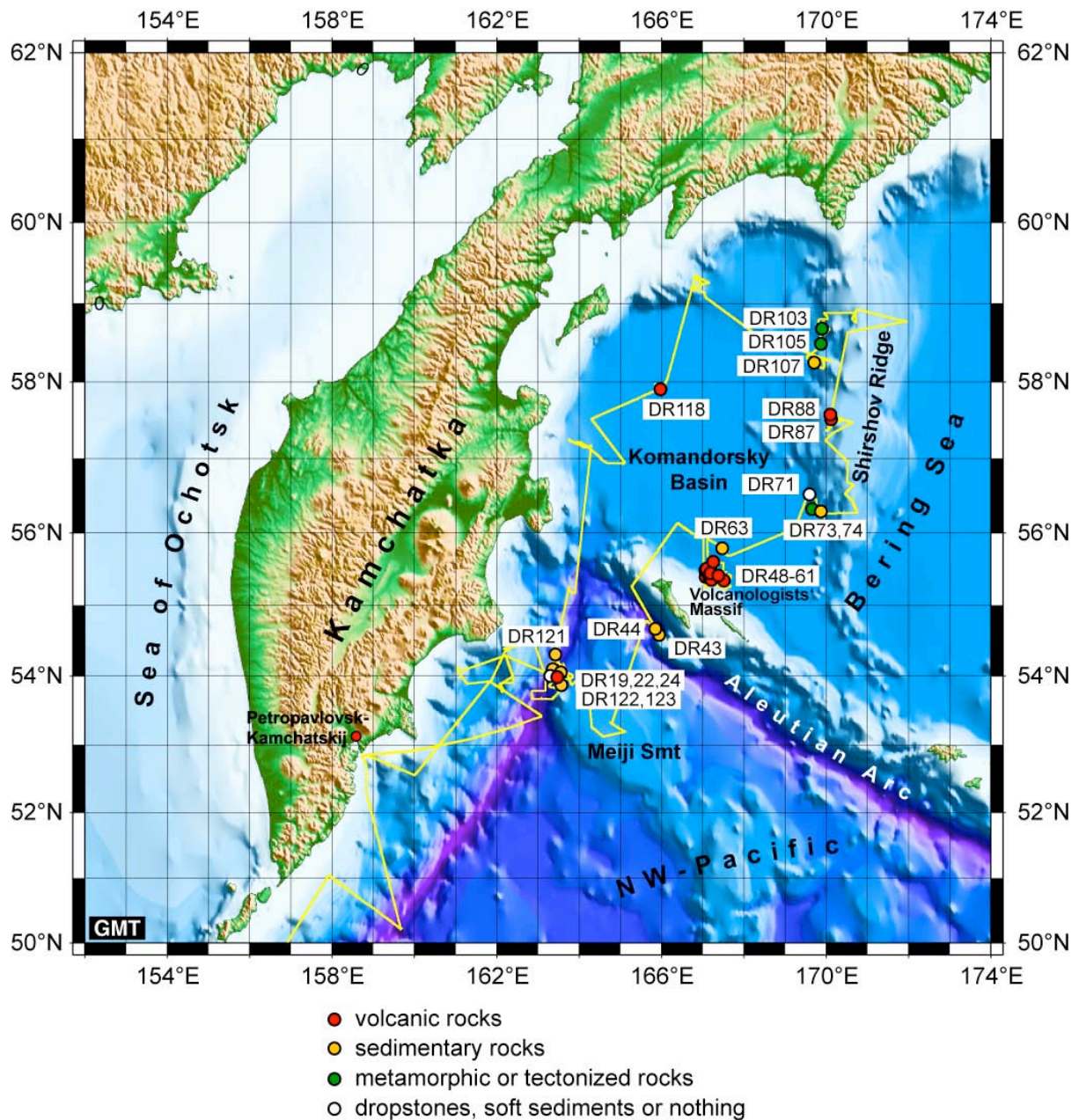


Fig. 5.5.1.: Dredge stations during SO201 Leg 2. Color coding of dredge stations refers to predominant type of rocks delivered on board.

dredging was carried out at 29 stations. Magmatic rocks of in situ origin were found in 18 hauls, partially to well solidified sediments in 10 hauls, Fe-Mn hydroxide crusts in 4 hauls, and volcanoclastic rocks in 6 hauls. Ice-rafted rocks (drop-stones) were common in all areas except the area of young volcanism at Volcanologists' massif. The drop-stones were recognized due to their highly variable lithology and sometimes apparent similarity to rocks found in neighboring areas in Kamchatka and Komandorsky Islands. In most cases the amount of rock in a dredge varied from a few rocks to $\frac{1}{4}$ full; two hauls were brought onboard $\frac{1}{2}$ to fully loaded. Overall, this statistically rather poor recovery of basement rocks reflects difficult conditions for dredging in most of the studied areas and only a few outcrops appropriate for dredging. In some cases bad weather conditions and strong currents also precluded choosing optimal location of dredge tracks.

5.5.2.1 Meiji Seamount

Dredging at Meiji Seamount was carried out at 6 stations located at trench-facing scarps of the trench-parallel faults cutting the western slope of the Meiji Seamount (DR19, 22, 24, 122, 123) and at a small NNE-striking ridge on the western (Kamchatka) side of the trench (DR121). This site was suggested to be an accreted fragment of the Meiji Seamount judging from on-board geomorphological analysis (Fig. 5.5.2). The dredging was primarily focused on sampling of volcanic rocks comprising basement of the Meiji seamount and testing the hypothesis of its ongoing accretion to the forearc of Kamchatka, associated with eventual small-step trench retreat.

Volcanic rocks which undoubtedly belong to the Meiji Seamount were obtained at station DR22 located on the steep scarp bordering the second (from the trench) step of the faulted western slope of the seamount. The rocks were represented by numerous fragments of moderately altered rare plagioclase and olivine-phyric basaltic pillow-lavas (Fig. 5.5.3 A) and more crystallized plagioclase-phyric dolerites (Fig. 5.5.3 B), likely originating from inner parts of sheet-lava flows. Other types of rocks from the haul were breccias with angular fragments of basalts cemented by limestone and Fe-Mn hydroxides (Fig. 5.5.3 C) and rounded fragments of terrigenous limestone with layers and co-sedimentary clasts of red clay (Fig. 5.5.3 D). Noticeable is the similarity of the sedimentary rocks to interbedded cherts and limestones associating with the Hawaiian-type basalts in the Kamchatsky Mys ophiolites (Chapter 3.3, Fig. 3.3.2), which have been proposed to host accreted fragments of older Hawaiian seamounts than preserved on the ocean floor (e.g. Portnyagin et al. 2008).

The appearance and petrographic features of volcanic rock obtained at DR22 station suggest that these rocks represent shield-stage submarine volcanism at the Meiji Seamount. Presence of carbonate sediments and fillings in pillow-lavas are suggestive of relatively shallow water conditions at the time of eruptions and substantial subsidence (well below CCD level) of this part of the seamount since Cretaceous time. The rocks are the first samples recovered from the Meiji basement since ODP Leg 19 drilling at Site 192. These rocks are undoubtedly less altered compared to the Site 192 basalts and provide invaluable material for future studies which will eventually provide missing information on the absolute age and geochemistry of the oldest seamount in the Emperor Seamount Chain.

Other dredges at the Meiji Seamount and Kamchatka side of the trench yielded a few fragments of volcanic rocks of questionable provenance (DR19, 121), dense carbonate rocks, possibly, strongly hydrothermally altered ultramafic protoliths (DR19), consolidated siliceous sediments, some with well preserved microfossils (DR123) and also common partly consolidated muddy sediments (DR24,122). These sedimentary rocks together with volcanic rocks from DR22 provide direct information on the oceanic plate input into the Kamchatka subduction zone. The material obtained during the SO201-2 cruise from the Meiji area is particularly important to clarify the contribution from subducted sediments into volcanism in central and northern Kamchatka hosting the largest volcanoes in the Pacific "Ring of Fire".

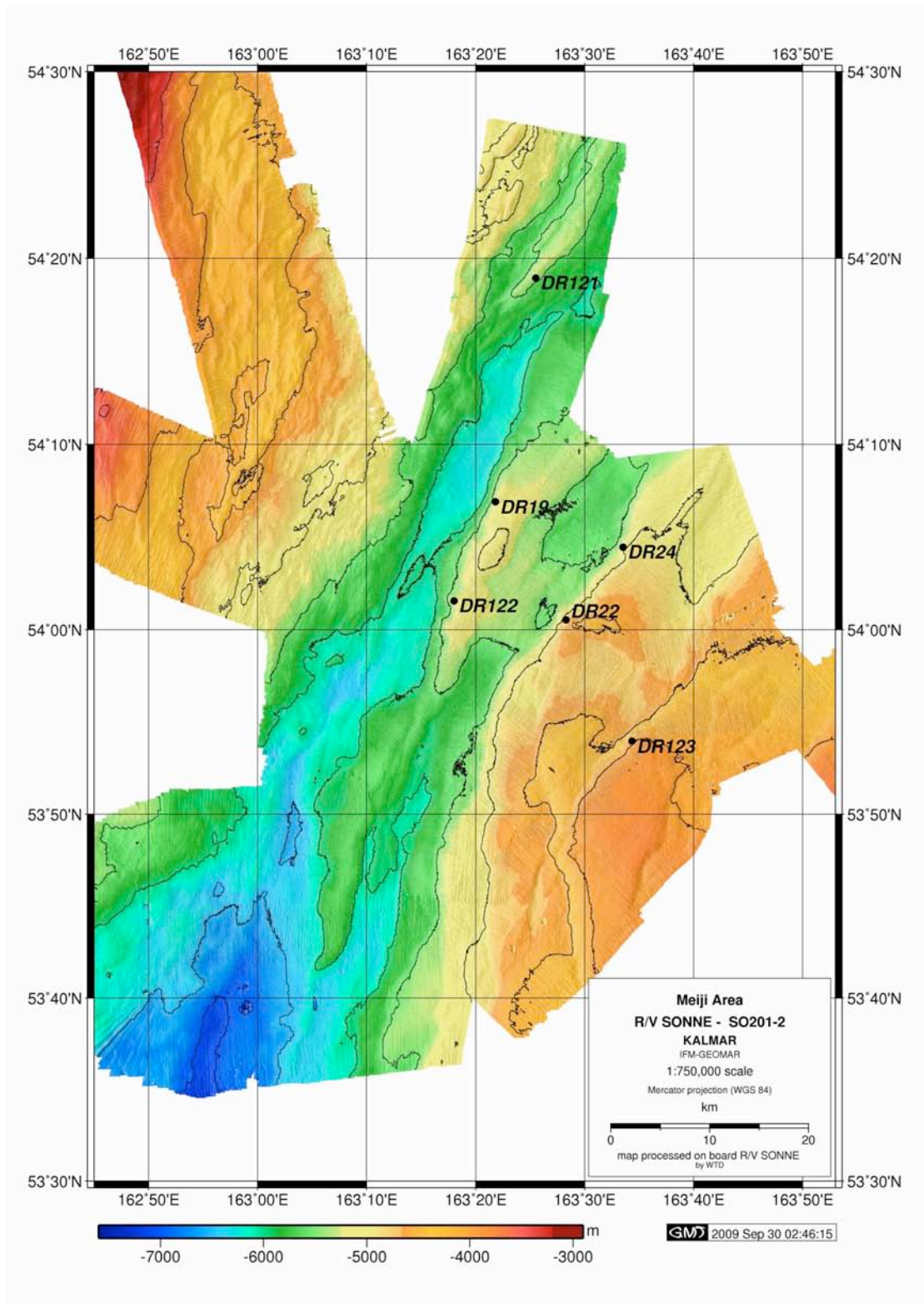


Fig. 5.5.2.: Bathymetric map of the western slope of Meiji Seamount obtained during SO201-2 and dredge stations.

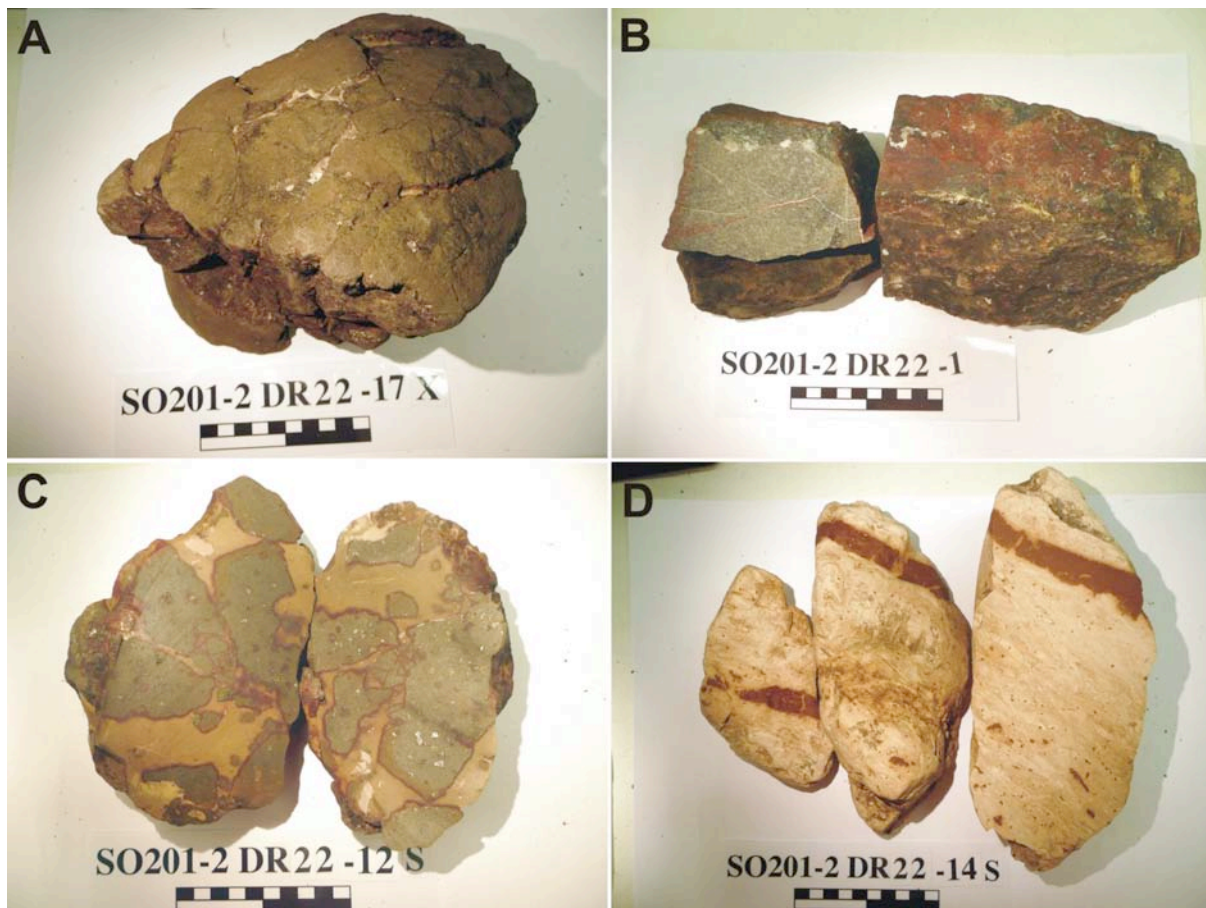


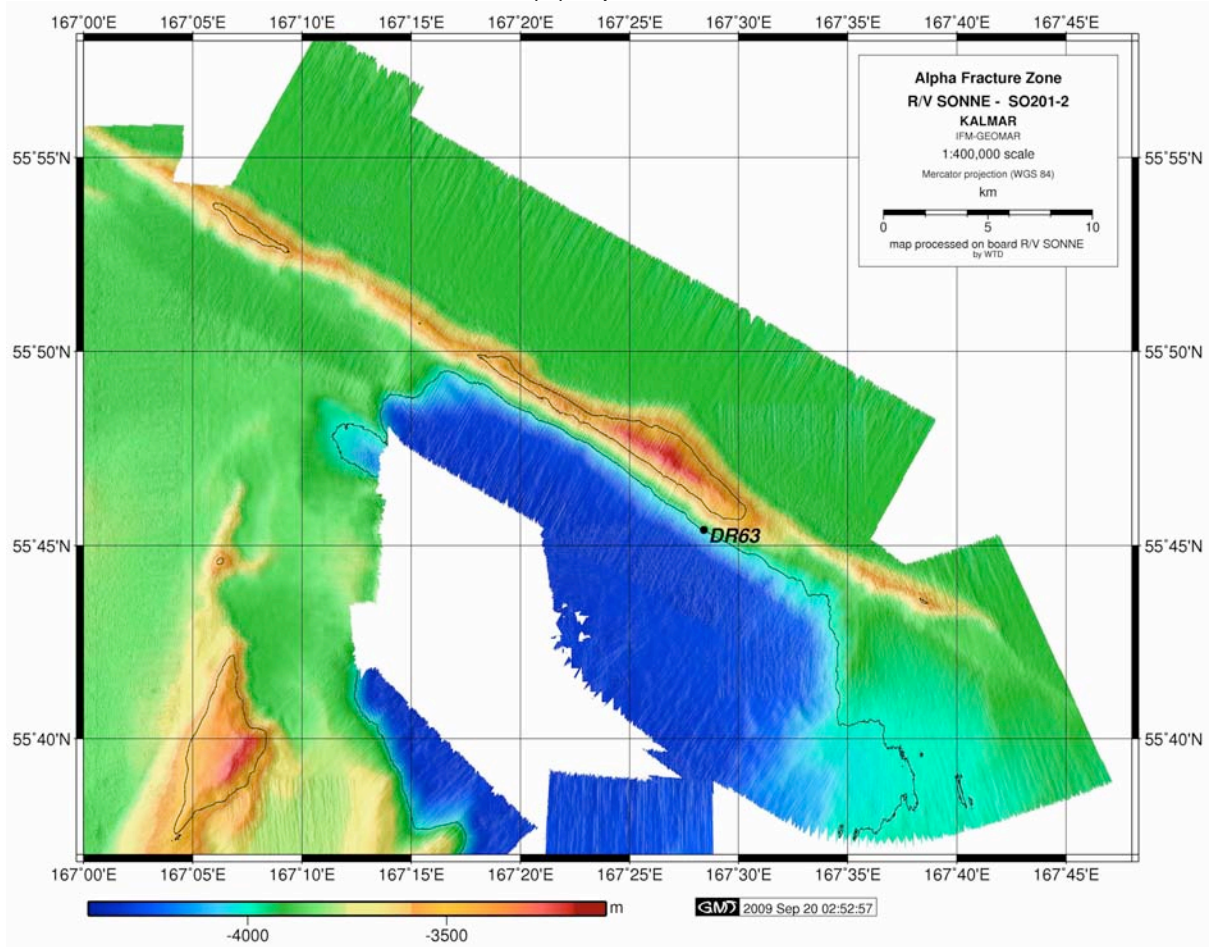
Fig. 5.5.3.: Representative volcanic and associated sedimentary rocks recovered from the Meiji Seamount. A) Fragment of pillow lava with well preserved outer margin. Moderately altered aphyric basalt, B) Dolerite from massive sheet lava flow or inner part of pillow; C) Breccia comprised by angular fragments of altered olivine-plagioclase-phyric basalt coated by thin Mn-crusts and small clasts of pink limestone cemented by pinkish-grey carbonate, D) Light pink clayish limestone with a layer and small clasts of red clay.

5.5.2.2. Komandorsky Basin and fracture zones

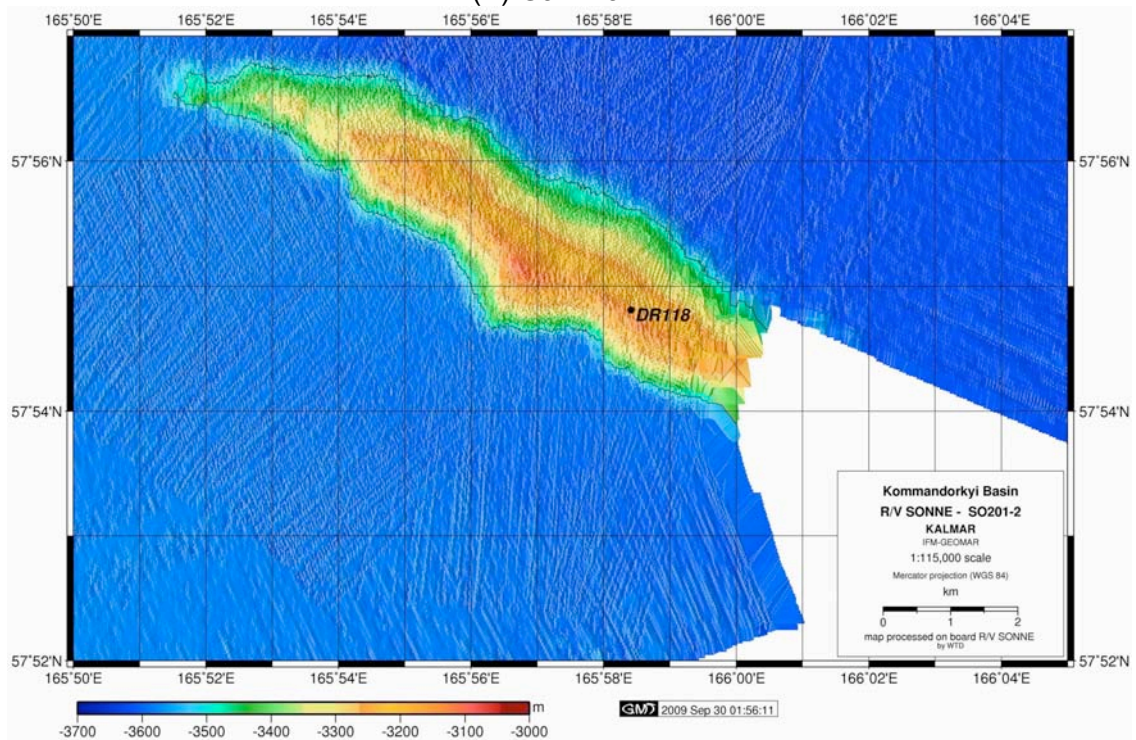
Dredging within the Komandorsky Basin and at related fracture zones was carried out at tectonic ridges associating with fracture zones, which provide the only opportunity to sample the basin basement by dredging, because other areas are largely covered by 0.5-1.0 km-thick blanket of sediment. Appropriate locations for dredging were found in 3 study areas: at the central part of the Alpha FZ ridge north of the Komandor Graben (DR 63), at the western part of the Gamma FZ ridge, in approximately the center of the Komandorsky Basin (DR 118) and at a tectonic block south of Medny Island, bordered by the Steller Basin to the north and Aleutian trench to the south (DR 43, 44) (Fig. 5.5.4). Mapping at the western end of the Alpha FZ ridge did not reveal appropriate locations for dredging.

Volcanic rocks which undoubtedly represent Komandorsky crust were recovered at station DR 118 on the SW slope of tectonic ridge of the Gamma FZ (Fig. 5.5.4 B). The rocks are relatively fresh fragments of pillow lavas ranging from nearly aphyric to olivine-plagioclase-phyric basalts with MORB-like appearance (Fig. 5.5.5). Olivine phenocrysts were likely altered. Plagioclase crystals (up to 1 cm large) appear to be fresh. The rocks obtained during SO201-2 are the first samples of the Komandorsky basement collected since ODP Leg 19 which penetrated a few meters of the basement at Site 191 in the central part of the basin (Stewart et al., 1973). These rocks provide valuable material to obtain new information about the age of the Komandorsky Basin crust and its composition.

(A) Alpha FZ



(B) Gamma FZ



(C) Tectonic block south of the Steller Basin

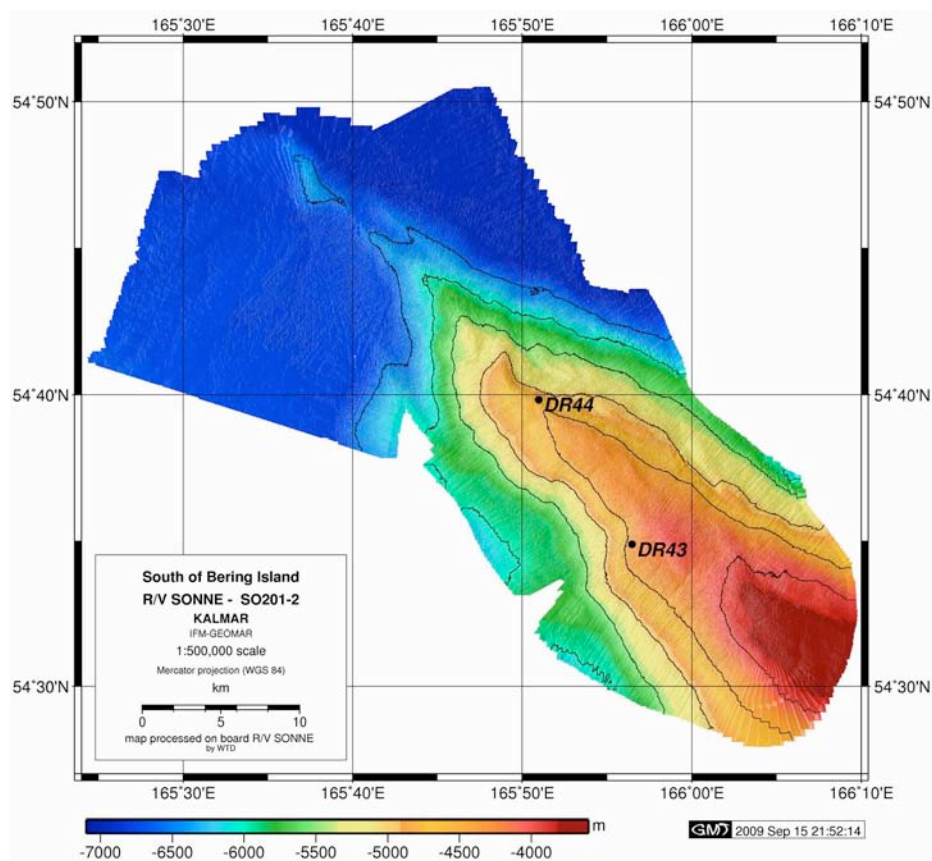


Fig. 5.5.4.: Bathymetric maps of uplifted parts of fracture zones and associated structures in the Komandorsky Basin and at the Aleutian trench with locations of dredge stations. A) central part of the Alpha FZ north of the Komandor Graben; B) western part of the Gamma FZ in the central Komandorsky Basin, C) tectonic block south of Medny Island between Aleutian trench (to the south) and Steller Basin (to the north).

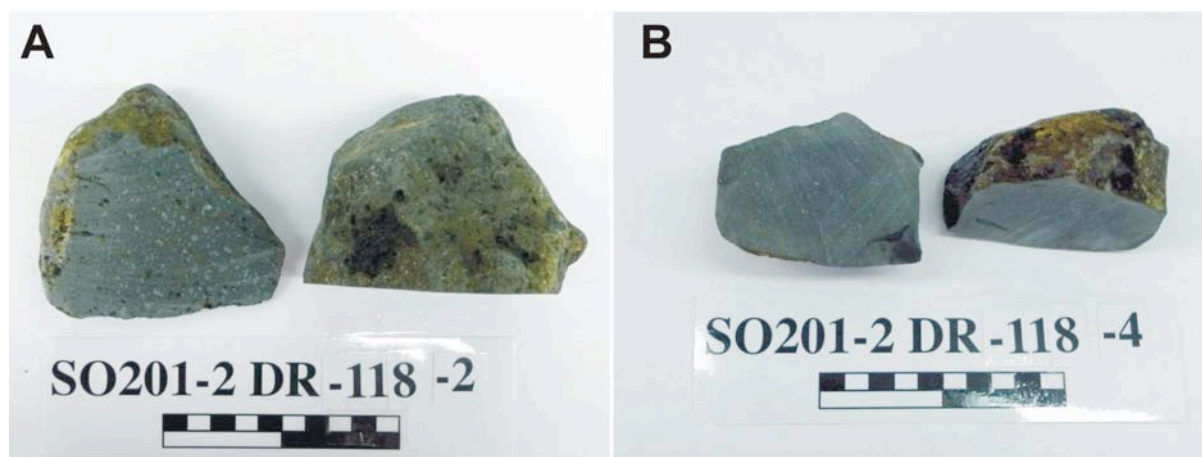


Fig. 5.5.5.: Representative volcanic rocks recovered from the Gamma Fracture Zone in the Komandorsky Basin. A) Fragment of strongly plagioclase-olivine-phyric vesicular pillow lava with well preserved rim-to-center pillow zoning; B) Rare plagioclase-phyric non-vesicular basalt.

The dredging at Alpha FZ (DR 63) yielded silty sandstones and fragments of Mn-crusts. Dredging at two stations on the tectonic block at the Steller Basin (DR 43, 44) delivered clay-silt and volcanogenic sandstones, which appear to be similar to those cropping out on

Komandorsky Islands, and thus suggesting that this tectonic fragment is most likely a displaced splinter of the Komandorsky block or other Aleutian crust and not an accreted fragment of oceanic crust.

5.5.2.3. Volcanologists' Massif and Piip Volcano

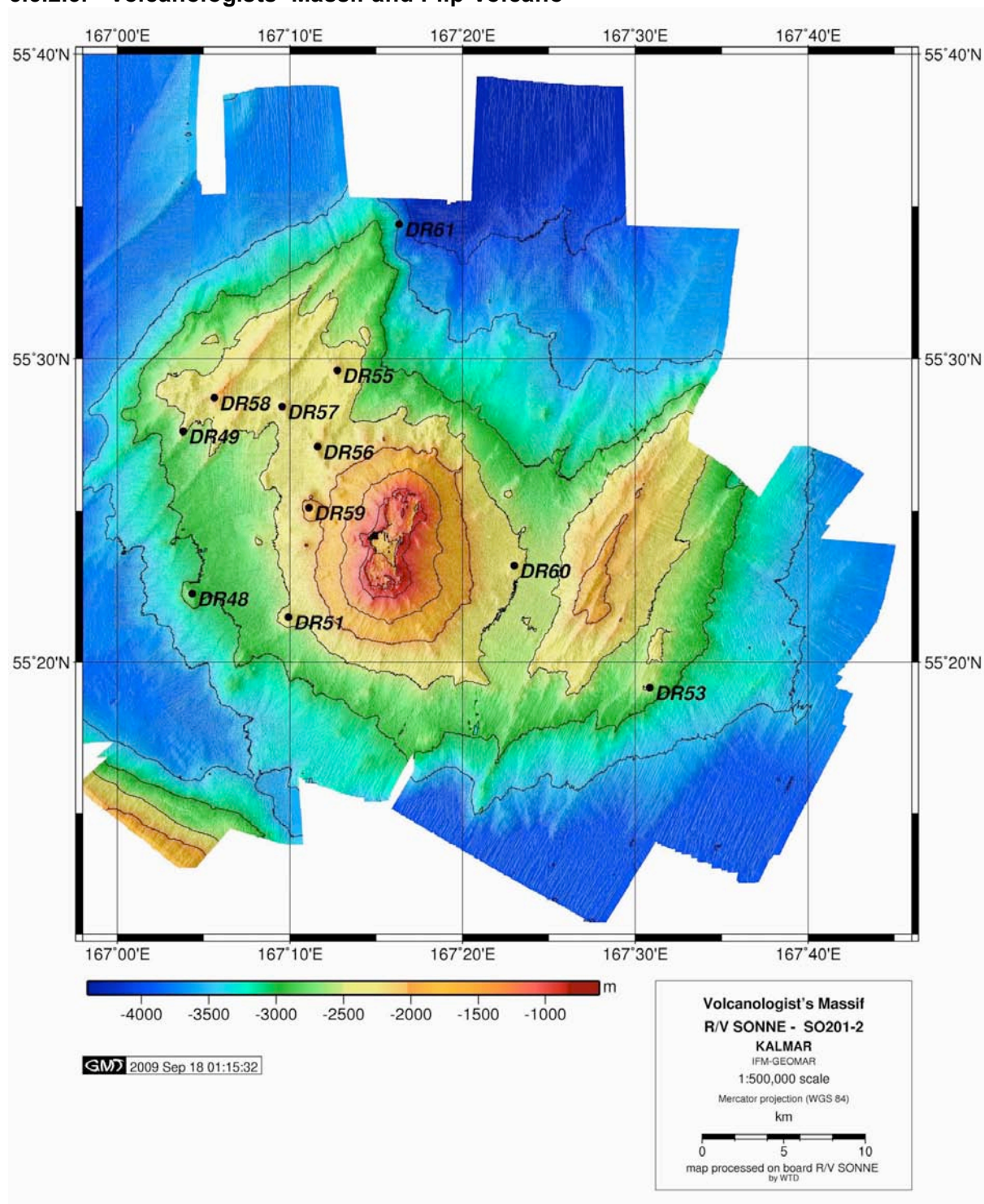


Fig. 5.5.6.: Bathymetric map of the Volcanologists' Massif and Piip volcano and SO201-2 dredge locations.

Dredging at the Volcanologists' Massif followed three previous sampling campaigns at this volcanic structure in 1986-1989 made with Russian research vessels "Volcanolog" and

“Akademik Keldish” (summarized in Yogodzinski et al. 1994). The SO201-2 expedition focused primarily on detailed bathymetric mapping of the massif and sampling of different volcanic units of the young Piip Volcano edifice. Dredging was performed at 11 stations (Fig. 5.5.6). Ten of these stations are considered to have been successful and delivered on board a representative amount of in-situ, mostly mafic and fresh volcanic rocks with clear features of submarine emplacement upon eruption.

Provisionally, the oldest rocks from the basement of the massif were obtained at stations DR 61 and DR 53. These rocks are represented by moderately to strongly altered aphyric basalts (DR 61; Fig. 5.5.7 B) and olivine-plagioclase-phyric basalts with preserved glassy pillow margins (DR 53; Fig. 5.5.7 A), both types associated with Mn-crusts. These types of basalts are clearly comparable to the older Komandor Series of Piip Volcano as described by Yogodzinski et al. (1994).

Dredging at other stations within the Volcanologists’ Massif yielded predominantly very fresh fragments of vesicular lavas with glassy rims ranging petrographically from almost aphyric (DR 57, 59, 60) to olivine-plagioclase- (DR 51, 59) and plagioclase-pyroxene-phyric (DR 58) basalts and andesites (Fig. 5.5.7 C-E). Abundant rare-plagioclase-magnetite phyric dacitic pumice fragments with fibrous texture were recovered at the dredge station DR 60 on the slope of Piip volcano (Fig. 5.5.7 F). These rocks as well as more mafic olivine-bearing rock varieties from other locations likely belong to the Piip Series of the massif following definition from Yogodzinski et al. (1994).

Overall, the studies at the Volcanologist’s Massif coincide with previously published results with regard to the presence of petrographically different rock varieties within the massif and possible evolution of its volcanism from MORB-like at early stages to widely differentiated island-arc volcanism on the later stage. The new collection of rocks contains abundant primitive samples with magnesian olivine in phenocrysts and glassy lava margins which were rather scarce in previous collections. These rocks provide an excellent material for various geochemical studies including absolute age dating, study of various trace elements isotopes and volatiles. These studies will shed further light on the origin and volcanic evolution of the Volcanologists’ Massif hosting important end-member type rocks in global systematics of island-arc volcanism.

5.5.2.4. Shirshov Ridge

Dredging of the Shirshov Ridge basement was carried out in three areas which are hereafter referred to as the Northern, Central and Southern Shirshov regions (Fig 5.5.1, 5.5.8 A-C). Preliminary dredge locations were chosen based on unpublished seismic profiling with R/V Volcanolog (provided by N. Seliverstov and B. Baranov).

Dredging in the Northern region (Fig 5.5.8 A) was focused on the area where metamorphic rocks (amphibolites) were previously recovered from the eastern slope of one of the NW-elongated rounded crustal blocks on the west-facing flank of the Shirshov Ridge (Silantiev et al., 1985). Station DR 103 was located on the western slope of the block where amphibolites were previously sampled. Station DR 105 was located on a separate block of smaller size further south, and DR 107 was on a morphologically different steep slope south of the former stations. Dredging at DR103 and DR105 yielded homogeneous compositions of predominantly metamorphic rocks: sheared and metamorphosed ultramafic rocks (DR 103, Fig. 5.5.9 E) and greenschist after siliceous sediments (DR 105, Fig. 5.5.9 F). Dredging at station DR 107 delivered partly solidified clay.

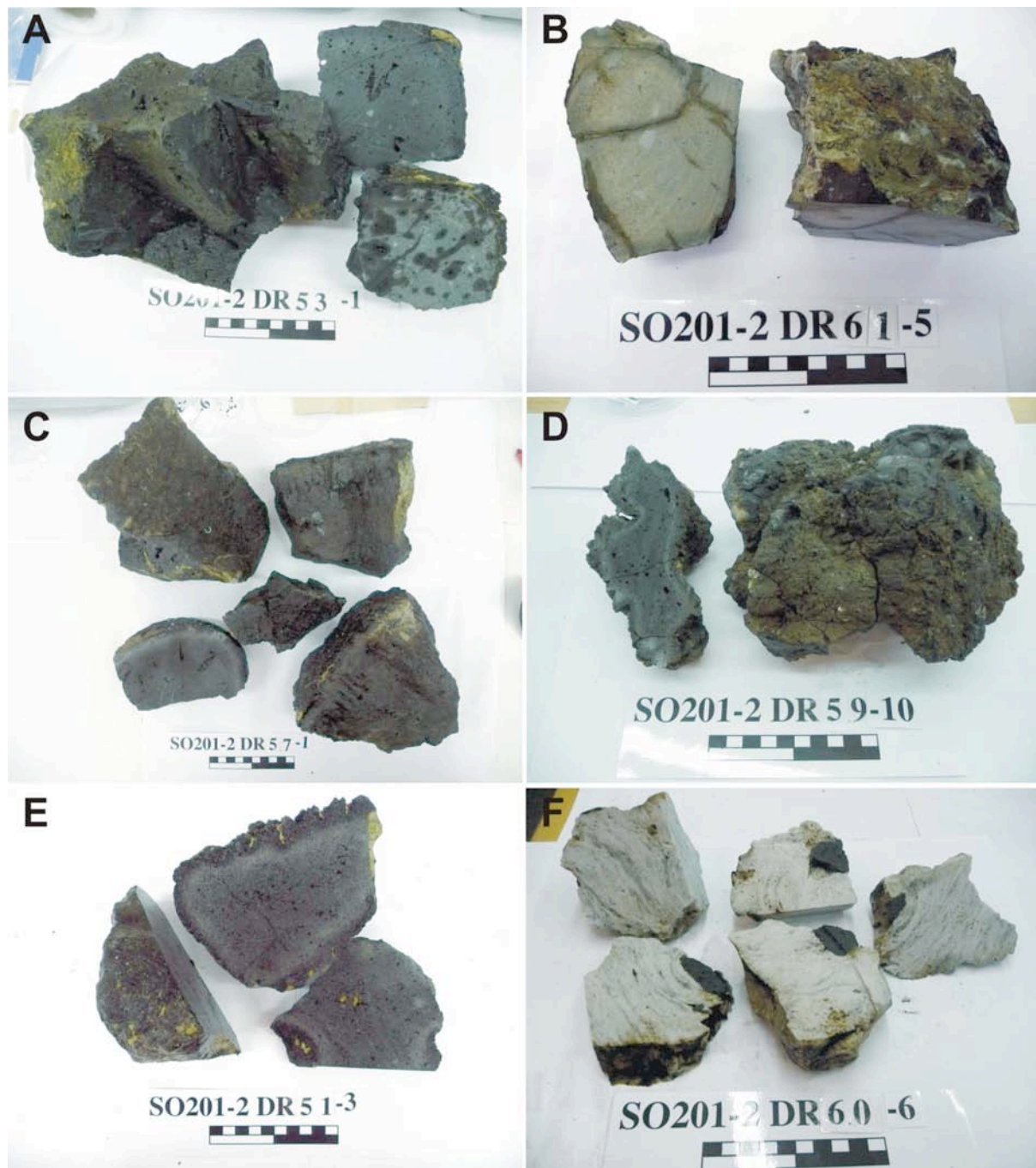
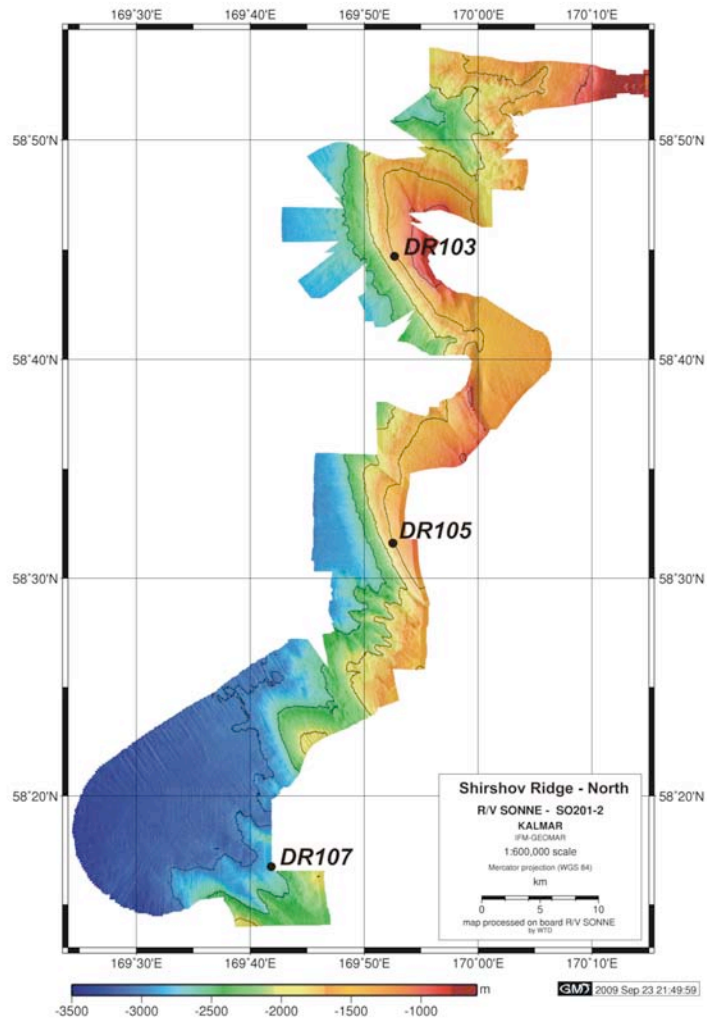
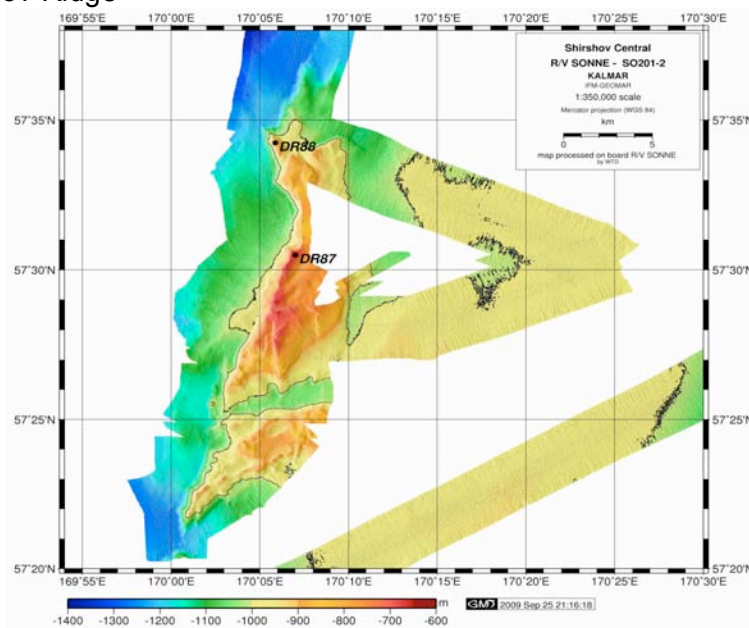


Fig. 5.5.7.: Representative types of volcanic rocks from the Volcanologist's Massif and Piip Volcano obtained during the SO201-2 expedition. A) Olivine-plagioclase-phyric basaltic pillow-lava from the southeastern flank of the massif (DR 53); B) Altered aphyric basalt from the basement at the northwestern tip of the massif (DR 61); C) Fragments of rare-olivine phyric andesitic(?) pillow lava from northwestern part of the massif (DR 57); D) Volcanic bomb of rare olivine-plagioclase-phyric basalt from satellite cone at the western foot of Piip volcano; E) Fragments of volcanic bomb (or lava flow "finger") of rare olivine-plagioclase phyric basalt from satellite cone on the southeastern foot of Piip volcano (DR 51); F) Fibrous dacitic pumice dredged from a high at the eastern slope of Piip volcano (DR 60).

A) Northern Shirshov Ridge



B) Central Shirshov Ridge



C) Southern Shirshov Ridge

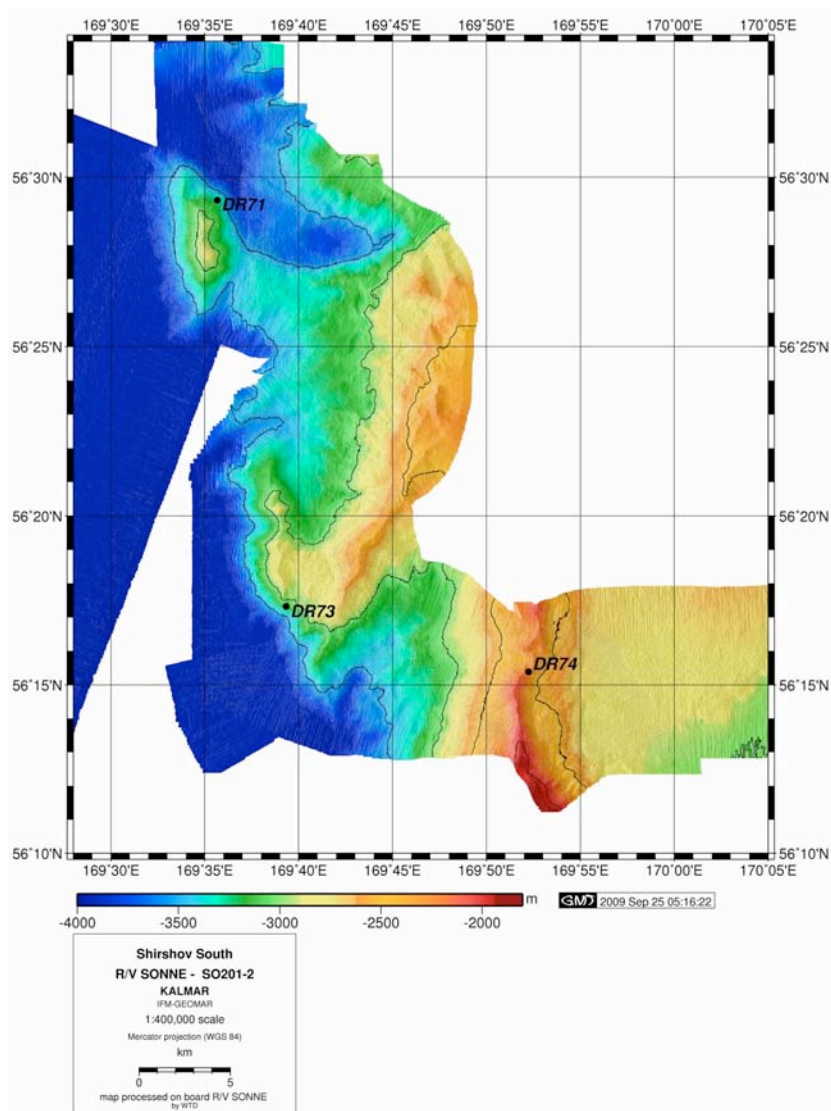


Fig. 5.5.8.: Bathymetric maps of northern (A), central (B) and southern (C) areas of the Shirshov Ridge and locations of SO201-2 dredge stations.

Dredging in the Central region (Fig 5.5.8 B) resulted in two successful attempts on the western slope of a small convex-to-the-east ridge, which appears to be a tectonic block on the west-facing side of the Shirshov Ridge. Dredging at both stations DR 87 and DR 88 recovered in-situ volcanic and sedimentary rocks. Rocks from the southern and slightly shallower station DR 87 were hornblende-bearing andesites (Fig. 5.5.9 A) and plagioclase-pyroxene phyric basaltic andesites and breccias (Fig. 5.5.9 B) with fragments of both types of the volcanic rocks (predominantly plagioclase-pyroxene-phyric basaltic andesites) placed in altered tuffaceous matrix. Dredging at the northern tip of the small ridge (DR 88) produced rocks of two types - massive aphyric basalts with rare phenocrysts of pyroxene and plagioclase (Fig. 5.5.9 C) and black cherts.

Dredging in the Southern region (DR 71, 73, 74; Fig 5.5.8 C) was carried out on the western slope of the Shirshov Ridge and on NS-striking tectonic blocks separated from the main ridge by a depression. The rocks recovered were strongly tectonized tuffs and breccias (DR 73) and a large fragment of sandstone (DR 74; Fig. 5.5.9 D). Besides the

mentioned in-situ rocks, several individual fragments of lavas and intrusive rocks of different types were recovered at station DR 71. The provenance of these rocks cannot be reconciled with confidence.

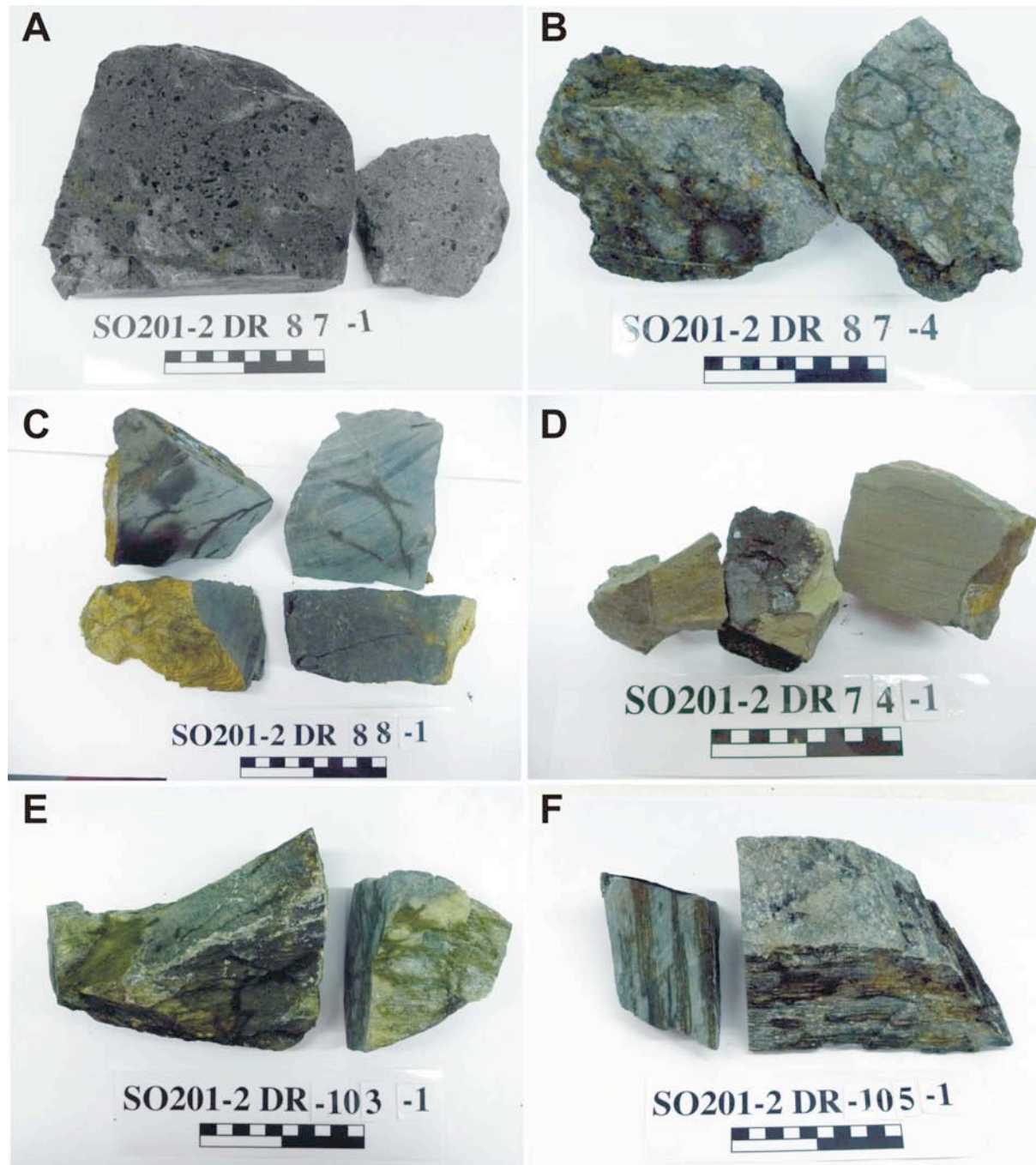


Fig. 5.5.9.: Representative basement rocks recovered from the Central (A-C), Southern (D) and Northern (E, F) Shirshov Ridge regions. A) Hornblende-pyroxene-phyric andesite (DR 87); B) Volcanic breccia consisting of clasts of plagioclase-pyroxene- and hornblende-phyric andesites(?) in tuffaceous matrix (DR 87); C) Massive aphyric basalt with fine-grained dolerite texture (DR 88); Volcanogenic sandstone (coarse-grained tuff) (DR 74); E) Sheared and metamorphosed ultramafic rock (DR 103); F) Greenschist after siliceous sediment (DR 105).

The results obtained on Shirshov Ridge during the SO201-2 expedition confirm previous

interpretations of this as a tectonic ridge, possibly split and torn away from the Kamchatka margin as a result of spreading in the Komandorsky Basin (Baranov et al., 1991). The rocks recovered from 3 areas along the Shirshov Ridge during the SO201-2 cruise are each of very different origin and composition and could not have originated in a single setting. These results suggest that the Shirshov Ridge is probably a complexly-structured terrane comprising some parts of an ophiolitic assemblage and wherein rocks of different age and provenance are tectonically superimposed. Interpretation of the Shirshov Ridge as a possible remnant of older Emperor Seamount Chain (originating prior to the crustal assemblages present in the NW Pacific today) as proposed recently by Steinberger and Gaina (2007) does not find supporting evidence in our new data obtained during SO201-2 cruise. Large parts of the Shirshov Ridge are likely of island-arc origin. Some blocks of oceanic crust (e.g. DR 88) could also have been incorporated into the ophiolite terrains as well as exhumed metamorphic blocks.

5.6. SEDIMENT SAMPLING (D. Nürnberg, R. Tiedemann)

5.6.1. Multicorer Deployment

In total, 14 multicorers were deployed during SO201-2. After several improvements of the device, the recovery of sediments became successful with mostly 12 tubes filled with sediment. The multicorer was lowered with an average speed of 0.7 m/s to about ~30-40 m above seafloor, where it was stopped for ~2-3 minutes. It was then lowered with a speed of 0.5 m/s until bottom contact. Contact with the seafloor was monitored through the cable tension. The multicorer was left on the seafloor for about 1 minute, then pulled out with a speed of 0.3 m/s and finally heaved with a speed of 0.7 m/s.

For ocean bottom observations, we mounted the deep-sea camera system of Fa. Marinetechnik Kawohl to the MUC. It consists of one camera and two lamps (DEEPSEA Power & Lights). The control unit is from Fa. Marinetechnik Kawohl. Power supply is by Coax cable with LWL (>600 V). Brightness of lamps can be variably chosen by changing the voltage from 300-600 V.



Height:	approx. 2250 mm
Diameter:	approx. 1900 mm
Weight of head:	approx. 180 Kg
Weight of framework:	approx. 465 Kg
Number of tubes:	12
Diameter of tubes:	100 mm

Tab. 5.6.1.: *Technical specifications of Kiel multicorer*

Fig. 5.6.1.: *Deployment and retrieval of multicorer mounted with the deep-sea color TV camera system of Fa. Marinetechnik Kawohl.*

Sampling

Sediment recovery in each of the 12 tubes was recorded, seawater was siphoned off (for bottom water analyses) and the sediment was briefly described. Core tops (1 cm thick) were either preserved in Rose Bengal and alcohol, or put into plastic bags and/or petridishes. All tubes were completely cut into 1 cm thick slices and put into plastic bags (Whirlpack) or petridishes, which were sealed with electric tape. Sediment samples were distributed to various working groups at the Alfred-Wegener-Institute (AWI) at Bremerhaven, at IFM-GEOMAR, at Shirshov Institute of Oceanology, and at the Pacific Oceanographic Institute (POI).

5.6.2. Gravity corer and piston corer

Deployment

In total, 15 piston cores and 1 gravity core were deployed during SO201-2 from water depths of < 3900 m to 630 m. Core recovery ranged from 2.70 m to 18.32 m. At selected locations, we recovered two piston cores (double coring) to guarantee sufficient amounts of sediment for future analyses. Appendix V lists the relevant data for the sediment records recovered.

The piston corer with split piston, developed by Fa. Marinetechnik Kawohl (marinetechnikawohl@t-online.de), can be fitted with a core barrel up to 30 m in length (in 5 m increments). On RV Sonne, the piston corer was deployed with a 18 mm steel cable attached to the ship's deep-sea winch (max. speed: 2 m/s for up to 70 kN or max. speed: 1 m/s for up to 140 kN). The piston corer was lowered with an average speed of 1.0 m/s to ~50 m above seafloor, where it was stopped for ~5 minutes. It was then lowered with a speed of 0.3 m/s until the pilot trigger core hit the seafloor. Contact with the seafloor was monitored through the cable tension. When the pilot core reached the seafloor, the piston corer was released, free falling by ~5 m before reaching the seafloor, and penetrating into the sediments. The device remained at seafloor for about 30 seconds after piston release in order to allow for deep penetration, then pulled out with a speed of 0.3 m/s. Once out of the sediment, it was heaved up with a speed of 1.0 m/s.



Fig. 5.6.2.: Recovery of a 15 m-Piston Corer during SO201-2

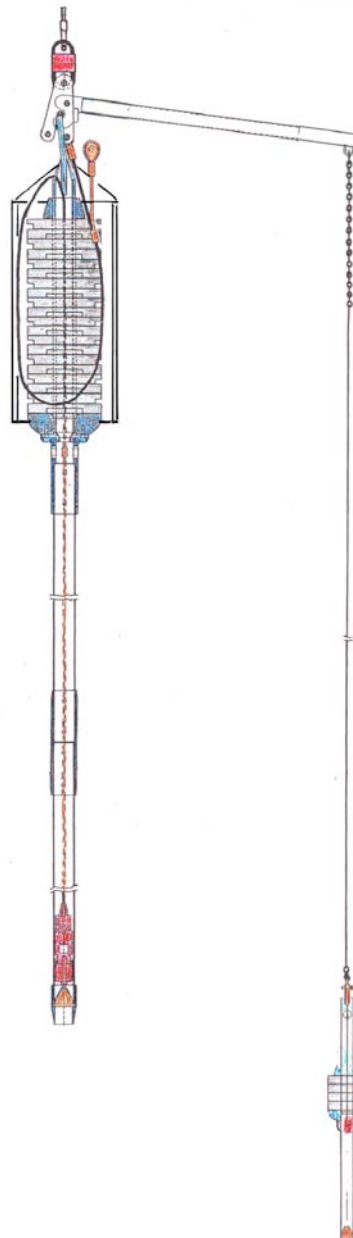


Fig. 5.6.3.: Schematic diagram of the Split-Piston Corer from Fa. Marinetechnik Kawohl, deployed during SO201-2

Core handling

The core liners of the piston cores were orientated, then labelled and cut into 1 m sections. After measuring magnetic susceptibility, each section was split into working and archive halves. The sediment surface was cleaned before lithological descriptions. Color reflectance measurements were made on the archive half. The archive halves were usually packed into plastic D-tubes and stored at $\sim 4^{\circ}\text{C}$, within a few hours of recovery. At selected cores, oriented cube-samples (1 cm^3) for paleomagnetic studies and bulk samples were taken continuously from the archive halves. The working halves were completely used up, providing sample material for the various working groups (s. chapter 5.6.2.1). The sediment from core catchers was packed whenever possible, and stored at $\sim 4^{\circ}\text{C}$. The pilot cores were

logged by magnetic susceptibility, and afterwards split into halves. The archive half was visually described and color scanned.

Labelling of core liners and D-tubes

The top and base of each section is marked with "Top" and "Base/Bottom", respectively, and the continuous depth along the core. Liners and D-Tube caps contain the following information:

- core number (e.g., SO201-2-127-KL)
- "A" for archive half, "W" for working half.
- arrow pointing to base with depths of section top and base

Visual core description and core photography

The sediment core descriptions (see Appendix VI) summarize data obtained during shipboard visual inspection of each core. All descriptions were documented with the software package APPLECORE, using a lithology custom file containing patterns following the standard ODP sediment classification scheme, a modified version of the lithologic classification of Mazzullo et al. (1988). Sediments were named on the basis of composition and texture using a principal name together with major and minor modifiers. Principal names define the degree of consolidation (induration) and granular sediment class. The location and nature of sedimentary structures, the occurrence of ichnofossils and major groups of macro- and microfossils, as well as accessories such as pyrite, iron sulfides, laminae, shell fragments, dropstones etc. are shown in the third column of the core description sheet. The symbols used to designate structures found in each core are shown in the legend to core description. Color was visually estimated and measured with the Minolta spectrophotometer.

Core sections were photographed using a digital camera. The single images were arranged and are presented as whole-core image series (see Appendix VII).

5.6.2.1 Sampling scheme of sediment cores

The 1m-long segments of the sediment cores were sampled according to the following scheme, repeating every 10 cm:

0-1 cm	Ti/Nü
1-2 cm	½ Ti/Nü + ½ Russ. Sci.
2-3 cm	AWI Diatoms
3-4 cm	Ti/Nü
4-5 cm	Russ. Sci.
5-6 cm	Ti/Nü
6-7 cm	½ Ti/Nü + ½ Russ. Sci.
7-10 cm	AWI Radiolarien-Isotops

The abbreviation Ti/Nü corresponds to samples for R. Tiedemann (AWI-Bremerhaven) and D. Nürnberg (IFM-GEOMAR, Kiel), whereas Russ. Sci. marks samples for Russian Scientists (POI-Vladivostok, Shirshov Institute, Moscow). Samples were taken as whole slices from the working half and were placed in plastic bags (Whirl-Paks). Every 5 cm, starting at a depth of 5 cm, a syringe with defined volume was taken for physical properties analyses by Tiedemann and Nürnberg.

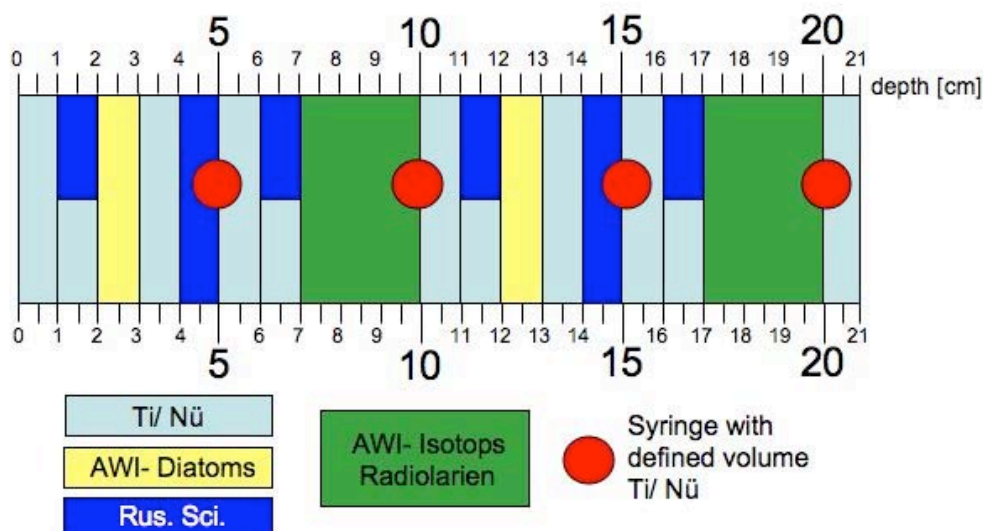


Fig. 5.6.4.: Sampling scheme applied for sediment cores recovered during SO201-2.

The working halves for the following sediment cores were completely sampled. Thus, only the archive halves of these sediment cores were stored.

<u>sediment core</u>	<u>length</u>
SO 201-2-09-KL	535 cm
SO 201-2-12-KL	905 cm
SO 201-2-14-KL	274 cm
SO 201-2-40-KL	895 cm
SO 201-2-77-KL	1178 cm

Samples taken from core SO201-2-77-KL for the Russian scientific party comprise the depth interval from 0-1178 cm. The archive half from 0-278 cm was sampled continuously each cm for paleomagnetic studies.

Working halves of the following sediment cores were completely sampled according to the above mentioned scheme only for listed sections:

<u>sediment core</u>	<u>length</u>	<u>completely sampled from/to</u>
SO 201-2-81-KL	1755 cm	0-555 cm
SO 201-2-85-KL	1813 cm	0-1213 cm
SO 201-2-101-KL	1832 cm	0-1332 cm

At core SO201-2-81, the archive-half was sampled continuously each cm from 555-1755 cm for paleomagnetic studies. The archive half from core SO201-2-85-KL (0-1813 cm) was also sampled for paleomagnetic studies. All above listed sediment cores have been visually described and scanned with the Minolta colorspectrometer.

Below mentioned sediment cores were cut into working and archive halves, and were visually described and scanned with the Minolta-colorspectrometer:

<u>sediment core</u>	<u>length</u>
SO 201-2-69-KL	675 cm
SO 201-2-114-KL	789 cm
SO 201-2-115-KL	430 cm
SO 201-2-127-KL	554 cm

The following sediment cores represent duplicates from other cores ("double coring") and were not opened:

<u>sediment core</u>	<u>length</u>
SO 201-2-80-KL	1220 cm
SO 201-2-84-KL	1800 cm
SO 201-2-100-KL	1754 cm

An exception from the described sampling scheme is one segment of sediment core SO201-2-09-KL. Here, sampling was accomplished by exclusively using syringes. As this procedure was ineffective and highly time consuming, we adopted the sampling scheme described above (Fig. 5.6.4.).

5.6.2.2. Shipboard core logging

5.6.2.2.1. Magnetic susceptibility data (*L. Max / R. Tiedemann*)

The magnetic susceptibility was measured aboard RV SONNE with the Multi-Sensor Core Logger designed and built by GEOTEK, Haslemere, UK. This system enables the amount of magnetic material in the sediment to be determined in unsplit sediment cores encased in cylindrical plastic liners. We measured magnetic susceptibility in core sections of 12 cm diameter, up to 100 cm long closed by plastic caps of 12.5 cm diameter. The section was placed on the rails of a conveyor system and aligned to the start position. A core pusher then moved the section in increments of 1 cm through the BARTINGTON MS2C sensor loop. The starting position of the section was 10 cm in front of the sensor loop. A low intensity (ca. 80 A/m RMS) non-saturating, alternating magnetic field (0.565 kHz) is produced by an oscillator circuit within the sensor. Any magnetic material in the near vicinity of the sensor causes a change in the oscillator frequency, which is electronically converted into (artificial) magnetic susceptibility values. Data were initially collected on a Macintosh computer and edited with EXCEL and KALEIDAGRAPH. Artificial susceptibility minima near core section breaks were eliminated. Magnetic susceptibility data, which are indicative of the terrigenous, siliciclastic sediment input are summarized in the Appendix VIII.

5.6.2.2.2. Color scan (*J. Riethdorf / D. Nürnberg*)

A Minolta CM 508d hand-held spectrophotometer was used to measure light reflectance on sediment cores after opening of the core. These measurements were carried out on the damp core surface, and clear plastic film was used to cover the core. The spectrum of the reflected light is measured by a multi-segment light sensor. The spectral reflectance is measured at a 20 nm pitch between wavelengths of 400 to 700 nm, and a double-beam feedback system automatically compensates for variation in the illumination from the CM 508d's pulsed xenon arc lamp. Routine measurements were carried out at 1 cm spaced intervals, and automatically recorded on a Toshiba Satellite 2060 DS laptop computer using Minolta's software Spectramagic v.2.11 (release 1998). Before measurement of each core segment, the spectrophotometer was first calibrated for white color reflectance and then "zero calibrated". This color calibration was made to avoid variation in color readings due to the laboratory environment (temperature, humidity, and background light) and instrument variations. From the reflectance data, the standard color-values X, Y, and Z are automatically calculated by the software Spectramagic, which are displayed in the L*, a* and b* CIELAB

color coordinates. Most valuable for the interpretation of our sediments were the L* and b*-values, shown in the Appendix IX (Figs. B1-B6). The L*-value represents brightness and can be directly correlated to grayvalue measurements (i.e. from video-systems). The color b*-value reflects green colors and hence, is indicative for cyclic changes in biogenic silica production in our sediment records.

5.6.2.2.3. Humidity (S. Gorbarenko / A. Derkachev)

The sediment humidity was measured by a microwave moisture meter (resonance ultrahigh frequency humidity meter RUFH-M-8, West Company LTD, Russia, Kaliningrad). 100% of humidity is a water. The sediment humidity was measured every 1 cm throughout the sediment cores (s. Appendix, Lithologs). The relative precision is ~2-3%. The sediment humidity records studied demonstrate a high variability, most likely related to climate changes and/or the accumulation of terrigenous, biogenic and volcanic material. Turbidity layers also strongly influence the sediment humidity.

5.6.3. Results and Discussion

5.6.3.1. Sediment Facies

Sedimentary facies at Area B (Kronotsky continental margin)

SO201-2-9, -12, -14, -127 (Fig. 5.6.5.)

The sediment records from the Kronotsky continental margin were recovered from ~1450 m, ~2100 m, and ~2600 m water depth. Site locations are max. 40 nm from the steep coast. The ~5.5 m long sediment record SO201-2-127 is composed entirely of greenish olive-gray diatomaceous ooze and diatomaceous sandy clayey silt, with calcitic shell fragments and dropstones across the entire sediment sequence. The Holocene diatomaceous sediment is regularly interrupted by turbiditic black sand layers, which commonly exhibit a sharp base and fining upwards sequences (Fig. 5.6.6.). Sediment particles are commonly angular and consist of quartz, feldspar, volcanic particles and few foraminifers.

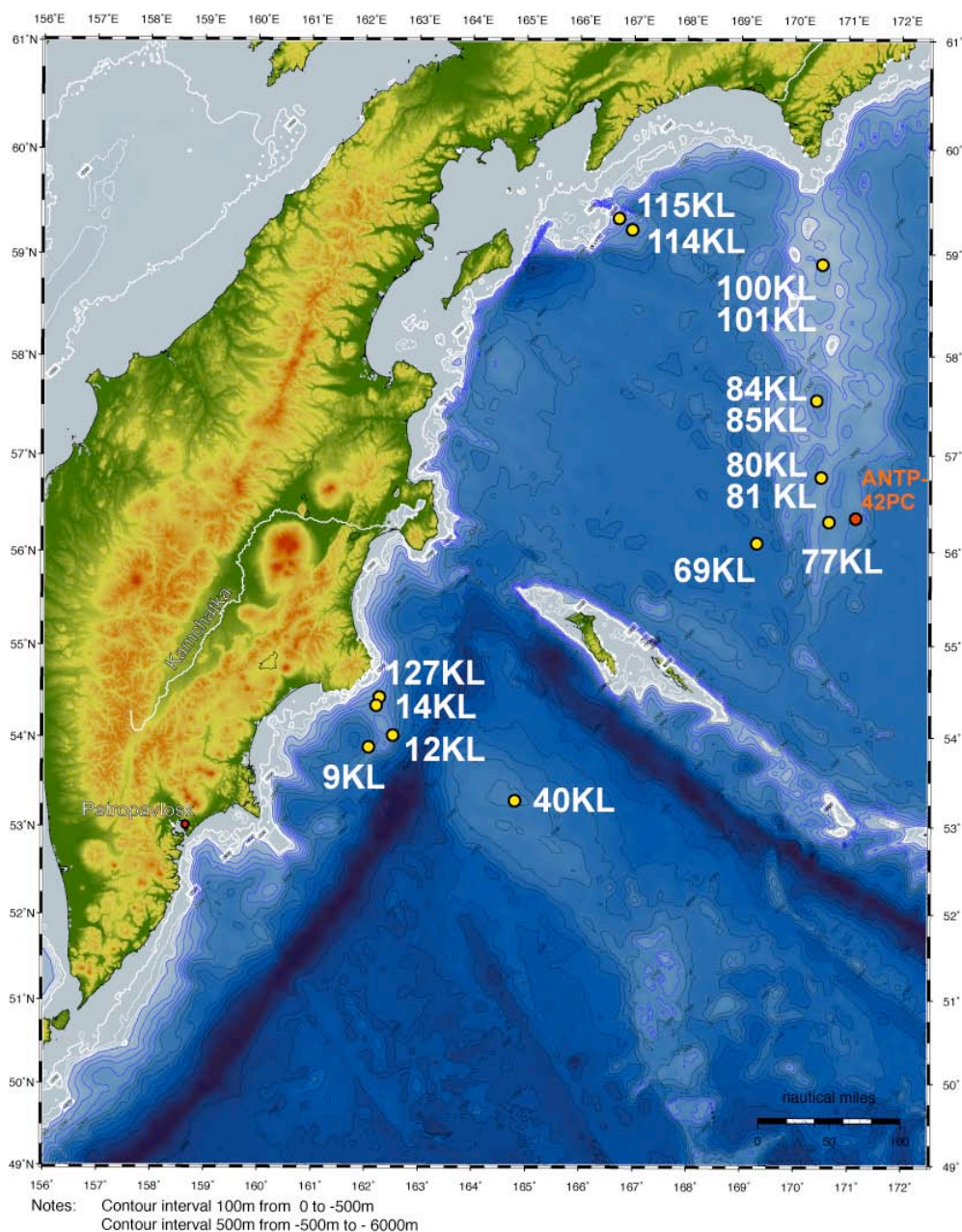


Fig. 5.6.5.: Location of sediment cores

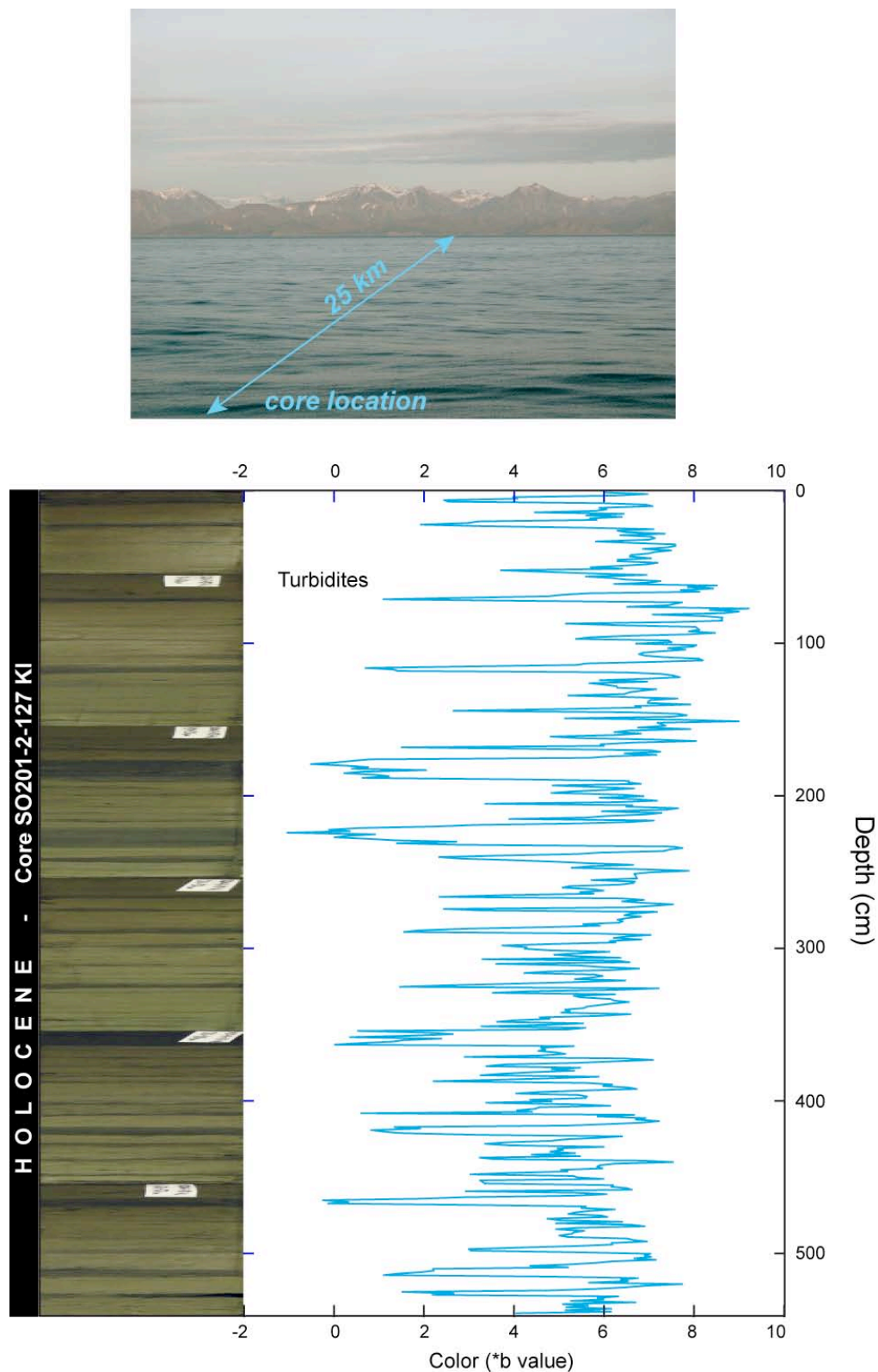


Fig. 5.6.6.: Core SO201-2-127: A high-resolution Holocene climate archive. Correlation of turbidite layers and color b^* -values from core SO201-2-127. Upper photo indicates the coastal distance to the core location. The coastal area is marked by a mountain range with elevations of up to 1500. This rough relief continues over 20 km to a water depth of 1500 m at core SO201-2-127.

Sediments below the diatomaceous sequence are best documented in the 9 m-long sediment core SO201-2-12. The diatomaceous sediment is replaced by monotonous, siliciclastic, olive gray sandy clayey silt series, which commonly contain calcitic shell fragments, dropstones, and high portions of terrestrial organic matter. Similar to the overlying diatomaceous sediment, the fine-grained siliciclastic sequence is intercalated by many well-defined turbiditic sand layers, which may reach >10 cm in thickness, and by volcanic ashes (see Chapter 5.6.3.3).

The frequent occurrence of small turbidites within the Holocene sequence at core SO201-2-127 is best represented by the color b^* -values (Fig. 5.6.7.). Spectral analyses of the color L^* and b^* -values (Fig. 5.6.7.) suggest a cyclic deposition of the turbidite layers with dominant cycles of 50 cm, 21 cm and 15 cm. This would imply a cyclic deposition of turbidites at centennial to millennial time scales, since core SO201-2-127 comprises a 5.5 m long incomplete Holocene sequence, assuming a sedimentation rate of 50 cm/kyr, at least. The cyclic occurrence of the turbidites suggests a climate-related process as a potential trigger mechanism rather than seismic activity. However, seismic activity may have contributed to sporadic turbidite deposition as this region is known as a very active seismic zone.

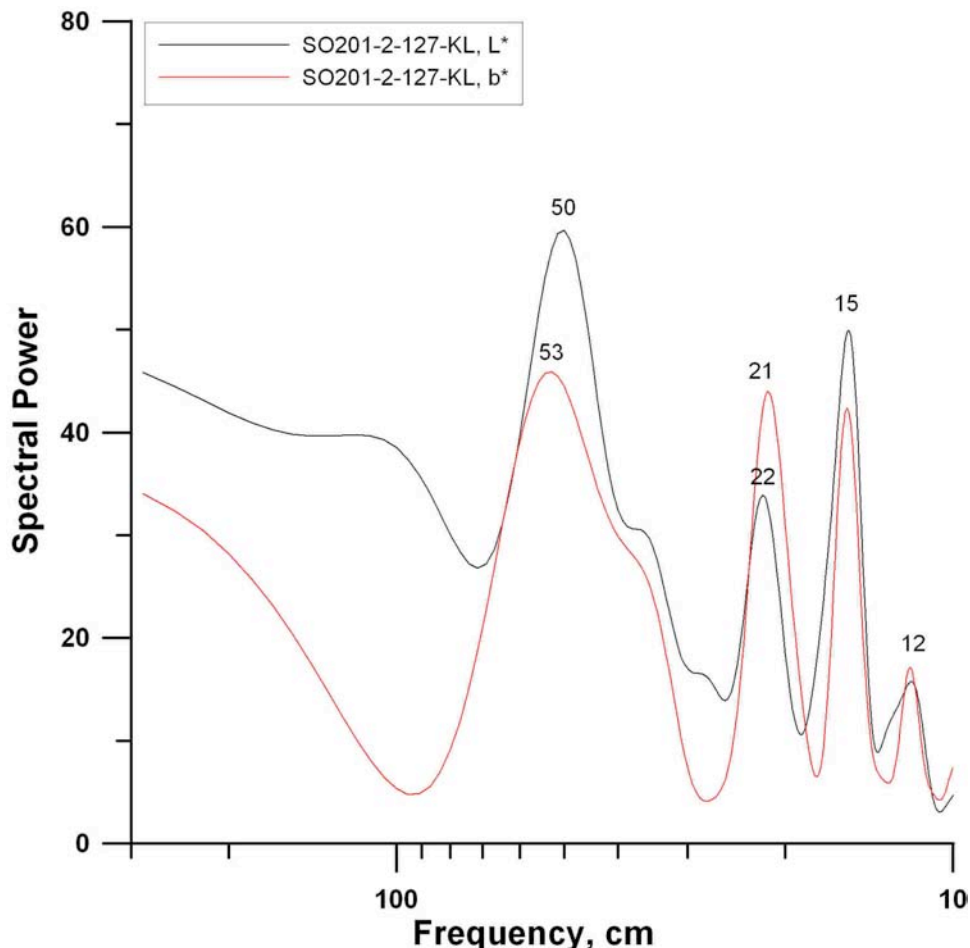


Fig. 5.6.7.: Blackman-Tukey power spectrum of the L^* - and b^* -values from the 5.54 m long sediment core SO201-2-127-KL recovered at the Kronotsky peninsula (Area B) in 1440 m water depth. Dominant frequencies are similar for both values and occur at 12 cm, 15 cm, 21-22 cm, and 50-53 cm, respectively. Spectral analysis was carried out using the program "Analyseries" (V.2.0.4.2). The Blackman-Tukey method was applied to the unsmoothed L^* - and b^* -values measured with a Minolta colorspectrophotometer at intervals of 1 cm. For the output a resampling interval of 0 to 0.2 cm^{-1} in steps of $5 \times 10^{-4} \text{ cm}^{-1}$ was chosen.

Sedimentary facies at Area B (Meiji Seamount)

SO201-2-40 (Fig. 5.6.5.)

The sediment record from Meiji Seamount (SO201-2-40) from ~2900 m water depth reveals a monotonous and commonly bioturbated terrigenous (siliciclastic) sequence. Below ~2.6 m, greenish horizons of diagenetically altered sediment occur increasingly. The siliciclastic sequence is only interrupted twice by diatomaceous sandy clayey silt, pointing to enhanced marine productivity in line with climatic optima. The near-surface diatomaceous, light brownish sediment is observed only in the trigger core. A second diatomaceous sediment layer occurs at ~5.3 - 5.6 m core depth. This horizon is clearly reflected in higher color b^* -values. Ice-rafted detritus is rare, although present in the entire sediment profile pointing to the presence of seasonal sea ice in the Meiji Seamount area. Most notably are the numerous tephra layers and lenses in sediment core SO201-2-40 (see Chapter 5.6.3.3).

Sedimentary facies at Area E (Shirshov Ridge)

SO201-2-77, -81, -85, -101 (Fig. 5.6.5.)

Cores from Shirshov Ridge were recovered along a N-S transect from 630, 970, 1150, and 2100 m water depth. The sedimentary records can be correlated based on comparable records of magnetic susceptibility (see Chapter 5.6.3.2.) and distinct tephra layers (see Chapter 5.6.3.3.). The correlation of cores implies that overall sedimentation rates are variable and do not change systematically with water depth as could be expected from undisturbed continental slope settings. Rather, the various catchment areas seem to be differentially affected by depositional, redistributional and/or erosional processes. Final conclusions, however, cannot be drawn as long as the age model is not established.

In accordance to the physical properties, lithologies can be traced among core locations. Core SO201-2-81 shows exemplarily the different lithologies changing over time and reflecting considerable changes in the depositional environment. Sedimentation at Shirshov Ridge is dominated by terrigenous (siliciclastic) material. The monotonous and often bioturbated terrigenous sequences, characterized by high portions of siliciclastics, relatively low magnetic susceptibilities and low b^* -values, are repeatedly interrupted by short events of diatomaceous ooze deposition, implying enhanced marine productivity. During these periods, the siliciclastic portion, which is mainly bound to the silt and clay fractions, rapidly declines. Color b -values commonly increase due to the typically greenish olive-gray colors of the ooze. Calcareous foraminifers are present. In accordance to the sedimentation pattern in the Sea of Okhotsk (Nürnberg & Tiedemann 2004), we relate the presence of diatomaceous oozes to warm climatic periods. Diatomaceous ooze or diatomaceous sandy clayey silt deposition repeatedly occurred through time, commonly followed by a „transitional sediment“, which gradually becomes more terrigenous, while percentages of biogenic silica decrease. The „transitional“ dark olive-gray sandy clayey silt facies change into pale dark gray and homogenous sandy silty clay, which most likely represents glacial intervals of sediment deposition. It is interesting to note that these fine full glacial sediments commonly do not contain ice-rafted detritus, implying either no sea-ice cover or perennial sea ice coverage across Shirshov Ridge. Diatomaceous ooze deposition commences directly above the pale dark gray glacial sediment, mostly characterized by a sharp boundary, sometimes by a gradational contact. The pelagic sediments from Shirshov Ridge are commonly rare in dropstones, although occurring over the entire sediment records and often enriched at the base of the diatomaceous oozes. Tephra layers and lenses occur repeatedly and can be correlated between cores (see Chapter 5.6.3.3.).

Biogenic opal sedimentation is clearly reflected in the color b^* -values, which exhibit distinct variations across the sediment column. Spectral analysis of b^* -records from cores SO201-2-85 and SO201-2-101 reveals high-frequency, cyclic variations in lithology most presumably caused by high-amplitude changes in the ratio of biogenic and terrigenous sediments. The frequency spectra from both cores suggest a dominant lithological variability at a wavelength of 71 cm (Fig. 5.6.8.). The studies from Cook et al. (2005) and Gorbarenko (unpublished data) congruently suggest for the time interval of the last 15 kyr sedimentation

rates of ca. 15 cm/kyr for the Shirshov Ridge region (see also Chapter 5.6.3.2.). Extrapolation of this sedimentation rate would translate the 71 cm cycle into a millennial-scale variability appearing within the range of Dansgaard-Oeschger cycles and Heinrich events.

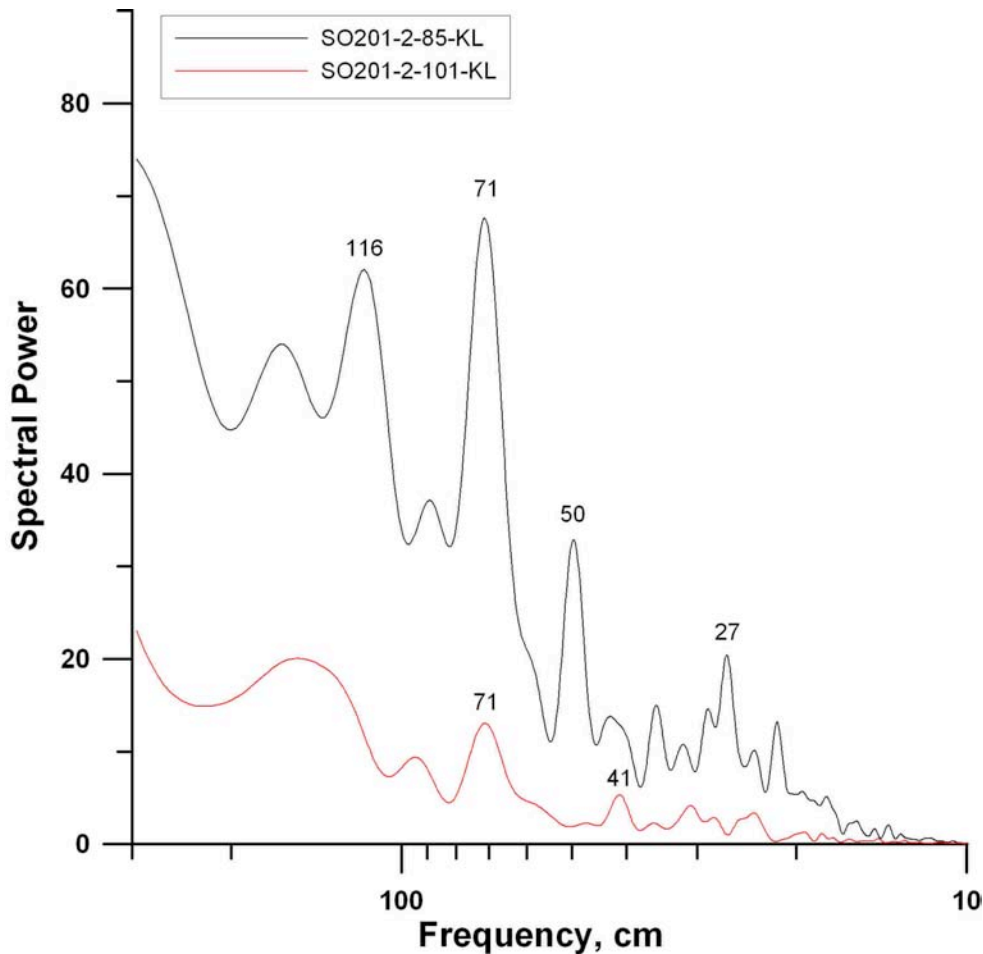


Fig. 5.6.8.: Blackman-Tukey power spectrum of the b^* -values from the sediment cores SO201-2-85-KL and SO201-2-101-KL. Both cores have been recovered at the Shirshov Ridge (Area E) and are 18.13 cm and 18.32 cm long, respectively. Dominant b^* -frequencies are 50 cm, 71 cm, and 116 cm for core SO201-2-85-KL from 968 m water depth, and 41 cm and 71 cm for core SO201-2-101-KL from 630 m water depth. Spectral analysis was carried out using the program "Analyseries" (V.2.0.4.2). The Blackman-Tukey method was applied to the unsmoothed b^* -values measured with a Minolta colorspectrophotometer at intervals of 1 cm for each core. For the output a resampling interval of 0 to 0.1 cm^{-1} in steps of 10^{-4} cm^{-1} was chosen.

Sedimentary facies at Area D (northern Bering Sea continental margin)

SO201-2-114, -115 (Fig. 5.6.5.)

Piston cores SO201-2-114 and SO201-2-115 were recovered from ~1400 m and ~720 m water depth, respectively, from the northern Bering Sea continental margin. The site locations were within 50-60 nm distance to the coast. In spite of the short distance between cores, they reveal quite different sedimentary archives. The shallow core SO201-2-115 is dominated by olive-gray to dark gray sandy silty clay to sandy clayey silt with common calcitic shell fragments and dropstones of considerable size (up to 8 cm in diameter). Most notably are numerous coarse sand and gravel layers intersecting the siliciclastic sediment,

pointing to considerable sediment supply and reworking of upper continental slope and shelf sediments.

The deeper core SO201-2-114 reflects a very different environmental setting. The strong H₂S odor while opening the core points to the decay of high organic carbon concentrations under dysoxic conditions. Sediments are commonly fine-grained and reveal a succession of sediment types already seen at Shirshov Ridge. Pale dark gray and homogenous glacial sandy silty clay deposits are followed by diatomaceous deposits, which repeatedly occur in the sediment record. The diatomaceous successions are commonly followed by a „transitional sediment“, which gradually becomes more terrigenous and less diatomaceous, and gradually changes into the pale dark gray glacial deposits. Surprisingly, we observed well-established laminated fine-grained sediments in the deglacial sediments of core SO201-2-114, providing evidence for low oxygen concentrations in the northwest Bering Sea at intermediate water depths (1400 m).

5.6.3.2. Magnetic susceptibility

In general, the magnetic susceptibility values in the NW-Pacific and the western Bering Sea are relatively low (<60 SI units) in comparison to other oceanic regions that are influenced by ice-rafted debris and fluvial sediment discharge. Pronounced maxima in magnetic susceptibility values exceeding >60 SI units characterize ash layers or turbidites (Appendix VIII Figures A1-A3). The magnetic susceptibility records from Shirshov Ridge display the lowest values (<15 SI units). Such values are typical for oceanic pelagic environments (Bloemendal et al. 1992), which are enriched in paramagnetic minerals (e.g. clay minerals, amphiboles, chlorite) and diamagnetic material (carbonate, opal). The hemipelagic sediments show, as expected, slightly higher magnetic susceptibility values of up to 60 SI units, probably due to both enhanced supply of terrigenous siliciclastic material and higher concentration of ferromagnetic minerals.

The high-resolution magnetic susceptibility records were also successfully used for between-core correlations at Shirshov Ridge (Fig. 5.6.9.) by matching prominent and similar structures. The core-to-core correlation is also in good agreement with the occurrence of identical ash layers. The correlation pattern for sediment records from Shirshov Ridge provided first information about local differences in sedimentation rates. Accordingly, cores SO201-2-85-KL and SO201-2-101-KL are marked by relatively high sedimentation rates. Core SO201-2-81-KL has distinctly lower sedimentation rates but reaches further back in time. Cook et al. (2005) and Gorbarenko (unpublished data) examined two short gravity cores from Shirshov Ridge and developed an age model for the last 15 kyr. These cores are close to the position of cores SO201-2-77-KL and SO201-2-81-KL and congruently suggest relatively high sedimentation rates of ca. 15cm/kyr.

5.6.3.3. Tephra layers in the NW-Pacific and Bering Sea

Volcanic activity on the Kurile Islands and the Kamchatka Peninsula produces large volumes of pyroclastic material and pumice, which are widely transported by wind and surface ocean currents and later, accumulate on the sea floor. Tephra layers may actually serve as excellent time markers and may help to establish the chronostratigraphy in this ocean area. In the adjacent Sea of Okhotsk, for example, Gorbarenko et al. (2004) identified several volcanic ash layers, which could not only be correlated over wide distances, but were also related to distinct volcano eruptions.

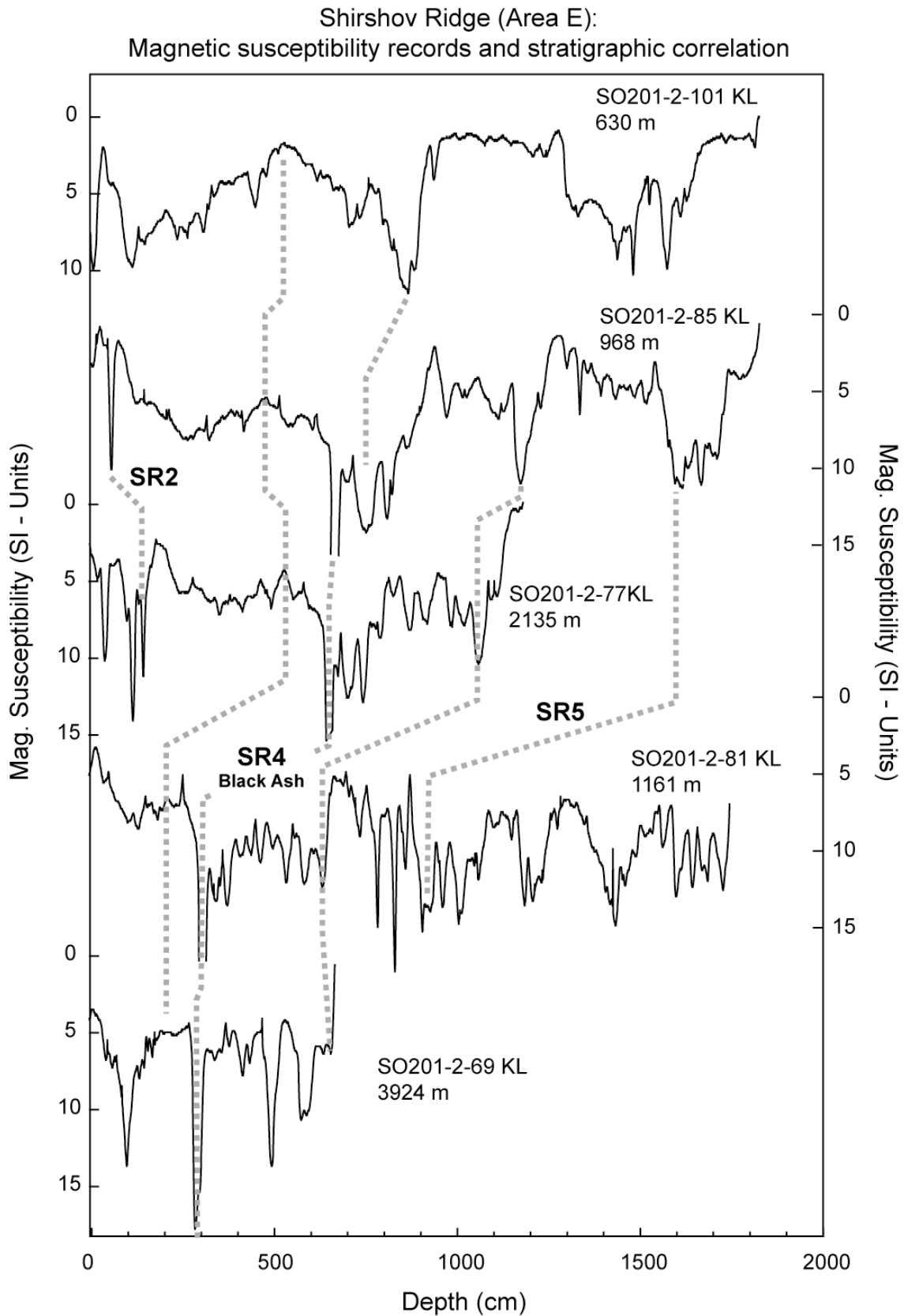


Fig. 5.6.9.: Magnetic susceptibility records from Shirshov Ridge and their stratigraphic correlation. SR2, SR4 and SR5 indicate ash layers.

During SO-201, distinct tephra layers and – when bioturbated - tephra lenses were found in nearly all sediment cores recovered: across the continental slope of the Kronotsky Bay (indicated by the prefix KB), at Meiji Seamount in the NW Pacific (indicated by WP), and on Shirshov Ridge (SR). Lenses of volcanic ash were indicated with the prefixes KBI, WPI, and SRI, respectively (Figs. 5.6.5.,5.6.6.). The volcanic ashes were sampled, described by visual inspection and later, studied in more detail using smear slides under the polarization microscope.

In core SO201-2-09-KL from the continental slope of Kronotsky Peninsula, five well-defined tephra layers (KB 1 to KB 5) and 4 horizons of tephra lenses (KBI 1 to KBI 4) with thicknesses of ~2-10 mm were differentiated (Fig. 5.6.10.-11.). As all the volcanic ash material was found in light olive gray sandy clayey silt, while the diatomaceous ooze typical for the Holocene is missing, we assume that the tephra layers and lenses are of Pleistocene age.

At Meiji Seamount (SO 201-2-40-KL), we detected 18 tephra layers and 6 tephra lenses in the ~18 m-record (Fig. 5.6.10.), which are all whitish-gray to gray to beige. Some tephra layers exhibit thicknesses of up to 10 cm, and quite a few show fining upward sequences. Age control cannot be derived yet from these volcanic ashes. However, if the occurrence of diatomaceous ooze and diatomaceous sandy clayey silt at 5.5 m core depth is indicative for marine oxygen isotope stage (MIS) 5, then the tephra layers in core SO201-2-40 might have been deposited during the last ~290 kyr.

In the Holocene-Late Pleistocene sediment sequences from Shirshov Ridge area (Bering Sea), 8 tephra layers and 6 tephra lense horizons (2-5 mm thickness) were identified in cores SO201-2-77-KL, SO201-2-81-KL and SO201-2-85-KL (Fig. 5.6.11.). Based on the study of the morphology of volcanic glass particles, of mineral inclusions, and color, the dark-gray tephra layers SR1 and SR2 were correlated with peat tephra from Bering Island (Kirianov et al. 1986), and hence, are presumably of Holocene age. SR1 found in core SO201-2-77 resembles tephra layer KD-5, which is dated to 4.5 kyr and is most likely connected to the Shiveluch volcano eruption (Braitseva et al. 1993). SR2, which was found in cores SO201-2-77 and SO2-85, may be correlated with tephra layer KD-8 of Bering Island, dated to 7.7 kyr and related to the Karymsky volcano eruption (tephra – KRM) (Braitseva et al. 1993).

The up to 4 cm thick, black tephra layer SR4 was found in all cores from the Shirshov Ridge area and thus, is of chronostratigraphic significance (Fig. 5.6.10., see also chapter 5.6.3.2.). The SR4 tephra is typically characterized by brown ash with plagioclase microlite inclusions, which up to now was only described in the NW Pacific and Bering Sea areas. It is most presumably related to the Shiveluch volcano eruption during the Late Pleistocene.

A very prominent stiff tephra layer occurs in core SO201-2-81 at ca. 15.5 m core depth. The whitish-gray SR7 tephra with a slight pink taint is up to 5 cm thick and is characterized by colorless thin-fragmental volcanic ash shards without mineral inclusions, and a greenish diagenetically altered base. SR7 is presumably of overregional stratigraphical importance as similar ashes were found in core SO201-2-09 from Kronotsky continental slope at 511-515 cm core depth, and in core SO201-2-40 from Meiji Seamount at 845-850 cm core depth, nicely indicated by high sediment reflectance values (Fig. 5.6.11.).

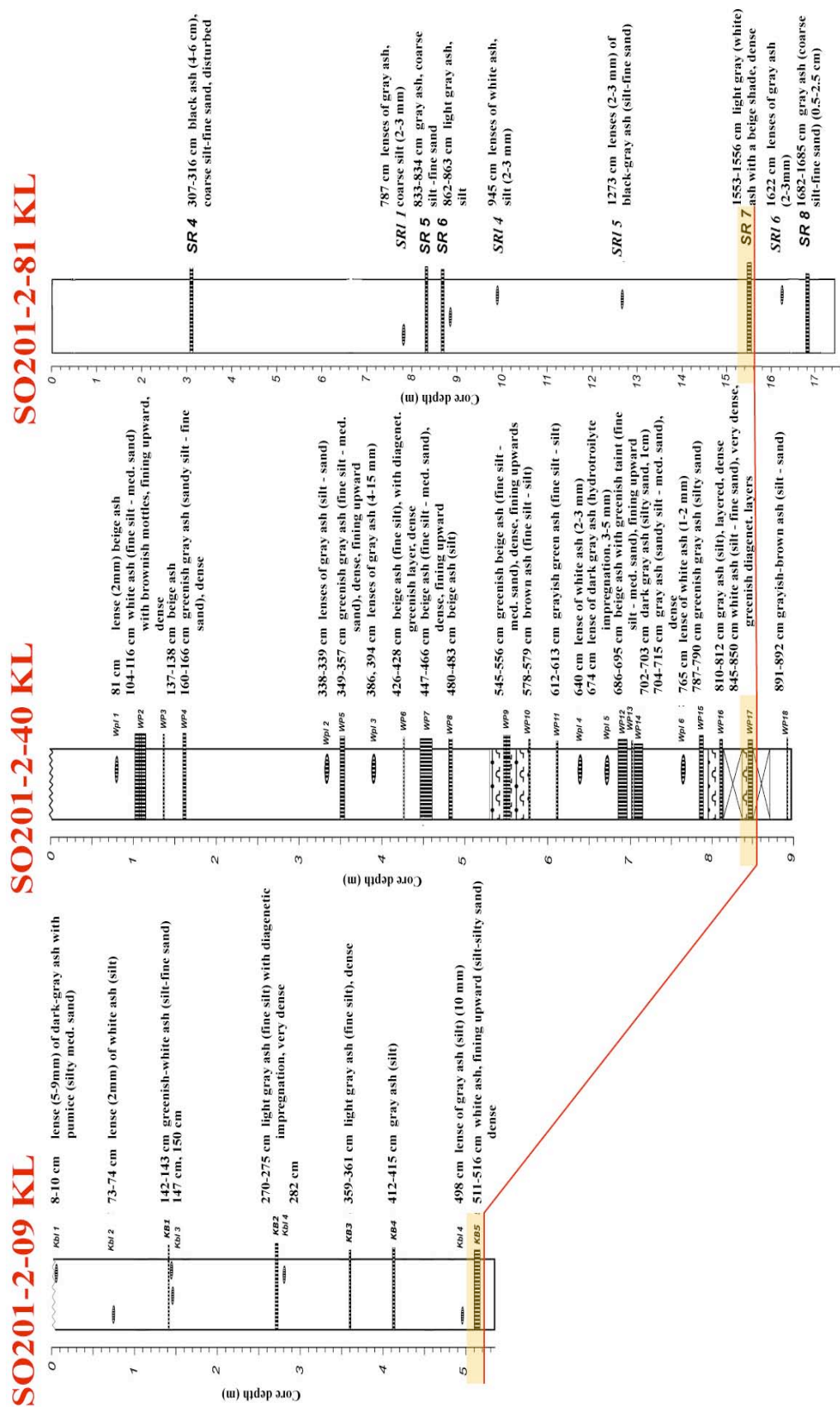


Fig. 5.6.10.: Tephra layers in core SO201-2-09 from the Kronotsky continental margin, in core SO201-2-40 from Meiji Seamount, and in core SO201-2-77 from Shirshov Ridge. Tephra layers are named KB 1 to KB 5 (KB = Kronotsky Bay), WP 2 to WP 18 (WP = West Pacific), and SR 1 to SR 4 (SR = Shirshov Ridge). Tephra lenses are named KBI 1 to KBI 4 in core SO201-2-09, Wpl 1 to Wpl 6 in core SO201-2-40, and SRI 1 to SRI 6 in core SO201-2-77. Note that the whitish-gray tephra layer SR7 is present in all regions and may serve as a stratigraphical time marker.

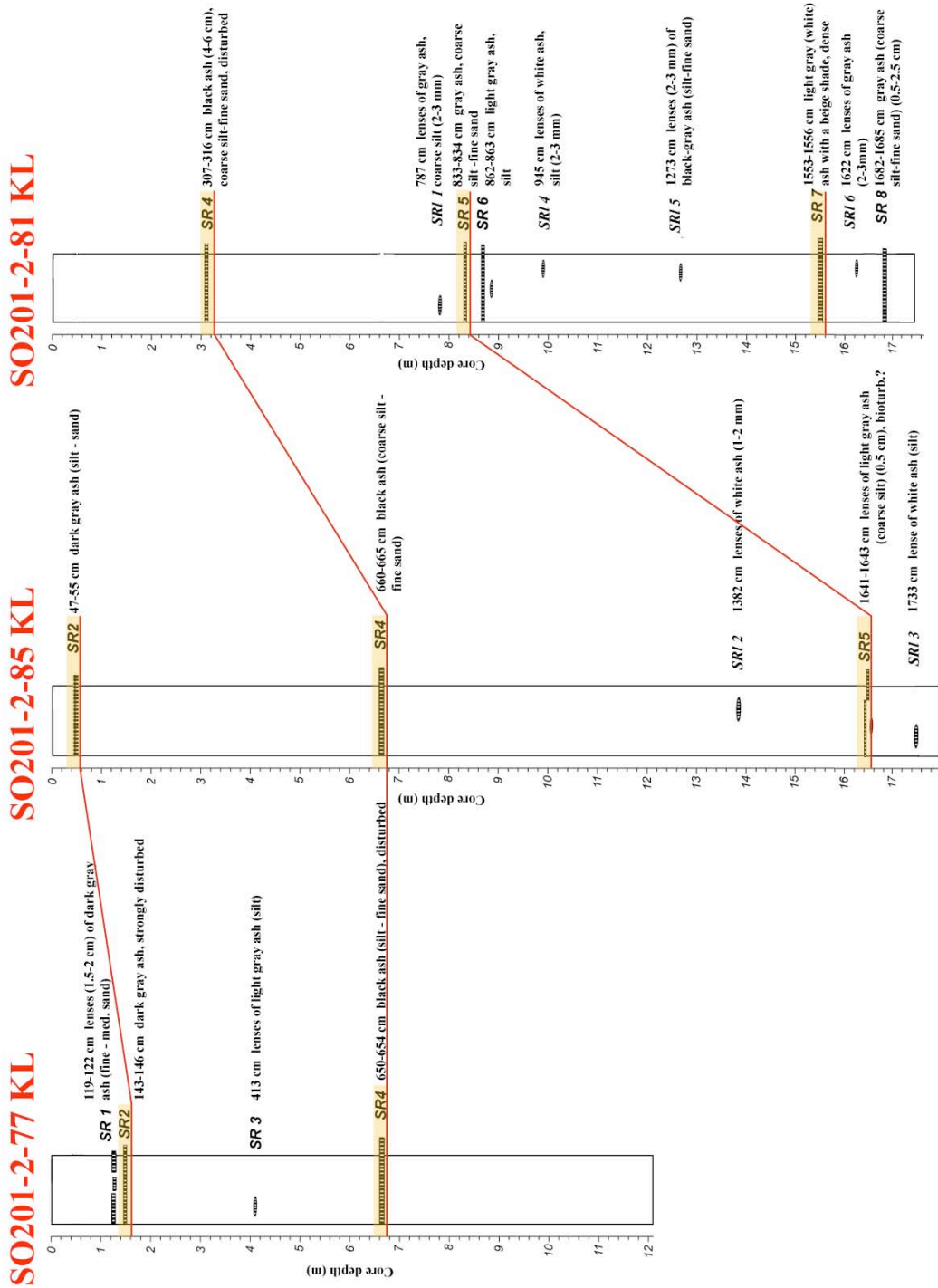


Fig. 5.6.11.: Tephra layers and lenses in cores SO201-2-77, SO201-2-85, and SO201-2-81 from Shirshov Ridge. Nomenclature of tephra layers and lenses is as in Figure 5.6.10. The prominent volcanic ash layers SR2, SR4, and SR5 can be traced across core locations.

6. SUMMARY

Oceanography

Hydrographic measurements encountered SST warming in combination with reduced values for salinity due to increased run off and ice melting during summer time. Winter water mainly forms in the northern Bering Sea and was detected within the Pacific stations which originate from the advection of Bering Sea Water through the Kamchatka Strait. Reduced values of oxygen in the northern stations within the Bering Sea enabled the identification of slightly laminated sediments for coring.

Heat flow

The heat flow measurements of this cruise have confirmed and further established a positive heat flow anomaly at the northwestern flank of the Meiji seamount. This anomaly is tentatively explained as the result of primarily fault controlled, vigorous fluid convection in fractured rocks of the descending limb of the oceanic crust toward the subduction zone. The alternative interpretation of the anomaly being caused by a deeper seated magmatic body will be investigated in further analysis as well. However, since this body would have to be the result of an isolated injection of magma from a much deeper seated (and small sized) mantle plume into a fast moving (8 cm a⁻¹) oceanic plate, this interpretation appears to be highly constructed and therefore less likely.

Volcanology

Mapping of volcanic and tectonic structures and dredging of basement rocks targeted on four major regions: (1) Meiji Seamount on the Pacific Plate, (2) Komandorsky Basin, (3) Volcanologist's Massif and Piip Volcano, and (4) Shirshov Ridge in the Bering Sea. None of the areas were previously mapped with multi-beam echo-sounding system and data on the basement rock compositions from these areas are sparse or even not available yet. Geological, volcanological, petrological, geochemical and geochronological analyses subsequent to the cruise are aimed to provide principle information the origin, age and evolution of these features. The integration of these results with existing data as well as with the data obtained during on-land and marine (SO201 Leg 1b) investigations within the KALMAR project will contribute to better understanding of the geodynamic evolution of the NW Pacific Ocean, its convergent margins and marginal seas. Complementing extensive bathymetric mapping, a total of 29 dredges were carried on cruise SO201 Leg 2. Of these deployments, 26 recovered basement rocks, among them a broad variety of volcanic rocks as well as metamorphic and sedimentary rocks.

Paleoceanography

During Leg SO201-2, we recovered a total of 164 m of sediment at 16 sites in the NW-Pacific and the Bering Sea (Fig. 5.6.5.), ranging in age from Late Pleistocene to Holocene. Our sediment cores form a north-south transect from 53°N to 60°N covering intermediate to deepwater levels from 630 to 3913 m water depth. These records will permit paleoceanographic studies on a variety of timescales, including centennial to millennial (10² to 10³ yr) and orbital (10⁴ to 10⁵ yr) time resolution and will allow to address a broad set of scientific hypotheses on these scales (see chapter 2.3).

Geographically, our sediment records cover four areas that are characterized by different environmental settings: the Pacific continental margin offshore the Kronotsky Peninsula of Kamchatka (Area B), the Meiji Seamount in the NW-Pacific (Area B), the Kommandorsky Basin and Shirshov Ridge in the Bering Sea (Area E) and the northwest Bering Sea continental margin (Area D). The pelagic sediment archives in Area E appeared to provide the stratigraphically most complete sediment sequence, covering at least two glacial/interglacial cycles. Full glacial sediments are surprisingly void of ice-rafted debris, suggesting that no or perennial sea ice existed in the Shirshov Ridge area. Deglacial and

interglacial sediments are typically abundant in diatoms and even calcitic foraminifers, pointing to an extremely enhanced marine productivity. The high-resolution records from Shirshov Ridge reveal a millennial-scale cyclic pattern of lithological changes within the frequency range of Dansgaard-Oeschger cycles and Heinrich events.

In Area B and Area D, sediments are characterized by monotonous siliciclastic sequences, interrupted by short periods of diatomaceous sediment deposition. The occurrence of turbidites is a common feature of these continental margin sediments. The high-resolution Holocene sequence at core SO201-2-127 is characterized by cyclic deposition of turbidites at centennial to millennial time scales. The cyclic occurrence of the turbidites suggests a climate-related process as a potential trigger mechanism rather than seismic activity. However, seismic activity may have contributed to sporadic deposition of turbidites as this region is known as a very active seismic zone.

One of the most exciting results was the successful recovery of ultra high-resolution, laminated, deglacial sediments from the northwest Bering Sea. The laminated sediment sequence was recovered from ~1400 m water depth and mark a time interval of low oxygen conditions at intermediate water depths.

Distinct tephra layers were identified, which could be related to distinct Kamchatka volcano eruptions and were used to correlate the sediment cores laterally over long distances. They will serve as important time markers and will help to establish the chronostratigraphy in this ocean area.

7. REFERENCES

- Ahagon, N., Ohkushi, K., Uchida, M., and Mishima, T., 2003, Mid-depth circulation in the northwest Pacific during the last deglaciation: evidence from foraminiferal radiocarbon ages. *Geophysical Research Letters* 30(21): 2097, doi:10.1029/2003GL018287.
- Aizawa, C., Tanimoto, M., Jordan, R.W., 2005, Living diatom assemblages from North Pacific and Bering Sea surface waters during summer 1999. *Deep Sea Research II*, 52: 2186-2205.
- Baranov, B.V., Seliverstov, N.I., Muravev, A.V. and Muzurov, E.L., 1991, The Komandorsky Basin as a product of spreading behind a transform plate boundary. *Tectonophysics*, 199: 237-269.
- Ben-Avraham, Z., Cooper, A.K., 1981, Early evolution of the Bering Sea by collision of oceanic rises and North Pacific subduction zones. *Geol. Soc. Am. Bull.* 92: 485-495.
- Bloemendal, J., King, J.W., Hall, F.R. and Doh, S.-J., 1992, Rock magnetism of Late Neogene and Pleistocene deep-sea sediments: relationship to sediment source, diagenetic processes, and sediment lithology. *Journal of Geophysical Research* 97(B4): 4361-4375.
- Bogdanov, N. A., Neprochnov, Yu, P., 1984, Geology of the Bering Sea deep basins. In: *Origin and History of the Marginal and Inland Seas. Proc. 27th Int. Geol. Congr. VNU Science Press, Utrecht*, 27: 1-17.
- Braitseva, O.A., Sulerzhitsky, S.D., Litasova, S.N., and Melekestsev, I.V., 1993, Radiocarbon dating and tephrochronology in Kamchatka. *Radiocarbon* 35: 463-476.
- Brigham-Grette, J., Gualtieri, L., 2004, Response to Grosswald and Hughes 2004, Brigham-Grette et al. 2003, Chlorine-36 and ¹⁴C chronology support a limited last glacial maximum across central Chukotka, northeastern Siberia, and no Beringian ice sheet, and: Gualtieri et al. 2003, Pleistocene raised marine deposits on Wrangel Island, northeastern Siberia: implications for Arctic ice sheet history. *Quaternary Research* 62: 227-232.
- Cook, M.S., Keigwin, L.D., and Sancetta, C.A., 2005, The deglacial history of surface and intermediate water of the Bering Sea. *Deep-Sea Research II*, 52: 2163-2173.
- Cooper, A.K., Scholl, D.W., Marlow, M.S., 1976, Plate tectonic model for the evolution of the eastern Bering Sea basin. *Geol. Soc. America Bull.* 87, 8: 1119-1126.
- Cormier, V.F., 1975, Tectonics near the junction of the Aleutian and Kuril-Kamchatka Arcs and a mechanism for Middle Tertiary magmatism in the Kamchatka Basin. *Geol. Soc. Am. Bull.* 86, 443-453.
- DeMets, C., Gordon, R.G., Argus, D.F., Stein, S., 1990, Current plate motions. *Geophys. J. Int.* 101: 425-478.
- Davaille, A., Lees, J.M. 2004, Thermal modelling of subducted plates: tear and hotspot at the Kamchatka corner. *Earth Planet. Sci. Lett.* 226: 293-304.
- Duncan, R.A., Keller, R.A., 2004, Radiometric ages for basement rocks from the Emperor Seamounts. ODP Leg 197. *Geochem. Geophys. Geosyst.* 5:Q08L03, doi:10.1029/2004GC000704.
- Dyke, A.S, Andrews, J.T., Clark, P.U., England, J.H., Miller, G.H., Shaw, J., Veillette, J.J., 2002, The Laurentide and Innuitian ice sheets during the Last Glacial Maximum. *Quaternary Science Reviews* 21(1-3): 9-31.
- Endoh, T., Mitsudera, H., Xie, S.P., Qiu, B., 2004, Thermohaline structure in the Subarctic North Pacific simulated in a general circulation model. *Journal of Physical Oceanography* 34: 360-371.
- Favorite, F., Dodimead, A.J., Nasu, K., 1976, Oceanography of the Subarctic Pacific region, 1960 – 71. *Bull. Int. North Pacific Comm.* 33: 1-187.

- Freitag, R., Gaedicke, C., Baranov, B., Tsukanov, N., 2001, Collisional processes at the junction of the Aleutian-Kamchatka arcs: New evidences from fission-track analysis and field observations. *Terra Nova* 13 (6): 433-442.
- Frey, F.A., Huang, S., Blichert-Toft, J., Regelous, M., Boyet, M., 2005, Origin of depleted components in lavas related to the Hawaiian Hotspot: Evidence from Hf isotope data. *Geochem. Geophys. Geosyst.* 6(2):Q02L07, doi:10.1029/2004GC000757.
- Gaedicke, C., Baranov, B., Seliverstov, N., Alexeiev, D., Tsukanov, N., Freitag, R., 2000, Structure of an active arc-continent collision area: the Aleutian-Kamchatka junction. *Tectonophysics*, 325: 63-85.
- Geist, E.L., Scholl, D.W., 1994, Large-scale deformation related to the collision of the Aleutian Arc with Kamchatka. *Tectonics* 13: 538-560.
- Gorbarenko, S.A., 1996, Stable isotope and lithologic evidence of late-glacial and Holocene oceanography of the North-western Pacific and its marginal seas. *Quaternary Research* 46: 230-250.
- Gorbarenko, S.A., Southon, J.R., Keigwin, L.D., Cherepanova, M.V. and Gvozdeva, I.G., 2004, Late Pleistocene-Holocene oceanographic variability in the Okhotsk Sea: geochemical, lithological and paleontological evidence. *Palaeogeography Palaeoclimatology Palaeoecology* 209: 281-301.
- Huang, S., Regelous, M., Thordarson, T., Frey, F.A., 2005, Petrogenesis of lavas from Detroit Seamount: Geochemical differences between Emperor Chain and Hawaiian volcanoes. *Geochem. Geophys. Geosyst.* 6(1):Q01L06, doi:10.1029/2004GC000756.
- Hughen, K., Lehman, S., Southon, J., Overpeck, J., Marchal, O., Herring, C. and Turnbull, J., 2004, ¹⁴C activity and global carbon cycle changes over the past 50,000 years. *Science* 303: 202-207.
- Hunt, G.L., Stabeno, P.J., 2005, Oceanography and ecology of the Aleutian Archipelago: spatial and temporal variation. *Fish. Oceanogr.* 14 (Suppl. 1), 292–306.
- Keigwin, L.D., and Jones, G.A., 1990, Deglacial climatic oscillations in the Gulf of California. *Paleoceanography* 5(6): 1009-1023.
- Keigwin, L.D., 1998, Glacial-age hydrography of the far northwest Pacific. *Paleoceanography* 13(4): 323-339.
- Kelemen, P.B., Yogodzinski, G.M., and Scholl, D.W., 2003, Along-strike variation in the Aleutian Island Arc: Genesis of high Mg# andesite and implications for continental crust. *Inside the Subduction Factory, Volume Geophysical Monograph 138, American Geophysical Union*, 223-276.
- Keller, R.A., Fisk, M.R., White, W.M., 2000, Isotopic evidence for Late Cretaceous plume-ridge interaction at the Hawaiian hotspot. *Nature* 405(8 JUNE 2000): 673-676.
- Kiefer, T., Sarnthein, M., Erlenkeuser, H., Grootes, P. and Roberts, A., 2001, North Pacific response to millennial-scale changes in ocean circulation over the last 60 ky. *Paleoceanography* 16: 179-189.
- Kiefer, T. and Kienast, M., 2005, Patterns of deglacial warming in the Pacific Ocean: a review with emphasis on the time interval of Heinrich event 1. *Quaternary Science Reviews* 24: 1063-1081.
- Kienle J., 1971, Gravity and magnetic measurements over Bowers Ridge and Shirshov Ridge, Bering Sea. *J. Geophys.* 76: 7138-7153.
- Kim, J.-H., Rimbu, N., Lorenz, S.J., Lohmann, G., Nam, S.-I., Schouten, S., Rühlemann, C. and Schneider, R.R., 2004, North Pacific and North Atlantic sea-surface temperature variability during the Holocene. *Quaternary Science Reviews* 23: 2141-2154. doi:10.1016/j.quascirev.2004.08.010.
- Kirianov, V.Y., Egorova, I.A. and Litasova, S.N., 1986, Volcanic ash on Bering Island (Commander Islands) and Kamchatka Holocene eruptions. *Volc Seism* 6: 18-28 (English translation 1990, 8: 850-868).
- Levin, V., Shapiro, N., Park, J., Ritzwoller, M., 2002, Seismic evidence for catastrophic slab loss beneath Kamchatka. *Nature* 418: 763-766.

- Levitus, S., and Boyer, T., 1994, World Ocean Atlas Volume 4: Temperature NOAA Atlas NESDIS 4, U.S. Department of Commerce, Washington, DC.
- Matsumoto, K., Oba, T., Lynch-Stieglitz, J. and Yamamoto, H., 2002, Interior hydrography and circulation of the glacial Pacific Ocean. *Quaternary Science Reviews* 21: 1693-1704.
- Mazzullo, J.M., Meyer, A., and Kidd, R.B., 1988, New sediment classification scheme for the Ocean Drilling Program. In Mazzullo, J., and Graham, A.G. (Eds.), *Handbook for Shipboard Sedimentologists*. ODP Tech. Note, 8: 45-67.
- McKay, J.L., Pedersen, T.F., and Kienast, S.S., 2004, Organic carbon accumulation over the last 16 kyr off Vancouver Island, Canada: evidence for increased marine productivity during the deglacial. *Quaternary Science Reviews* 23: 261-281.
- McKenzie, D.P., Parker, R.L., 1967, The North Pacific: an example of tectonics on a sphere. *Nature* 216: 1276-1280.
- Minolta Co. Ltd., 1995, Spectrophotometer CM-508d Instruction Manual, 1-32
- Mordasova, N., Metreveli, M.P., Ventsel, M.V., 1995, Phytoplankton enzymes in the west Bering Sea. In: Kotenev BN, Sapozhnikoiv VV (Editors) *Complex studies of the Bering Sea ecosystem*. Moscow, VNIRO Press: 256-264 (in Russian).
- Moroz, V.V., Bogdanov, K.T., 2007, Variability of Hydrophysical Fields in the Regions of Islands Arcs in Far East Seas. In «Far East Seas of Russia», book 1, *Oceanological Studies*, 387-404 (in Russian).
- Nakatsuka, T., Watanabe, K., Handa, N., Matsumoto, E., Wada, E., 1995, Glacial to interglacial surface nutrient variations of Bering deep basins recorded by $d^{13}C$ and $d^{15}N$ of sedimentary organic matter. *Paleoceanography* 10: 1047-1061.
- Narita, H., Sato, M., Tsunogai, S., Murayama, M., Ikehara, M., Nakatsuka, T., Wakatsuchi, M., Harada, N. and Ujiie, Y., 2002, Biogenic opal indicating less productive northwestern North Pacific during the glacial ages. *Geophysical Research Letters* 29(15): 1732. doi:10.1029/2001GL014320.
- Newberry, J.T., Laclair, D.L., Fujita, K., 1986, Seismicity and tectonics of the far western Aleutian Islands. *Geodynamics* 6: 13-32.
- Nürnberg, D. and Tiedemann, R., 2004, Environmental change in the Sea of Okhotsk during the last 1.1 Ma. *Paleoceanography* 19: PA4011. doi:10.1029/2004PA001023.
- Ohkouchi, N., Kawamura, K., Kawahata, H., and Okada, H., 1999, Depth ranges of alkenone production in the central Pacific Ocean. *Global Biogeochemical Cycles* 13: 695-704.
- Ohtani, K., Akiba, Y., Takenouti, A.Y., 1972, Formation of western subarctic water in the Bering Sea. In: Takenouti, A.Y. (Ed.), *Biological oceanography of the northern North Pacific Ocean*. Idemitsu Shoten Publ. Co, 32-44.
- Pagani, M., Freeman, K.H., Ohkouchi, N., and Caldeira, K., 2002, Comparison of water column $[CO_{2aq}]$ with sedimentary alkenone-based estimates: a test of the alkenone- CO_2 proxy. *Paleoceanography* 17: 1069. doi:10.1029/2002PA000756.
- Portnyagin, M., Hoernle, K., Avdeiko, G., Hauff, F., Werner, R., Bindeman, I., Uspensky, V., Garbe-Schonberg, D., 2005, Transition from arc to oceanic magmatism at the Kamchatka-Aleutian junction. *Geology* 33(1): 25-28.
- Portnyagin, M.V., Savelyev, D.P., Hoernle, K., Hauff, F., Garbe-Schönberg, D., 2008, Mid-Cretaceous Hawaiian tholeiites preserved in Kamchatka. *Geology* 36(11): 903-906, doi: 10.1130/G25171A.25171.
- Rabinowitz, P.D. and Cooper, A.K., 1977, Structure and sediment distribution in the Western Bering Sea. *Marine Geology* 24: 309-320.
- Ranero, C., Phipps Morgan, J., McIntosh, K., Reichert, C., 2003, Bending-related faulting and mantle serpentinization at the Middle America trench. *Nature* 425: 367-373.
- Regelous, M., Hofmann, A.W., Abouchami, W., Galer, S.J.G., 2003, Geochemistry of lavas from the Emperor Seamounts, and the geochemical evolution of Hawaiian Magmatism from 85 to 42 Ma. *J. Petrol.* 44(1):113-140.

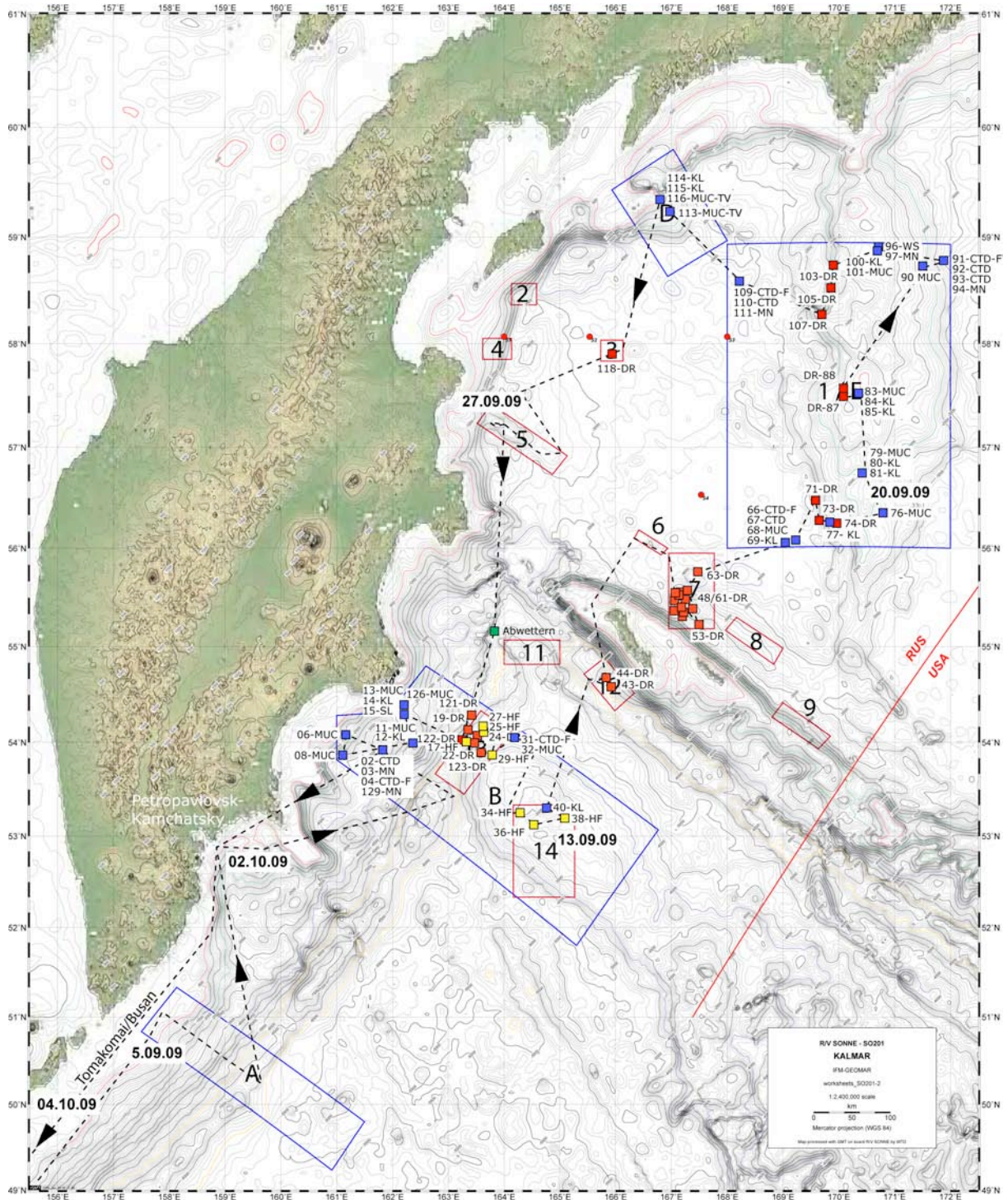
- Roden, G. I., 1991, Subarctic-Subtropical transition zone of the North Pacific: Large-scale aspects and meso-scale structure. NOAA Tech. Rep. NMFS, 105, 1–38.
- Rogachev, K., Shlyk, N., Carmack, E., 2007, The shedding of mesoscale anticyclonic eddies from the Alaskan Stream and westward transport of warm water. *Deep-Sea Res.*, 54, 2643-2656.
- Saenko, O., Schmittner, A., Weaver, A.J., 2004, The Atlantic-Pacific seesaw. *J. Climate* 17: 2033-2038.
- Sarmiento, J.L., Gruber, N., Brzezinski, M.A., Dunne, J.P., 2004, High-latitude controls of thermocline nutrients and low latitude biological productivity. *Nature* 427: 56-60.
- Sarnthein, M., Gebhardt, H., Kiefer, T., Kucera, M. and Erlenkeuser, H., 2004, Mid-Holocene origin of the sea surface salinity low in the subarctic North Pacific. *Quaternary Science Reviews* 23(20-22): 2089-2100.
- Savostin, L.A., Baranov, B.V., Grigoryan, T.Z. and Merklin, L.R., 1986, Tectonics and origin of the western Bering Sea. *Dokl. Akad. Nauk SSSR* 286: 942-946.
- Scholl, D.W., Buffington, E.C. and Marlow, M.S., 1975, Plate tectonics and the structural evolution of the Aleutian-Bering Sea Region. *Geol. Soc. Am. Spec. Pap.*, v. 151, p.1-32.
- Seliverstov, N.I., Avdeiko, G.P., Ivanenko, A.N., Shkira, V.A., Khabunaya S.A., 1986, New submarine volcano on western Aleutian Arc. *Volcanology and Seismology* 5, 3-16 (in Russian).
- Seliverstov, N.I., 1987, Seismoacoustic investigations of the ocean-continent transitional zones. *Science Pub.*, Moscow, 112 p. (in Russian).
- Seliverstov N.I., Torokhov P.V., Baranov B.V., 1995, Piip Submarine Volcano: Structural-Tectonic Control, Geological Structure, and Hydrothermal Activity. *Volcanology and Seismology*, 17: 169-192.
- Seliverstov, N.I., 1998, Sea bottom structure off Kamchatka and geodynamics of the Kamchatka/Aleutian junction area. *Science Pub.*, Moscow, 164 (in Russian).
- Seliverstov, N.I., 1998, Structure of sea-floor offshore Kamchatka and geodynamics of the Kuril-Kamchatka and Aleutian island-arc junction. *Moscow, Nauchny Mir*, 164 (in Russian).
- Silantiev, S.A., Baranov, B.V., Kolesov, G.M. 1985, Geochemistry and petrology of the Shirshov Ridge's amphibolites (Bering Sea). *Geokhimiya* 12: 1694-1705 (in Russian).
- Smirnov, Y.B., Sugrobov, V.M., 1979, Terrestrial heat flow in the Kurile-Kamchatka & Aleutian provinces – I Heat flow and tectonics, *Volcanol. Seismol.* 1: 59-73 (in Russian).
- Smirnov, Y.B., Sugrobov, V.M., 1980, Terrestrial heat flow in the Kurile-Kamchatka & Aleutian provinces – II The map of measured and background heat flow. *Volcanol. Seismol.* 1: 16-31 (in Russian).
- Smith, W.H.F., Sandwell D.T., 1997, Global seafloor topography from satellite altimetry and ship depth soundings. *Science* 277: 1956-1962.
- Stabeno, P.J. and Reed, R.K. 1994, Circulation in the Bering Sea basin observed by satellite-tracked drifters: 1986–1993. *J. Phys. Oceanogr.* 24: 848–854.
- Stabeno, P.J., Reed, R.K. and Schumacher, J.D., 1995, The Alaska Coastal Current: Continuity of transport and forcing. *JGR VOL. 100, NO. C2, PAGES 2477-2485.*
- Stabeno, P.J., Schumacher, J.D., Ohtani, K., 1999, The physical oceanography of the Bering Sea. In: Loughlin TR, Ohtani, K (Eds), *Dynamics of the Bering Sea. Univ. Alaska Sea Grant, Fairbanks*, 1 – 28.
- Stabeno, P.J., Kachel, D.G., Kachel, N.B. and Sullivan, M.E., 2005, Observations from moorings in the Aleutian passes: temperature, salinity and transport. *Fish. Oceanogr.* 14 (Suppl. 1): 39–54.
- Steinberger, B. and Gaina, C., 2007, Plate-tectonic reconstructions predict part of the Hawaiian hotspot track to be preserved in the Bering Sea. *Geology*, 35: 407-410.

- Stewart, R.J., Natland, J.H., and Glassley, W.R., 1973, Petrology of Volcanic Rocks Recovered on DSDP Leg 19 from the North Pacific Ocean and the Bering Sea, in Creager, J.S., Scholl, D.W., and Supko, P.R., eds., Initial Reports of the Deep Sea Drilling Project. Volume 19: Washington D.C., U.S. Government Printing Office, 615-627.
- St. John, K.E.K., Krissek, L.A., 1999, Regional patterns of Pleistocene ice-rafted debris flux in the North Pacific. *Paleoceanography* 14(5): 653-662.
- Sugrobov, V.M., Yanovsky, F.A., 1993, Terrestrial heat flow, estimation of deep temperature and seismicity of the Kamchatka region. *Tectonophysics* 217: 43-53.
- Takahashi, K., 1999, Paleoceanographic changes and present environment of the Bering Sea. In: Loughlin TR, Ohtani K (Eds.), *Dynamics of the Bering Sea*. University of Alaska Sea Grant, Fairbanks, pp. 365–385.
- Takahashi, K., 2005, The Bering Sea and paleoceanography. *Deep-Sea Res.* 52: 2080-2091.
- Tanaka, S., and Takahashi, K., 2005, Late Quaternary paleoceanographic changes in the Bering Sea and the western subarctic Pacific based on radiolarian assemblages. *Deep-Sea Research II*, 52(16-18): 2131-2149.
- Tarduno, J.A., Duncan, R.A., Scholl, D.W., Cottrell, R.D., Steinberger, B., Thordarson, T., Kerr, B.C., Neal, C.R., Frey, F., Toril, M., Carvallo, C., 2003, The Emperor seamounts: southward motion of the Hawaiian hotspot plume in Earth's mantle. *Science* 301(22 August 2003):1064-1069.
- Tsvetkov, A.A., 1990, Magmatism and geodynamics of the Komandorsk-Aleutian island arc. Moscow, Nauka, p 325 (in Russian).
- Tsuda, A., Takeda, S., Saito, H., Nishioka, J., Nojiri, Y., Kudo, I., Kiyosawa, H., Shiimoto, A., Imai, K., Ono, T., Shimamoto, A., Tsumune, D., Yoshimura, T., Aono, T., Hinuma, A., Kinugasa, M., Suzuki, K., Sohrin, Y., Noiri, Y., Tani, H., Deguchi, Y., Tsurushima, N., Ogawa, H., Fukami, K., Kuma, K., Saino, T., 2003, A mesoscale iron enrichment in the western subarctic Pacific induces a large centric diatom bloom. *Science* 300: 958-961.
- Tsuchiya, M., Talley, L.D., 1996, Water-property distributions along an eastern Pacific hydrographic section at 135W. *J. of Marine Research* 54, 541–564.
- Valyashko, G.M., Chernyavsky, G.B., Seliverstov, N.I., Ivanenko, A.N., 1993, Back-arc spreading in the Komandorsky Basin. *Paper of Academy of Sciences of USSR* 338, 3: 212-216 (in Russian).
- Van Geen, A., Zheng, Y., Bernhard, J.M., Cannariato, K.G., Carriquiry, J., Dean, W.E., Eakins, B.W., Ortiz, J.D., and Pike, J., 2003, On the preservation of laminated sediments along the western margin of North America. *Paleoceanography* 18(4): 1098.
- Volynets, O.N., Koloskov, A.V., Yogodzinski, G.M., Seliverstov, N.I., Egorov, Y.O., Shkira, V.A., Matveenko, V.V., 1992, Boninite tendency in the lavas of the submarine Piip volcano and its framing (western part of the Aleutian Arc). 1. Geology, petrochemistry and mineralogy. *Volcanology and seismology* 1: 3-23 (in Russian).
- Wessel, P., Smith, W.H.F., 1995, *The Generic Mapping Tools (GMT) version 3.0*. Technical Reference Cookbook, SOEST/NOAA.
- Yasuda, I., 2004, North Pacific intermediate water: progress in SAGE and related projects. *Journal of Oceanography* 60: 385–395.
- Yogodzinski, G.M., Volynets, O.N., Koloskov, A.V., Seliverstov, N.I., Matvenkov, V.V., 1994, Magnesian andesites and the subduction component in a strongly calc-alkaline series at Piip volcano, Far Western Aleutians. *J. Petrol.* 35(1): 163-20.
- Yogodzinski, G.M., Volynets, O.N., Koloskov, A.V., Seliverstov, N.I., Matveenko, V.V., 1994, Magnesian andesites and the subduction component in a strongly calc-alkaline series at Piip volcano, Far Western Aleutians. *J. Petrol.* 35(1): 163-204.

- Yogodzinski, G.M., Kay, R.W., Volynets, O.N., Koloskov, A.V., and Kay, S.M., 1995, Magnesian andesite in the western Aleutian Komandorsky region: Implications for slab melting and processes in the mantle wedge. *Geol Soc Am Bull* 107: 505-519.
- Yogodzinski, G.M., Lees, J.M., Churikova, T.G., Dorendorf, F., Woerner, G., Volynets, O.N., 2001, Geochemical evidence for the melting of subducting oceanic lithosphere at plate edges. *Nature* 409: 500-504.

Appendix I
Overview Station Map

Appendix I



Cruise track, working areas and stations of SO201-KALMAR Leg 2. Areas in blue (A-E) were permitted for paleoceanographic work, areas in red (1-14) were permitted for volcanological work and for heat flow measurements (12-14). Numbers mark the cruise stations (1-129) blue symbols: CTD, Multinet MN, Multicorer MUC, Pistoncorer KL, red symbols: Dredges DR, yellow symbols: Heat Flow HF.

Appendix II
Station List

Appendix II

Station No.	Gear	Date (UTC)	Start (UTC)	Water depth (m)	Latitude (deg/min)	Longitude (deg/min)	On Bottom (UTC)	Rope length (m)	Water depth (m)	Latitude (deg/min)	Longitude (deg/min)	Off Bottom (UTC)	Rope length (m)	Water depth (m)	Latitude (deg/min)
SO201-2-01	PS-1	05.09.2009	17:47	250,8	50°46,18'N	157°38,53'E	17:47		250,8	50°46,18'N	157°38,53'E	17:47		250,8	50°46,18'N
	PS-2	05.09.2009	19:25	6300,1	51°03,05'N	157°53,50'E	19:25		6300,1	51°03,05'N	157°53,50'E	19:25		6300,1	51°03,05'N
	PS-3	06.09.2009	0:39	5050,4	50°31,95'N	159°00,09'E	0:39		5050,4	50°31,95'N	159°00,09'E	0:39		5050,4	50°31,95'N
	PS-4	06.09.2009	3:51	6553,0	50°12,93'N	159°39,63'E	3:51		6553,0	50°12,93'N	159°39,63'E	3:51		6553,0	50°12,93'N
	PS-5	06.09.2009	6:34	5760,9	50°40,69'N	159°28,44'E	6:34		5760,9	50°40,69'N	159°28,44'E	6:34		5760,9	50°40,69'N
SO201-2-02	CTD	07.09.2009	20:50	3664	53°55,14'N	161°49,83'E	22:38	3666	3665	53°54,54'N	161°50,07'E	22:39		3665	53°54,54'N
SO201-2-03	MN	08.09.2009	0:16	3662	53°55,16'N	161°49,79'E	0:50	1000	3663	53°55,14'N	161°49,76'E	0:51		3663	53°55,14'N
SO201-2-04	CTD-F	08.09.2009	2:30	3656	53°55,19'N	161°49,87'E	2:37	1000	3657	53°55,13'N	161°49,67'E				
SO201-2-05	PS	08.09.2009	3:05	3654	53°55,19'N	161°49,36'E									
SO201-2-06	MUC	08.09.2009	7:31	936	53°03,42'N	161°03,75'E	8:01	941	931	53°03,42'N	161°03,72'E	8:02		931	53°03,43'N
SO201-2-07	PS-1	08.09.2009	9:05	1760	54°06,30'N	161°09,90'E									
SO201-2-08	MUC	08.09.2009	18:20	2640	53°52,19'N	162°03,96'E	19:30	?	2635	53°52,18'N	162°03,96'E				
SO201-2-09	KL	08.09.2009	21:32	2627	53°52,14'N	162°04,03'E	22:22	2606	2627	53°52,16'N	162°04,05'E	22:24	2581	2623	53°52,17'N
SO201-2-10	PS	09.09.2009	0:06	2579	53°52,90'N	162°05,38'E									
SO201-2-11	MUC	09.09.2009	1:32	2169	53°59,49'N	162°22,44'E	2:31	2178	2169	53°59,47'N	162°22,53'E	2:33		2170	53°59,48'N
SO201-2-12	KL	09.09.2009	4:07	2173	53°59,56'N	162°22,55'E	4:49	2170	2145	53°59,47'N	162°22,51'E	4:50		2170	53°59,47'N
SO201-2-13	MUC	09.09.2009	8:03	1482	54°17,34'N	162°11,83'E	8:47	1485	1483	54°17,32'N	162°11,85'E	8:50		1483	54°17,32'N
SO201-2-14	KL	09.09.2009	10:01	1483	54°17,30'N	162°11,85'E	10:33	1462	1482	54°17,31'N	162°11,87'E	10:35		1482	54°17,31'N
SO201-2-15	SL	09.09.2009	11:37	1483	54°17,33'N	162°11,87'E	12:10	1495	1483	54°17,31'N	162°11,86'E	12:11		1482	54°17,32'N
SO201-2-16	PS	09.09.2009	12:54	1482	54°17,26'N	162°11,89'E									
SO201-2-17	HF	09.09.2009	18:07	5220	54°00,00'N	163°20,00'E	19:46	5285	5252	54°00,00'N	163°20,00'E	20:09	5252	5252	54°00,00'N
SO201-2-18	PS	09.09.2009	22:00	5200	53°59,90'N	163°19,97'E									
SO201-2-19	DR	10.09.2009	0:05	5763	54°07,14'N	163°21,24'E	1:49	5920	5805	54°07,15'N	163°21,16'E	3:20	5212	5174	54°06,91'N
SO201-2-20	PS	10.09.2009	5:34	4814	54°06,88'N	163°22,39'E									
SO201-2-21	PS	10.09.2009	21:20	4461	53°58,66'N	163°49,47'E									
SO201-2-22	DR	11.09.2009	2:30	5104	54°00,72'N	163°27,87'E	4:01	5073	4958	54°00,72'N	163°28,12'E	5:30	4675	4581	54°00,53'N
SO201-2-23	PS	11.09.2009	7:45	4530	54°00,56'N	163°28,90'E									
SO201-2-24	DR	11.09.2009	9:04	5412	54°04,33'N	163°32,58'E	10:54	5389	5372	54°04,37'N	163°32,86'E	12:03	5070	5073	54°04,46'N
SO201-2-25	HF	11.09.2009	14:46	4998	54°05,00'N	163°37,00'E	16:31	4994	4994	54°05,00'N	163°37,00'E	16:31	5018	4994	54°05,00'N
SO201-2-26	PS	11.09.2009	18:14	5046	54°05,29'N	163°37,09'E									
SO201-2-27	HF	11.09.2009	19:01	5468	54°09,38'N	163°36,60'E	20:42	5471	5471	54°09,40'N	163°36,50'E	21:03	5500	5471	54°01,40'N
SO201-2-28	PS	11.09.2009	22:55	5469	54°09,50'N	163°36,18'E									
SO201-2-29	HF	12.09.2009	1:27	3893	53°52,00'N	163°48,00'E	2:38	3891	3891	53°52,00'N	163°47,99'E	2:59	3921	3895	53°52,00'N

Appendix II

Longitude (deg/min)	Station End (UTC)	Water depth EM120 (m)	Latitude (deg/min)	Longitude (deg/min)	Area	Depth interval (m)	Pilot core recovery (m)	Core recovery (m)	Gear	Remarks	Station No.	
157°38,53'E	17:47	250,8	50°46,18'N	157°38,53'E	Area A Continental slope off Kamchatka				EM/PS		SO201-2-01	
157°53,50'E	19:25	6300,1	51°03,05'N	157°53,50'E					EM/PS	Change in route		
159°00,09'E	0:39	5050,4	50°31,95'N	159°00,09'E					EM/PS	Change in route		
159°39,63'E	3:51	6553,0	50°12,93'N	159°39,63'E					EM/PS	Change in route		
159°28,44'E	6:34	5760,9	50°40,69'N	159°28,44'E					EM/PS	Ende		
161°50,08'E	23:59	3662	53°54,64'N	161°49,71'E	Area B Kronotsky Halbinsel				CTD	Water sampling	SO201-2-02	
161°49,76'E										MN		SO201-2-03
	3:00	3656	53°55,17'N	161°49,55'E						CTD-F		SO201-2-04
	7:30	936	54°03,42'N	161°03,75'E						EM/PS	Search for ideal coring position	SO201-2-05
161°03,73'E	8:26	937	54°03,42'N	161°03,72'E						MUC	1 x Watersample	SO201-2-06
	17:43	?	53°47,82'N	162°08,79'E						EM/PS	Search for ideal coring position	SO201-2-07
	20:48	2657	53°52,01'N	162°03,80'E						MUC	Surface sediments	SO201-2-08
162°04,06'E	23:45	2625	53°52,15'N	162°04,05'E				0,50	5,35	KL	Piston corer 15 m, core recovery 5m Banana	SO201-2-09
	1:14	2112	53°59,07'N	162°21,47'E						EM/PS		SO201-2-10
162°22,52'E	4:07	2173	53°59,56'N	162°22,55'E						MUC		SO201-2-11
162°22,51'E	5:59	2171	53°59,47'N	162°22,51'E				0,82	9,05	KL	Core recovery 9,05 m	SO201-2-12
162°11,84'E	9:35	1483	54°17,32'N	162°11,85'E						MUC		SO201-2-13
162°11,87'E	11:30	1482	54°17,34'N	162°11,88'E				0,61	2,74	KL	Banana	SO201-2-14
162°11,87'E	12:51	1483	54°17,33'N	162°11,80'E				0,00	0,00	SL	Gravity coring	SO201-2-15
	17:25	5191	54°00,14'N	163°19,99'E		Area B /13 Meiji Seamount				PS		SO201-2-16
163°20,00'E	22:00	5252	53°59,90'N	163°19,97'E						HF	Heat Flow	SO201-2-17
	23:37	5370	54°09,03'N	163°23,51'E						PS	SIMRAD profiling, mapping and location of dredge stations	SO201-2-18
163°21,84'E	5:10	5163	54°06,88'N	163°22,26'E			631			DR	Dredging	SO201-2-19
	8:47	5300	54°02,81'N	163°30,19'E						PS	Profiling stopped because of bad weather conditions	SO201-2-20
	2:26	5200	54°00,77'N	163°27,71'E						PS	SIMRAD Profiling	SO201-2-21
163°28,29'E	7:10	4675	54°00,58'N	163°28,97'E			377			DR	Dredging	SO201-2-22
	8:59	3504	54°04,42'N	163°32,55'E						PS	SIMRAD Profiling	SO201-2-23
163°33,52'E	13:58	5054	54°04,40'N	163°33,54'E			299			DR	Dredging	SO201-2-24
163°37,00'E	18:10	4994	54°05,00'N	163°37,00'E						HF	Heat Flow	SO201-2-25
	18:45	5418	54°09,59'N	163°36,53'E						PS	Parasound	SO201-2-26
163°36,50'E	0:00									HF	Heat Flow	SO201-2-27
	1:01	4038	53°53,10'N	163°47,00'E						PS	Parasound	SO201-2-28
163°47,97'E	4:20	3895	53°52,00'N	163°48,13'E						HF	Heat Flow	SO201-2-29

Appendix II

Station No.	Gear	Date (UTC)	Start (UTC)	Water depth (EM120 (m))	Latitude (deg/min)	Longitude (deg/min)	On Bottom (UTC)	Rope length (m)	Water depth (EM120 (m))	Latitude (deg/min)	Longitude (deg/min)	Off Bottom (UTC)	Rope length (m)	Water depth (EM120 (m))	Latitude (deg/min)	
SO201-2-30	PS	12.09.2009	4:37	4026	53°53,33'N	163°50,61'E										
SO201-2-31	CTD-F	12.09.2009	6:39	4290	54°03,69'N	164°10,92'E	6:52	500	4292	54°03,67'N	164°09,40'E					
SO201-2-32	MUC	12.09.2009	7:20	4295	54°03,64'N	164°10,98'E	9:18	4298	4291	54°03,60'N	164°11,01'E					
SO201-2-33	PS	12.09.2009	11:07	4286	54°02,95'N	164°11,11'E										
SO201-2-34	HF	12.09.2009	16:17	2996	53°15,50'N	164°17,43'E	17:16	2996	2996	53°15,45'N	164°17,50'E	17:35	3011	2996	53°15,45'N	
SO201-2-35	PS	12.09.2009														
SO201-2-36	HF	12.09.2009	20:05	3222	53°07,16'N	164°34,48'E	21:09	3223	3223	53°07,16'N	164°34,35'E	21:28	3244	3224	53°07,15'N	
SO201-2-37	PS	12.09.2009	22:38	3226	53°57,11'N	164°34,25'E										
SO201-2-38	HF	13.09.2009	1:01	3214	53°11,34'N	165°05,50'E	2:00	3205	3205	53°11,34'N	165°05,49'E	2:20	3228	3206	53°11,34'N	
SO201-2-39	PS	13.09.2009	3:37	3200	53°11,66'N	164°04,64'E										
SO201-2-40	KL	13.09.2009	5:40	2951	53°18,59'N	164°46,58'E	6:35	2930	2984	53°18,63'N	164°46,67'E	6:39	2874	2984	53°18,64'N	
SO201-2-41	PS	13.09.2009	8:08		53°18,50'N	164°46,49'E										
SO201-2-42	PS	13.09.2009	17:03	6688	54°39,77'N	165°32,21'E										
SO201-2-43	DR	13.09.2009	21:08	4700	54°35,19'N	165°55,77'E	20:47	4708	4694	54°35,20'N	165°35,79'E	0:07	4356	4354	54°34,88'N	
SO201-2-44	DR	14.09.2009	2:50	4922	54°40,24'N	165°50,36'E	4:20	5040	5053	54°40,27'N	165°50,61'E	5:45	4642	4627	54°39,82'N	
SO201-2-45	PS	14.09.2009	7:42	4996	54°40,20'N	165°50,75'E										
SO201-2-46	PS	14.09.2009	19:01	3771	56°06,00'N	166°20,00'E										
SO201-2-47	PS	14.09.2009	23:52	3837	55°55,98'N	166°57,15'E										
SO201-2-48	DR	15.09.2009	7:15	3127	55°21,89'N	167°04,03'E	8:09	3052	3035	55°21,90'N	167°03,96'E	9:12	2748	2782	55°22,27'N	
SO201-2-49	DR	15.09.2009	11:12	2677	55°27,29'N	167°03,80'E	12:08	2667	2634	55°27,31'N	167°03,82'E	12:53	2388	2391	55°27,62'N	
SO201-2-50	PS	15.09.2009	14:50	2387	55°27,66'N	167°03,84'E										
SO201-2-51	DR	15.09.2009	21:24	2600	55°21,02'N	167°09,89'E	22:14	2643	2580	55°21,05'N	167°09,89'E	23:34	2200	2183	55°21,49'N	
SO201-2-52	PS	16.09.2009	2:15	2273	55°21,91'N	167°11,06'E										
SO201-2-53	DR	16.09.2009	5:24	3011	55°13,66'N	167°31,04'E	6:21	3013	3000	55°18,69'N	167°31,07'E	7:45	2490	2430	55°18,16'N	
SO201-2-54	SimRS	16.09.2009	8:55	2516	55°19,26'N	167°30,80'E										
SO201-2-55	DR	16.09.2009	20:02	2374	55°29,22'N	167°12,56'E	20:52	2375	2358	55°29,21'N	167°12,56'E	22:00	1990	2005	55°29,62'N	
SO201-2-56	DR	16.09.2009	23:21	2338	55°26,84'N	167°11,17'E	0:09	2374	2369	55°26,86'N	167°11,11'E	1:06	2005	2025	55°27,11'N	
SO201-2-57	DR	17.09.2009	2:27	2380	55°28,01'N	167°09,51'E	3:11	2409	2377	55°28,02'N	167°09,49'E	4:12	2062	2082	55°28,43'N	
SO201-2-58	DR	17.09.2009	5:28	2459	55°28,19'N	167°05,35'E	6:14	2416	2374	55°28,32'N	167°05,36'E	7:19	2104	2089	55°28,72'N	
SO201-2-59	DR	17.09.2009	8:54	2259	55°24,90'N	167°10,20'E	9:39	2180	2222	55°24,98'N	167°10,35'E	10:40	1820	1798	55°25,10'N	
SO201-2-60	DR	17.09.2009	12:45	2456	55°22,79'N	167°23,10'E	13:39	2461	2431	55°22,80'N	167°23,15'E	14:20	2203	2221	55°23,19'N	
SO201-2-61	DR	17.09.2009	16:35	3943	55°34,08'N	167°16,81'E	17:49	3937	3910	55°34,11'N	167°16,76'E	19:02	3435	3435	55°34,49'N	

Appendix II

Longitude (deg/min)	Station End (UTC)	Water depth EM120 (m)	Latitude (deg/min)	Longitude (deg/min)	Area	Depth interval (m)	Pilot core recovery (m)	Core recovery (m)	Gear	Remarks	Station No.	
	6:15	4289	54°03,60'N	164°10,80'E					PS	Parasound mapping	SO201-2-30	
	7:08	4293	54°03,67'N	164°10,97'E					CTD-F	only Flurometer Data	SO201-2-31	
	11:00	4292	54°03,41'N	164°11,03'E					MUC	Water sampling	SO201-2-32	
	16:23	2997	53°15,48'N	164°17,45'E					PS	Parasound profiling (Heat Flow)	SO201-2-33	
164°17,50'E	18:37	2997	53°15,42'N	164°17,51'E	Area B/14 Meiji Seamount				HF	Heat Flow	SO201-2-34	
											Parasound profiling (Heat Flow)	SO201-2-35
164°34,33'E	22:35	3224	53°07,13'N	164°34,30'E					HF	Heat Flow	SO201-2-36	
	0:49	3219	53°11,47'N	165°05,69'E					PS	Parasound profiling (Heat Flow)	SO201-2-37	
165°05,47'E	3:30	3206	53°11,33'N	165°05,47'E					HF	Heat Flow	SO201-2-38	
												SO201-2-39
164°46,67'E	8:02	2981	53°18,53'N	164°46,54'E				0,25	8,95	KL	piston corer 20 m / damaged core, ca. 8 m retrieved	SO201-2-40
	11:32		53°47,34'N	165°02,61'E						PS	Parasound mapping	SO201-2-41
	21:00	4806	54°35,20'N	165°55,58'E		Area 12				PS	Parasound mapping	SO201-2-42
165°56,46'E	1:45	4383	54°34,77'N	165°56,33'E			340			DR	Dredging	SO201-2-43
165°50,97'E	7:45	4655	54°39,87'N	165°50,97'E	Area 12 Bering Island	426			DR	Dredging	SO201-2-44	
	8:46	6935	54°49,28'N	165°41,67'E	Area 12				PS	Parasound mapping	SO201-2-45	
	23:09	3875	55°56,26'N	166°48,11'E	Area 6 Alpha Fracture Zone				PS	Parasound mapping	SO201-2-46	
	7:12	3108	55°21,79'N	167°04,04'E	Area 7 Massiv Volcanologov				PS	Parasound mapping	SO201-2-47	
167°04,34'E	10:12	2926	55°22,54'N	167°04,14'E			253			DR	Dredging	SO201-2-48
167°03,82'E	13:47	2387	55°27,66'N	167°03,84'E			243			DR	Dredging	SO201-2-49
	20:54	2601	55°23,68'N	167°08,68'E						PS	Parasound mapping	SO201-2-50
167°09,90'E	2:05						397			DR	Dredging, knot in wire with 209 m wire in water	SO201-2-51
	5:53	2296	55°20,73'N	167°25,62'E						PS	Parasound mapping	SO201-2-52
167°30,84'E	8:37	2316	55°19,24'N	167°30,79'E			570			DR	Dredging	SO201-2-53
	18:49	2749	55°26,67'N	167°29,00'E						SimRS	Simrad Survey	SO201-2-54
167°12,75'E	22:40	2047	55°29,64'N	167°12,86'E			353			DR	Dredging	SO201-2-55
167°11,59'E	1:55	2040	55°22,09'N	167°11,56'E			344			DR	Dredging	SO201-2-56
167°09,55'E	4:52	2098	55°28,43'N	167°09,52'E			295			DR	Dredging	SO201-2-57
167°05,61'E	8:04	2065	55°28,78'N	167°05,56'E			285			DR	Dredging	SO201-2-58
167°11,10'E	11:20	1822	55°25,12'N	167°11,18'E			424			DR	Dredging	SO201-2-59
167°22,99'E	15:10	2225	55°23,00'N	167°23,00'E			210			DR	Dredging	SO201-2-60
167°16,33'E	20:15	3425	55°34,62'N	167°16,15'E			475			DR	Dredging	SO201-2-61

Appendix II

Station No.	Gear	Date (UTC)	Start (UTC)	Water depth (EM120 (m))	Latitude (deg/min)	Longitude (deg/min)	On Bottom (UTC)	Rope length (m)	Water depth (EM120 (m))	Latitude (deg/min)	Longitude (deg/min)	Off Bottom (UTC)	Rope length (m)	Water depth (EM120 (m))	Latitude (deg/min)	
SO201-2-62	SimRad	17.09.2009	21:08	3436	55°34,82'N	167°15,91'E										
SO201-2-63	DR	18.09.2009	1:53	4010	55°45,40'N	167°28,40'E	3:05	4012	3978	55°45,44'N	167°28,34'E	4:11	3622	3601	55°45,90'N	
SO201-2-64	PS	18.09.2009	5:41	3709	55°45,88'N	167°28,03'E										
SO201-2-65	PS	18.09.2009	11:35	3940	56°00,04'N	169°00,20'E										
SO201-2-66	CTD-F	18.09.2009	14:22	3917	56°04,10'N	169°14,21'E	14:27	150	3917	56°04,10'N	169°14,16'E					
SO201-2-67	CTD	18.09.2009	14:49	3919	56°04,10'N	169°14,22'E	15:09	1000	3919	56°04,09'N	169°14,21'E	15:42				
SO201-2-68	MUC	18.09.2009	16:05	3920	56°04,12'N	169°14,19'E	17:41	3915	3919	56°04,13'N	169°14,11'E	17:42	3922			
SO201-2-69	KL	18.09.2009	20:23	3913	56°04,15'N	169°14,14'E	21:36	3899	3924	56°04,14'N	169°14,22'E	21:37	3887	3918	56°04,14'N	
SO201-2-70	PS	18.09.2009	23:17	3938	56°04,34'N	169°14,37'E										
SO201-2-71	DR	19.09.2009	3:01	3651	56°29,17'N	169°36,46'E	4:04	3681	3668	56°29,20'N	169°36,50'E	5:15	3280	3281	56°29,32'N	
SO201-2-72	PS	19.09.2009	6:30	3289	56°29,33'N	169°35,65'E										
SO201-2-73	DR	19.09.2009	8:54	3720	56°16,83'N	169°39,16'E	10:04	3700	3677	56°16,85'N	169°39,18'E	11:21	3111	3074	56°17,32'N	
SO201-2-74	DR	19.09.2009	14:27	2531	56°15,03'N	169°52,90'E	15:14	2525	2517	56°15,07'N	169°52,83'E	16:14	2220	2199	56°15,38'N	
SO201-2-75	PS	19.09.2009	17:26	2800	56°15,00'N	169°59,00'E										
SO201-2-76	MUC	19.09.2009	22:35	2133	56°19,79'N	170°41,96'E	23:10		2137	56°19,80'N	170°41,96'E	23:21		2130	56°19,80'N	
SO201-2-77	KL	20.09.2009	0:52	2130	56°19,82'N	170°41,93'E	1:34	2110	2135	56°19,83'N	170°41,98'E					
SO201-2-78	PS	20.09.2009	3:17	2075	56°24,21'N	170°38,61'E										
SO201-2-79	MUC	20.09.2009	6:45	1150	56°43,12'N	170°29,85'E	7:23	1159	1161	56°42,99'N	170°29,78'E	7:24		1160		
SO201-2-80	KL	20.09.2009	9:23	1159	56°42,97'N	170°29,80'E	9:50	1137	1159	56°42,98'N	170°29,74'E					
SO201-2-81	KL	20.09.2009	12:31	1164	56°42,99'N	170°29,77'E	12:59	1133	1161	56°42,99'N	170°29,77'E					
SO201-2-82a	PS	20.09.2009														
SO201-2-82b	PS	20.09.2009	22:08	920	57°32,83'N	170°06,92'E										
SO201-2-83	MUC	21.09.2009	2:27	972	57°30,25'N	170°24,84'E	2:57	972	970	57°30,28'N	170°24,82'E	3:02	970			
SO201-2-84	KL	21.09.2009	4:32	968	57°30,31'N	170°24,77'E	4:56	943	943	57°30,31'N	170°24,79'E					
SO201-2-85	KL	21.09.2009	7:41	975	57°30,30'N	170°24,79'E	8:05	941	968	57°30,30'N	170°24,77'E	8:06		967		
SO201-2-86	PS	21.09.2009	8:58	967	57°30,13'N	170°24,25'E										
SO201-2-87	DR	21.09.2009	10:31	965	57°30,47'N	170°01,90'E	10:32	959	959	57°30,47'N	170°06,19'E	11:47	697	694	57°30,49'N	
SO201-2-88	DR	21.09.2009	15:08	1160	57°34,10'N	170°05,27'E	15:31	1165	1158	57°34,09'N	170°05,32'E	16:18	838	835	57°34,24'N	
SO201-2-89	PS	21.09.2009	16:49	837	57°34,22'N	170°05,93'E										

Appendix II

Longitude (deg/min)	Station End (UTC)	Water depth EM120 (m)	Latitude (deg/min)	Longitude (deg/min)	Area	Depth interval (m)	Pilot core recovery (m)	Core recovery (m)	Gear	Remarks	Station No.
	1:46	4099	55°45,10'N	167°28,80'E					SimRS	Simrad Survey, Mapping, locating of dredge site	SO201-2-62
167°28,29'E	5:29	3721	55°45,90'N	167°28,25'E	Area 7 Alpha fracture Zone	377			DR	Dredging	SO201-2-63
	6:59	3912	55°42,15'N	167°44,94'E	Area 7 Massiv Volcanologov				SimRS	EM120 Profiling	SO201-2-64
	12:43	3928	56°04,08'N	169°14,56'E	Area A				PS	Border of working Area E, profiling	SO201-2-65
	14:35	3915	56°04,09'N	169°14,21'E					CTD-F	Flurometer	SO201-2-66
	15:42	3918	56°04,12'N	169°14°16,00'E	Shirshov Ridge				CTD	water sampling	SO201-2-67
	19:23	3912	56°04,19'N	169°14,16'E	Kommandorsky Basin				MUC	3 Rohre nicht ausgelöst, 5 Rohre voll, 4 Rohre leer, Videosystem bei 2360m ausgefallen	SO201-2-68
169°14,22'E	23:03	3940	56°04,17'N	169°14,21'E	Kommandorsky Basin		0,60	6,75	KL	piston corer 10 m	SO201-2-69
	2:44	3650	56°29,07'N	169°38,60'E	Area E				PS	Mapping, transit to next dredge station	SO201-2-70
169°35,66'E	6:21	3283	56°29,31'N	169°39,71'E		387			DR	Dredging	SO201-2-71
	8:45	3526	56°16,48'N	169°39,58'E					PS	Mapping for dredging	SO201-2-72
169°39,33'E	12:31	3092	56°17,32'N	169°39,24'E	Area E Shirshov Ridge	603			DR	Dredging	SO201-2-73
169°52,25'E	17:05	2209	56°15,37'N	169°52,16'E		318			DR	Dredging	SO201-2-74
	21:22	2064	56°26,03'N	170°37,23'E					PS	Parasound profiling	SO201-2-75
170°41,96'E	22:49	2132	56°19,78'N	170°41,96'E					MUC	Close to IODP site	SO201-2-76
	2:36	2163	56°19,90'N	170°41,97'E			0,90	11,78	KL	piston corer 15 m, close to IODP site	SO201-2-77
	6:42	1175	56°43,02'N	170°29,93'E					PS	Parasound profiling	SO201-2-78
	8:07	1164	56°42,99'N	170°29,80'E					MUC	with camera, (Site 13)	SO201-2-79
	10:42	1160	56°43,00'N	170°29,78'E	Area E Shirshov Ridge		0,86	12,20	KL	piston corer 15 m, overpenetrated	SO201-2-80
	13:50	1165	56°42,99'N	170°29,63'E			0,17	17,55	KL	piston corer 20 m	SO201-2-81
	22:08	920	57°32,80'N	170°06,93'E					PS	Parasound profiling	SO201-2-82a
	1:13	1002	57°34,03'N	170°07,88'E					PS	Mapping for dredging	SO201-2-82b
	3:31	972	57°30,30'N	170°24,80'E					MUC	MUC with camera	SO201-2-83
	5:34	976	57°30,32'N	170°24,77'E			0,00	18,00	KL	piston corer, Pilotcore nicht funktioniert, kein Kerngewinn, nur Oberflächenprobe	SO201-2-84
	8:49	967	57°30,31'N	170°24,75'E			0,00	18,13	KL	piston corer 20 m	SO201-2-85
	10:29	968	57°30,47'N	170°06,18'E					PS	Mapping for dredging	SO201-2-86
170°07,01'E	12:08	698	57°30,49'N	170°07,06'E		265			DR	Dredging	SO201-2-87
170°05,89'E	16:40	837	57°34,23'N	170°05,90'E		323			DR	Dredging	SO201-2-88
	2:29	1638	58°43,00'N	171°23,72'E					PS	Parasound profiling	SO201-2-89

Appendix II

Station No.	Gear	Date (UTC)	Start (UTC)	Water depth (deg/min) EM120 (m)	Latitude (deg/min)	Longitude (deg/min)	On Bottom (UTC)	Rope length (m)	Water depth (deg/min) EM120 (m)	Latitude (deg/min)	Longitude (deg/min)	Off Bottom (UTC)	Rope length (m)	Water depth (deg/min) EM120 (m)	Latitude (deg/min)
SO201-2-90	MUC-TV	22.09.2009	2:37	1614	58°43,00'N	171°23,75'E	3:22	1621	1616	58°42,01'N	171°23,77'E	3:24	1606	1616	58°42,01'N
SO201-2-91	PS	22.09.2009	4:13	1614	58°43,02'N	171°23,75'E									
SO201-2-92	CTD-F	22.09.2009	6:02	3116	58°46,04'N	171°55,02'E	6:15	300	3123	58°46,03'N	171°54,91'E				
SO201-2-93	CTD	22.09.2009	6:29	3116	58°45,98'N	171°54,85'E	7:42	3115	3117	58°46,01'N	171°55,01'E				
SO201-2-94	MN	22.09.2009	9:25	3115	58°46,02'N	171°54,95'E	10:00	1000	3117	58°46,01'N	171°55,10'E				
SO201-2-95	PS	22.09.2009	11:03	3145	58°45,97'N	171°55,04'E									
SO201-2-96	atersampl	22.09.2009	15:03	659	58°55,12'N	170°44,45'E	15:21	652	664	58°55,12'N	170°44,45'E				
SO201-2-97	MN	22.09.2009	15:59	650	58°55,14'N	170°44,46'E	16:24	600	650	58°55,12'N	170°44,53'E				
SO201-2-98	PS	22.09.2009	17:30	630	58°53,26'N	170°42,26'E									
SO201-2-99	MUC-TV	22.09.2009	19:22	643	58°52,52'N	170°41,40'E	19:50		643	58°52,53'N	170°41,48'E				
SO201-2-100	KL	22.09.2009	21:22	630	58°52,55'N	170°41,43'E	21:29	606	630	58°52,55'N	170°41,40'E	21:39		630	58°52,55'N
SO201-2-101	KL	22.09.2009	23:30	630	58°52,52'N	170°41,45'E	0:06	607	630	58°52,52'N	170°41,45'E	0:07	607	630	58°52,52'N
SO201-2-102	PS	23.09.2009	0:53	620	58°52,51'N	170°40,68'E									
SO201-2-103	DR	23.09.2009	5:37	1614	58°44,15'N	169°53,33'E	6:07	1609	1587	58°44,17'N	169°53,33'E	8:02	1375	1353	58°44,28'N
SO201-2-104	PS	23.09.2009	8:51	1405	58°44,21'N	169°53,75'E									
SO201-2-105	DR	23.09.2009	11:27	2087	58°31,69'N	169°51,38'E	12:07	2120	2078	58°31,77'N	169°51,36'E	13:37	1508	1520	58°31,87'N
SO201-2-106	PS	23.09.2009	14:30	1690	58°31,49'N	169°52,40'E									
SO201-2-107	DR	23.09.2009	18:00	2737	58°16,59'N	169°41,77'E	18:51	2736	2742	58°16,58'N	169°41,85'E	19:46	2399	2412	58°16,64'N
SO201-2-108	PS	23.09.2009	20:46	2426	58°16,48'N	169°42,37'E									
SO201-2-109	CTD-F	24.09.2009	7:26	3535	58°35,68'N	168°17,84'E	7:34	300	3535	58°35,68'N	168°17,84'E				
SO201-2-110	CTD	24.09.2009	7:50	3537	58°35,69'N	168°17,86'E	9:13	3536	3537	58°35,65'N	168°17,81'E				
SO201-2-111	MN	24.09.2009	11:15	3535	58°35,71'N	168°17,79'E	11:48	1000	3535	58°35,69'N	168°17,90'E				
SO201-2-112	PS	24.09.2009	18:07	1700	59°07,91'N	167°00,64'E									
SO201-2-113	MUC-TV	24.09.2009	23:34	1393	59°13,86'N	166°59,25'E	0:10	1398	1392	59°13,86'N	166°59,24'E	0:11		1392	59°13,86'N
SO201-2-114	KL	25.09.2009	1:37	1394	59°13,84'N	166°59,33'E	2:21	1376	1417	59°13,87'N	166°59,32'E				
SO201-2-115	KL	25.09.2009	5:13	725	59°19,50'N	166°47,75'E	5:58	702	726	59°19,51'N	166°47,75'E				
SO201-2-116	MUC-TV	25.09.2009	7:08	725	59°19,50'N	166°47,70'E	7:03		725	59°19,51'N	166°47,70'E	7:35		724	59°19,51'N
SO201-2-117	PS	25.09.2009	16:13	3600	58°01,79'N	166°07,32'E									
SO201-2-118	DR	25.09.2009	18:24	3584	57°54,43'N	165°57,62'E	19:43	3590	3554	57°54,52'N	165°57,82'E	20:45	3141	3124	57°54,81'N
SO201-2-119	PS	26.09.2009	9:12	3374	56°55,62'N	165°04,78'E									
SO201-2-120	PS	28.09.2009	11:38	5190	54°26,28'N	163°27,05'E									
SO201-2-121	DR	28.09.2009	13:22	5697	54°18,53'N	163°25,98'E	15:03	5703	5660	54°18,56'N	163°25,96'E	16:11	5314	5303	54°18,95'N
SO201-2-122	DR	28.09.2009	20:38	5662	54°01,08'N	163°17,31'E	22:21	5600	5569	54°01,12'N	163°17,51'E	23:32	5238	5238	54°01,55'N

Appendix II

Longitude (deg/min)	Station End (UTC)	Water depth EM120 (m)	Latitude (deg/min)	Longitude (deg/min)	Area	Depth interval (m)	Pilot core recovery (m)	Core recovery (m)	Gear	Remarks	Station No.	
171°22,75'E	4:12	1610	58°43,03'N	171°23,75'E	Area E Shirshov Rücken				MUC-TV		SO201-2-90	
	5:55	3118	58°45,79'N	171°54,81'E						PS	Parasound profiling	SO201-2-91
	6:22	3117	58°46,87'N	171°54,88'E						CTD-F		SO201-2-92
	8:55	3116	58°46,02'N	171°54,98'E						CTD		SO201-2-93
	10:57	3117	58°84,60'N	171°55,22'E						MN		SO201-2-94
	14:58	660	58°55,15'N	170°44,47'E						PS	No images taken after 14:06, because of PC failure	SO201-2-95
	15:45	659	58°55,14'N	170°44,46'E						Watersampling		SO201-2-96
	17:03	650	58°55,11'N	170°44,50'E						MN		SO201-2-97
	19:21	643	58°52,57'N	170°41,89'E						PS	The control PC was out of control for 10:15 min of survey	SO201-2-98
	20:15	630	58°52,55'N	178°41,46'E						MUC-TV		SO201-2-99
170°41,40'E	22:00	630	58°52,53'N	170°41,42'E				0,73	17,54	KL	piston core 20 m	SO201-2-100
170°41,45'E								0,57	18,32	KL		SO201-2-101
										PS		SO201-2-102
169°53,72'E	8:37	1406	58°44,19'N	169°53,77'E			234			DR	Dredge got stuck	SO201-2-103
										PS		SO201-2-104
169°52,30'E	14:15	1499	58°31,89'N	169°52,39'E			558			DR	Dredging	SO201-2-105
	17:38	2401	50°14,37'N	169°42,41'E						PS	EM120 Profiling for Dredging	SO201-2-106
169°42,46'E	20:35	2392	58°16,68'N	169°42,48'E			330			DR	Dredging	SO201-2-107
	5:54	3565	58°35,65'N	168°17,86'E						PS	Parasound profiling for sediment coring	SO201-2-108
	7:41	3535	58°35,68'N	168°17,85'E					CTD-F	E-NW Corner Fluorometer	SO201-2-109	
	10:50	3534	58°35,68'N	168°17,80'E					CTD	water sampling	SO201-2-110	
	12:48	3535	58°35,69'N	168°17,90'E					MN	E-NW Corner	SO201-2-111	
	21:54	700	59°20,60'N	166°47,70'E					PS	Parasound profiling for coring site	SO201-2-112	
166°59,24'E	0:50	1393	59°13,85'N	166°59,26'E	Area D				MUC-TV	Area D, Ausfall der Kamera ab Einsetzen des MUC, keine Eindringung nur Oberfläche gewonnen viel IIRD	SO201-2-113	
	3:17	1401	59°13,65'N	166°59,73'E	Area D		1,00	7,89	KL	Piston core 10 m	SO201-2-114	
	6:30	726	59°19,51'N	166°47,72'E	Area D		0,74	4,22	KL	Piston core 15 m	SO201-2-115	
166°47,70'E	8:01	731	59°19,55'N	166°47,78'E	Area D				MUC-TV	nicht ausgelöst wegen zu hartem Untergrund	SO201-2-116	
	17:58	3603	57°97,74'N	165°50,75'E	Area 3 Kommandorsky Basin				PS	EM120 Profiling for Dredging	SO201-2-117	
165°58,41'E	21:49	3205	57°54,84'N	165°58,68'E	Area 3 Kommandorsky Basin	430			DR	Dredging	SO201-2-118	
	14:50	3507	57°12,80'N	163°47,88'E	Area 5				PS		SO201-2-119	
	12:53	5831	54°16,57'N	163°23,58'E	Area B Meiji Seamount				PS	EM120 profiling	SO201-2-120	
163°25,54'E	18:23	5275	54°19,03'N	163°29,38'E	Area B Meiji Area / trench	357			DR	Dredging	SO201-2-121	
163°18,03'E	1:31	5239	54°01,62'N	163°18,09'E	Area B Meiji Seamount	331			DR	Dredging	SO201-2-122	

Appendix II

Station No.	Gear	Date (UTC)	Start (UTC)	Water depth (EM120 (m))	Latitude (deg/min)	Longitude (deg/min)	On Bottom (UTC)	Rope length (m)	Water depth (EM120 (m))	Latitude (deg/min)	Longitude (deg/min)	Off Bottom (UTC)	Rope length (m)	Water depth (EM120 (m))	Latitude (deg/min)
SO201-2-123	DR	29.09.2009	3:16	4576	53°54,39'N	163°33,76'E	4:35	4556	4536	53°54,38'N	163°33,79'E	5:52	4072	4072	53°53,97'N
SO201-2-124	PS	29.09.2009	7:31	4139	53°54,09'N	163°34,24'E									
SO201-2-125	PS	29.09.2009	18:47	3350	54°42,11'N	162°44,06'E									
SO201-2-126	MUC	29.09.2009	0:42	1440	54°23,70'N	162°13,33'E	1:15	1451	1443	54°23,64'N	162°13,37'E	1:17	0	1440	54°23,65'N
SO201-2-127	KL	30.09.2009	2:21	1443	54°23,66'N	162°13,36'E	3:15	1415	1440	54°23,66'N	162°13,34'E	3:07	1408	1441	54°23,66'N
SO201-2-128	MN	30.09.2009													
SO201-2-129	MN	30.09.2009	9:11	3658	53°54,54'N	161°50,02'E	9:44	1000	3658	53°54,51'N	161°49,96'E				
SO201-2-130	PS	30.09.2009	11:08	3662	53°54,39'N	161°50,39'E	16:42			53°25,00'N	163°04,15'E	16:53			53°15,00'N
END															

Appendix II

Longitude (deg/min)	Station End (UTC)	Water depth EM120 (m)	Latitude (deg/min)	Longitude (deg/min)	Area	Depth interval (m)	Pilot core recovery (m)	Core recovery (m)	Gear	Remarks	Station No.
163°34,34'E	7:20	4139	53°54,09'N	163°34,24'E	Area B Meji Seamount	464			DR	Dredging	SO201-2-123
	14:16	6055	53°59,97'N	163°09,96'E	Area B Meji Seamount				PS	EM120 profiling	SO201-2-124
	0:25	1387	54°23,56'N	162°11,79'E	Area B Meji Seamount				PS	Parasound profiling for core site	SO201-2-125
162°13,34'E	2:05	1440	54°23,65'N	162°13,33'E	Area B				MUC	ohne TV	SO201-2-126
162°13,37'E	4:07	1444	54°23,70'N	162°13,51'E	Area B Krontosky Peninsula		0,90	5,54	KL	Piston core 15 m	SO201-2-127
									MN	Failure of the engine	SO201-2-128
	10:49	3662	53°54,56'N	161°41,61'E	Area B				MN	Same station as 201-2-3 MN, Repetition	SO201-2-129
162°20,00'E	19:38	6966	53°15,00'N	01°62,20'E	Area B					Parasound mapping	SO201-2-130
							8,65	164,01			END

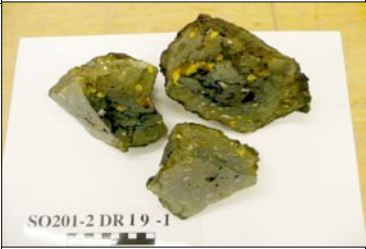
Appendix III
Sampling Summary Dredges

Appendix III

Type	Stat.	Location	total volume	Rock summary	on bottom lat °N long °E	off bottom lat °N long °E	depth (m) max min	Mag rock	Mn rock	Sed rock	Volcani- clastics
DR	19	Meiji Seamount (Area B)	few rocks	sedimentary rocks, dropstones	54,119 163,353	54,115 163,364	5805 5174	0	0	1	0
DR	22	Meiji Seamount (Area B)	full	lavas, volcanoclastics, sedimentary rocks	54,012 163,469	54,009 163,472	4958 4581	1	0	1	1
DR	24	Meiji Seamount (Area B)	few rocks	sedimentary rocks	54,073 163,548	54,074 163,559	5372 5073	0	0	1	0
DR	43	South of Bering Island (Area 12)	few rocks	sedimentary rocks, dropstones	54,587 165,597	54,581 165,941	4694 4354	0	0	1	0
DR	44	South of Bering Island (Area 12)	few rocks	sedimentary rocks	54,671 165,844	54,664 165,85	5053 4627	0	0	1	0
DR	48	Volcanologist's Massif (Area 7)	1/4 full	lavas, dropstones	55,365 167,066	55,371 167,072	3035 2782	1	0	0	0
DR	49	Volcanologist's Massif (Area 7)	???	lavas	55,455 167,064	55,46	2634 2391	1	0	0	0
DR	51	Volcanologist's Massif (Area 7)	1/4 full	lavas	55,351 167,165	55,358 167,165	2580 2200	1	0	0	0
DR	53	Volcanologist's Massif (Area 7)	1/4 full	(pillow) Lavas, dropstones, Mn crusts	55,312 167,518	55,319 167,514	3000 2490	1	1	0	0
DR	55	Volcanologist's Massif (Area 7)	1/6 full	lavas	55,487 167,209	55,327 167,213	2375 1990	1	0	0	0
DR	56	Volcanologist's Massif (Area 7)	few rocks	lavas, dropstones	55,448 167,185	55,452 167,193	2369 2025	1	0	0	0
DR	57	Volcanologist's Massif (Area 7)	few rocks	lavas	55,467 167,158	55,474 167,159	2377 2082	1	0	0	0
DR	58	Volcanologist's Massif (Area 7)	few rocks	lavas	55,472 167,089	55,479 167,094	2374 2089	1	0	0	0
DR	59	Volcanologist's Massif (Area 7)	1/3 full	lavas, volcanic bombs?, dropstones	55,416 167,173	55,418 167,185	2186 1798	1	0	0	1
DR	60	Volcanologist's Massif (Area 7)	1/4 full	lavas, light pumice, dropstones	55,380 167,386	55,387 167,383	2431 2221	1	0	0	1
DR	61	Volcanologist's Massif (Area 7)	1/4 full	lavas, volcanoclastics, Mn crusts	55,569 167,279	55,574 167,256	3910 3435	1	1	0	1
DR	63	Alpha Fracture Zone (Area 7)	1/4 full	sedimentary rocks, Mn crusts	55,757 167,472	55,757 167,473	3978 3601	0	1	1	0
DR	71	Shirshov Ridge South (Area E)	few rocks	lavas, intrusiva (may be dropstones)	56,487 169,608	56,489 169,594	3681 3280	0	0	0	0
DR	73	Shirshov Ridge South (Area E)	few rocks	tectonized lavas and tuffs	56,281 169,653	56,289 169,656	3677 3074	1	0	0	0
DR	74	Shirshov Ridge South (Area E)	1/6 full	sedimentary rocks, Mn crusts, dropstones	56,251 169,881	56,256 169,871	2517 2199	0	1	1	0
DR	87	Shirshov Ridge Central (Area E)	full	lavas, volcanoclastics, dropstones	57,508 170,105	57,508 170,117	945 694	1	0	0	1
DR	88	Shirshov Ridge Central (Area E)	1/2 full	lavas, volcanoclastics, sedimentary rocks, sponges	57,568 170,089	57,571 170,098	1158 835	1	0	1	1
DR	103	Shirshov Ridge North (Area E)	1/6 full	metamorphic rocks, dropstones	58,736 169,889	58,738 169,895	1587 1353	1	0	0	0
DR	105	Shirshov Ridge North (Area E)	1/6 full	metamorphic rocks, dropstones	58,530 169,855	58,531 169,872	2078 1520	1	0	0	0
DR	107	Shirshov Ridge North (Area E)	few rocks	sedimentary rocks	58,276 169,698	58,277 169,708	2742 2412	0	0	1	0
DR	118	Kommandorkyi Basin (Area 3)	1/6 full	lavas, dropstones	57,909 165,964	57,914 165,974	3554 3124	1	0	0	0
DR	121	Meiji Area (Area B)	few rocks	most likely dropstones	54,309 163,433	54,316 163,426	5660 5303	0	0	0	0
DR	122	Meiji Seamount (Area B)	few rocks	sediments, dropstones	54,019 163,292	54,026 163,301	5569 5238	0	0	0	0
DR	123	Meiji Seamount (Area B)	1/4 full	sedimentary rocks	53,906 163,563	53,9	4536 4072	0	0	1	0
Total:								18	4	10	6

Appendix IV
Rock Description

Appendix IV

SO201-2-DR19												
Location: Area B, Meiji Seamount												
Dredge on bottom UTC 10/09/09 1:49hrs, lat 54°7.15'N, long 163°21.16'E, depth 5805m												
Dredge off bottom UTC 10/09/09 3:20hrs, lat 54°6.91'N, long 163°21.84'E, depth 5174m												
Total volume: some rocks												
Comments: 1 large piece of lava, solidified sediments, altered ultramafic (?) rocks, sandstones												
SAMPLE #	SAMPLE DESCRIPTION	TS	CHEM	Ar	Rest	GU/MIN	ARCH	VULC	SED	MIN	NOTES	SAMPLE PHOTOS
DR19-1	<p>1. Rock Type: Volcanic moderately altered rock, lava</p> <p>2. Size: ca. 30x30x30 cm</p> <p>3. Shape/Angularity: subangular</p> <p>4. Color: Dark grey, somewhat yellowish at ca. 3 cm altered margin</p> <p>5. Rock texture: Almost aphyric with rare Pl microphenocrysts (ca. 0.5 mm), well crystallized groundmass. Vesicularity ca. 20 % heterogeneously distributed. Vesicles are highly variable in size from mm-sized up to 2x5 cm filled with monocrystalline to polymorphic color-less to honey-yellow calcite, some voids are open.</p> <p>6. Phenocrysts: Pl microphenocrysts up to ca. 0.5 mm</p> <p>7. Matrix: well crystallized to doleritic</p> <p>8. Secondary Minerals: chlorite in groundmass</p> <p>9. Encrustations: Very thin Fe-Mn crust (0.5 mm or less)</p> <p>10. Comment: Inner parts maybe good for chemistry. Careful picking required to avoid vesicles. Depending on XRF data the rock maybe good for Ar-Ar dating. This is a single block or lava, perhaps, basalt, which maybe in situ volcanic rock. It cannot be excluded however that this block of crust was formerly a part of Kamchatka forearc merged with Meiji when the trench jumped to the west.</p>	x	x					x			+ 2 TS to D.Savelyev and N.Tsukanov	
DR19-2	<p>1. Rock Type: Very dense massive carbonate (?) rock of unclear origin</p> <p>2. Size: 20x10x10</p> <p>3. Shape/Angularity: rounded</p> <p>4. Color: Light greenish grey</p> <p>5. Rock texture: massive ophitic</p> <p>6. Phenocrysts: none</p> <p>7. Matrix: none</p> <p>8. Secondary Minerals: none</p> <p>9. Encrustations: carbonate crust with clay fragments</p> <p>10. Comment: High density suggests ultramafic protolith, maybe harzburgite or dunite fragment completely replaced with carbonate. Or it maybe sedimentary rock by origin - a limestone inclusion in clay. Definitely in-situ rock.</p>	x	x								+ 2 TS to D.Savelyev and N.Tsukanov	
DR19-3	<p>1. Rock Type: Similar to DR19-2</p> <p>2. Size: 20x15x5</p> <p>3. Shape: rounded</p> <p>5. Rock texture: Has a 'fluidal' texture formed by network of very thin subparallel veins</p>	x									+ 1 TS to D.Savelyev	
DR19-4	<p>1. Rock Type: similar to sample #2 and 3, 'inclusion' in coarse grained calcite cement</p> <p>2. Size: 10x5x4</p> <p>3. Shape/Angularity: subrounded</p> <p>4. Color: dark grey slightly brownish</p> <p>5. Rock texture: dense massive</p>	x									+ 1 TS to D.Savelyev	
DR19-5	<p>1. Rock Type: Dense rock composed by intergrowths of large elongate crystals.</p> <p>2. Size: 12x7x4</p> <p>3. Shape/Angularity: rounded</p> <p>4. Color: light greenish grey</p> <p>5. Rock texture: crystalline - the rock is entirely composed by intergrowths of crystals</p> <p>10. Comment: The origin of this rock is not clear. This can be completely reworked volcanic/intrusive rock replaced by actinolite or epidote (?).</p>	x									+ 1 TS to D.Savelyev	
DR19-6	<p>1. Rock Type: Dense coarse grained rock</p> <p>2. Size: 10x15x5</p> <p>3. Shape/Angularity: rounded</p> <p>4. Color: light greenish grey</p> <p>5. Rock texture: massive, looks amorphous, coarse grained crystalline crust</p> <p>10. Comment: the rock was included in clay</p>	x									+ 1 TS to D.Savelyev	

Appendix IV

SAMPLE #	SAMPLE DESCRIPTION	TS	CHEM	Ar	Rest	GL/MIN	ARCH	VULC	SED	MIN	NOTES	SAMPLE PHOTOS
DR19-7S	1. Rock Type: Massive plate-joined volcanogenic sandstone 2. Size: 70x20x7 3. Shape/Angularity: angular 4. Color: dark grey 5. Rock texture: middle grained with poor layering 6. Phenocrysts: contains grains of plag, cpx, hbl (?) 8. Secondary Minerals: chloritization 10. Comment: contains prints of plants (?) - must be shown to paleontologist!	x							x		1 TS to N.Tsukanov	
DR19-8S	1. Rock Type: Volcanogenic sandstone, similar to # 7S but more fine-grained 2. Size: 30x30x20 3. Shape/Angularity: angular 4. Color: dark grey 5. Rock texture: massive with poor layering, fine grained with rare clasts up to 1.5 mm 10. Comment: clasts up to 1.5 mm, has no flora prints. D.Savelyev suggests that 7S and 8S may come from Kronotskaya Series in Kamchatka.	x							x		1 TS to N.Tsukanov	
DR19-9S	1. Rock Type: Allevrolite 2. Size: 20x15x8 3. Shape/Angularity: angular 4. Color: light greenish grey 10. Comment: Very common type of rock in DR19, comprises about 1/2 of total volume - clearly in situ rock.	x							x			
DR19-10S	1. Rock Type: Similar to #9S but has a clearly layered zone 2. Size: 10x10x7 3. Shape/Angularity: angular 5. Rock texture: massive to layered in the middle part of the sample. The layered zone is 1 cm thick and composed by several more to less coarse-grained 1 mm layers .	x							x			
DR19-11S	1. Rock Type: Dense coarse grained rock 2. Size: 10x10x10 3. Shape/Angularity: rounded 4. Color: greenish grey at the margin to grey in the core. 10. Comment: this rock looks like crystalline calcite which concentrically overgrew rock of other type in the core.	x							x			
DR19-1-X	Backup of sample DR19-1							x	x			
DR19-7S-X	Backup of sample DR19-7S							x		x		

SO201-2-DR22


Location: Area B, Meiji Seamount. Western slope, 2nd step, from lower slope to top at small 'noose'

Dredge on bottom UTC 11/09/09 04:01hrs, lat 54°00,72'N, long 163°28,12'E, depth 4958m








Dredge off bottom UTC 11/09/09 05:30hrs, lat 54°00,53'N, long 163°28,29'E, depth 4581m

Total volume: Full






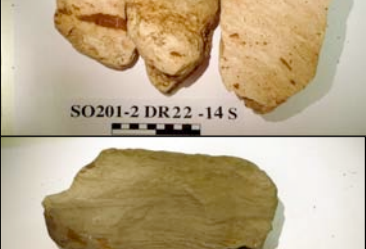

Comments: Several large blocks and numerous fragments of pillow lavas and sediments. No dropstones.

SAMPLE #	SAMPLE DESCRIPTION	TS	CHEM	Ar	Rest	GL/MIN	ARCH	VULC	SED	MIN	NOTES	Sample Photos
DR22-1	1. Rock Type: Volcanic moderately altered rock 2. Size: 30x30x30 3. Shape/Angularity: Angular 4. Color: Dark grey to blueish grey 5. Rock texture: Massive homogeneous Pl-phyr. No vesicules. 6. Phenocrysts: Plag - ca. 30%, 2-3 mm in size, appears to be altered. 7. Matrix: Well crystallized (= doleritic). 8. Secondary Minerals: Calcite and hematite fillings of veins (up to 1 mm thick). Secondary minerals after plag (chlorite, albite ?) 9. Encrustations: Thin Fe-Mn hydroxide crust, Fe-oxides and calcite in veins. 10. Comment: The sample was taken from one of two large blocks, which looked identically with regard to rock type and alteration (maybe two halves of the same larger block). This rock can be inner	x	x					x			1 TS N.Tsukanov	

Appendix IV

SAMPLE #	SAMPLE DESCRIPTION	TS	CHEM	Ar	Rest	GL/MI	N	ARCH	VULC	SED	MIN	NOTES	Sample Photos
DR22-2	<ol style="list-style-type: none"> 1. Rock Type: Volcanic, fragment of pillow lava, moderately to strongly altered. 2. Size: 20x20x15 3. Shape/Angularity: Subangular 4. Color: Dark grey 5. Rock texture: Massive, almost aphyric, slightly vesicular (<=5%), voids filled with calcite. 6. Phenocrysts: none 7. Matrix: Cryptocrystalline (or hyalopilitic). Outer margin is glassy. Glass was not preserved and replaced with yellow palagonite 8. Secondary Minerals: palagonite after glass 9. Encrustations: Rare limestone filling of cracks up to 5 mm thick 10. Comment: This sample is representative for the predominant type of rocks in the dredge DR22. A lot of pillow fragments (slightly petrographically variable but all with outer pillow margin) were taken as archive sample DR22-18X 	x	x						x				
DR22-3	<ol style="list-style-type: none"> 1. Rock Type: Volcanic, fragment of pillow lava similar to sample no. DR22-2 2. Size: ca. 15x12x10 3. Shape/Angularity: Subangular 4. Color: Dark grey 5. Rock texture: Vesicular rare ol-phyric, vesicles are open 6. Phenocrysts: Ol - <2% up to 1 mm, replaced with Fe-oxides; rare Spl phenocrysts <<1% up to 0.3 mm 7. Matrix: Microcrystalline/hyalopilitic 8. Secondary Minerals: Palagonite, Fe oxides 10. Comment: maybe good for chemistry. Petrographically similar fragments of pillow basalts were placed as archive sample 18X and should be used to separate spinel crystals if necessary. 	x	x						x			1 TS to N.Tsukanov	
DR22-4	<ol style="list-style-type: none"> 1. Rock Type: Fragment of pillow lava similar to sample no. 2,3 2. Size: 20x15x10 3. Shape/Angularity: subangular 4. Color: dark grey 5. Rock texture: almost aphyric, visicular 6. Phenocrysts: rare Ol <1% 7. Matrix: hyalopilitic 8. Secondary Minerals: Palagonite replacing glass, Fe-hydroxides 9. Encrustations: Limestone filling cracks 10. Comment: Large surface of pillow, glass not preserved. Needs careful picking prior powdering to avoid limestone and vesicles. Analogs can be found in archive DR22-18X 	x	x						x				
DR22-5	<ol style="list-style-type: none"> 1. Rock Type: Massive volcanic rock, moderately altered 2. Size: 20x15x15 3. Shape/Angularity: Rounded 4. Color: Brownish grey 5. Rock texture: Massive doleritic with rare Pl phenocrysts 6. Phenocrysts: Pl - ca. 5% up to 5 mm long, altered (?) 7. Matrix: Doleritic, plag maybe fresh (xls <=1 mm) 8. Secondary Minerals: chlorite hematite 9. Encrustations: thin Fe-Mn hydroxide crust, limestone fragments on the surface 10. Comment: the sample represents several large blocks of petrographically similar rocks, maybe good for chemistry and Ar-Ar dating of groundmass. 	x	x						x			1 TS to N.Tsukanov	
DR22-6	<ol style="list-style-type: none"> 1. Rock Type: Massive volcanic rock moderately altered, overall similar to sample no. 5 but has more fine-grained groundmass. 2. Size: 20x10x8 3. Shape/Angularity: subrounded 4. Color: dark grey 5. Rock texture: rare Pl-phyric, slightly visicular, 2-3% vesicules filled with calcite 6. Phenocrysts: pl - ca. 5% <=3mm 7. Matrix: microlithic 8. Secondary Minerals: palgonite, Fe-oxides 9. Encrustations: Crusts of limestone containing fragments of basalt 10. Comment: The sample is likely inner part of pillow lava, good for chemistry. 	x	x						x				
DR22-7	<ol style="list-style-type: none"> 1. Rock Type: Massive volcanic rock, probably inner part of pillow lava, 2. Size: 20x12x6 3. Shape/Angularity: subrounded 10. Comment: Looks very simikar to sample # 6 but appears to be more fresh, maybe good for chemistry and Ar-Ar dating on groundmass 	x	x						x				
DR22-8	<ol style="list-style-type: none"> 1. Rock Type: Massive well crystallized volcanic rock, moderately altered. 2. Size: 15x12x10 3. Shape/Angularity: subrounded 4. Color: dark grey 5. Rock texture: rare Pl-phyric 6. Phenocrysts: Plag ca. 5% <=3 mm - appears to be fresh 7. Matrix: doleritic 8. Secondary Minerals: chlorite, hematite in marginal parts 9. Encrustations: none 10. Comment: Plag maybe fresh, good for chemistry and Ar-Ar dating 	x	x						x				

Appendix IV

SAMPLE #	SAMPLE DESCRIPTION	TS	CHEM	Ar	Rest	GL/MI	N	ARCH	VULC	SED	MIN	NOTES	Sample Photos
DR22-9	1. Rock Type: Volcanic visicular moderately altered rock, fragment pillow 2. Size: 30x40x10 3. Shape/Angularity: Rounded 4. Color: dark grey, somewhat brownish 5. Rock texture: Rare Pl-phyric, visicular. Vesiculues heterogeneously distributed ca. 20-30%, rounded, up to 1 cm in diameter, open or filled with calcite. 6. Phenocrysts: Pl <=5% <=5 mm, Ol may be present as small microphenocrysts replaced by Fe oxides 7. Matrix: doleritic 8. Secondary Minerals: some chloritization 9. Encrustations: thin Fe-Mn hydroxide crust 10. Comment: this rock is likely a fragment of pillow. It is different	x	x						x				 SO201-2 DR22 -9
DR22-10	1. Rock Type: Volcanic breccia, moderately to low altered 2. Size: 25x17x8 3. Shape/Angularity: angular 4. Color: dark grey to black 5. Rock texture: clasts are aphyric cemented by dark cryptocrystalline cement 6. Phenocrysts: none 7. Matrix: cryptocrystalline 8. Secondary Minerals: not clear 9. Encrustations: appears to be good for chemistry 10. Comment:	x	x						x				 SO201-2 DR22 -10
DR22-11-CL	1. Rock Type: Volcanic breccia 2. Size: 15x10x10 3. Shape/Angularity: subangular 4. Color: dark grey to black 5. Rock texture: angular clasts (from mm-sized to 10 cm) of rare ol-phyric basalt cemented by dark grey cryptocrystalline material 6. Phenocrysts: plag, ol 7. Matrix: hyalopilitic 8. Secondary Minerals: chlorite, palagonite, Fe oxides 9. Encrustations: 10. Comment: the sample has clear shape of pillow fragment with well preserved rounded surface (former glassy margin). The inner parts are however completely brecciated and cemented by	x							x	x		D.Maicher is interested to study this sample in detail.	 SO201-2 DR22 -11 CL
DR22-12-S	1. Rock Type: sedimentary breccia 2. Size: 20x20x10 3. Shape/Angularity: subrounded 4. Color: basaltic clasts - dark grey surrounded by brown halos, matrix - light brown 5. Rock texture: clast are angular fragments of pillow basalts 1-8 cm in size with Fe-Mn crusts and also angular clasts of light pink limestone 0.5-2 cm. clasts:cement=60:40 6. Phenocrysts: Ol and Plag phenocrysts in basaltic clasts 10. Comment: One half was cut into several slices which went to C.Dullo (for IFM-GEOMAR longue), N.Tsukanov and D.Savelyev. Two slices composed mainly by basalt were stored in the second bag, these pieces are good for chemistry.	x							x	x		Sample stored in two separate bags. 3 slices went to C.Dullo, N.Tsukanov, D.Savelyev.	 SO201-2 DR22 -12 S
DR22-13-S	1. Rock Type: Sedimentary breccia with basaltic clasts cemented by pink limestone. Similar to #12-S. 10. Comment: Well preserved spheric pillow margin. the basalt was likely broken after eruption, cracks were filled with lime stone later.	x							x	x		1 fragment of pink limestone goes to D.Savelyev for paleontological investigations.	 SO201-2 DR22 -13 CL
DR22-14-S	1. Rock Type: Light pink clayish limestone with a layer of red clay, contains clasts of limestone and red clay. 10. Comment: The origin of the limestone and clasts is likely consedimentary.	x								x		1 piece goes to D.Savelyev, 1 piece to N.Tsukanov.	 SO201-2 DR22 -14 S
DR22-15-S	1. Rock Type: Alevrolite 2. Size: 20x10x5 4. Color: grey 5. Rock texture: layered with lenses. 10. Comment: This sample is a fragment of one of ca.3 large (>30cm) blocks of allevolite.	x								x		1 TS to N.Tsukanov. 1 piece goes to D.Savelyev.	 SO201-2 DR22 -15 S

Appendix IV

SAMPLE #	SAMPLE DESCRIPTION	TS	CHEM	Ar	Rest	GL/MIN	ARCH	VULC	SED	MIN	NOTES	Sample Photos
DR22-16-S	1. Rock Type: Diatomite 4. Color: white 5. Rock texture: slightly layered	x							x		1 TS to N.Tsukanov	
DR22-17-X	1. Rock Type: Large fragment of pillow of nice shape			x								
DR22-18 X	1. Rock Type: Numerous fragments of pillow basalts 10. Comment: Likely close analogues of samples # 2-4. Some can be used for chemistry and separation of minerals (spinel)			x							Several pieces of pillow went to D.Savelyev to separate spinel phenocrysts	
DR22-19 X	1. Rock Type: Fragment of pillow. 10. Comment: Looks pretty fresh. It went into archive because it was found on the latest stage of sample description when other samples were packed already.			x								

SO201-2-DR24

Location: Area B, Meiji Smt. 2nd step of western slope close to the base of the slope.
Dredge on bottom UTC 11/09/09 10:54hrs, lat 54°04,37'N, long 163°32,86'E, depth 5372m






Dredge off bottom UTC 11/09/09 12:03hrs, lat 54°04,46'N, long 163°33,52'E, depth 5073m

Total volume: a few rocks





Comments: Rocks of different lithology and provenance (amf-andesites, harzburgites, sediments). Predominantly drop-stones except for sediments.

SAMPLE #	SAMPLE DESCRIPTION	TS	CHEM	Ar	Rest	GL/MIN	ARCH	VULC	SED	MIN	NOTES	Sample Photos
DR24-1-S	1. Rock Type: Clay allevolite 10. Comment: Soft, contains sand particles, tunnels made by worms.								x			

Appendix IV

SO201-2-DR43												
Location: Area 12, Southern flank of Komandorsky block, sw-slope, upper part Dredge on bottom UTC 13/09/09 22:47hrs, lat 54°35,20'N, long 165°35,79'E, depth 4694m Dredge off bottom UTC 13/09/09 00:07hrs, lat 54°34,88'N, long 165°56,46'E, depth 4354m Total volume: a few rocks, appr. 20 pieces: sediment, volcanic (1 piece) Comments: Mostly interpreted to be ice-rafted. Local samples of poorly indurated sediment only. One basalt interpreted to be ice-rafted												
SAMPLE #	SAMPLE DESCRIPTION	TS	CHEM	Ar	Rest	GU/MIN	ARCH	VJ/LC	SED	MN	NOTES	Sample Photos
DR43-1-S	1. Rock Type: Sediment, mostly clay-some silt 2. Size: 10x10x12 3. Shape/Angularity: Sub-angular, sub-rounded 4. Color: Pale gray-green 5. Rock texture: Moderately indurated, fine, massive, unlayered 6. Phenocrysts: No visible minerals								X			
DR43-2-S	1. Rock Type: Sediment, breccia 2. Size: 27x15x15 3. Shape/Angularity: Angular 4. Color: Gray-green 5. Rock texture: Poorly indurated, coarse sedimentary breccia, angular clay and sandstone clasts up to 7 sm long 7. Matrix: Similar (possibly crushed) material 10. Comment: possible tectonic origin?								X			
DR43-3-X	1. Rock Type: Sedimentary rock, grauwacke-sandstone (?) 2. Size: 15x10x6 3. Shape/Angularity: Angular 4. Color: Dark blueish-gray 5. Rock texture: Well indurated 10. Comment: Turbidite? Probably ice-rafted?						X					
DR43-4-X	1. Rock Type: Sedimentary rock, sandy siltstone 2. Size: 20x11x7 3. Shape/Angularity: Angular 4. Color: Dark brownish-gray 5. Rock texture: Well indurated 10. Comment: Probably ice-rafted						X					
DR43-5-X	1. Rock Type: Mafic volcanic, amagdaloidal basalt 2. Size: 8x7x5 3. Shape/Angularity: Subangular 4. Color: Dark gray to black 5. Rock texture: Aphonitic 6. Phenocrysts: Rare pyroxene phenocrysts 7. Matrix: 15 % vesicles, mostly filled 8. Secondary Minerals: Calcite (?) and zeolite (?) vesicle fillings 9. Encrustations: 10. Comment: Probably ice-rafted						X					

Appendix IV

SO201-2-DR44 Location: Area 12, northern flank of Komandorsky block, upper northern slope Dredge on bottom UTC 14/09/09 04:20hrs, lat 54°40,27'N, long 165°50,61'E, depth 5053m Dredge off bottom UTC 14/09/09 05:45hrs, lat 54°39,82'N, long 165°50,97'E, depth 4627m Total volume: a few rocks Comments: sandstones, cherts, alevrolites												
SAMPLE #	SAMPLE DESCRIPTION	TS	CHEM	Ar	Rest	GU/MIN	ARCH	VJLC	SED	MIN	NOTES	Sample Photos
DR44-1-S	1. Rock Type: Sandstone 2. Size: 12x8x8 3. Shape/Angularity: Subangular 4. Color: Grey 5. Rock texture: Mid to coarse grained, clear layering. 4 cm coarse grained, 5 cm intercalated mid and c.gr. sandstones layers 2-3 mm. Clasts are various including shells fragments cemented by carbonate. Veins of cutting carbonates (<2 mm) 10. Comment: Look similar to Komandorsky rocks	X							X		+ 2 TS to D.Savelyev and N.Tsukanov	 <p style="text-align: center;">SO201-2 DR44 -1 S</p>
DR44-2-S	1. Rock Type: Sandstone with attached fragment of more soft clay sandstone 2. Size: 15x10x8 3. Shape/Angularity: Well rounded 4. Color: Grey 5. Rock texture: Massive (no layering) with carbonate cement	X							X		+ 1 TS to D. Savelyev	 <p style="text-align: center;">SO201-2 DR44 -2 S</p>
DR44-3-S	1. Rock Type: Chert (a cut fragment of large piece) 2. Size: 25x12x10 3. Shape/Angularity: Rounded 4. Color: Dark grey to black 5. Rock texture: Massive 10. Comment: Pure chert (no reaction with acid) Veins of SiO2 (Halzedon, <2 mm). Small piece of large sample								X			 <p style="text-align: center;">SO201-2 DR44 -3 S</p>
DR44-4-S	1. Rock Type: Clay sandstone / alevrolite 2. Size: 20x18x8 3. Shape/Angularity: Rounded 4. Color: Olive-grey 5. Rock texture: Coarse layered to lense layered, 1/2 sandstone, 1/2 sandy alevrolite with gradual transition. 10. Comment: Similar to alevrolite from the DR43								X			 <p style="text-align: center;">SO201-2 DR44 -4 S</p>

Appendix IV


SO201-2-DR48
Location: Area 7, Volcanologist massif, "cone" south-eastern part of the massif

Dredge on bottom UTC 15/09/09 08:09hrs, lat 55°21,90'N, long 167°03,96'E, depth 3035m

Dredge off bottom UTC 15/09/09 09:12hrs, lat 55°22,54'N, long 167°04,14'E, depth 2926m

Total volume: appr. 1/4 full

Comments: Numerous fragments of lavas with glassy margins. 1 large block of andesite. Some dropstones (sandstone, sediments)

SAMPLE #	SAMPLE DESCRIPTION	TS	CHEM	Ar	Rest	GU/MIN	ARCH	VJLC	SED	MIN	NOTES	Sample Photos
DR48-1	1. Rock Type: Volcanic, fragment of lava flow (lava tube), fresh 2. Size: 20x12x7 3. Shape/Angularity: Subangular 4. Color: Dark grey 5. Rock texture: Ol-Cpx-Pl phytic, visicular appr. 50% + large void in the middle of sample (appr. 2x10); glassy matrix (appr. 1 cm on both sides) 6. Phenocrysts: Ol - 10-15% <=3 mm - fresh, Cpx - appr. 10% <=3 mm - fresh, Pl - <=10% microphenocrysts <=2 mm - fresh 7. Matrix: Glassy to cryptocrystalline 8. Secondary Minerals: none 9. Encrustations: none 10. Comment: Very good for chemistry, Ol, Cpx, Plag - fresh. Glass for volatiles, melt inclusions.	X				!					+ Gene	
DR48-2	1. Rock Type: Volcanic, lava fragment with glassy margin, similar to #1 2. Size: 10x10x8 5. Rock texture: Somewhat less porhiritic (total amount of phenocrysts <= 20%)	X				!					+ Gene	
DR48-3	1. Rock Type: Volcanic fragment of lava flow, appears similar to #1 2. Size: 10x7x7 3. Shape/Angularity: Subangular 5. Rock texture: Vesicular with glassy margin 10. Comment: Has well preserved glassy margins	X				X						
DR48-4	1. Rock Type: Volcanic fragment of lava flow, fresh, vesicular; overall similar to 1-3 2. Size: 12x10x7 3. Shape/Angularity: Subangular 5. Rock texture: Vesicular with glassy margin, vesicularity appr. 50% (<=5 mm, rounded) 6. Phenocrysts: (Ol, Cpx, Plag) <=20 %; Ol <= 10% up to 3 mm 9. Encrustations: Some of vesiculars are filled with green material 10. Comment: Good for chemistry, glass	X				X						
DR48-5	1. Rock Type: Volcanic, small fragment of lava flow with glassy margin on 2 sides. Appears very similar to #1 =Ol,Cpx,Pl basalt 2. Size: 7x6x6 3. Shape/Angularity: Subangular	X				X						
DR48-6	1. Rock Type: Small fragment of Ol-Cpx-Pl phytic basalt with glassy margin similar to #1 2. Size: 5x6x6 3. Shape/Angularity: Subrounded 5. Rock texture: vesicular 6. Phenocrysts: amount of phenocrysts <=15% 10. Comment: Too small for chemistry. Glass !	X				X						

Appendix IV

SAMPLE #	SAMPLE DESCRIPTION	TS	CHEM	Ar	Rest	GL/MI N	ARCH	VULC	SED	MN	NOTES	Sample Photos	
DR 48-7	<ol style="list-style-type: none"> 1. Rock Type: Volcanic lava, dense, vesicular, fresh. Ol-Cpx-Pl basalt 2. Size: 20x13x7 3. Shape/Angularity: Subrounded 4. Color: Dark grey 5. Rock texture: Massive, somewhat vesicular. Vesicles (appr. 50%) mostly <=1 mm, some 5% large (<=5 mm) rounded 6. Phenocrysts: Ol: <=15-20% < 3mm, fresh 7. Matrix: Microlytic, glassy (?) 8. Secondary Minerals: Green fillings in vesicles 9. Encrustations: Greenish yellow clay on the surface 10. Comment: Very good for chemistry. Fresh Ol! 	X				Ol						+ Gene	 <p style="text-align: center;">SO201-2 DR 48 -7</p>
DR48-8	<ol style="list-style-type: none"> 1. Rock Type: Volcanic lava flow, similar to #7 2. Size: 15x12x12 3. Shape/Angularity: Subrounded 5. Rock texture: Dense, vesicular 10. Comment: Good for chemistry, good large Ol crystals 	X				X						+ Gene	 <p style="text-align: center;">SO201-2 DR 48 -8</p>
DR48-9	<ol style="list-style-type: none"> 1. Rock Type: Volcanic lava flow, similar to #7-8 2. Size: 10x10x15 3. Shape/Angularity: Subrounded 5. Rock texture: Vesicular, in comparison to 7-8 somewhat more porphyric - up to 20-25% 10. Comment: Fresh, Good for chemistry, + Olivine 	X										+ Gene	 <p style="text-align: center;">SO201-2 DR 48 -9</p>
DR48-10	<ol style="list-style-type: none"> 1. Rock Type: Volcanic lava flow, slightly altered, petrographically similar to #7-8 2. Size: 10x7x7 3. Shape/Angularity: Subrounded 5. Rock texture: Rare vesicular, in comparison to 7-8 more altered (appr. 1 cm outer marine) 6. Phenocrysts: Ol appr. 20% <=3 mm fresh, rare Cpx < 5% 8. Secondary Minerals: Vesicles filled with calcite 10. Comment: Should be analyzed for majors, Good for Olivine 	X				X							 <p style="text-align: center;">SO201-2 DR 48 -10</p>
DR48-11	<ol style="list-style-type: none"> 1. Rock Type: Volcanic lava flow, vesicular, fresh with glassy margin 2. Size: 15x15x10 3. Shape/Angularity: Subrounded 4. Color: Dark grey 5. Rock texture: Ol phyric, vesicular (appr. 50%, open), well preserved glassy margin (appr. 1 cm) on one side 6. Phenocrysts: Ol <= 10%, <=1.5 m, few Cpx appr. 1 mm 7. Matrix: Glassy at margin to microlitic in the inner part 8. Secondary Minerals: None 9. Encrustations: Clay on surface 10. Comment: Good for chemistry ! May be primitive rock. 	X				X						+ Gene	 <p style="text-align: center;">SO201-2 DR 48 -11</p>
DR48-12	<ol style="list-style-type: none"> 1. Rock Type: Volcanic lava flow. Similar to #11. 2. Size: 20x20x10 3. Shape/Angularity: Subangular 5. Rock texture: Vesicular. Somewhat fluidal. Vesicles are heterogeneously distributed. 10. Comment: Fresh. Good for chemistry. A little glass preserved. 	X											 <p style="text-align: center;">SO201-2 DR 48-12</p>
DR48-13-X	<ol style="list-style-type: none"> 1. Rock Type: Fragment of lava with glassy margin and sandy clay, similar to #1. Vesicular Ol-Cpx-Pl phyric basalt 2. Size: 10x7x6 3. Shape/Angularity: Subrounded 5. Rock texture: Vesicular 					X	X						 <p style="text-align: center;">SO201-2 DR 48 -13 X</p>







Appendix IV

SAMPLE #	SAMPLE DESCRIPTION	TS	CHEM	Ar	Rest	GL/MI	Ol	ARCH	VULC	SED	MIN	NOTES	Sample Photos
DR48-14-X	1. Rock Type: Lava, Ol-Cpx-Plag phyric, similar to #1 2. Size: 10x6x6 5. Rock texture: Vesicular	X				Ol	X						 SO201-2 DR 48 -14 X
DR48-15-X	1. Rock Type: Vesicular Ol-Cpx-Pl lava fragment 2. Size: 10x3x7 6. Phenocrysts: Some large Ol crystals up to 3 mm					Ol	X						 SO201-2 DR 48 -15 X
DR48-16-X	1. Rock Type: Vesicular rare Ol phyric lava, similar to #7 2. Size: 10x5x10 3. Shape/Angularity: Subangular 10. Comment: Fresh							X					 SO201-2 DR 48 -16 X
DR48-17-X	1. Rock Type: Vesicular Ol-Cpx basalt lava 2. Size: 20x10x7 10. Comment: Some vesicles filled with clay							X					 SO201-2 DR 48 -17 X
DR48-18-X	1. Rock Type: Rare Ol-Pl phyric vesicular basalt similar to 7 2. Size: 10x8x5 3. Shape/Angularity: Subrounded							X					 SO201-2 DR 48 -18 X
DR48-19-X	1. Rock Type: Volcanic, rare Cpx-Ol(?) andesite 2. Size: 15x10x4 3. Shape/Angularity: Rounded 5. Rock texture: vesicular, fluidal 10. Comment: Most likely dropstone! Composition may be HMB							X				+ Gene	 SO201-2 DR 48 -19 X
DR48-20-X	1. Rock Type: Cpx-Hbl-Pl andesite 2. Size: fragment of large (30x20x20) block 3. Shape/Angularity: Subangular 5. Rock texture: Massive 10. Comment: Likely dropstone! Moderately altered							X				+ Gene	 SO201-2 DR 48 -20 X




Appendix IV

SO201-2-DR49												
Location: Area 7 - Volcanologist's massif - "lava flow": small ridge at SW side massif Dredge on bottom UTC 15/09/09 12:08hrs, lat 55°27,31'N, long 167°03,82'E, depth 2634m Dredge off bottom UTC 15/09/09 12:53hrs, lat 55°27,62'N, long 167°03,82'E, depth 2391m Total volume: few rocks Comments:												
SAMPLE #	SAMPLE DESCRIPTION	TS	CHEM	Ar	Rest	GL/MIN	ARCH	VULC	SED	MIN	NOTES	Sample Photos
DR49-1	1. Rock Type: Volcanic lava flow 2. Size: 10x8x8 3. Shape/Angularity: Subangular 4. Color: Grey 5. Rock texture: Ol phyric vesicular to aphyric more dense in the central part, vesicles are open 6. Phenocrysts: Ol: appr. 10-15% up to 3 mm fresh 7. Matrix: microlitic / glassy 9. Encrustations: Cavities in the central part have incrustations of yellowish mineral. Thin Mn crust on the surface + clay 10. Comment: Good for chemistry + Ol	X				X					+ Gene	 <p style="text-align: center;">SO201-2 DR 4 9 -1</p>
SO201-2-DR51												
Location: Area 7, Volcanologist's massif, cone on SW slope Dredge on bottom UTC 15/09/09 21:24hrs, lat 55°21,05'N, long 167°09,89'E, depth 2580m Dredge off bottom UTC 15/09/09 05:30hrs, lat 55°21,49'N, long 167°09,90'E, depth 2183m Total volume: 1/4 full Comments: abundant fresh vesicular, pillow lava basalts, minor andesite with Hbl												
SAMPLE #	SAMPLE DESCRIPTION	TS	CHEM	Ar	Rest	GL/MIN	ARCH	VULC	SED	MIN	NOTES	Sample Photos
DR51-1	1. Rock Type: Volcanic fresh, Pl-Ol basalt 2. Size: 25x25x20 3. Shape/Angularity: Angular 4. Color: dark grey - black interior 5. Rock texture: Rounded vesicles appr. 25%, abundant microvesicles, no filling 6. Phenocrysts: appr. 5-10% phenocrysts up to 2-3 mm, Ol, Pl, tr Cpx? 7. Matrix: Aphanitic 8. Secondary Minerals: no 9. Encrustations: no	X	X			X						 <p style="text-align: center;">SO201-2 DR 5 1 -1</p>
DR51-1-X	1. Rock Type: The same as #1 10. Comment: The same as #1 but in large quantity with abundant glass						X					
DR51-2	1. Rock Type: Volcanic, fresh, Pl-Ol basalt 2. Size: 20x15x12 3. Shape/Angularity: Subangular 4. Color: Gray to dark gray interior 5. Rock texture: Vesicles appr. 20%, no fillings 6. Phenocrysts: up to 2-3 mm, 10-15%, Ol, Pl, tr Cpx (?) 7. Matrix: Aphanitic 9. Encrustations: Glassy rim	X	X			Glass Oliv, Plag						 <p style="text-align: center;">SO201-2 DR 5 1 -2</p>
DR51-3	1. Rock Type: Volcanic, fresh, Plag-Ol basalt 2. Size: 25x12x15 3. Shape/Angularity: Angular 4. Color: Dark to dark grey 5. Rock texture: vesicles variable, 10%, no fillings 6. Phenocrysts: up to 1-2 mm, appr. 10%, Ol, Pl, fresh 10. Comment: Glassy rim	X	X			Glass Oliv, Plag						 <p style="text-align: center;">SO201-2 DR 5 1 -3</p>
DR51-4	1. Rock Type: Volcanic fresh, Plag-Ol basalt 2. Size: 12x12x12 3. Shape/Angularity: Angular 4. Color: Dark grey interior 5. Rock texture: vesicles variable, 10% 6. Phenocrysts: 5-10% up to 1-2 mm, olivine, pagoclase fresh 7. Matrix: Aphanitic 8. Secondary Minerals: no 9. Encrustations: No 10. Comment: Glass not evident as in #1-3	X	X			Oliv, Pl						 <p style="text-align: center;">SO201-2 DR 5 1 -4</p>

Appendix IV



SAMPLE #	SAMPLE DESCRIPTION	TS	CHEM	Ar	Rest	GU/MIN	ARCH	VJLC	SED	MN	NOTES	Sample Photos
DR51-5	1. Rock Type: Volcanic, fresh, Plag-Oliv basalt 2. Size: 15x15x10 3. Shape/Angularity: Angular 4. Color: Gray- dark grey 5. Rock texture: vesicular, abundant large rounded vesicles, up to 1 cm, appr. 30% 6. Phenocrysts: appr. 5-10% fresh, Pl, Ol 7. Matrix: Aphanitic 10. Comment: Some fresh glass, less then #1-3	X	X			Oliv, Pl, Glass						
DR51-6	1. Rock Type: Volcanic fresh, Pl-Ol basalt 2. Size: 10x10x15 3. Shape/Angularity: Angular 4. Color: gray to dark gray 5. Rock texture: vesicles 15-20%, no fillings 6. Phenocrysts: 10-20% up to 1-2 mm, Ol, Pl, Cpx 7. Matrix: Aphanitic 8. Secondary Minerals: 9. Encrustations: no 10. Comment: Some glassy margins	X	X			Oliv, Pl, Cpx Glass						
DR51-7	1. Rock Type: Volcanic, fresh, Plag-Ol basalt 2. Size: 20x20x12 3. Shape/Angularity: Angular 4. Color: Dark grey interior 5. Rock texture: vesicles, highly variable up to 1 cm, appr. 15-20%, no fillings 6. Phenocrysts: 15-20%, Plag, Ol 9. Encrustations: no 10. Comment: Fresh glassy rim; large slab, 20x12 cm is taken by Dima Savelyev for display in Volcanological museum (Petropavlovsk, IVIS)	X	X			Oliv, Pl, Glass						
DR51-8	1. Rock Type: Volcanic, fresh, Hb andesite 2. Size: 30x15x20 3. Shape/Angularity: Angular 4. Color: fresh interior colour is grey to light grey 5. Rock texture: no vesicles, dense and massive 6. Phenocrysts: 5-10%, Cpx, Hbl, Plag 7. Matrix: Aphanitic 8. Secondary Minerals: 9. Encrustations: no 10. Comment: no glass	X	X			Cpx, Hb, Plag						
DR51-9	1. Rock Type: Volcanic fresh, Basalt with inclusion 2. Size: 25x20x20 3. Shape/Angularity: Angular 4. Color: Dark grey fresh interior 5. Rock texture: vesicles sparce <10% 6. Phenocrysts: 15-20%, Ol, Plag 7. Matrix: Aphanitic 10. Comment: Cut surface reveals inclusion of Plag basalt or andesite	X	X			Ol, Plag						
DR51-9-X	1. Rock Type: Same as #9 10. Comment: In larger quantity then #9 for archive						X					
DR51-10	1. Rock Type: Volcanic fresh, Plag-Ol basalt 2. Size: 10x10x12 3. Shape/Angularity: Angular 4. Color: Gray to dark gray interior 5. Rock texture: vesicles small <5 mm, <10% 6. Phenocrysts: 5-10%, Pl and Ol 7. Matrix: Aphanitic 9. Encrustations: no 10. Comment: Fresh glassy margins	X	X			Plag, Ol, Glas s						
DR51-11	1. Rock Type: Volcanoclastic (?), fresh, Andesitic volcanic breccia 2. Size: 30x25x25 3. Shape/Angularity: Angular 4. Color: Cut surface reveals interior of gray volcanic rock in a matrix of red volcanic rock 5. Rock texture: Dense, unvesiculated 6. Phenocrysts: Gray rock is Hb-Cpx-Pl andesite with 10-20% phenocrysts up to 6-7 mm. This grey andesite is in fragments from 5 to 7 cm in a red matrix containing phenocrysts of similar mineralogy	X	X			Hb, Cpx, Plag						

Appendix IV



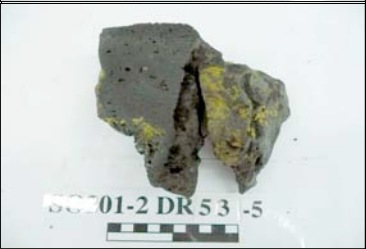


SAMPLE #	SAMPLE DESCRIPTION	TS	CHEM	Ar	Rest	GL/MI	N	ARCH	VULC	SED	MIN	NOTES	Sample Photos
DR51-11-X	1. Rock Type: Same as #11 10. Comment: in large quantity							X					
DR51-12-X	1. Rock Type: Fresh lava, Plag-Ol basalt 10. Comment: Similar to abundant lava in this dredge					Plag, Ol		X					
DR51-13-X	1. Rock Type: Same as #12X					Plag, Ol		X					
DR51-14-X	1. Rock Type: Same as #12X-13X					Plag, Ol		X					

SO201-2-DR53

Location: AREA 7 VOLCANOLOGIST'S MASSIF, SE slope of eastern edifice
Dredge on bottom UTC 16/09/09 06:21hrs, lat 55°18,69'N, long 167°31,07'E, depth 3000m
Dredge off bottom UTC 16/09/09 07:45hrs, lat 55°19,16'N, long 167°30,84'E, depth 2430m
Total volume: 1/4
Comments: 3 large (appr. 0.5 m) blocks of pillow lavas numerous fragments, some dropstones (chert, andesites)

SAMPLE #	SAMPLE DESCRIPTION	TS	CHEM	Ar	Rest	GL/MI	N	ARCH	VULC	SED	MIN	NOTES	Sample Photos
DR53-1	1. Rock Type: Volcanic, fragment of pillow lava with glassy margin, fresh 2. Size: 60x40x30 3. Shape/Angularity: Subrounded 4. Color: Dark grey 5. Rock texture: Rare Ol-Pl phyric, vesicular. Vesicles are more abundant toward the margin, from 10 to 20 %. Some rare large voids with "bubbled" surface are also present 6. Phenocrysts: Pl - appr. 10% some are up to 1 cm, mostly 2-3 mm; Ol - <=2-3% some are appr. 2-3 mm, + microphenocrysts (<=1 mm) 7. Matrix: Cryptocrystalline, hyalopilitic. Glassy margin appr. 5-7 mm 8. Secondary Minerals: none 9. Encrustations: clay and thin (appr. 0.5 mm) Fe-Mn crust 10. Comment: Very good for chemistry. Plag, Ol - fresh. Glass. Glassy margins from all big sample were collected and stored in separate bag.	X	X									+ Gene	
DR53-2	1. Rock Type: Volcanic, large fragment of pillow lava with glassy margin 2. Size: 40x30x30 3. Shape/Angularity: Subangular 5. Rock texture: Petrographically identical to #1. 6. Phenocrysts: Some Ol are up to 5 mm 10. Comment: Glassy margins were collected in separate bag	X	X									+ Gene	

Appendix IV

SAMPLE #	SAMPLE DESCRIPTION	TS	CHEM	Ar	Rest	GL/MIN	ARCH	VJJC	SED	MIN	NOTES	Sample Photos
DR53-3	1. Rock Type: Volcanic, fragment of pillow lava 2. Size: 20x10x8 3. Shape/Angularity: Subangular 10. Comment: Petrographically identical to #1, has wide well preserved glassy margin	X	X								+ Gene	
DR53-4	1. Rock Type: Volcanic, fragment of pillow lava with glassy margin 2. Size: 13x13x8 3. Shape/Angularity: Subangular 5. Rock texture: Petrographically very similar to #1. 6. Phenocrysts: Plag crystals are somewhat smaller (<=0.7 cm)	X									+ Gene	
DR53-5	1. Rock Type: Volcanic, fragment of pillow with glassy margin 2. Size: 13x10x8 3. Shape/Angularity: Subangular 10. Comment: Very similar to #1	X									+ Gene	
DR53-6	1. Rock Type: Volcanic pillow lava fragment with fresh glass 2. Size: 15x8x6 3. Shape/Angularity: Subrounded	X									+ Gene	
DR53-7-M	1. Rock Type: Fragment of pillow - analogues to all other samples from the dredge 9. Encrustations: Coated with appr. 1 to 1.5 cm thick crust of Fe-Mn hydroxides 10. Comment: 1/2 has been given to Dima Savelyev									X	+ D.Savelyev	

SO201-2-DR55


Location: Area 7, Volcanologist's massif, northern block, small cone in eastern part, ridge-like structure, NE - end (SW - DR57)

Dredge on bottom UTC 16/09/09 20:52hrs, lat 55°29,21'N, long 167°12,56'E, depth 2358m


Dredge off bottom UTC 16/09/09 22:00hrs, lat 55°29,62'N, long 167°12,75'E, depth 2005m

Total volume: appr. 10 rocks

Comments: Small but consistent collection of fresh volcanic rocks in this dredge - all interpreted to be olivine basaltic andesites or andesite lava

SAMPLE #	SAMPLE DESCRIPTION	TS	CHEM	Ar	Rest	GL/MIN	ARCH	VJJC	SED	MIN	NOTES	Sample Photos
DR55-1	1. Rock Type: Volcanic, fresh, olivine basaltic andesite 2. Size: 13x15x15 3. Shape/Angularity: Angular, fresh flow surface and glass 4. Color: Gray - dark gray interior 5. Rock texture: vesicles - irregular, often flattened and angular, appr. 10%, no fillings 6. Phenocrysts: appr. 5-10%, mostly olivine up to 2 mm, some Ol megacrysts to 8 mm, Plag in microphenocrysts < 1mm 7. Matrix: aphanitic 8. Secondary Minerals: no 9. Encrustations: no 10. Comment: This rock has phenocryst mineralogy of a basalt but may be basaltic andesite or andesite. Two bags of this large sample	X	X			Ol, Plag, Glas s						

Appendix IV

SAMPLE #	SAMPLE DESCRIPTION	TS	CHEM	Ar	Rest	GU/MIN	ARCH	VJ/LC	SED	MN	NOTES	Sample Photos
DR55-2	1. Rock Type: Volcanic, fresh, olivine basaltic andesite 2. Size: 15x8x10 3. Shape/Angularity: Angular 4. Color: Gray to dark gray interior 5. Rock texture: Vesicles irregular appr. 15% 6. Phenocrysts: Mostly Ol up to 2-3 mm, some larger Ol crystals to 7-8 mm, no Plag phenocrysts evident, microphenocrysts of Pl (<1mm) may be present 7. Matrix: 8. Secondary Minerals: no 9. Encrustations: no 10. Comment: Glassy margins	X	X			Ol, Plag, Glas s						
DR55-3	1. Rock Type: Volcanic, fresh, olivine basaltic andesite 2. Size: 8x10x5 3. Shape/Angularity: Angular 4. Color: Gray to dark gray interior 5. Rock texture: Vesicles rounded appr. 15-20% 6. Phenocrysts: Mostly Ol up to 2-3 mm, some larger Ol crystals to 6-7 mm, microphenocrystic laths of Pl (?) (<1mm) 7. Matrix: Aphanitic 10. Comment: Similar to #1 in this dredge. Glassy margins.	X	X			Ol, Plag, Glas s						
DR55-4	1. Rock Type: Volcanic fresh, olivine basaltic andesite 2. Size: 6x4x3 3. Shape/Angularity: Angular 4. Color: Gray to dark gray interior 5. Rock texture: Vesicles irregular appr. 20%, no fillings 6. Phenocrysts: Mostly Ol 5-10%, to 3 mm, but some up to 6-7 mm. No Plag phenocrysts or microphenocrysts are evident 9. Encrustations: no 10. Comment: Similar to #1. Glassy margins.	X	X			Ol, Plag, Glas s						
DR55-5	1. Rock Type: Volcanic, fresh, olivine basaltic andesite 2. Size: 5x3x3 3. Shape/Angularity: angular 4. Color: Gray to dark gray interior 5. Rock texture: vesicles irregular 10-20% 6. Phenocrysts: mostly Ol up to 2-3 mm, some larger crystals of Ol to 6-7 mm, appr. 5-10%. Plag phenocr. or microphen. were not observed 7. Matrix: Aphanitic 8. Secondary Minerals: no 9. Encrustations: no 10. Comment: Fresh glassy margins	X	X			Ol, Plag, Glas s						
DR55-6	1. Rock Type: Volcanic, fresh, olivine basaltic andesite 2. Size: 5x3x3 3. Shape/Angularity: Angular 4. Color: Gray to dark gray interior 5. Rock texture: Vesicles flattened and angular appr. 10% 6. Phenocrysts: appr. 5%, Ol up to 2-3 mm, no Plag phenocr. or microph. observed 8. Secondary Minerals: no 9. Encrustations: no 10. Comment: fresh glassy margins	X	X			Ol, Plag, Glas s						

SO201-2-DR56


Location: Area 7, Volcanologist's massif, Northern block, "2" (bend ridge)

Dredge on bottom UTC 17/09/09 00:09hrs, lat 55°26,86'N, long 167°11,11'E, depth 2369m

Dredge off bottom UTC 17/09/09 01:06hrs, lat 55°27,11'N, long 167°11,53'E, depth 2025m

Total volume: Few rocks





Comments: Mostly ice-rafted, one sample (small) of fresh basalt counted and interpreted to be "in place" here

SAMPLE #	SAMPLE DESCRIPTION	TS	CHEM	Ar	Rest	GU/MIN	ARCH	VJ/LC	SED	MN	NOTES	Sample Photos
DR56-1	1. Rock Type: Volcanic, fresh, Pl-Ol basalt 2. Size: 10x6x6 3. Shape/Angularity: Angular, fresh flow surface features 4. Color: dark gray interior 5. Rock texture: Vesicles small and irregular, < 5%, no fillings 6. Phenocrysts: appr. 5%, mostly Plag phenocrysts up to 6-7 mm, fewer olivine phenocr. up to 3-4 mm 7. Matrix: Aphanitic 8. Secondary Minerals: no 9. Encrustations: no	X	X			Plag, Ol						

Appendix IV

SO201-2-DR57												
Location: Area 7. Volcanologist's massif. Northern block. ridge like structure. SW end (NE: DR55)												
Dredge on bottom UTC 17/09/09 03:11hrs, lat 55°28.02'N, long 167°09.49'E, depth 2377m												
Dredge off bottom UTC 17/09/09 04:12hrs, lat 55°28.43'N, long 167°09.55'E, depth 2082m												
Total volume: Few rocks												
Comments: One large angular block (>80 kg) and several smaller blocks. All similar fresh lavas. With Glass												
SAMPLE #	SAMPLE DESCRIPTION	TS	CHEM	Ar	Rest	GL/MIN	ARCH	VULC	SED	MN	NOTES	Sample Photos
DR57-1	1. Rock Type: Volcanic, fresh, olivine bearing andesite 2. Size: 70x40x50 3. Shape/Angularity: Angular, fresh flow surfaces 4. Color: Gray interior 5. Rock texture: Vesicles mostly <2mm, irregular, appr. 5% 6. Phenocrysts: Few phenocrysts-sparsely phyric, olivine phenocrysts appr. 3% up to 1-2 mm, plagphenocr not observed 7. Matrix: Aphanitic 8. Secondary Minerals: no 9. Encrustations: no 10. Comment: Fresh glassy rims	X	X									 SO201-2 DR 5 7 -5
DR57-1-X	1. Rock Type: the same as #1						X					
DR57-2	1. Rock Type: Volcanic fresh, olivine bearing andesite 2. Size: 16x11x7 3. Shape/Angularity: Angular, fresh flow surfaces 4. Color: gray interior 5. Rock texture: Vesicles, mostly rounded 10-15% - no filling 6. Phenocrysts: few phenocrysts - sparsely phyric <1%, Ol up to 3 mm, Plag phenocr. not observed 7. Matrix: Aphanitic 8. Secondary Minerals: no 9. Encrustations: no	X	X									 SO201-2 DR 5 7 -2
DR57-3	1. Rock Type: Volcanic fresh 2. Size: 16x11x9 3. Shape/Angularity: Angular, fresh flow features 4. Color: Gray interior 5. Rock texture: Abundant large vesicles > 3mm, appr. 15-20%, no fillings 6. Phenocrysts: few phenocrysts, sparsely phyric <5%, mostly Ol up to 3 mm, some microilitic laths possibly Plag 8. Secondary Minerals: no 9. Encrustations: no 10. Comment: Fresh glassy margins	X	X									 SO201-2 DR 5 7 -3
DR57-4	1. Rock Type: Volcanic, fresh, olivine bearing andesite 2. Size: 10x10x8 3. Shape/Angularity: Angular, fresh flow surfaces 4. Color: Gray interior 5. Rock texture: Vesicularity appr. 20%, no fillings 6. Phenocrysts: Few phenocrysts-sparsely phyric <3%, mostly olivines up to 2-3 mm, microphenocrysts < 1mm appear to be mostly olivine but may include Plag 7. Matrix: Aphanitic 8. Secondary Minerals: no 9. Encrustations: no	X	X									 SO201-2 DR 5 7 -4
DR57-5	1. Rock Type: Volcanic, fresh, olivine bearing andesite 2. Size: 8x12x8 3. Shape/Angularity: Angular, fresh flow surfaces 4. Color: gray interior 5. Rock texture: Vesicularity appr. 20%, nearly aphyric 6. Phenocrysts: w/wt phenocrysts - <1%, microphenocrysts of Ol < 1mm, no Plag observed 7. Matrix: Aphanitic 8. Secondary Minerals: no 9. Encrustations: no 10. Comment: Glassy margins	X	X									 SO201-2 DR 5 7 -5
DR57-6	1. Rock Type: Volcanic, fresh, olivine bearing andesite 2. Size: 10x4x4 3. Shape/Angularity: Angular, fresh flow features 4. Color: Gray interior 5. Rock texture: Vesicularity appr. 20% - no fillings 6. Phenocrysts: few phenocrysts < 1%, mostly olivine microphenocrysts < 1mm, no Plag observed 7. Matrix: Aphanitic 8. Secondary Minerals: no 9. Encrustations: no	X	X									 SO201-2 DR 5 7 -6

Appendix IV

SO201-2-DR58 Location: Area 7. Volcanologists Massif, Northern block ridge like structure similar to DR57. appr. 2.3 nm W of DR57 Dredge on bottom UTC 17/09/09 06:14hrs, lat 55°28,32'N, long 167°05,36'E, depth 2374m Dredge off bottom UTC 17/09/09 07:19hrs, lat 55°28,72'N, long 167°05,61'E, depth 2089m Total volume: few rocks Comments:												
SAMPLE #	SAMPLE DESCRIPTION	TS	CHEM	Ar	Rest	GL/MIN	ARCH	VJLC	SED	MN	NOTES	Sample Photos
DR58-1	1. Rock Type: Volcanic, lava, vesicular, fresh 2. Size: 20x10x10 3. Shape/Angularity: Subangular 4. Color: Grey 5. Rock texture: Vesicular, vesicles: appr. 15-20% rounded <=5mm, evenly distributed 6. Phenocrysts: Pl appr. 20%, < 3mm, fresh; Cpx <=5% <=2 mm, fresh; Ol <=1-2% with Px rims (?) 7. Matrix: Microlitic / finely crystallized 8. Secondary Minerals: none 9. Encrustations: Clay on the surface, very thin Mn crust 10. Comment: Good for chemistry	X	X								+ Gene	
DR58-2	1. Rock Type: Volcanic, lava, vesicular, fresh, Cpx-Plag basalt 2. Size: 8x4x3 3. Shape/Angularity: Subangular 4. Color: Grey 5. Rock texture: Dense vesicular 6. Phenocrysts: Pl <=20% up to 2mm, evenly distributed, Cpx <=5% <=1.5 mm 7. Matrix: microlitic to doleritic 8. Secondary Minerals: none 9. Encrustations: grey film on the surface, also filling some cracks 10. Comment: Looks similar to #1, somewhat altered from surface	X	X									
DR58-3	1. Rock Type: Volcanic, fragment of sheet flow (?), fresh 2. Size: 15x10x5 3. Shape/Angularity: Subangular 4. Color: Grey 5. Rock texture: Rare Ol, Cpx, Plag phyrlic; vesicles <=15% - two types: 1) Relatively large flattened (1:5) 2) small (appr. 1 mm) forming chains parallel top each other. Due to the 2nd type of vesicularity the rock has "fluidal" texture, plate joining 6. Phenocrysts: Pl, Cpx, Ol : <=1-2% <=1 mm fresh 7. Matrix: glassy with microlites 8. Secondary Minerals: none 9. Encrustations: very thin film on surface. 10. Comment: Perfectly fresh and good for chemistry. The rock looks similar to the "Table mountains" trachybasalts from Bering isl.	X	X								+ Gene	
DR58-4	1. Rock Type: Volcanic, likely fragment of pillow lava (a segment glass not preserved) 2. Size: 15x7x7 3. Shape/Angularity: Subrounded 4. Color: Dark grey 5. Rock texture: Strongly Ol-Plag (Cpx) phyrlic, Vesicles <=20-25%, evenly distributed, rounded <= 1cm, often elongate 6. Phenocrysts: Plag <=20%, <=5mm, osten intergrows with Ol; Ol - appr. 5-7% <=2 mm, Cpx - not clear, rather rare <=1%, intergrows with Ol, Plag 7. Matrix: Microlitic 8. Secondary Minerals: none 9. Encrustations: Thin Fe-Mn crust, clay. 10. Comment: The sample may be readily in situ, although it doesn't look similar to any dredge before. Good for chemistry	X	X								+ Gene	

Appendix IV

SO201-2-DR59												
Location: Area 7. Volcanologists massif, cone on the western flank of Piip volcano												
Dredge on bottom UTC 17/09/09 09:39hrs, lat 55°24.98'N, long 167°10.35'E, depth 2186m												
Dredge off bottom UTC 17/09/09 10:40hrs, lat 55°25.10'N, long 167°11.10'E, depth 1798m												
Total volume: 1/3 full												
Comments: Mostly fragments of lavas and bombs of variably Pl phyric andesites, few dropstones												
SAMPLE #	SAMPLE DESCRIPTION	TS	CHEM	Ar	Rest	GL/MIN	ARCH	VJULC	SED	MN	NOTES	Sample Photos
DR59-1	1. Rock Type: Volcanic, fragment of lava or bomb with glassy margin. Young and fresh 2. Size: 15x12x15 3. Shape/Angularity: Angular 4. Color: Grey 5. Rock texture: Dense, rare Pl-Ol phyric, vesicular, vesicles <=1 cm nonequally distributed (from appr. 60% to few %) 6. Phenocrysts: Plag <=5% <=1mm; Ol <=2-3 % <= 0.5 mm 7. Matrix: Glassy to hyalopilitic 8. Secondary Minerals: none 9. Encrustations: none 10. Comment: Good for chemistry. The aphyric rock type. Glassy margin!	X	X								+ Gene	
DR59-2	1. Rock Type: Volcanic, fragment of lava or bomb 2. Size: Large block appr. 30 cm diameter 3. Shape/Angularity: Angular 4. Color: Grey 5. Rock texture: Massive, Ol-Pl phyric (with rare Cpx?) with glassy margin. Vesicles (<=2cm) rounded 6. Phenocrysts: Plag appr. 10% <=3 mm (Pl>Ol), Ol <=5% <=1 mm, Cpx <=1-2% <=0.5 mm 7. Matrix: Glassy to microlitic 10. Comment: Glassy margin!	X	X									
DR59-3	1. Rock Type: Volcanic, fragment of lava, glassy margin 2. Size: large block appr. 30 cm diameter 5. Rock texture: Overall looks similar to #2, that is more porphyritic compared to #1 10. Comment: Good for chemistry. Glassy margin	X	X								+ Gene	
DR59-4	1. Rock Type: Volcanic, bomb (?) 2. Size: A part of large block appr. 30 cm diameter 3. Shape/Angularity: Angular 5. Rock texture: Overall similar to #2,3 (Ol - small and rare) 10. Comment: It has quenched margin on both sides. Well quenched, has good glass. Good for chemistry	X	X									
DR59-5	1. Rock Type: Volcanic, lava (?) 2. Size: 10x7x7 3. Shape/Angularity: Subangular 4. Color: Dark grey to black 5. Rock texture: Dense Ol-Plag phyric, vesicular (<= 20 %), voids are angular (overall is less vesicular than other samples) 6. Phenocrysts: PL <=30% <=7mm, elongate; Ol <=2% <=0.5 mm, Cpx - a few xls (<1% <=1mm) 7. Matrix: glassy 10. Comment: Glassy margin. The most porphyritic sample in the dredge	X	X								+ Gene	
DR59-6	1. Rock Type: Volcanic bomb (?) highly vesicular 2. Size: 10x8x8 3. Shape/Angularity: Subangular 5. Rock texture: Rare Pl phyric, highly vesicular (appr. 60%), vesicles rounded (<=5mm) get smaller toward glassy margin (<=0.5 mm). Inclusions of aphyric basalt 6. Phenocrysts: Plag <=5% <=3mm, rare Ol, Cpx (?). 7. Matrix: Glassy to microlitic 10. Comment: May be interesting to see how glass composition changes from central to marginal parts and correlates with the size of vesicles	X	X								+ Gene	

Appendix IV

SAMPLE #	SAMPLE DESCRIPTION	TS	CHEM	Ar	Rest	GU/MIN	ARCH	VJJC	SED	MN	NOTES	Sample Photos
DR59-7	1. Rock Type: Volcanic, bomb (?) 2. Size: 15x15x10 3. Shape/Angularity: Angular 5. Rock texture: Mixed sample. Central part is Pl phyric (like #5), margin is almost aphyric and contains inclusions of very vesicular aphyric rock 10. Comment: If analyzed to bulk composition it should be carefully picked to avoid mixing different types of rocks. Glassy margin=aphyric basalt	X									+ Gene	 SO201-2 DR 5 9-7
DR59-8	1. Rock Type: Volcanic, bomb ? 2. Size: 20x10x10 3. Shape/Angularity: Angular 5. Rock texture: Dense, moderately vesicular, rare Ol-Plag phyric, glassy margin. Overall similar to #1. Has some very large (appr. 5 cm long) elongate voids flattened and oriented along margin 10. Comment: Good for chemistry, glass.	X	X									 SO201-2 DR 5 9-8
DR59-9	1. Rock Type: Volcanic pumice 2. Size: 3 fragments (A,B,C). The largest is appr. 8 cm in diameter 5. Rock texture: Almost aphyric, glassy, very vesicular 6. Phenocrysts: Rare Plag xls 10. Comment: Represents talus from the most N cone of the major edifice	X	X									 SO201-2 DR 5 9-9
DR59-10X	1. Rock Type: Nice sample of volcanic bomb with 2 chilled margins 2. Size: 20x20x12 3. Shape/Angularity: Angular 6. Phenocrysts: Rare Pl-Ol phyric rock						X					 SO201-2 DR 5 9-10
DR59-11X	1. Rock Type: Volcanic, bomb or lava 2. Size: Part of large (appr. 30 cm diameter) angular block 10. Comment: Can be used to separate rare Ol, has good chilled margin						X					 SO201-2 DR 5 9-11




Appendix IV

SO201-2-DR60 Location: Area 7. Volcanologist massif, southern slope of small cone on the eastern flank of Piip Dredge on bottom UTC 17/09/09 13:29hrs, lat 55°22,80'N, long 167°23,15'E, depth 2431m Dredge off bottom UTC 17/09/09 14:20hrs, lat 55°23,19'N, long 167°22,99'E, depth 2221m Total volume: 1/4 full Comments: appr. 80% of pumice, appr. 20 % middle to small fragments of basaltic pillows, few dropstones. With red crab.												
SAMPLE #	SAMPLE DESCRIPTION	TS	CHEM	Ar	Rest	GL/MIN	ARCH	VJLC	SED	MN	NOTES	Sample Photos
DR60-1	1. Rock Type: Volcanic, fragment of lava, vesicular, fresh 2. Size: appr. 12 cm diameter 3. Shape/Angularity: Subangular 4. Color: Dark grey to light grey 5. Rock texture: Dense rare Ol phyric, vesicles appr. 50% in central part to appr. 30% at glassy margin, some angular voids (<=1 cm long) 6. Phenocrysts: Ol microphen. <=10%, fresh (<=1mm), a few Cpx (<1 mm), Glass at chilled margin (appr. 0.5 cm on both sides) 7. Matrix: glassy to hyalopilitic 9. Encrustations: Thin Mn crust, clay on surface and filling some vesicles	X	X								+ Gene	 <p style="text-align: center;">SO201-2 DR 6 0 -1</p>
DR60-2	1. Rock Type: Volcanic, fragment of lava with glassy margin 2. Size: 10x10x6 3. Shape/Angularity: Angular 6. Phenocrysts: Overall similar to #1 but has more Ol (up to 20%), some xls appr. 2 mm, a few Cpx, Plag 10. Comment: Glass at margin	X	X								+ Gene	
DR60-3	1. Rock Type: Volcanic fragment of lava with quenched margin 2. Size: 10x8x5 3. Shape/Angularity: Subangular 10. Comment: Similar to #2. Good for chemistry. Glass!	X	X									 <p style="text-align: center;">SO201-2 DR 6 0 -3</p>
DR60-4	1. Rock Type: Volcanic, fragment of lava, glassy margins 2. Size: 10x6x6 3. Shape/Angularity: Angular 10. Comment: Petrographically similar to #2-3	X	X									 <p style="text-align: center;">SO201-2 DR 6 0 -4</p>
DR60-5	1. Rock Type: Pumice 2. Size: Large piece appr. 20 cm diameter 3. Shape/Angularity: Subangular 4. Color: Dirty white to brownish 5. Rock texture: Almost aphyric, "wood"-like texture 6. Phenocrysts: Rare xls TiMt, Plag 7. Matrix: Glassy 10. Comment: This type of rock predominates in the haul.	X	X									 <p style="text-align: center;">SO201-2 DR 6 0 -5</p>
DR60-6	1. Rock Type: Volcanic, white pumice with xenoliths of basalts 2. Size: appr. 20 cm diameter 3. Shape/Angularity: Angular 5. Rock texture and other petrographic features (plus comments): PUMICE - white to light grey similar to #6, but somewhat more dense. Large rare vesicles, almost aphyric with rare xls Plag (<=3mm), TiMt (<=0.5 mm). XENOLITHS - 3 fragments of large size (appr. 2-3 cm diameter) and numerous small fragments evenly distributed in host pumice. BASALTS are dark grey, massive to slightly vesicular, Ol-Plag phyric. Ol <=5-7 %, <=2mm, Plag <=5% <=2 mm. Look similar to some rocks from eastern flank of volcano and also to some aphyric basaltic andesites, the size of xenoliths is big enough for chemistry	X	X								+ Gene	 <p style="text-align: center;">SO201-2 DR 6 0 -6</p>
DR60-7X	1. Rock Type: Many fragments of lava with quenched margins 2. Size: from appr. 3 cm to 8 cm. Some are cut 10. Comment: The rocks are similar to #1-4											

Appendix IV

SO201-2-DR61											Sample Photos	
Location: Area 7, Volcanologists massif, northern block, lower slope of northernmost extension Dredge on bottom UTC 17/09/09 17:49hrs, lat 55°34,11'N, long 167°16,76'E, depth 3910m Dredge off bottom UTC 17/09/09 19:02hrs, lat 55°34,49'N, long 167°16,33'E, depth 3435m Total volume: appr. 20% Comments: mainly volcanics												
SAMPLE #	SAMPLE DESCRIPTION	TS	CHEM	Ar	Rest	GL/MIN	ARCH	VJLC	SED	MN	NOTES	
DR61-1	1. Rock Type: Volcanic, aphyric basalt 2. Size: 15x15x13 3. Shape/Angularity: Angular, but without fresh flow surfaces preserved 4. Color: Gray interior surface 5. Rock texture: Rare vesicles filled with dark minerals - uncertain 6. Phenocrysts: rare phenocrysts 2-3 mm - Plag (?) - uncertain due to alteration, appr. 4% 7. Matrix: crystalline, appr. diabasic, Px and Plag probably 8. Secondary Minerals: veins of calcite 9. Encrustations: no	X	X								+ Gene	 <p style="text-align: center;">SO201-2 DR 6 1 -1</p>
DR61-2	1. Rock Type: Volcanic, aphyric basalt 2. Size: 12x12x9 3. Shape/Angularity: Angular but without fresh flow surface 4. Color: Gray interior surface 5. Rock texture: rare vesicles <1% filled with soft dark mineral 6. Phenocrysts: Rare phenocrysts <1% - altered 7. Matrix: Appears crystalline, possibly diabasic, Px and Pl 8. Secondary Minerals: vein and vesicle fillings 9. Encrustations: no	X	X								+ Gene	 <p style="text-align: center;">SO201-2 DR 6 1 -2</p>
DR61-3	1. Rock Type: Volcanic, aphyric basalt 2. Size: 18x12x13 3. Shape/Angularity: Angular but without fresh flow surfaces 4. Color: Gray interior 5. Rock texture: Rare vesicles (<1%) filled with dark secondary mineral 6. Phenocrysts: Rare <1%; Plag (altered) 7. Matrix: Crystalline, appears diabasic with intergrowth pyroxene and Plag	X	X								+ Gene	 <p style="text-align: center;">SO201-2 DR 6 1 -3</p>
DR61-4	1. Rock Type: Volcanic, altered, metavolcanic - spilitic basalt 2. Size: 12x9x8 3. Shape/Angularity: Angular - subangular 4. Color: Green - Gray - white interior 5. Rock texture: no vesicles evident 6. Phenocrysts: no preserved 8. Secondary Minerals: fine rim but crystalline interior of this rock has been replaced by altering minerals, probably mostly kaolinite and calcite. Some igneous texture preserved but mineralogy is mostly secondary. Trace sulfide mineralization - pyrite.										+ Gene	 <p style="text-align: center;">SO201-2 DR 6 1 -4</p>
DR61-5	1. Rock Type: Volcanic, aphyric basalt 2. Size: 17x11x9 3. Shape/Angularity: Subangular but no fresh surfaces 4. Color: Gray-green interior 5. Rock texture: Rare vesicles filled by dark mineral (<1%). Many igneous textures preserved, including fine rim (formerly glass?) 6. Phenocrysts: Rare (<1%) not replaced by secondary minerals 10. Comment: More altered than samples 1-3 in this dredge but texturally similar	X	X								+ Gene	 <p style="text-align: center;">SO201-2 DR 6 1 -5</p>
DR61-6	1. Rock Type: Volcanic, spilitic basalt or greenstone 2. Size: 12x8x6 3. Shape/Angularity: Subangular 4. Color: Dark greenish-gray interior 5. Rock texture: no vesicles. Porphyritic igneous texture partly preserved 6. Phenocrysts: 10-20% mostly Pl and Px. Plag now chalky and altered to clay 7. Matrix: Finely crystalline 8. Secondary Minerals: chlorite, kaolinite, calcite (?)	X	X									 <p style="text-align: center;">SO201-2 DR 6 1 -6</p>
DR61-7	1. Rock Type: Volcanic, Plagioclase basalt altered 2. Size: 15x10x8 3. Shape/Angularity: Subangular 4. Color: Gray interior 5. Rock texture: no vesicles 6. Phenocrysts: Plag, some few preserved Plag up to appr. 6 mm, appr 5-10% 8. Secondary Minerals: rock is fractured with veins of secondary minerals. Veins are probably carbonate. Rim of sample is green with chalky white feldspar phenocrysts											 <p style="text-align: center;">SO201-2 DR 6 1 -7</p>

Appendix IV

SAMPLE #	SAMPLE DESCRIPTION	TS	CHEM	Ar	Rest	GL/MIN	ARCH	VJ/LC	SED	MN	NOTES	Sample Photos
DR61-8	1. Rock Type: Volcanic breccia, mafic 2. Size: 16x14x6 3. Shape/Angularity: Angular 4. Color: Greenish-gray angular clasts in a dark green matrix. This appears to be crushed or shattered mafic volcanic rock in a fine matrix of similar material 5. Rock texture: Some igneous textures of the volcanic fragments are preserved 10. Comment: Most appear to be the abundant aphyric basalts											 SO201-2 DR 6 -8
DR61-9	1. Rock Type: Volcanic, altered basalt 2. Size: 20x7x10 3. Shape/Angularity: Subangular 4. Color: Greenish-Gray interior 5. Rock texture: no vesicles, dense lava 6. Phenocrysts: rare, probably Plag <5%, olivine, now altered to secondary minerals 7. Matrix: Aphanitic 8. Secondary Minerals: yes 10. Comment: Many igneous features well preserved but minerals and glass largely replaced by secondary minerals											 SO201-2 DR 6 1-9
DR61-10M	1. Rock Type: Manganese crust surrounding altered basalt 2. Size: size of a fragment 5x6x5 3. Shape/Angularity: 4. Color: basalt is greenish- gray interior 5. Rock texture: vesicles appr. 3% filled by dark minerals 6. Phenocrysts: Rare phenocr. partially or wholly replaced by secondary minerals	X										 SO201-2 DR 6 1-10 -M
DR61-11	1. Rock Type: Volcanic, fresh, olivine basalt / basaltic andesite 2. Size: 7x5x6 3. Shape/Angularity: Angular with fresh flow surfaces and with glass 4. Color: Gray to dark gray interior 5. Rock texture: vesicles appr. 20%, no fillings 6. Phenocrysts: Mostly olivine up to 1-2 mm, <5% 10. Comment: Suspect that this sample may not be representative of this place	X	X									

SO201-2-DR63



Location: Area 7, Alpha Fracture zone, SW slope

Dredge on bottom UTC 18/09/09 03:05hrs, lat 55°45,44'N, long 167°28,34'E, depth 3978m






Dredge off bottom UTC 18/09/09 04:11hrs, lat 55°45,90'N, long 167°28,25'E, depth 3601m

Total volume: 20% full




Comments: Abundant Mn-oxide crusts coating fragments of sedimentary rock

SAMPLE #	SAMPLE DESCRIPTION	TS	CHEM	Ar	Rest	GL/MIN	ARCH	VJ/LC	SED	MN	NOTES	Sample Photos
DR63-1S	1. Rock Type: Sandy siltstone with Mn crusts 2. Size: 12x9x9 3. Shape/Angularity: Angular fragments 4. Color: Dark-gray sandy siltstone 5. Rock texture: Manganese crusts cementing fragments of sedimentary rock. No internal structure evident, well-indurated								X			 SO201-2 DR 63-1S
DR63-2S	1. Rock Type: Sedimentary, sandy siltstone 2. Size: 7x7x5 3. Shape/Angularity: Angular 4. Color: Dark gray interior, dark well sorted silty sediment 5. Rock texture: Massive, no internal structure, well indurated. Some sand-size particles visible											 SC201-2 DR 63-2 S

Appendix IV

SAMPLE #	SAMPLE DESCRIPTION	TS	CHEM	Ar	Rest	GL/MIN	ARCH	VJ/LC	SED	MN	NOTES	Sample Photos
DR63-3M	1. Rock Type: Manganese oxide crust 2. Size: 12x10x6 3. Shape/Angularity: 4. Color: Dark reddish brown crusts 5. Rock texture: some concentric structure visible											 <p style="text-align: center;">SO201-2 DR 63-3 M</p>
SO201-2-DR71 Location: Area E, Shirshov Ridge, small ridge-like structure W of southern tip of Shirshov, eastern flank Dredge on bottom UTC 19/09/09 04:04hrs, lat 56°29,20'N, long 169°36,50'E, depth 3668m Dredge off bottom UTC 19/09/09 05:15hrs, lat 56°29,32'N, long 169°35,66'E, depth 3281m Total volume: almost nothing Comments: Two small rocks in this dredge might provide information on this location in the context of other more successful dredging in nearby areas which are planned												
SAMPLE #	SAMPLE DESCRIPTION	TS	CHEM	Ar	Rest	GL/MIN	ARCH	VJ/LC	SED	MN	NOTES	Sample Photos
DR71-1	1. Rock Type: Volcanic, Spilitic basalt 2. Size: 10x7x5 3. Shape/Angularity: Subangular, no fresh flow surfaces 4. Color: Dark gray-grayish-green 5. Rock texture: no vesicles 6. Phenocrysts: appr. 20-30% appear to be mostly Plag. With indistinct crystal boundaries and greenish color indicate significant alteration 7. Matrix: Aphanitic 8. Secondary Minerals: Sulfide minerals present 9. Encrustations: no	X	X									 <p style="text-align: center;">SO201-2 DR 71 -1</p>
DR71-2	1. Rock Type: Intrusive 2. Size: 9x7x3 3. Shape/Angularity: Subangular 4. Color: Pale green to grayish-green and black 5. Rock texture: Medium grain, phaneritic (massive) texture 6. Phenocrysts: Mafic composition, Plag and two Px + oxides. Plag is pale green to white, Cpx is black and appear well preserved. Opx (?) is gray and brown with metallik bronze cleavage planes, also appears well preserved. Minor oxide minerals. Sulfide also present 10. Comment: Composition and state of preservation / alteration is similar to #1 (above)	X	X									 <p style="text-align: center;">SO201-2 DR 71 -2</p>
SO201-2-DR73 Location: Area E, Shirshov Ridge, western flank of southern part Dredge on bottom UTC 19/09/09 10:04hrs, lat 56°16,85'N, long 169°39,18'E, depth 3677m Dredge off bottom UTC 19/09/09 11:21hrs, lat 56°17,32'N, long 169°39,33'E, depth 3074m Total volume: few rocks Comments: Highly tectonized tuffs, basalts, volcanic breccia												
SAMPLE #	SAMPLE DESCRIPTION	TS	CHEM	Ar	Rest	GL/MIN	ARCH	VJ/LC	SED	MN	NOTES	Sample Photos
DR73-1	1. Rock Type: Metamorphic after tuff / strongly tectonized 2. Size: 20x5x10 3. Shape/Angularity: Subangular 4. Color: Reddish green 5. Rock texture: Middle grained volcanogenic tuff. Tectonized 8. Secondary Minerals: Cut by veins of second. minerals 10. Comment: Completely altered	X										 <p style="text-align: center;">SO201-2 DR 73 -1</p>
DR73-2	1. Rock Type: Strongly tectonized tuff similar to #1 2. Size: 8x2x6 3. Shape/Angularity: Subrounded 8. Secondary Minerals: chlorite, epidote, carbonate 10. Comment: Strongly altered	X										 <p style="text-align: center;">SO201-2 DR 73 -2</p>

Appendix IV

SAMPLE #	SAMPLE DESCRIPTION	TS	CHEM	Ar	Rest	GL/MIN	ARCH	VJJC	SED	MN	NOTES	Sample Photos
DR73-3	1. Rock Type: Tectonic breccia after finegrained tuff (?) 2. Size: 10x4x6 3. Shape/Angularity: Angular 4. Color: light green to greenish grey 5. Rock texture: Dence with aphanitic texture of unclear provenance	X										
DR73-4	1. Rock Type: Volcanic, highly altered and tectonized 2. Size: 5x4x3 3. Shape/Angularity: Angular 4. Color: Greenish grey 5. Rock texture: Pl phyric basalt (appr. 20% <=2 mm) 6. Phenocrysts: No fresh minerals preserved 8. Secondary Minerals: Highly altered (chlorite, epidote) cut by veins of SiO2	X										
SO201-2-DR74 Location: Area E. Shirshov Ridge, small "step" at upper eastern flank at Ridge-like structure at S-part of Shirshov Dredge on bottom UTC 19/09/09 15:14hrs, lat 56°15,07'N, long 169°52,83'E, depth 2517m Dredge off bottom UTC 19/09/09 16:14hrs, lat 56°15,38'N, long 169°52,25'E, depth 2199m Total volume: 1 block + a few rocks Comments: Large block = sandstone, small ones = Fe-Mn crusts, granite, basalts												
SAMPLE #	SAMPLE DESCRIPTION	TS	CHEM	Ar	Rest	GL/MIN	ARCH	VJJC	SED	MN	NOTES	Sample Photos
DR74-1S	1. Rock Type: Sandstone 2. Size: 40x40x25 3. Shape/Angularity: Angular 4. Color: Light greenish grey 5. Rock texture: Fine grained, layered, layers are <=1 mm to 1 cm thick with sharp boundaries. Grain size varies from appr. 0.5 mm to very fine 7. Matrix: Clayish matrix, soft 10. Comment: The sample is likely paleogene	X							X		+ D. Savelyev, + N. Tsukanov	
DR74-2M	1. Rock Type: Mn crust 4. Color: Brown 5. Rock texture: Soft, dirty											







Appendix IV

SO201-2-DR87											Sample Photos	
Location: Area E, Shirshov Ridge, top area in the central part of Shirshov, W-facing step Dredge on bottom UTC 21/09/09 10:51hrs, lat 57°30.50'N, long 170°06.32'E, depth 945m Dredge off bottom UTC 21/09/09 11:47hrs, lat 57°30.49'N, long 170°07.01'E, depth 694m Total volume: Full Comments: Tuffs, breccia of Hbl, Cpx phyric andesites (?), mega Hbl andesites. A few dropstones (granite)												
SAMPLE #	SAMPLE DESCRIPTION	TS	CHEM	Ar	Rest	GL/MIN	ARCH	VJLC	SED	MN	NOTES	
DR87-1	1. Rock Type: Volcanic lava, moderately altered 2. Size: 20x20x30 3. Shape/Angularity: Subrounded 4. Color: Brownish grey 5. Rock texture: Cpx-Hbl phyric andesite, nonvesicular 6. Phenocrysts: Hbl - appr. 20% <=1cm fresh; Cpx - <=5% <=1cm fresh 7. Matrix: Microlitic (Pl<=1.5mm) 8. Secondary Minerals: Somewhat altered, numerous veins (<=0.5mm) filled with white mineral 9. Encrustations: 10. Comment: Good for chemistry, Ar-Ar (!)	X	X									 <p style="text-align: center;">SO201-2 DR 8 7 -1</p>
DR87-2	1. Rock Type: Volcanic, vesicular andesitic basalt fragment in tuff matrix. Moderately altered 2. Size: 50x40x30 (whole block), andesitic fragments are upto appr. 10cm diameter 6. Phenocrysts: Andesitic clasts - Cpx-Plag phyric and-bas., Cpx appr. 15% <=2mm (augite), Plag <=30% <=2mm, vesicles rounded diameter <=6mm, filled with calcite (?) 7. Matrix: andesite clasts - microlitic with colour variable from brownish to grey; Matrix tuff - greenish-grey, middle grained 10. Comment: Good for chemistry, should be picked to avoid altered parts	X	X									 <p style="text-align: center;">SO201-2 DR 8 7 -2</p>
DR87-3	1. Rock Type: Volcanic, rare vesicular andesite basalt 2. Size: diameter appr. 30 cm 3. Shape/Angularity: Subangular fragment 4. Color: Dark grey 5. Rock texture: Cpx-Plag phyric, vesicular 6. Phenocrysts: Cpx <=10% <=2mm fresh; Plag - <=10% <=5mm, altered (?), vesicles - rare <=5mm, flattened 7. Matrix: Microlithic 8. Secondary Minerals: Moderate (altered Plag, Fe oxides) 10. Comment: Relatively good for chemistry, may require some picking to avoid obviously altered parts	X	X									 <p style="text-align: center;">SO201-2 DR 8 7 -3</p>
DR87-4	1. Rock Type: Tuffobrecia, andesitic 2. Size: 20x30x35 3. Shape/Angularity: Rounded 5. Rock texture: Contains clasts of andesites Hbl bearing, Cpx-Plag basalts, single megacrysts of Cpx, Hbl (<=1cm), clast of hornblende. Size of clasts is typically appr. 1.5 to 3 cm 10. Comment: Most of andes-bas. clasts look similar to #3	X										 <p style="text-align: center;">SO201-2 DR 8 7 -4</p>
DR87-5	1. Rock Type: Tuff, coarse grained 2. Size: appr. 30 cm diameter 3. Shape/Angularity: flattened rounded 4. Color: Greenish grey 5. Rock texture: Coarse grained, non layered 6. Phenocrysts: Plag, Cpx, Hbl (?) crystals 8. Secondary Minerals: Moderately altered 10. Comment: The sample represents one of numerous blocks of this type in the haul	X										 <p style="text-align: center;">SO201-2 DR 8 7 -5</p>
DR87-6	1. Rock Type: Tuffobrecia similar to #4 5. Rock texture: Similar to #4 but contains larger clasts of Pl-Cpx basalts (?) <=5-6 cm in diameter, Amf bearing andesites, also a lot of single crystals 7. Matrix: Hbl and Cpx in tuff matrix 10. Comment: Some clasts are good for chemistry	X										 <p style="text-align: center;">SO201-2 DR 8 7 -6</p>





Appendix IV

SAMPLE #	SAMPLE DESCRIPTION	TS	CHEM	Ar	Rest	GL/MIN	ARCH	VULC	SED	MIN	NOTES	Sample Photos
DR87-7	1. Rock Type: Sponges											
SO201-2-DR88 Location: Area E, Shirshov ridge, top area in the central part of Shirshov, SW facing step (lower level than 87 DR) Dredge on bottom UTC 21/09/09 15:31hrs, lat 57°34,09N, long 170°05,32E, depth 1158m Dredge off bottom UTC 21/09/09 16:18hrs, lat 57°34,24N, long 170°05,89E, depth 835m Total volume: 1/2 full Comments: sheet lavas, cherts, breccia, a lot of sponges												
SAMPLE #	SAMPLE DESCRIPTION	TS	CHEM	Ar	Rest	GL/MIN	ARCH	VULC	SED	MIN	NOTES	Sample Photos
DR88-1	1. Rock Type: Volcanic, sheet flow? 2. Size: 30x10x15 3. Shape/Angularity: Angular 4. Color: Dark grey / brownish grey 5. Rock texture: Massive with fine fluidality, nonvesicular. Almost aphyric 6. Phenocrysts: minor phenocrysts of Pl, Cpx 7. Matrix: microdoleritic 8. Secondary Minerals: Thin veins, Fe oxides, Mn 10. Comment: Good for chemistry and probably Ar-Ar	X	X									
DR88-2	1. Rock Type: Volcanic, massive, aphyric, lava flow 2. Size: 12x8x10 3. Shape/Angularity: Angular 4. Color: Brownish grey 8. Secondary Minerals: Vesicles filled, some <=1mm veins of halzedon 10. Comment: Similar to # 1 and # 3 but more altered	X	X									
DR88-3	1. Rock Type: Volcanic, massive aphyric basalt 2. Size: 15x5x6 3. Shape/Angularity: Angular 4. Color: Dark grey / brownish grey 5. Rock texture: Rare vesicles, open 10. Comment: Overall looks similar to #1. Good for chemistry	X	X									-1 

Appendix IV

SAMPLE #	SAMPLE DESCRIPTION	TS	CHEM	Ar	Rest	GU/MIN	ARCH	VJULC	SED	MN	NOTES	Sample Photos
DR88-4	1. Rock Type: Aphyric massiv basalt (or possibly tuff) 2. Size: 10x4x5 3. Shape/Angularity: Subangular 5. Rock texture: Aphyric with rare Pl crystals 10. Comment: Similar to # 1-3	X										 SO201-2 DR 88 -4
DR88-5	1. Rock Type: Volcanic, Sheet flow 2. Size: 7x7x6 3. Shape/Angularity: Subangular 8. Secondary Minerals: many veins of sec minerals (<=0.5 mm thick) very rare vesicles rounded, filled with white mineral 10. Comment: Similar to # 1-3	X										 SO201-2 DR 88 -5
DR88-6	1. Rock Type: Rare Pl-Px phytic basalt 2. Size: 12x3x4 3. Shape/Angularity: Subangular 4. Color: Brownish grey 5. Rock texture: Aphyric, massive 10. Comment: altered, similar to #3, may be good for chemistry at least voids are open and not many veining	X										 SO201-2 DR 88 -6
DR88-7	1. Rock Type: Volcanic breccia, strongly altered 2. Size: several pieces, diameter 5-10 cm 5. Rock texture: Consists of fragments of aphyric to rare phytic basalts 10. Comment: Alteration: pervasive. If analyzed for major and trace elements must be picked to avoid veins and vesicles filling	X										 SO201-2 DR 88 -7
DR88-8S	1. Rock Type: Chert with a mixture of a bit volcanoclastic material 4. Color: Bluish grey to brownish grey										+ D. Savelyev	 SO201-2 DR 88 -8 S
DR88-9X	1. Rock Type: Six pieces of aphyric basalts and probably tuffs 10. Comment: Similar petrographically to # 1-6. It is worth to look at these fragments in detail if geochemistry of first samples is interesting						X					 SO201-2 DR 88 -9 X

Appendix IV

SO201-2 DR103 Location: Western flank of Shirshov Ridge, northern part of Shirshov, "block" off western slope Dredge on bottom UTC 23/09/09 06:07hrs, lat 58°44,17'N, long 169°53,33'E, depth 1587m Dredge off bottom UTC 23/09/09 08:02hrs, lat 58°44,28'N, long 169°53,72'E, depth 1353m Total volume: Some rocks Comments: Sheared peridotites, few dropstones												
SAMPLE #	SAMPLE DESCRIPTION	TS	CHEM	Ar	Rest	GL/MIN	ARCH	VULC	SED	MIN	NOTES	Sample Photos
DR103-1	1. Rock Type: Ultramafic metamorphosed sheared rock 2. Size: sized up to appr. 30 cm 3. Shape/Angularity: one of several angular pieces 4. Color: light to dark green 5. Rock texture: Sheared texture, dark rounded fragments of harzburgite (?) in serpentinite matrix 10. Comment: This rock comes from the same tectonic block of amphibolites dredged here before on the E slope. Probably this is serpentinite melange including amphibolites	X									+ S. Silantyev	
SO201-2-DR105 Location: Area E, Shirshov Ridge, northern part of Shirshov, lower western flank Dredge on bottom UTC 23/09/09 12:07hrs, lat 58°31,77'N, long 169°51,36'E, depth 2078m Dredge off bottom UTC 23/09/09 13:37hrs, lat 58°31,87'N, long 169°52,30'E, depth 1520m Total volume: Some rocks Comments: Several angular blocks of green schists, small subrounded andesites, tufts, 1 stone - amphibolite												
SAMPLE #	SAMPLE DESCRIPTION	TS	CHEM	Ar	Rest	GL/MIN	ARCH	VULC	SED	MIN	NOTES	Sample Photos
DR105-1	1. Rock Type: Metamorphic, green schist, metasediment likely with admixture of volcanic material 5. Rock texture: Layered 6. Phenocrysts/matrix: Quartz and chlorite										+ S. Silantyev	
DR105-2	1. Rock Type: Amphibolite 2. Size: appr. 10x2x8 3. Shape/Angularity: small, rounded, flattened 4. Color: Black										+ S. Silantyev	
SO201-2-DR107 Location: Area E, Shirshov Ridge, northern part of Shirshov, small step at lower western flank Dredge on bottom UTC 23/09/09 18:51hrs, lat 58°16,58'N, long 169°41,85'E, depth 2742m Dredge off bottom UTC 23/09/09 19:46hrs, lat 58°16,64'N, long 169°42,46'E, depth 2412m Total volume: Few rocks Comments: Partly solidified sediments (clay)												
SAMPLE #	SAMPLE DESCRIPTION	TS	CHEM	Ar	Rest	GL/MIN	ARCH	VULC	SED	MIN	NOTES	Sample Photos
DR107-1S	1. Rock Type: Partly solidified sediment, clay 2. Size: One of similar fragments upto appr. 50x30x30 cm 3. Shape/Angularity: 4. Color: Yellowish grey 5. Rock texture: No clasts 10. Comment: No carbonates											
SO201-2-DR118 Location: Area 3, Komandorskiy basin, small NW-SE trending ridge, SW flank from base to top Dredge on bottom UTC 25/09/09 19:43hrs, lat 57°54,52'N, long 165°57,82'E, depth 3554m Dredge off bottom UTC 25/09/09 20:45hrs, lat 57°54,81'N, long 165°58,41'E, depth 3124m Total volume: appr. 10% full Comments: Many small pillow fragments, mostly <15cm, in long dimension - homogeneous, Ol-Plag basalt, few dropstones												
SAMPLE #	SAMPLE DESCRIPTION	TS	CHEM	Ar	Rest	GL/MIN	ARCH	VULC	SED	MIN	NOTES	Sample Photos
DR118-1	1. Rock Type: Volcanic, partially altered, Pl-Ol basalt 2. Size: 30x20x15 3. Shape/Angularity: Angular 4. Color: Dark gray interior 5. Rock texture: Sparse vesicles < 1% filled by dark mineral-dark green amygdules 6. Phenocrysts: <2-3 %, mostly Plag-fresh, sparse Ol appears mostly altered. 7. Matrix: Appears holo-crystalline and fresh 9. Encrustations: no 10. Comment: Ar-Ar - good crystalline gr. mass. Relatively large pillow fragment with distinctive core that appears to be largely crystalline and fresh. Rims of pillow are more altered and lack glass	X	X	X		Plag						

Appendix IV


SAMPLE #	SAMPLE DESCRIPTION	TS	CHEM	Ar	Rest	GL/MI	N	ARCH	VULC	SED	MN	NOTES	Sample Photos
DR118-1X	1. Rock Type: the same as #1 10. Comment: Extra pieces for archive							X					
DR118-2	1. Rock Type: Volcanic - partially altered, Ol-Pl basalt, pillow fragment 2. Size: 13x9x9 3. Shape/Angularity: Subangular 4. Color: Gray-dark gray interior 5. Rock texture: vesicles - absent. Glass rind is in-place but altered - pillow fragment 6. Phenocrysts: 5-10% - mostly Ol- mostly altered. Plag phenocr. partially fresh 9. Encrustations: no	X	X			Plag, Glas s							 SO201-2 DR -118 -2
DR118-3	1. Rock Type: Volcanic-partially altered, Plag-Ol basalt 2. Size: 13x8x6 3. Shape/Angularity: Subangular 4. Color: Dark gray interior 5. Rock texture: Vesicles sparse - filled by dark green mineral 6. Phenocrysts: 10-20 % mostly Plag, some fresh and up to 6-8 mm. Ol are fewer, smaller and mostly altered 7. Matrix: Aphanitic - appears mostly crystalline 9. Encrustations: no	X	X			Plag							 SO201-2 DR -118 -3
DR118-4	1. Rock Type: Volcanic - partially altered, Pl-Ol basalt 2. Size: 9x8x5 3. Shape/Angularity: Subangular 4. Color: Dark gray interior 5. Rock texture: Vesicles - absent (?), sparsely phyrlic 6. Phenocrysts: appr. 2-4% up to 2-3 mm, mostly Plag - some fresh. Ol phenocrysts appear mostly altered 7. Matrix: Aphanitic and appears mostly crystalline 9. Encrustations: no	X	X			Plag							 SO201-2 DR -118 -4
DR118-5	1. Rock Type: Volcanic-partially altered, Pl-Ol basalt 2. Size: 7x9x10 3. Shape/Angularity: Subangular 4. Color: Dark gray interior 5. Rock texture: Vesicles - absent (?) 6. Phenocrysts: 10-20%, Plag and Ol up to 6-8 mm, Pl - mostly fresh, Ol - mostly altered 7. Matrix: Aphanitic 9. Encrustations: no	X	X			Plag							 SO201-2 DR -118 -5
DR118-6	1. Rock Type: Volcanic - partially altered, Pl-Ol basalt 2. Size: 10x8x5 3. Shape/Angularity: Subangular 4. Color: Dark gray interior 5. Rock texture: Sparsely vesicular <1% vesicles filled with dark green mineral 6. Phenocrysts: 15-20%, mostly Plag, some fresh. Ol mostly altered 7. Matrix: Aphanitic, appears mostly crystalline 9. Encrustations: no	X	X			Plag							 SO201-2 DR -118 -6
DR118-7	1. Rock Type: Volcanic-partially altered, Ol-Pl basalt 2. Size: 12x8x5 3. Shape/Angularity: Angular 4. Color: Dark gray interior 5. Rock texture: Very sparsely vesicular - vesicles filled with dark green mineral 6. Phenocrysts: appr. 5%, some glomerocrysts of Ol up to 10-12 mm long. Ol appears mostly altered. Plag phenocr are smaller - up to 2-3 mm and appear mostly fresh 10. Comment: Pillow rind in this sample but no glass	X	X			Plag							 SO201-2 DR -118 -7
DR118-8	1. Rock Type: Volcanic - partially altered, Plag-Ol basalt 2. Size: 12x10x8 3. Shape/Angularity: Angular 4. Color: Dark gray interior 5. Rock texture: vesicles filled with dark green mineral 6. Phenocrysts: 15-20 %, Plag up to 6-8 mm - some fresh. Ol up to 4-6 mm - mostly altered 7. Matrix: Aphanitic 9. Encrustations: no	X	X			Plag							 SO201-2 DR -118 -8 X

Appendix IV





SAMPLE #	SAMPLE DESCRIPTION	TS	CHEM	Ar	Rest	GL/MI	ARCH	VULC	SED	MIN	NOTES	Sample Photos
DR118-9X	1. Rock Type: partially altered PI-OI basalt 2. Size: 9x6x7 10. Comment: Similar to abundant pillow fragments in this dredge					Plag	X					
DR118-10X	1. Rock Type: Partially altered, PI-OI basalt 2. Size: 10x8x6 6. Phenocrysts: fresh Plag 10. Comment: Similar to abundant pillow fragments in this dredge. Rind present but not glassy					Plag	X					
DR118-11X	1. Rock Type: Partially altered - PI-OI basalt 2. Size: 8x5x5 10. Comment: Similar to abundant pillow fragments in this dredge					Plag	X					
DR118-12X	1. Rock Type: partially altered PI-OI basalt 2. Size: 9x7x7 6. Phenocrysts: Some large Plag up to 8 mm 10. Comment: Similar to abundant pillow fragments in this dredge					Plag	X					
DR118-13X	1. Rock Type: Partially altered, PI-OI basalt 2. Size: 7x6x4 10. Comment: Similar to abundant pillow fragments in this dredge. Glassy rind appears mostly altered					Plag, Glas s?	X					
DR118-14X	1. Rock Type: Mixture of bulk pillow fragments from this dredge 10. Comment: Many pieces all uncut						X					

SO201-2-DR121

Location: Area B, Meiji area, NE-SW trending ridge W of trench - accreted block/crust?
Dredge on bottom UTC 28/09/09 15:03hrs, lat 54°18.56'N, long 163°25.96'E, depth 5660m
Dredge off bottom UTC 28/09/09 16:11hrs, lat 54°18.95'N, long 163°25.34'E, depth 5303m
Total volume: few rocks
Comments: volcanics, granite - dropstones

SAMPLE #	SAMPLE DESCRIPTION	TS	CHEM	Ar	Rest	GL/MI	ARCH	VULC	SED	MIN	NOTES	Sample Photos
DR121-1	1. Rock Type: Volcanic, moderately altered, Cpx-Pl phyrlic basalt 2. Size: 12x8x8 3. Shape/Angularity: Subrounded 4. Color: Dark greenish grey 6. Phenocrysts: Cpx - appr. 20-30% <=1 cm, Plag - <=15% <=0.5 cm 7. Matrix: Doleritic 8. Secondary Minerals: at margin - pervasive, some veining 10. Comment: Most likely dropstone	X	X									

Appendix IV

SO201-2-DR122 Location: Area B, Meiji Seamount, 1 (deepest) step at NW flank of Meiji small scarp Dredge on bottom UTC 28/09/09 22:21hrs, lat 54°01,12'N, long 163°17,51'E, depth 5569m Dredge off bottom UTC 28/09/09 23:32hrs, lat 54°01,55'N, long 163°18,03'E, depth 5238m Total volume: few rocks Comments: many small fragments, rounded to angular, mostly andesitic lava and various sedimentary rocks, some basaltic lava, one large piece of poorly lithified mud is regarded to be local. The rest is exotic												Sample Photos		
SAMPLE #	SAMPLE DESCRIPTION	TS	CHE	M	Ar	Rest	GL/MN	ARCH	H	VULC	SED	MN	NOTES	Sample Photos
DR122-1	1. Rock Type: Muddy sediment 2. Size: 30x35x20 3. Shape/Angularity: Smoothed edges due to transportation 4. Color: Light grayish green colour 5. Rock texture: Poorly consolidated													 <p style="text-align: center;">SO201-2 DR -12 2-1</p>
SO201-2-DR123 Location: Area B, Meiji Seamount, 3 step at NW flank of Meiji (most shallow step) Dredge on bottom UTC 29/09/09 04:35hrs, lat 53°54,38'N, long 163°33,79'E, depth 4536m Dredge off bottom UTC 29/09/09 05:52hrs, lat 53°53,97'N, long 163°34,34'E, depth 4072m Total volume: 1/4 Comments: Solidified sediments - allevolites. D. Savelyev took duplicates of #1-3 and also a number of other samples of similar lithology, numbered continuously from #4...														
SAMPLE #	SAMPLE DESCRIPTION	TS	CHEM	Ar	Rest	GL/MN	ARCH	VULC	SED	MN	NOTES	Sample Photos		
DR123-1S	1. Rock Type: Siliceous allevolite 2. Size: 30x20x15 3. Shape/Angularity: Subrounded 4. Color: Light to dark grey 5. Rock texture: "lens"-type layering. 10. Comment: Thin layers enriched in microfossils. Admixture of tuff material. Radiolarians and foraminiferas present								X		+ D. Savelyev	 <p style="text-align: center;">SO201-2 DR -12 3-1 S</p>		
DR123-2S	1. Rock Type: Siliceous allevolite 2. Size: diameter 10 cm 3. Shape/Angularity: Subrounded 4. Color: Transition from light grey to dark grey 5. Rock texture: Fine layered								X		+ D. Savelyev	 <p style="text-align: center;">SO201-2 DR -12 3-2 S</p>		
DR123-3S	1. Rock Type: Siliceous allevolite, partly consolidated 2. Size: appr. 10x5x7 3. Shape/Angularity: 4. Color: Light olive grey 5. Rock texture: "Lens"-type layering. Plate joining perpendicular to layering								X		+ D. Savelyev	 <p style="text-align: center;">SO201-2 DR -12 3-3 S</p>		

Appendix V
Sampling Summary Sediment

Appendix V

Station No.	Gear	Date (UTC)	On Bottom (UTC)	Water depth EM120 (m)	Latitude (deg/min) WGS84	Longitude (deg/min) WGS84	Area	Recovery Pilot Core (m)	Recovery Core (m)	Remarks
SO201-2-09	KL	08.09.2009	22:22	2627	53°52,16'N	162°04,05'E	Area B Kronotsky Peninsula	0,50	5,35	Piston corer 15 m; Banana
SO201-2-12	KL	09.09.2009	4:49	2170	53°59,47'N	162°22,51'E	Area B Kronotsky Peninsula	0,82	9,05	Piston corer 15 m
SO201-2-14	KL	09.09.2009	10:33	1482	54°17,31'N	162°11,87'E	Area B Kronotsky Peninsula	0,61	2,74	Piston coring; Banana
SO201-2-15	SL	09.09.2009	12:10	1483	54°17,31'N	162°11,86'E	Area B Kronotsky Peninsula	0,00	0,00	Gravity coring; only CC recovered
SO201-2-40	KL	13.09.2009	6:35	2984	53°18,63'N	164°46,67'E	Area B Meiji Seamount	0,25	8,95	Piston corer 20 m; Banana
SO201-2-69	KL	18.09.2009	21:36	3924	56°04,14'N	169°14,22'E	Area E Kommandorsky Basin	0,60	6,75	Piston corer 10 m
SO201-2-77	KL	20.09.2009	1:34	2135	56°19,83'N	170°41,98'E	Area E Shirshov Ridge	0,90	11,78	Piston corer 15 m; close to IODP site
SO201-2-80	KL	20.09.2009	9:50	1159	56°42,98'N	170°29,74'E	Area E Shirshov Ridge	0,86	12,20	Piston corer 15 m; overpenetrated
SO201-2-81	KL	20.09.2009	12:59	1161	56°42,99'N	170°29,77'E	Area E Shirshov Ridge	0,17	17,55	Piston corer 20 m
SO201-2-84	KL	21.09.2009	4:56	943	57°30,31'N	170°24,79'E	Area E Shirshov Ridge	0,00	18,00	Piston corer; Pilotcore did not function properly, therefore no recovery except for surface sample
SO201-2-85	KL	21.09.2009	8:05	968	57°30,30'N	170°24,77'E	Area E Shirshov Ridge	0,00	18,13	Piston corer 20 m; Pilotcore did not function properly
SO201-2-100	KL	22.09.2009	21:39	630	58°52,55'N	170°41,40'E	Area E Shirshov Ridge	0,73	17,54	Piston corer 20 m
SO201-2-101	KL	22.09.2009	0:06	630	58°52,52'N	170°41,45'E	Area E Shirshov Ridge	0,57	18,32	Piston corer 20 m
SO201-2-114	KL	25.09.2009	2:21	1417	59°13,87'N	166°59,32'E	Area D	1,00	7,89	Piston corer 10 m
SO201-2-115	KL	25.09.2009	5:58	726	59°19,51'N	166°47,75'E	Area D	0,74	4,30	Piston corer 15 m
SO201-2-127	KL	30.09.2009	3:05	1440	54°23,66'N	162°13,34'E	Area B Kronotsky Peninsula	0,90	5,54	Piston corer 15 m
SUM								8,65	164,09	

Locations of piston (KL) and gravity cores (SL) recovered during SO201-2 and relevant information.

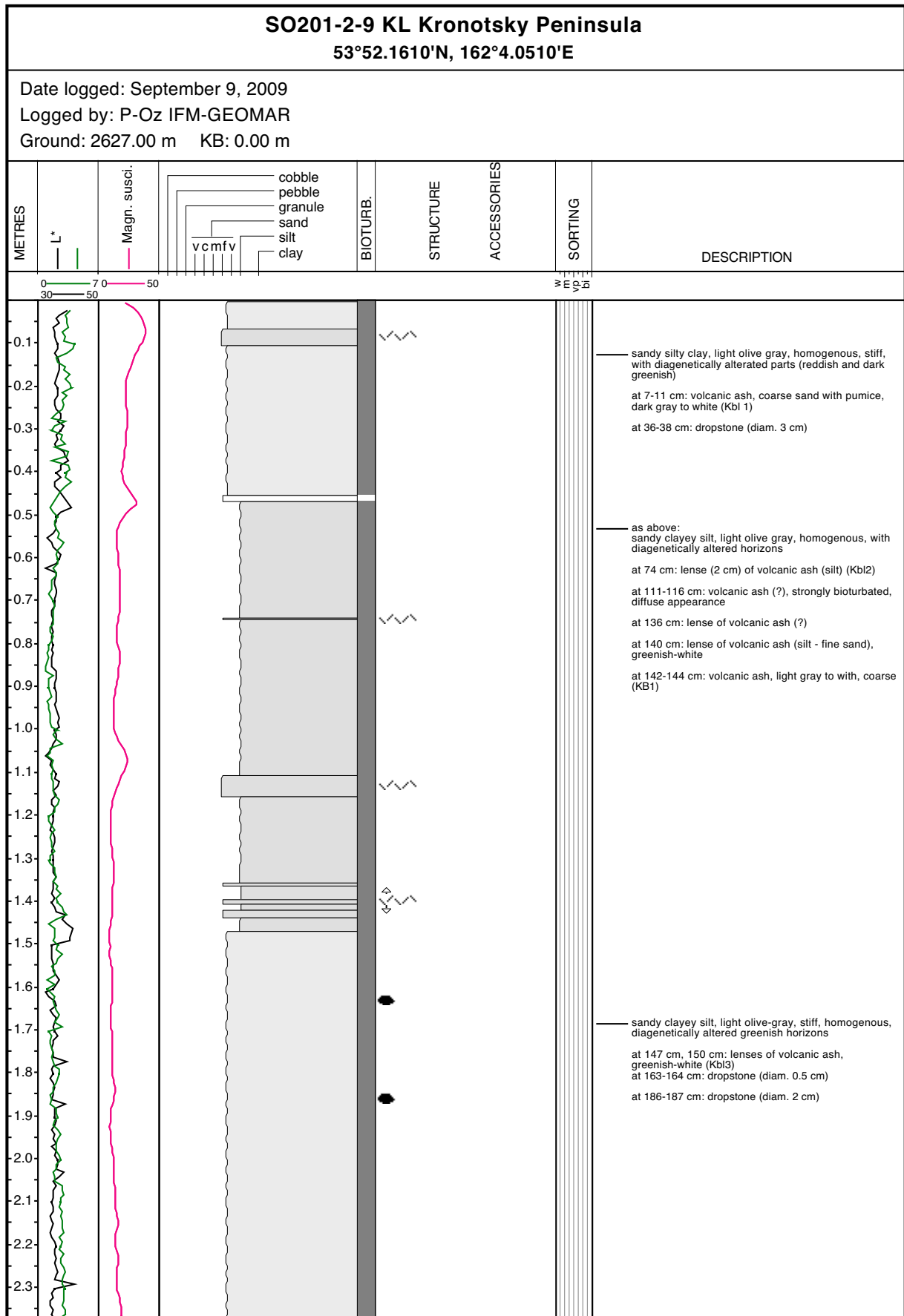
Appendix V

Station No.	Gear	Date (UTC)	On Bottom (UTC)	Water depth EMT20 (m)	Latitude (deg/min) WGS84	Longitude (deg/min) WGS84	Area	Amount of Cores	Total Recovery (cm)	TI1 (cm)	TI2 (cm)	NU1 (cm)	NU2 (cm)	NU3 (cm)	AW1 I (cm)	AW1 II (cm)	AW1 III (cm)	AW1 IV (cm)	Go (cm)	Iv (cm)	Ko (cm)	Remarks	
SO201-2-06	MUC	08.09.2009	8:01	931	53°03.42'N 161°03.72'E	161°03.72'E	Area B Kronotsky Peninsula	0	1	1										src	src	- almost no penetration - sample T1 treated with Rose Bengal - 6 cm of unlamiated dark-greyish sediment - silt to fine sand - 2 gravels (1 cm diam.)	
SO201-2-08	MUC	08.09.2009	19:30	2635	53°52.18'N 162°03.96'E	162°03.96'E	Area B Kronotsky Peninsula	2	10	4		src			6					src	src	- no oxidation horizon visible - homogeneous greenish-brown sediment - silt-dominated - smell of sulfur hydroxide	
SO201-2-11	MUC	09.09.2009	2:31	2169	53°59.47'N 162°22.53'E	162°22.53'E	Area B Kronotsky Peninsula	6	56	11		9			10	8	8			10		- no oxidation horizon visible - homogeneous greenish-brown sediment - silt-dominated - smell of sulfur hydroxide - sampling problems according to not fitting MUC-plugs - sediment in 1 tube was completely lost - Russian colleagues share 1 tube of 13 cm - no oxidation horizon visible - homogeneous greenish-grey sediment - silt-dominated - smell of sulfur hydroxide - only water sampling	
SO201-2-13	MUC	09.09.2009	8:47	1463	54°17.32'N 162°11.85'E	162°11.85'E	Area B Kronotsky Peninsula	6	74			12	13		13	10	13			13		- 5 full tubes, 4 empty tubes, 3 tubes did not function - TV-system failure at 2360 m water depth 0-13cm: silty, brownish oxidation horizon 13cm-EOC: pale grey clay	
SO201-2-32	MUC	12.09.2009	9:18	4231	54°03.60'N 164°11.01'E	164°11.01'E	Area B Meili Seamount															- location close to IODP site	
SO201-2-68	MUC	18.09.2009	17:41	3915	56°04.13'N 169°14.11'E	169°14.11'E	Area E Kommandorsky Basin	5	97	19		24			16	23				15		- MUC with TV-System (Site 13) - 1 tube did not close	
SO201-2-76	MUC	19.09.2009	23:10	2137	56°19.80'N 170°41.96'E	170°41.96'E	Area E Shishov Ridge	9	258	23	24	31	31	24	28	27	28	28	22	20		- MUC with TV-System (Site 13) 0-12cm: brownish-green silty clay; foram-bearing 12cm-EOC: green-to olive-grey clay; foram-bearing 0-8cm: light olive-grey silty sand, rich in benthic organisms; 8cm-EOC: stiff, dark olive-grey sandy clay; silt; dropstones common; foraminifers - homogeneous greyish-green to brownish-green silty mud	
SO201-2-79	MUC	20.09.2009	7:23	1161	56°42.99'N 170°29.78'E	170°29.78'E	Area E Shishov Ridge	7	118		24				24	24	22					- TV-system failure during deployment - few penetration, only surface sediments recovered - brownish-grey sandy mud with gravel (f.f.d.) - gear did not function entirely due to hard seafloor	
SO201-2-83	MUC	21.09.2009	2:57	970	57°30.28'N 170°24.82'E	170°24.82'E	Area E Shishov Ridge	8	110	17		16			11	16	13			12		- 8 full tubes, 2 empty tubes, sediment in 1 tube was lost during recovery - from tubes 9 and 10 only surface sediments have been recovered 0-1cm: dark greyish clay with bioturbation 1-8cm: greenish-grey clay with bioturbation and gastropod shells 8cm-EOC: dark grey silty mud	
SO201-2-90	MUC-TV	22.09.2009	3:22	1616	58°42.01'N 171°23.77'E	171°23.77'E	Area E Shishov Ridge	12	151		31	30	30	31	29								- TV-system failure during deployment - few penetration, only surface sediments recovered - brownish-grey sandy mud with gravel (f.f.d.) - gear did not function entirely due to hard seafloor
SO201-2-99	MUC-TV	22.09.2009	19:50	643	58°52.53'N 170°41.48'E	170°41.48'E	Area E Shishov Ridge	3	6			3			2	1						- 8 full tubes, 2 empty tubes, sediment in 1 tube was lost during recovery - from tubes 9 and 10 only surface sediments have been recovered 0-1cm: dark greyish clay with bioturbation 1-8cm: greenish-grey clay with bioturbation and gastropod shells 8cm-EOC: dark grey silty mud	
SO201-2-113	MUC-TV	24.09.2009	0:10	1392	59°13.86'N 166°59.24'E	166°59.24'E	Area D	4	10			5			4	1						- TV-system failure during deployment - few penetration, only surface sediments recovered - brownish-grey sandy mud with gravel (f.f.d.) - gear did not function entirely due to hard seafloor	
SO201-2-116	MUC	25.09.2009	7:34	725	59°19.51'N 166°47.70'E	166°47.70'E	Area D	0	0													- 8 full tubes, 2 empty tubes, sediment in 1 tube was lost during recovery - from tubes 9 and 10 only surface sediments have been recovered 0-1cm: dark greyish clay with bioturbation 1-8cm: greenish-grey clay with bioturbation and gastropod shells 8cm-EOC: dark grey silty mud	
SO201-2-126	MUC	30.09.2009	1:15	1443	54°23.64'N 162°13.37'E	162°13.37'E	Area B Kronotsky Peninsula	7	96		15		16	15	13	11	13			13		- 8 full tubes, 2 empty tubes, sediment in 1 tube was lost during recovery - from tubes 9 and 10 only surface sediments have been recovered 0-1cm: dark greyish clay with bioturbation 1-8cm: greenish-grey clay with bioturbation and gastropod shells 8cm-EOC: dark grey silty mud	
							SUM	69	987	75	94	125	95	112	128	122	96	28	75	0	37		

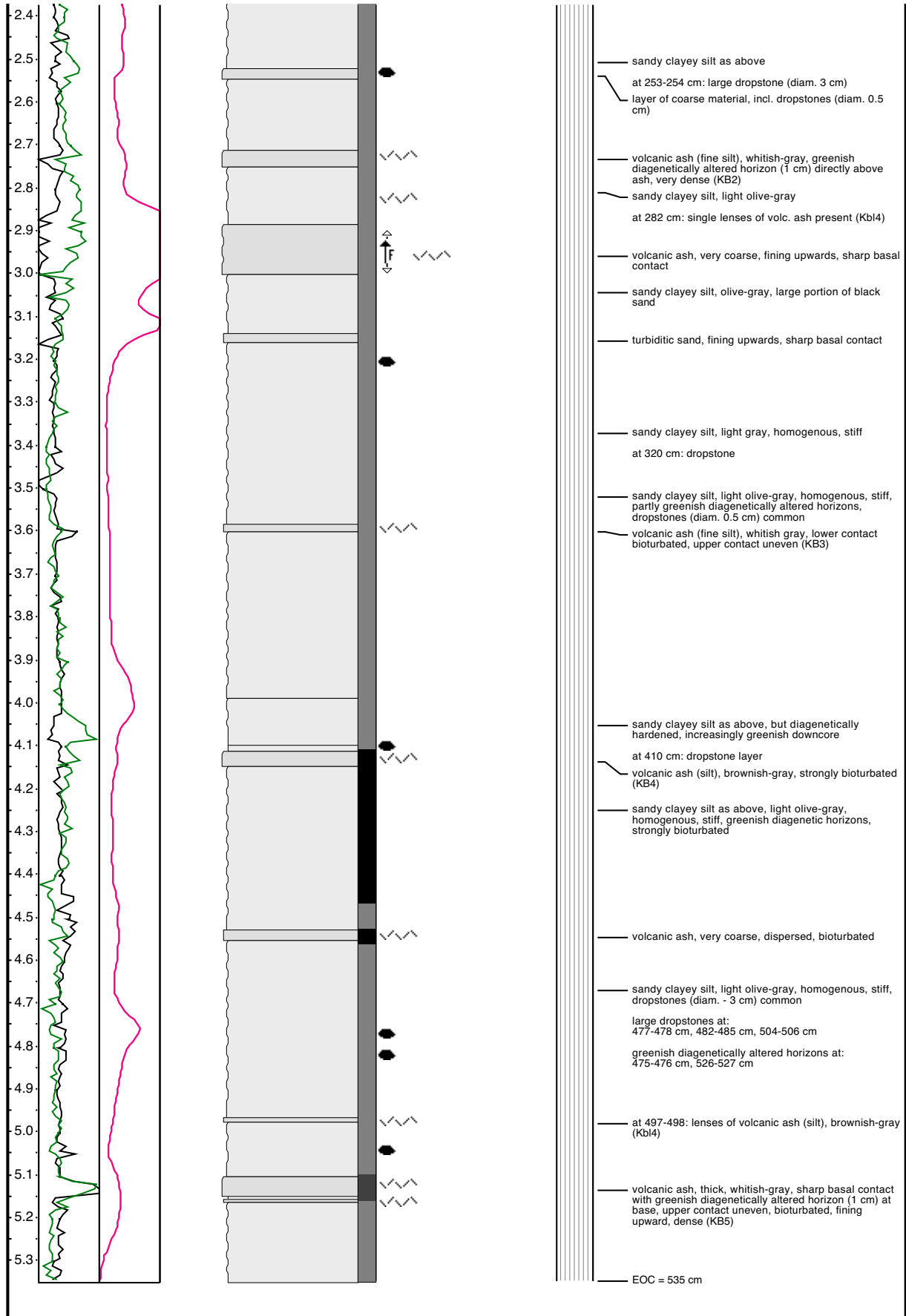
Locations of multicorers (MUC) recovered during SO201-2 and scheme of sample distribution among participating institutions.

Appendix VI
Core Description

Appendix VI

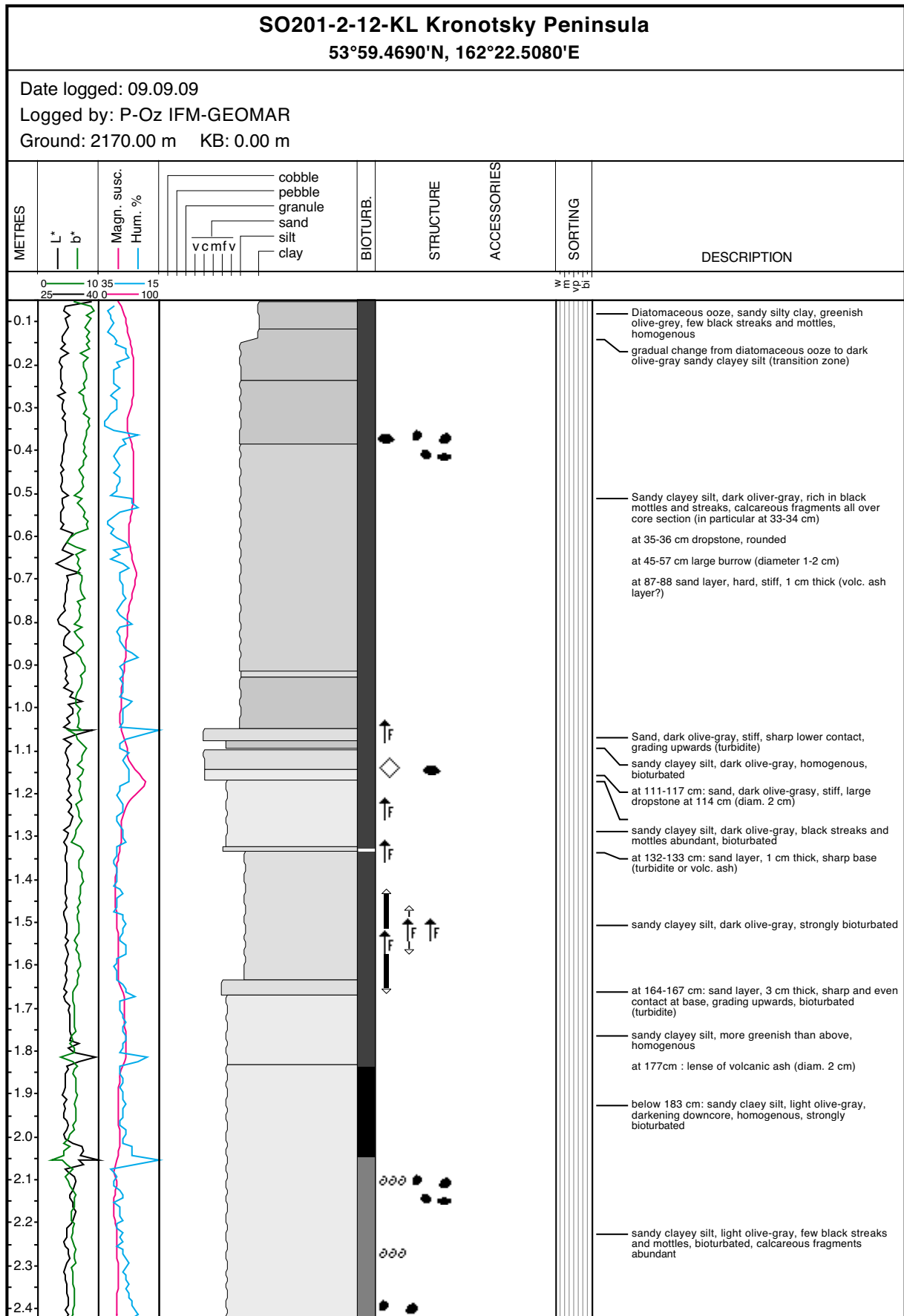


Appendix VI

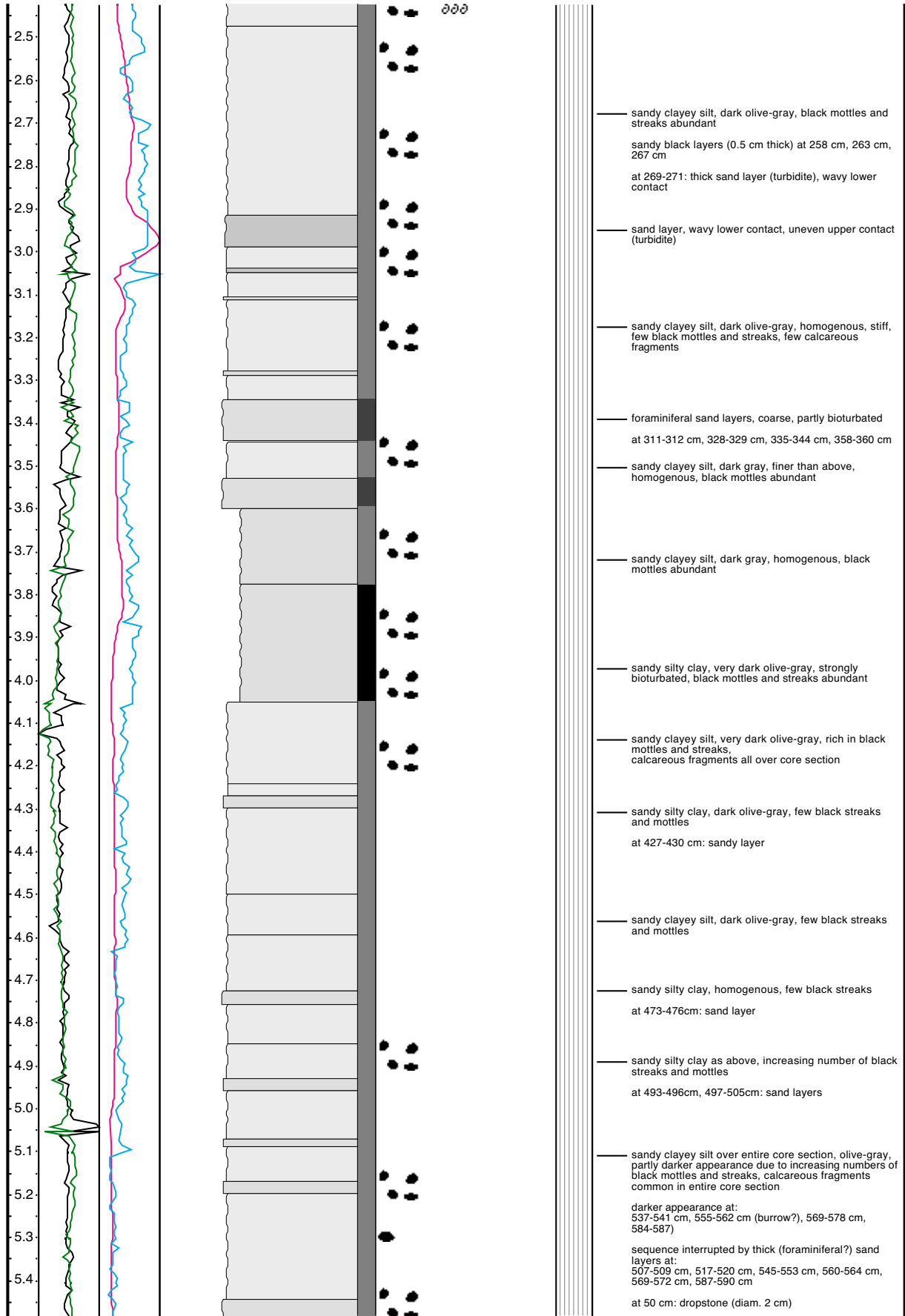




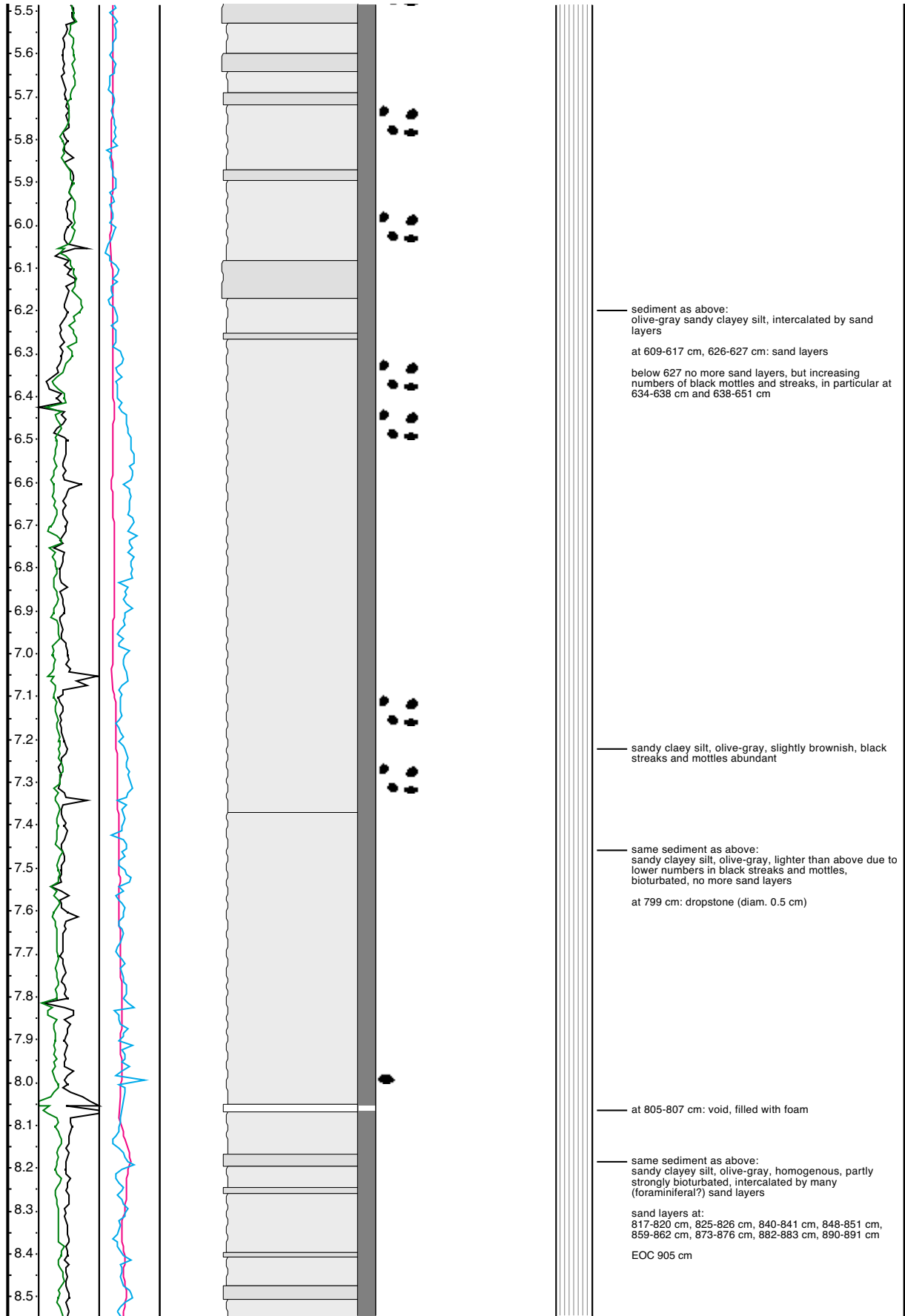
Appendix VI



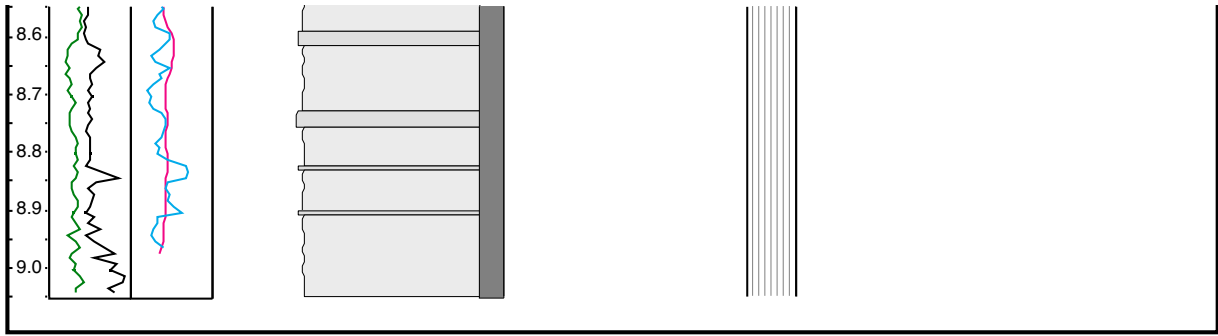
Appendix VI



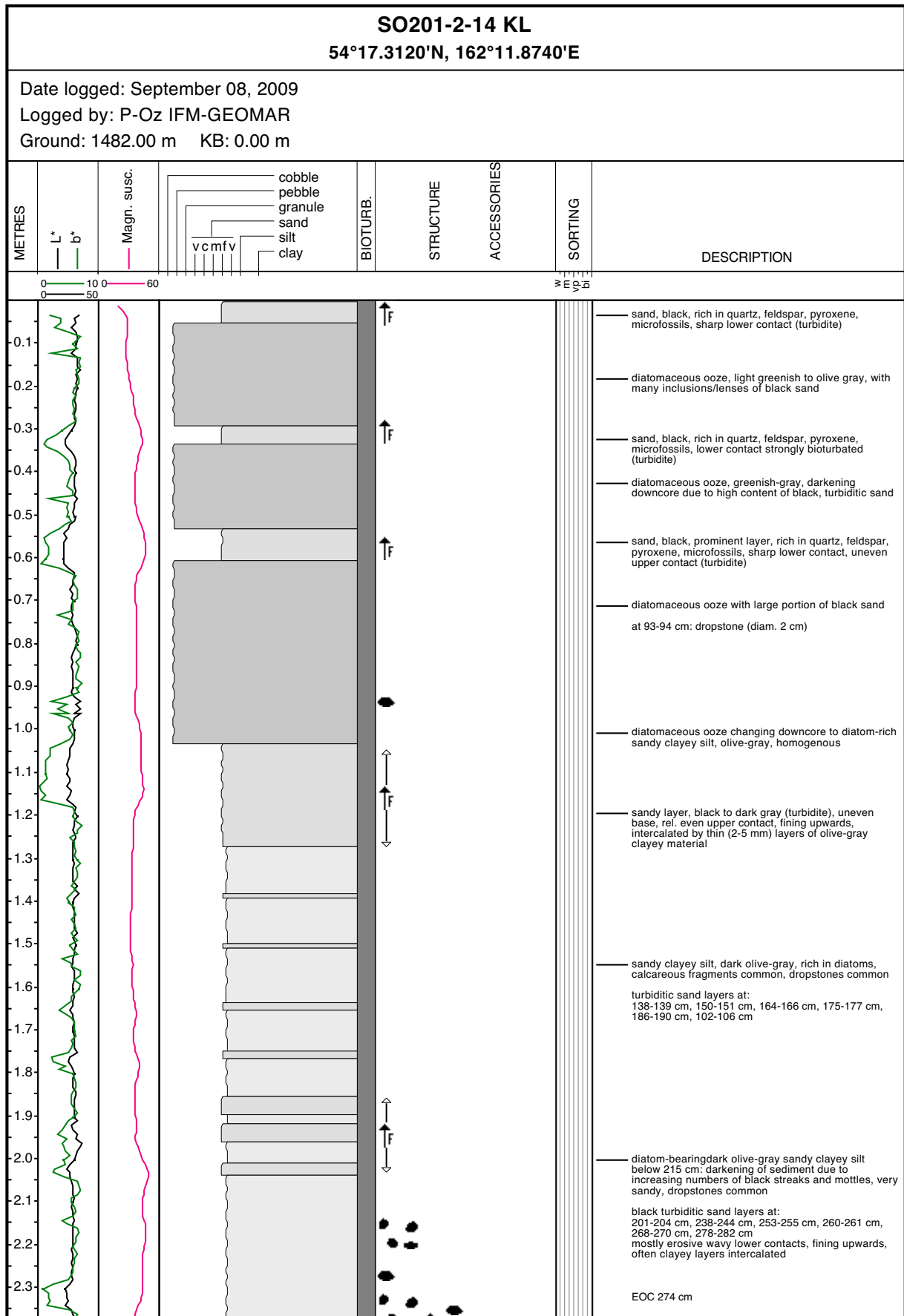
Appendix VI



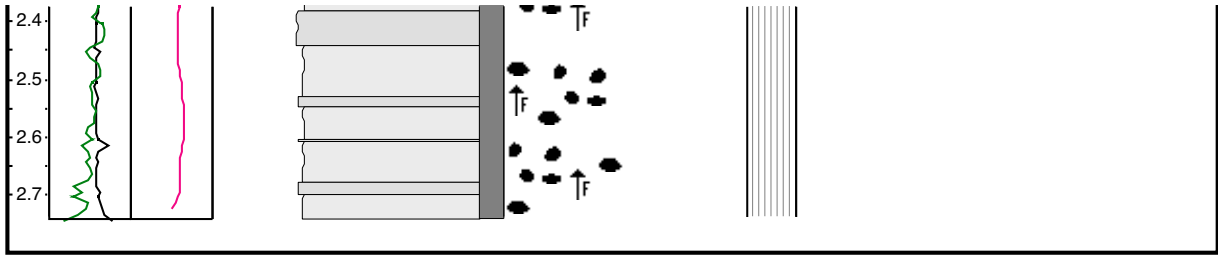
Appendix VI



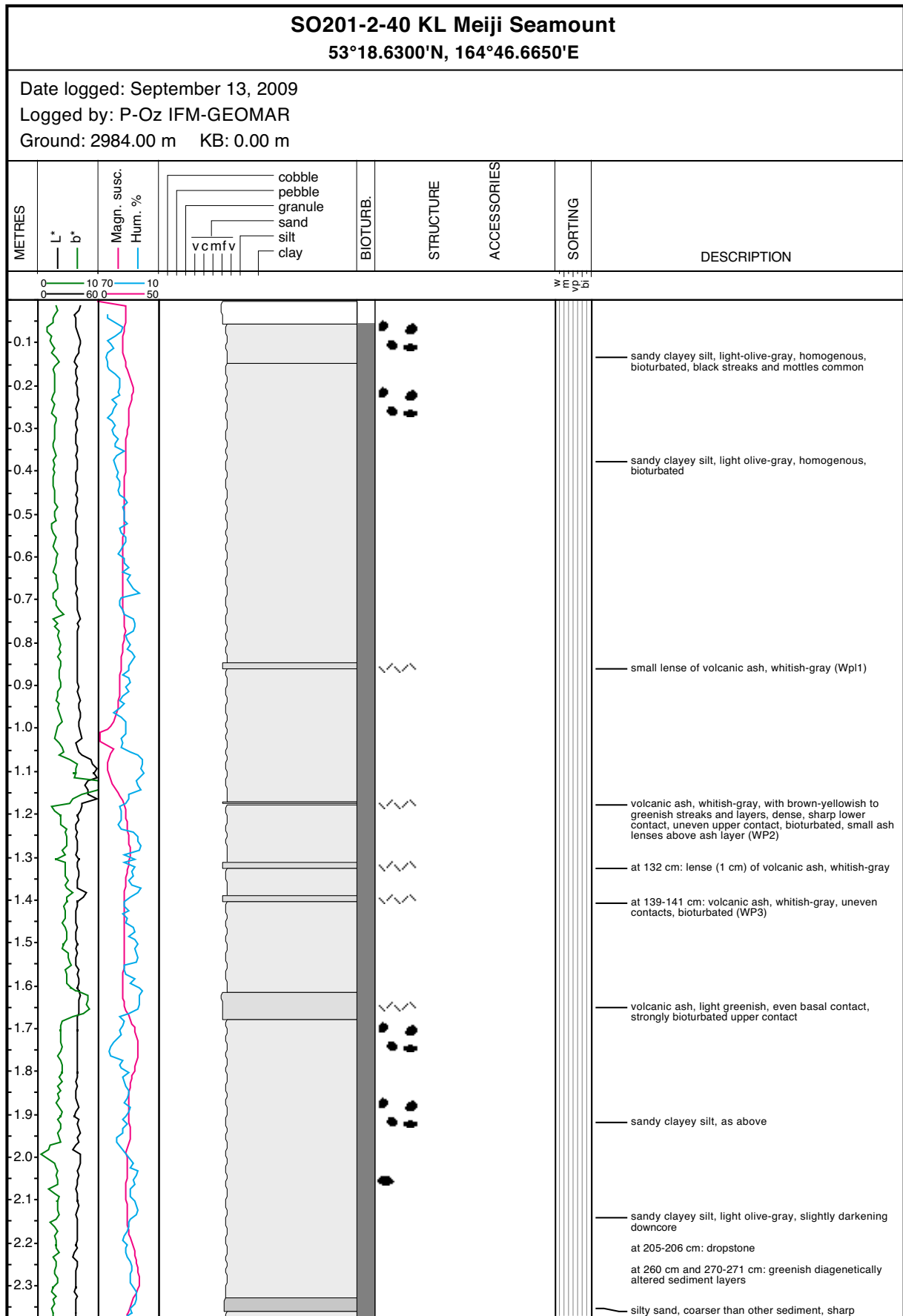
Appendix VI



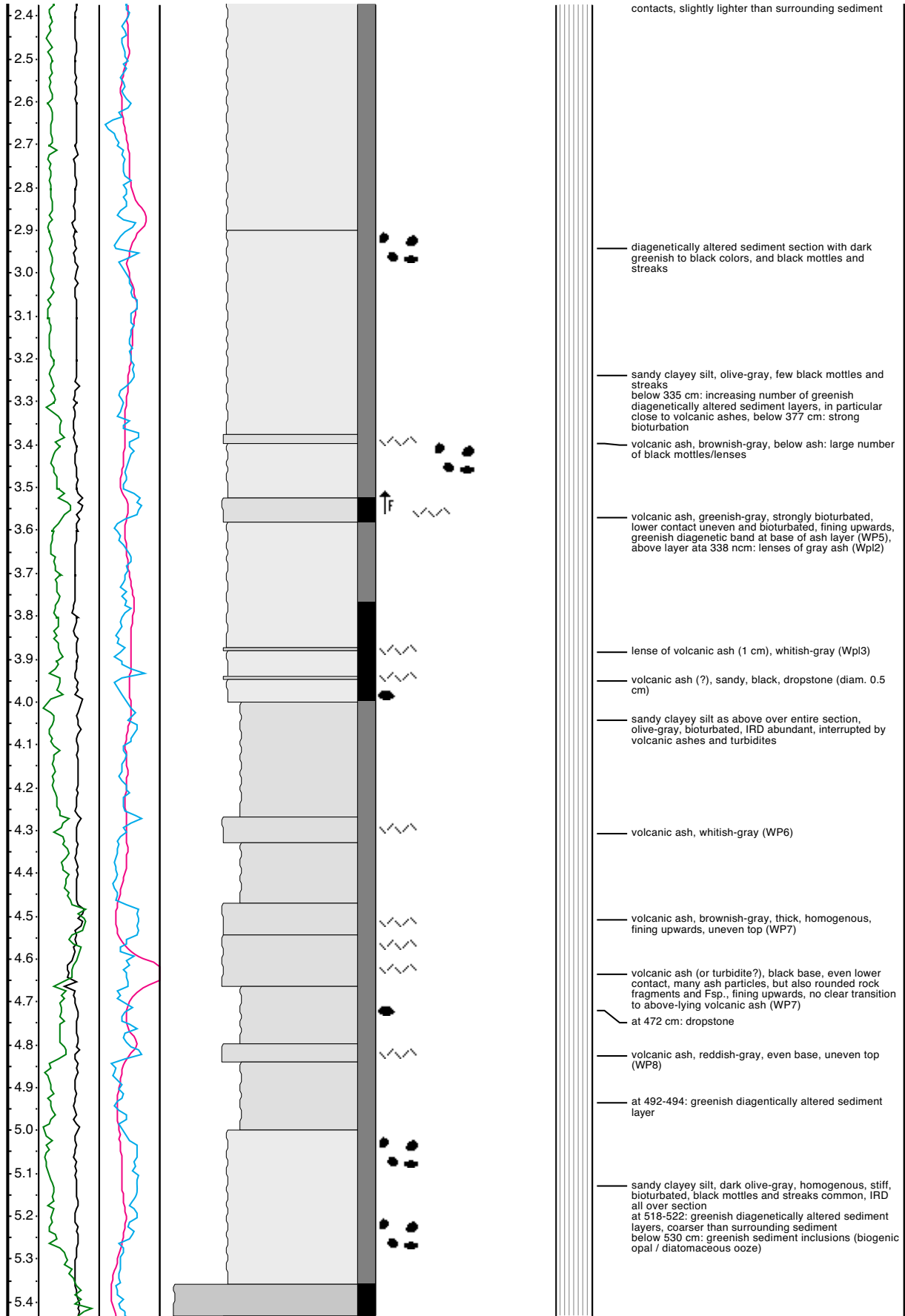
Appendix VI



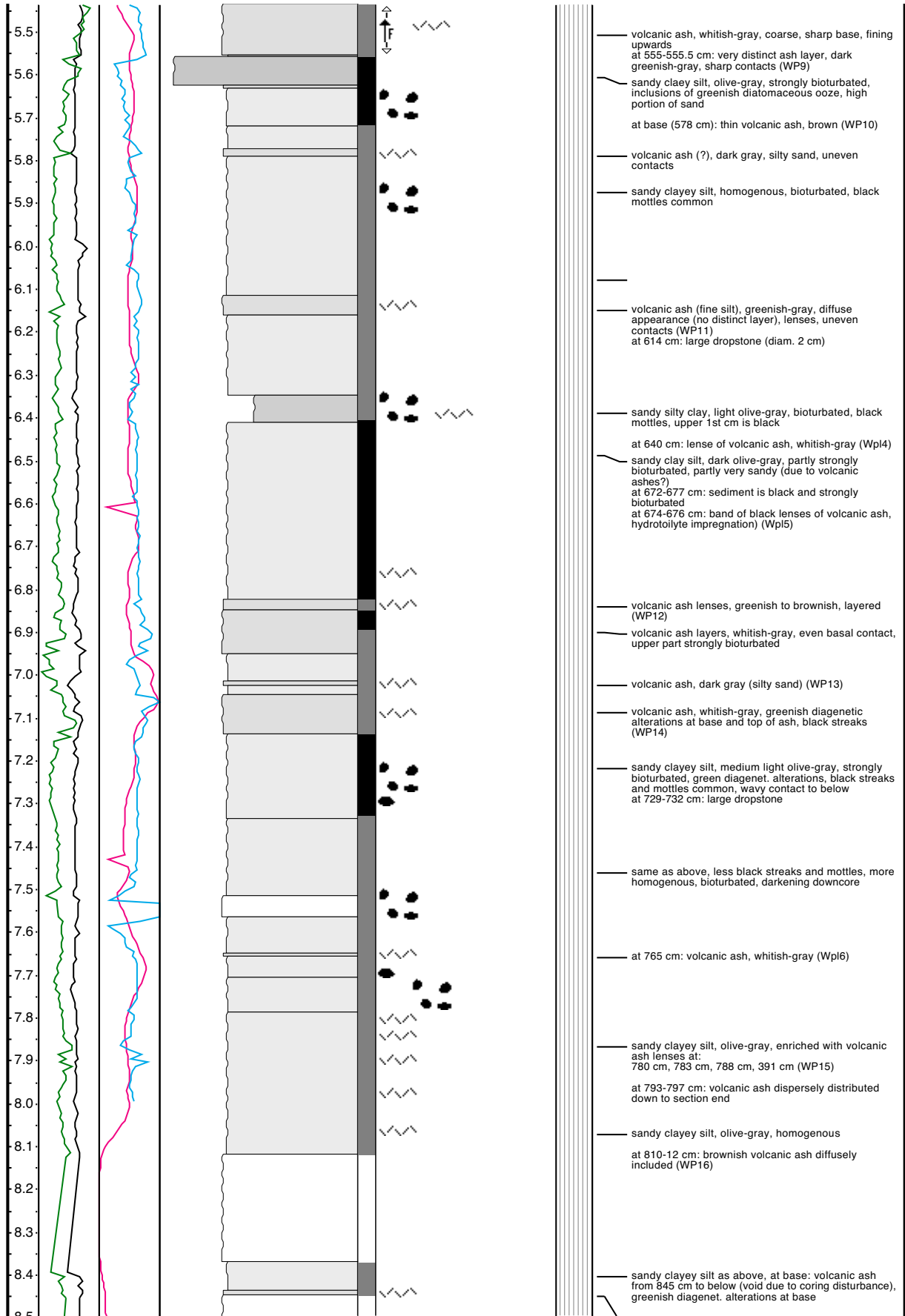
Appendix VI



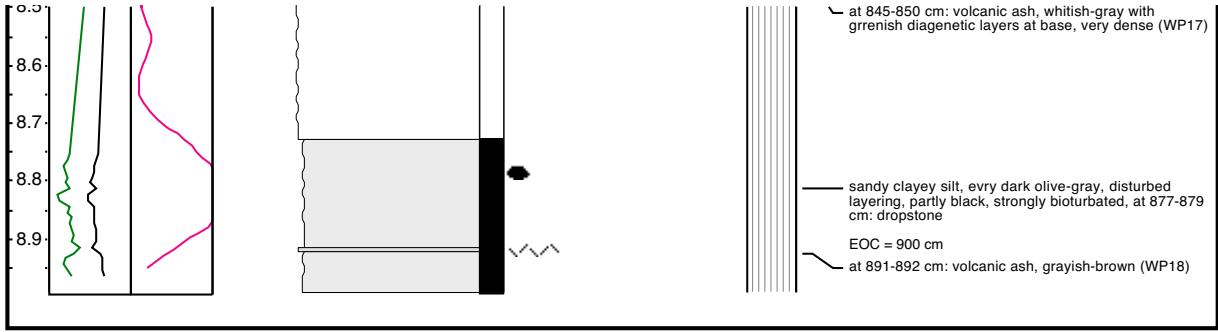
Appendix VI



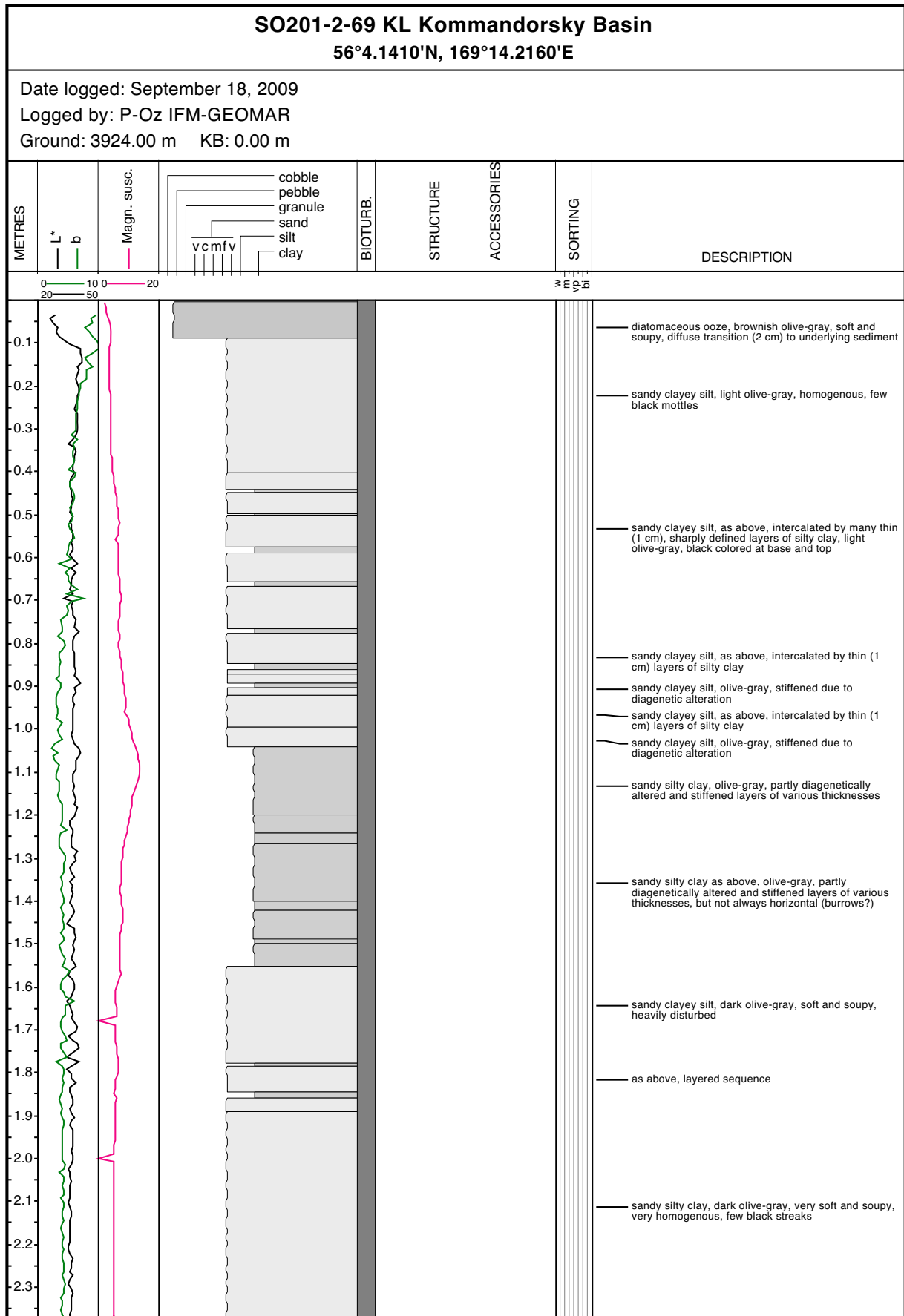
Appendix VI



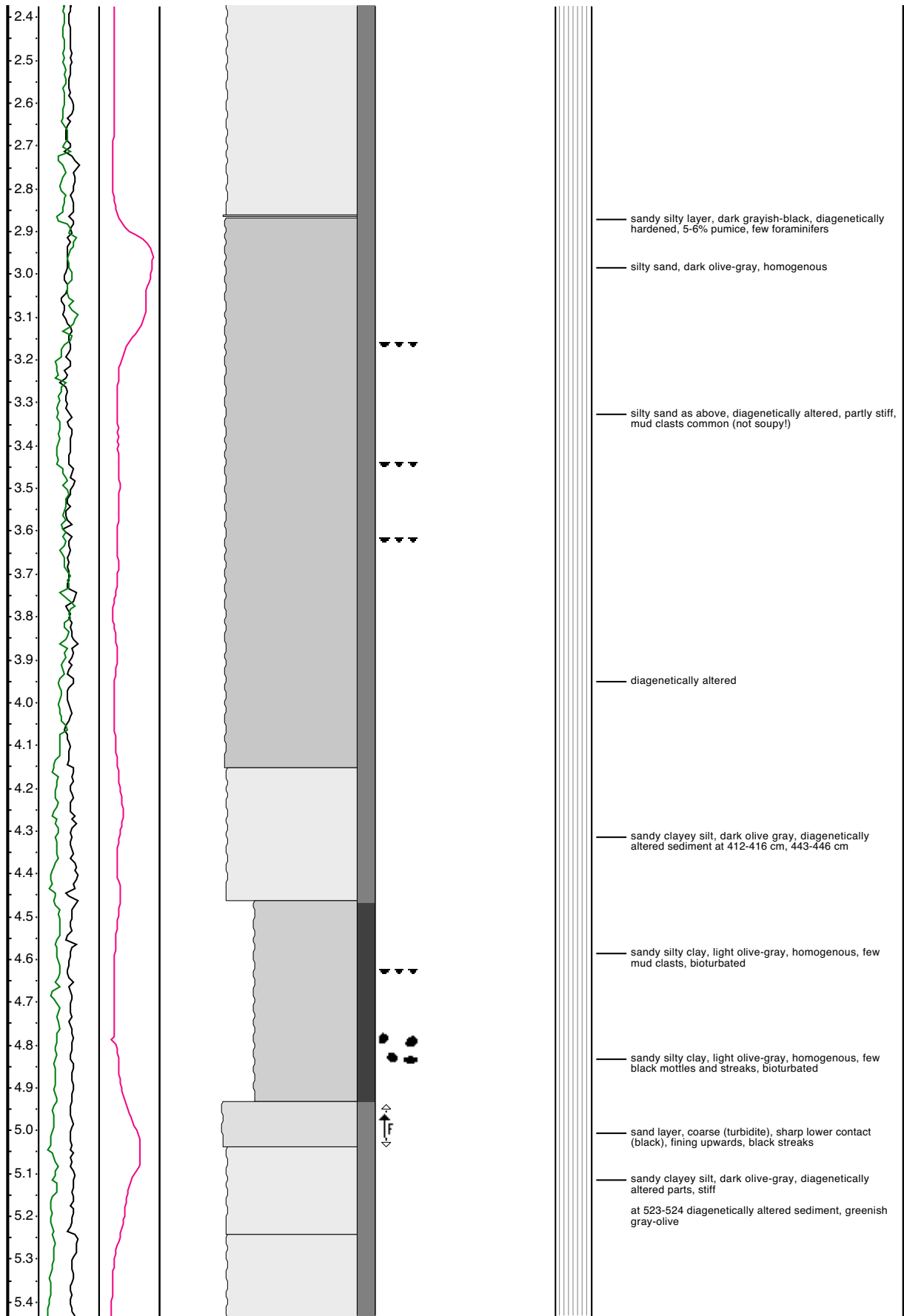
Appendix VI



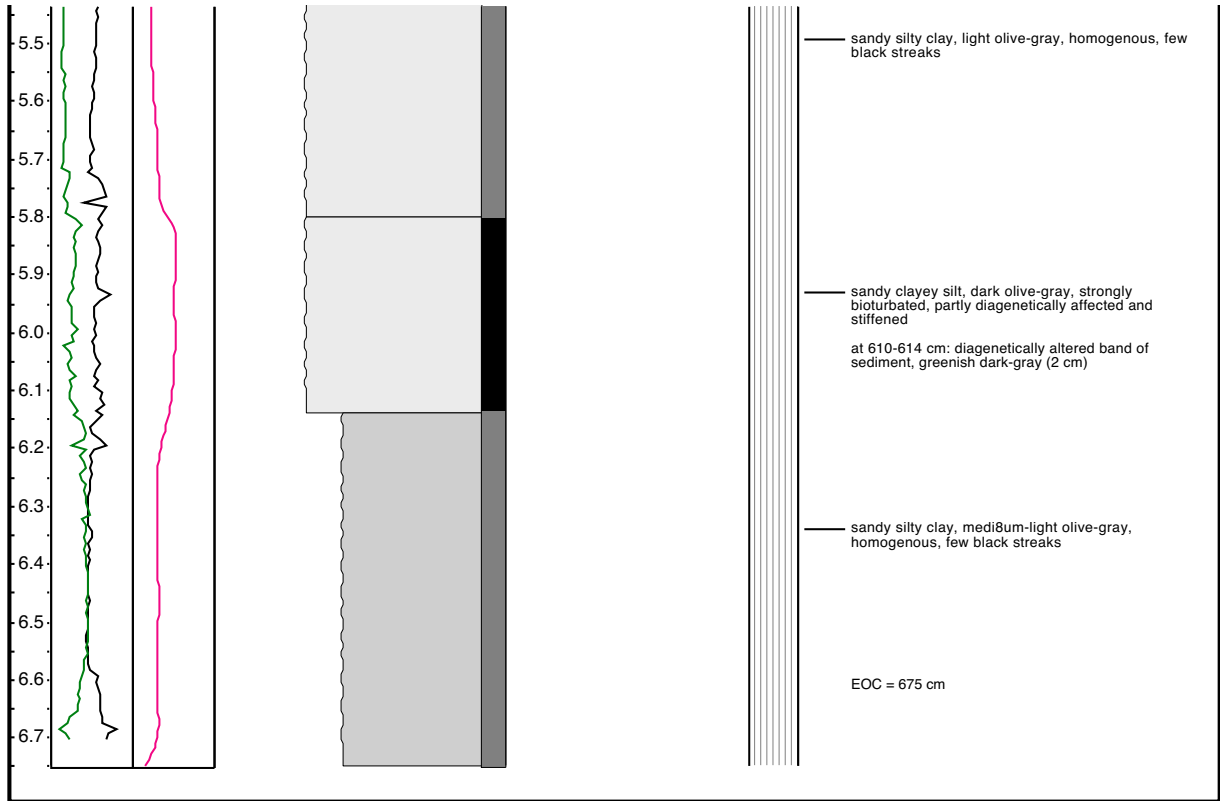
Appendix VI



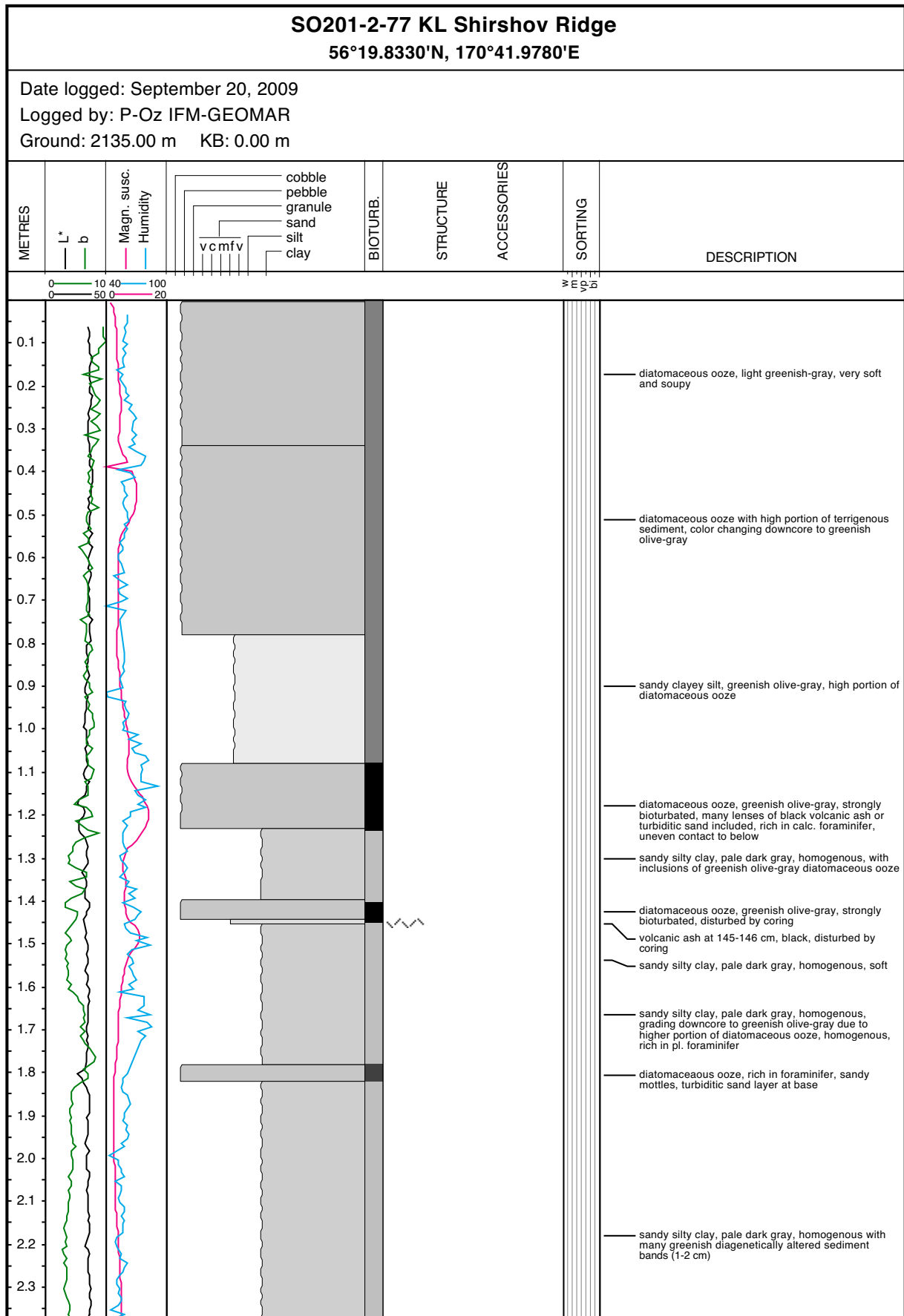
Appendix VI



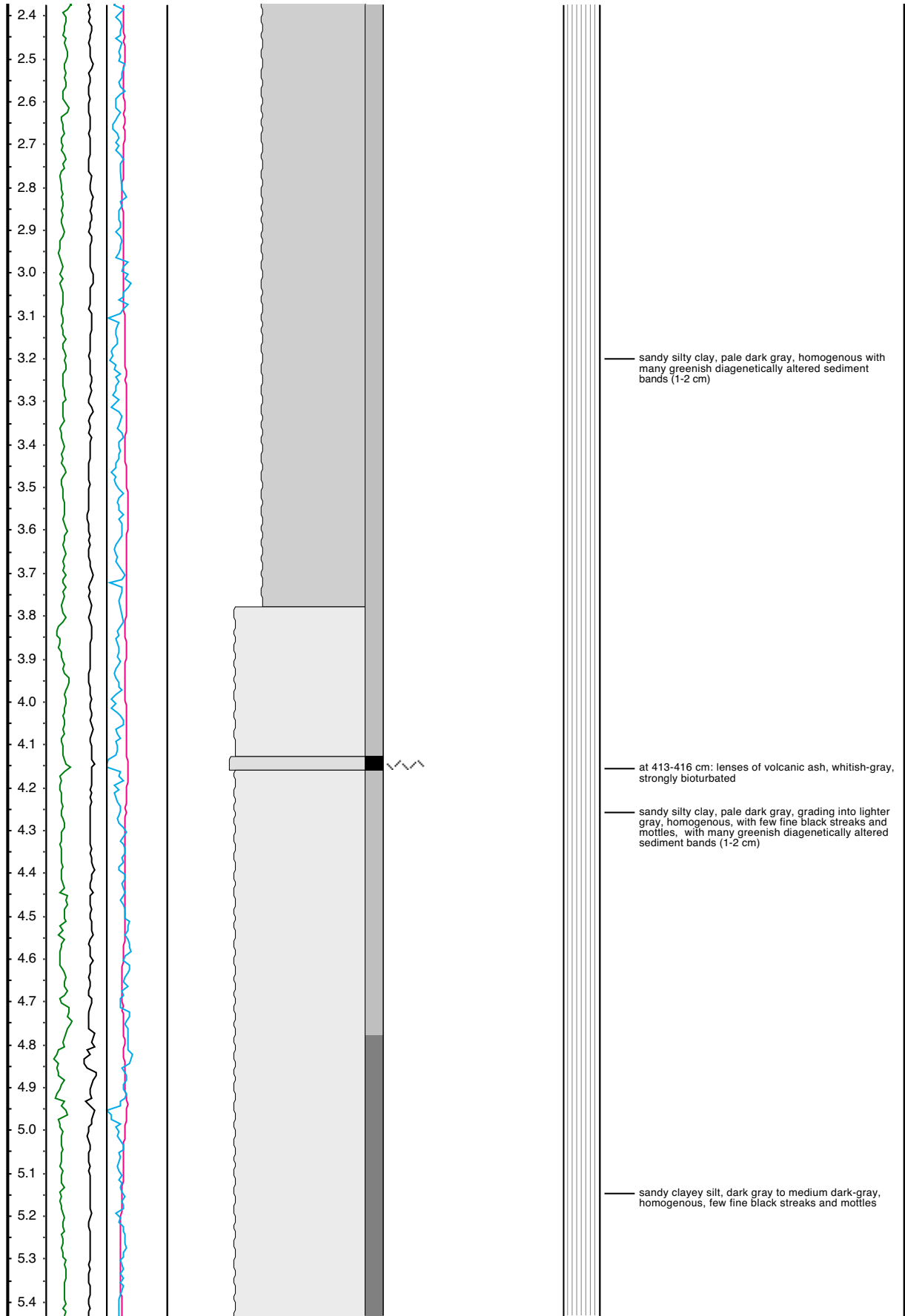
Appendix VI



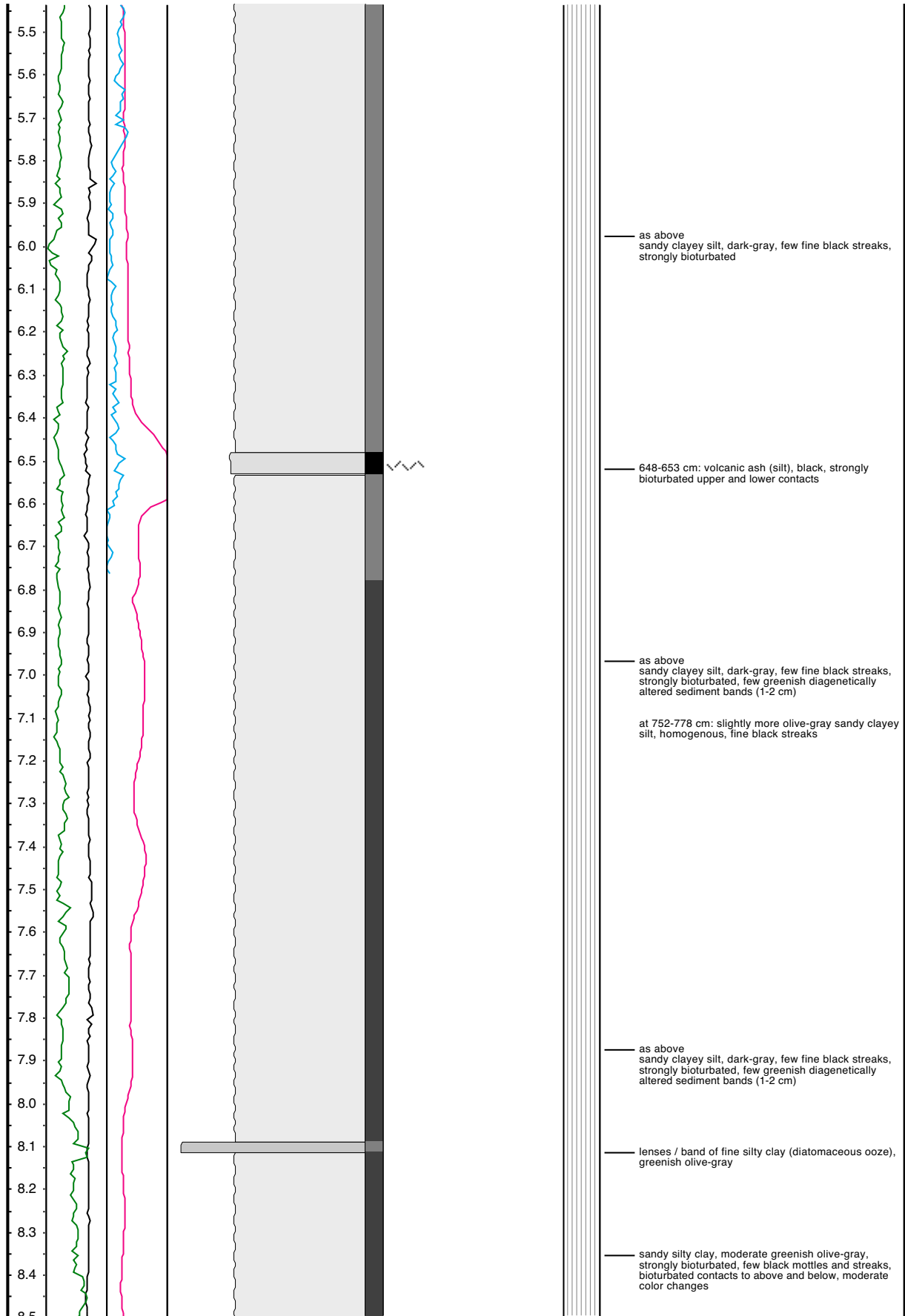
Appendix VI



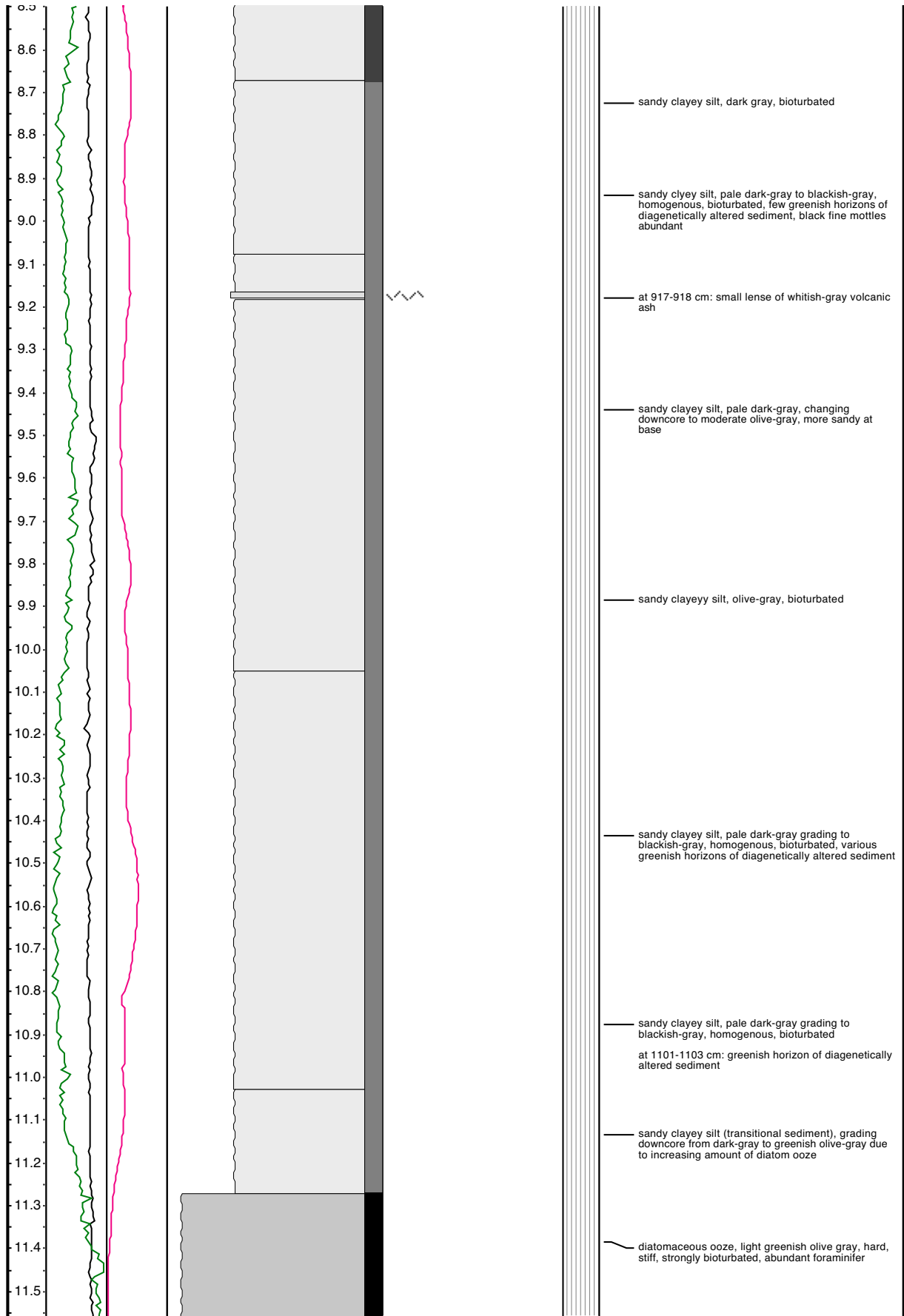
Appendix VI



Appendix VI



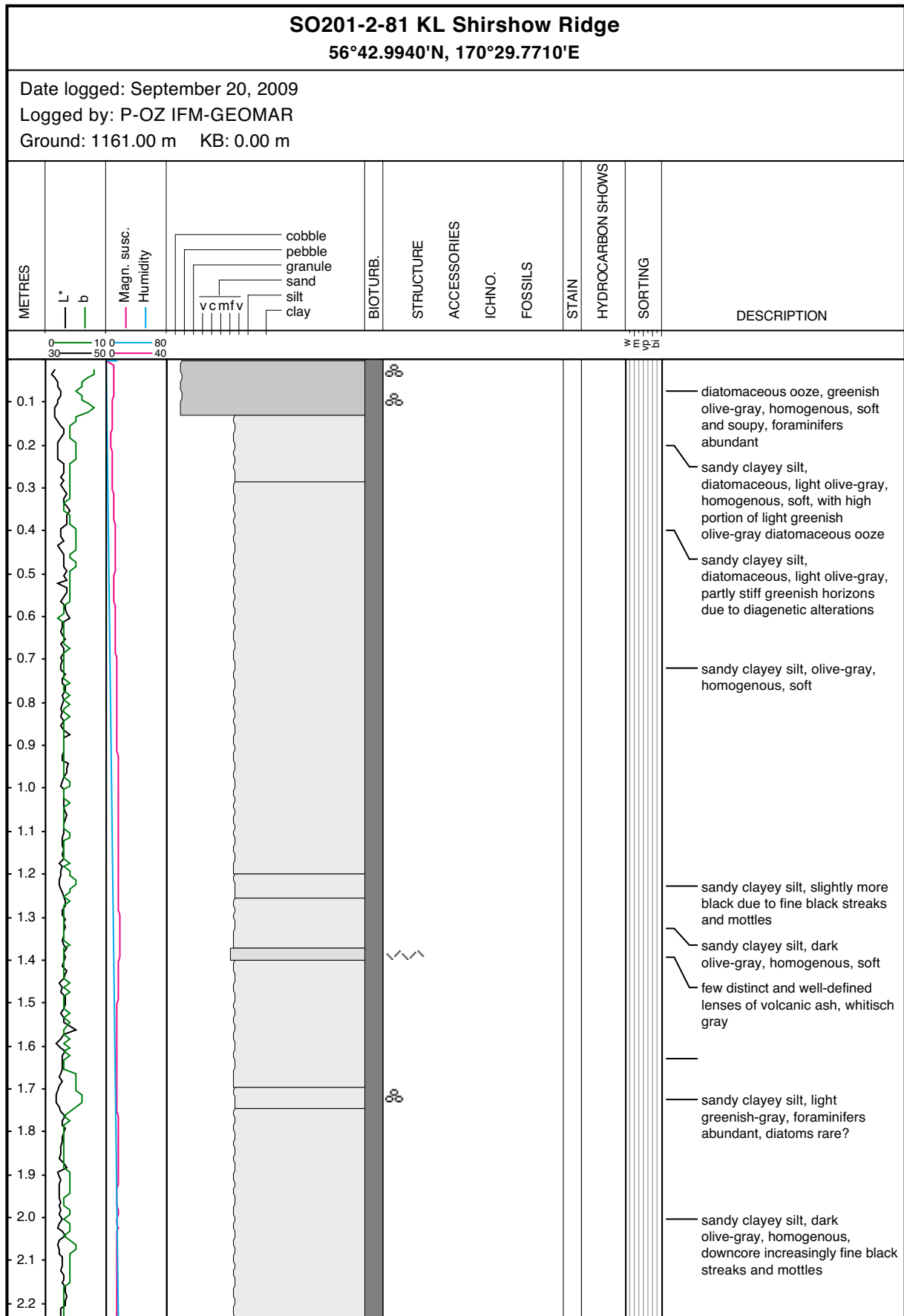
Appendix VI



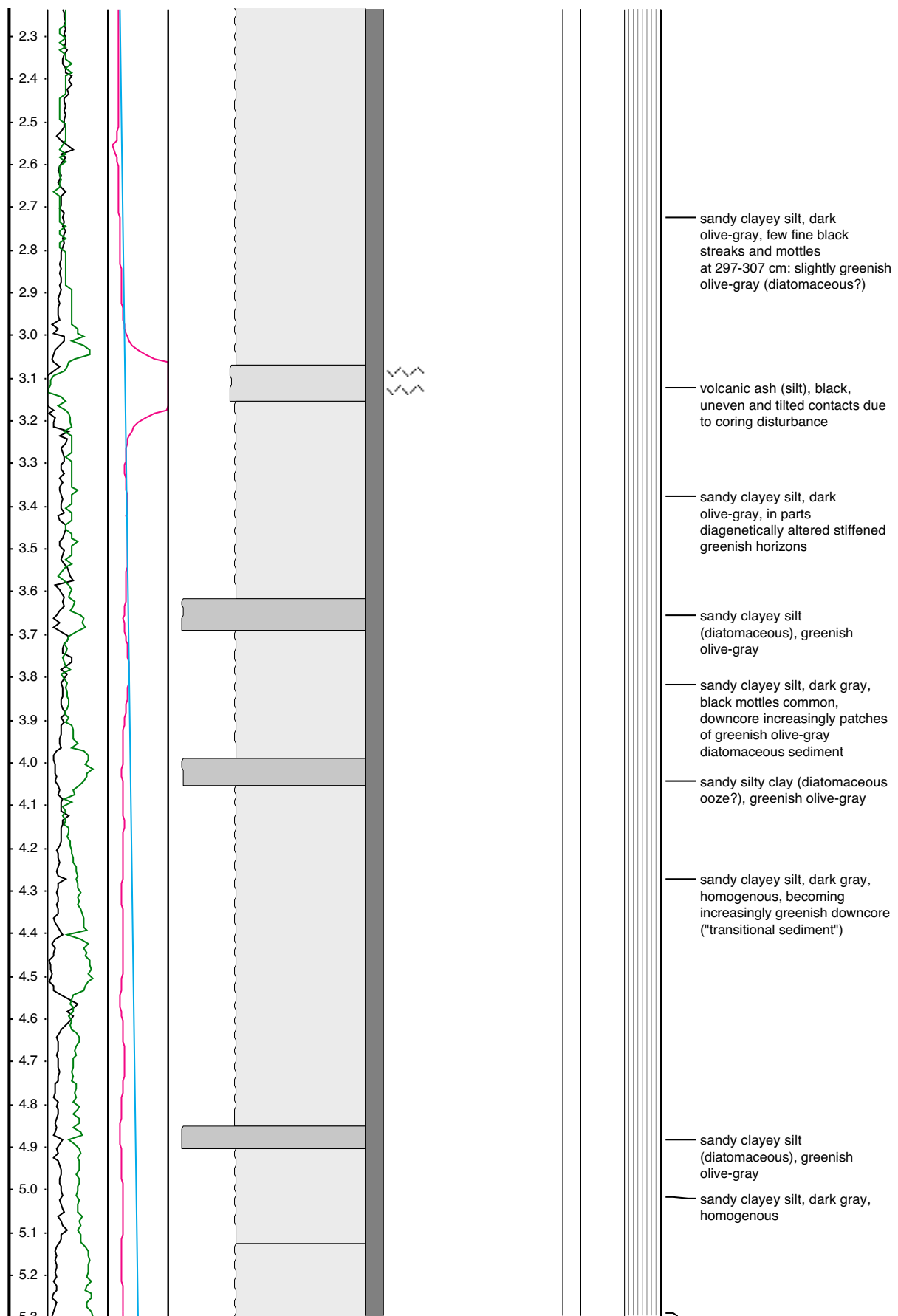
Appendix VI



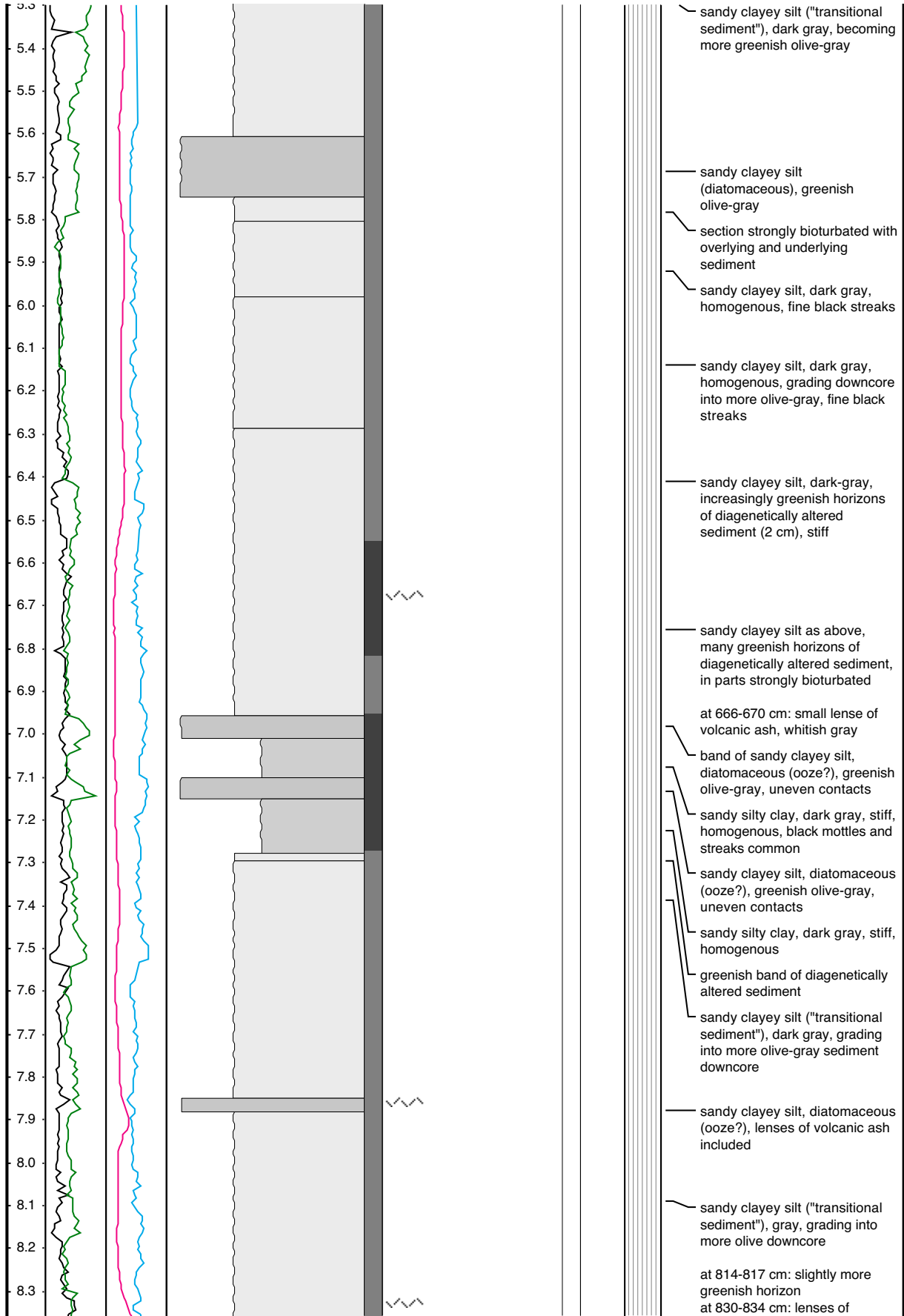
Appendix VI



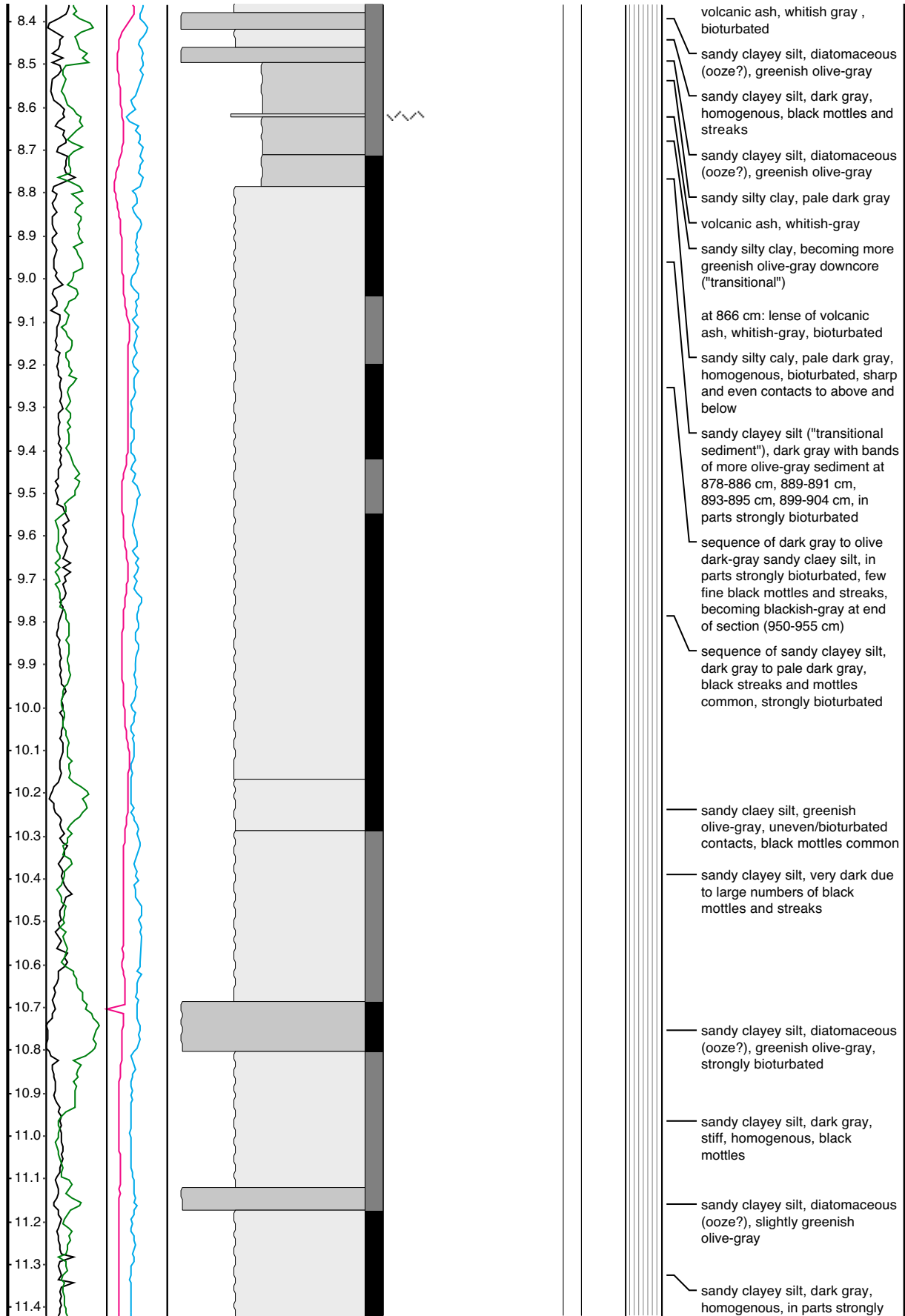
Appendix VI



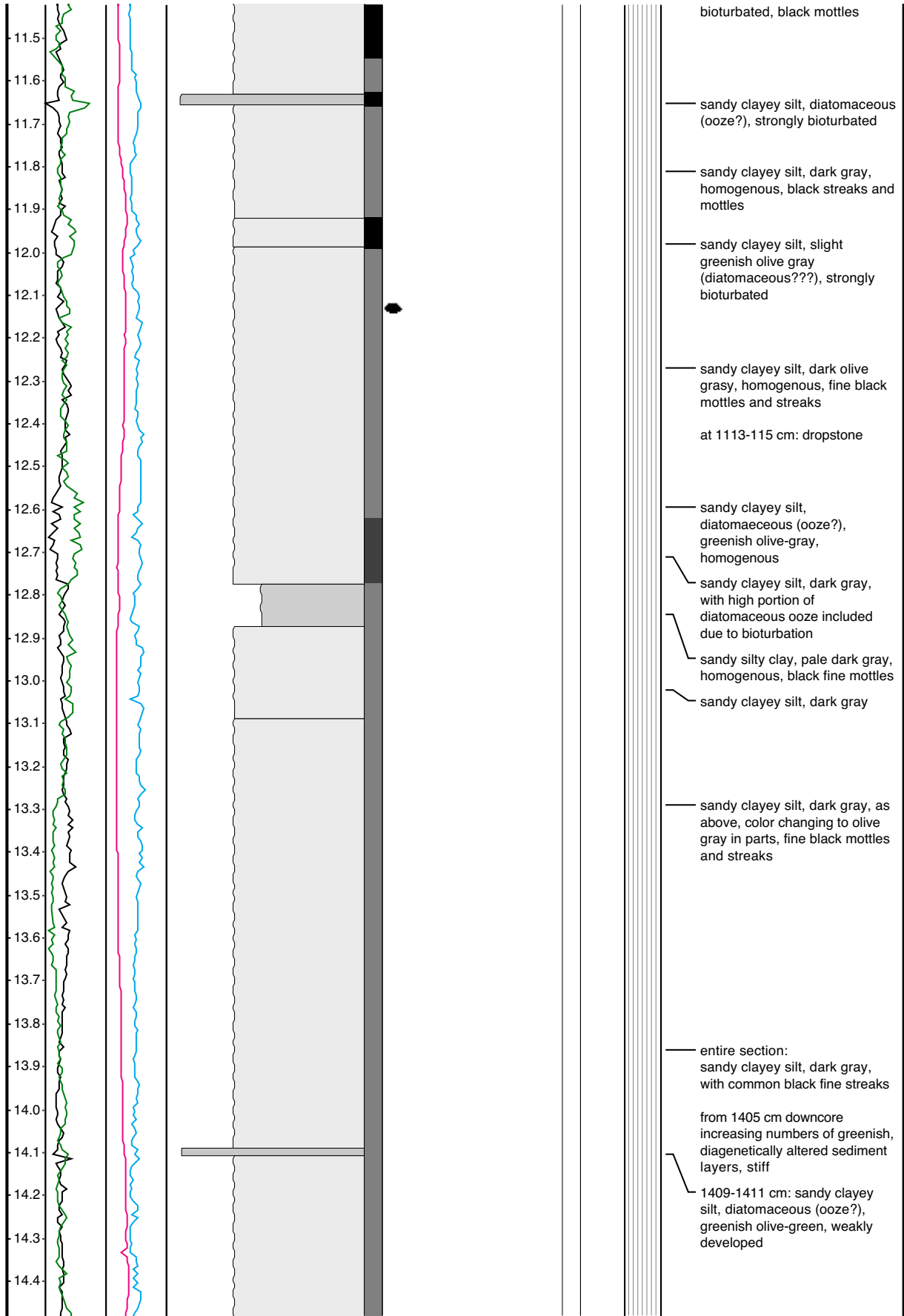
Appendix VI



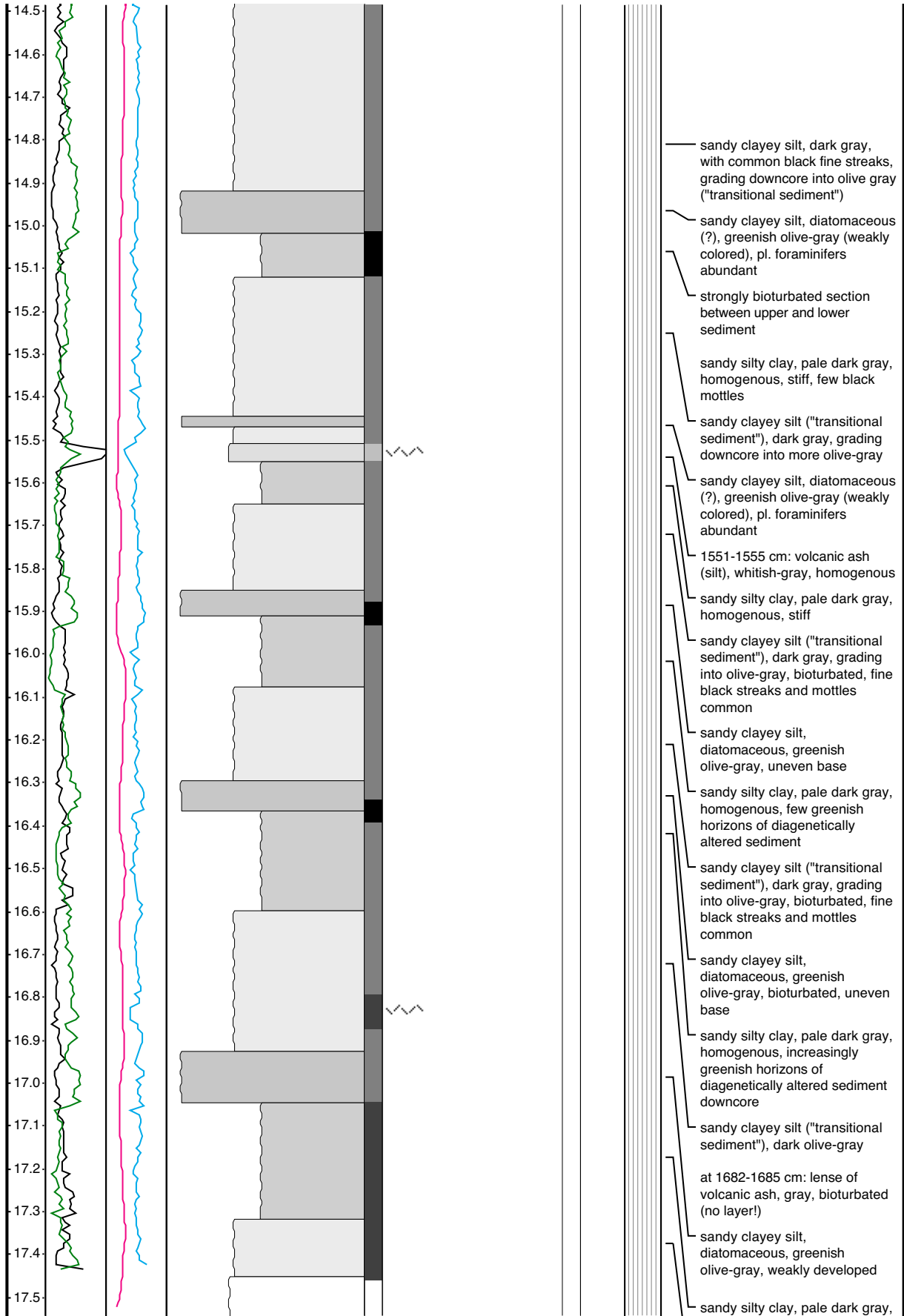
Appendix VI



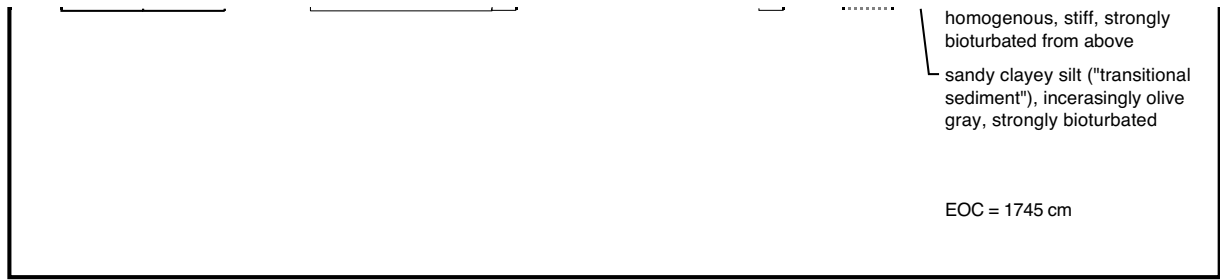
Appendix VI



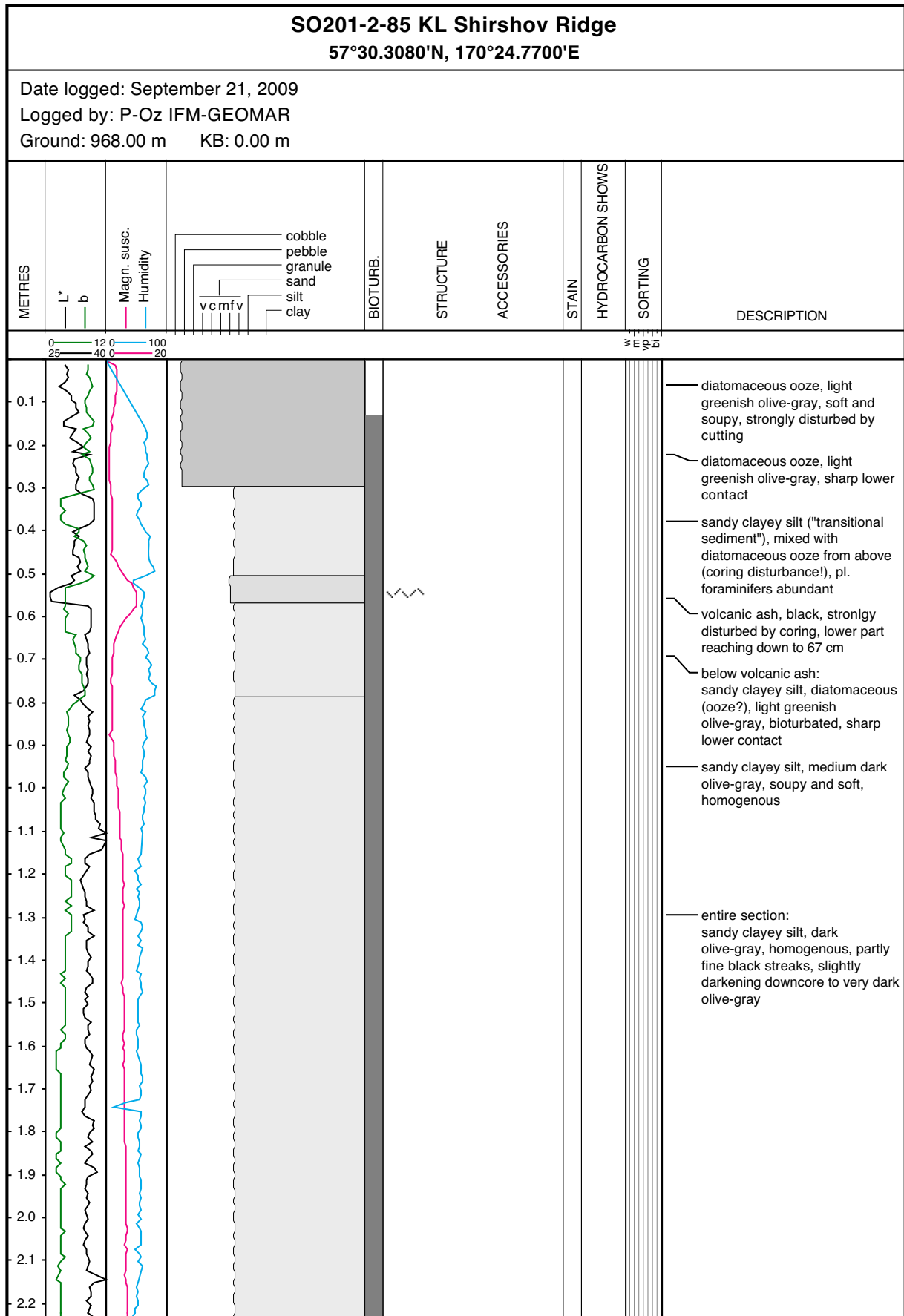
Appendix VI



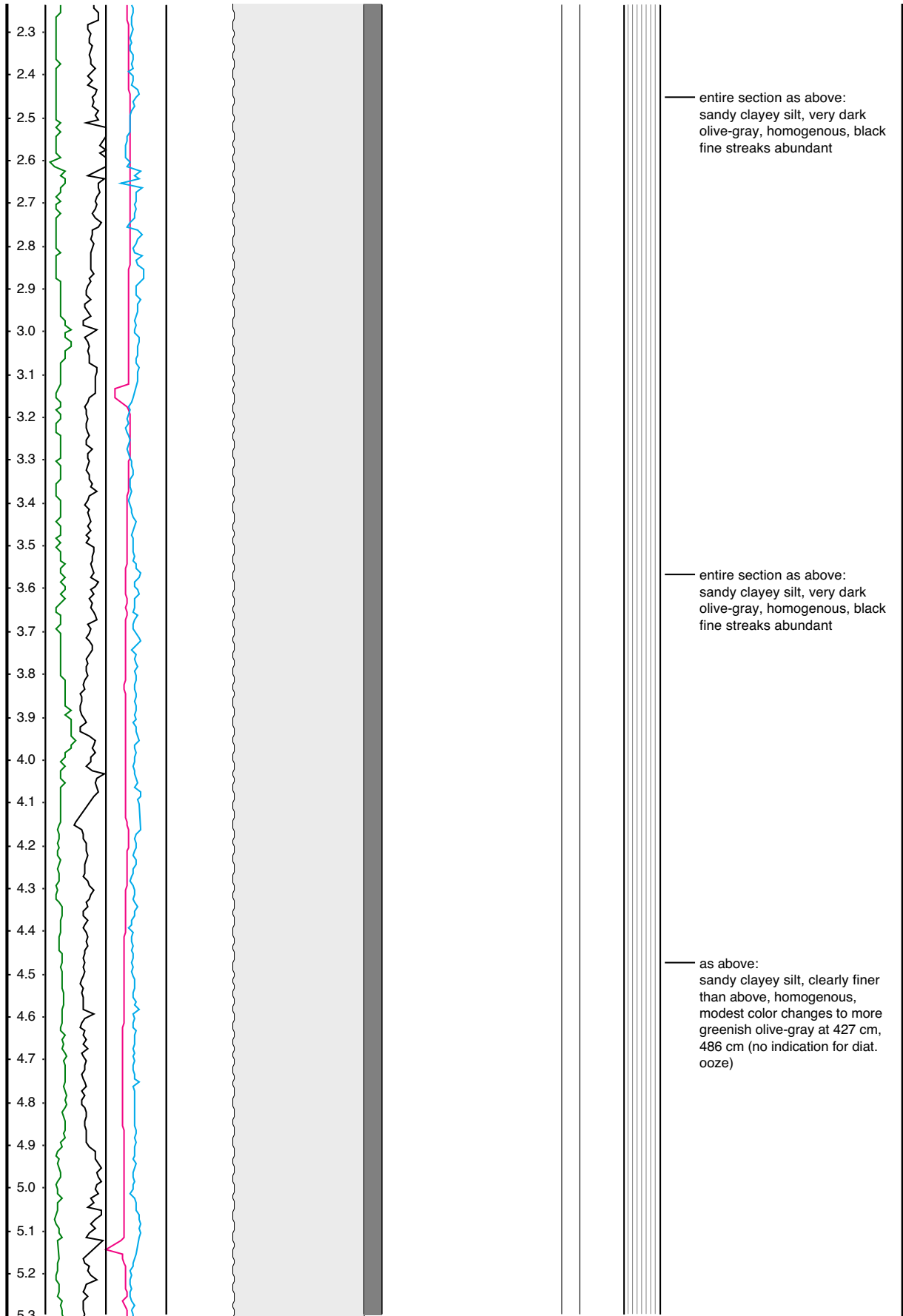
Appendix VI



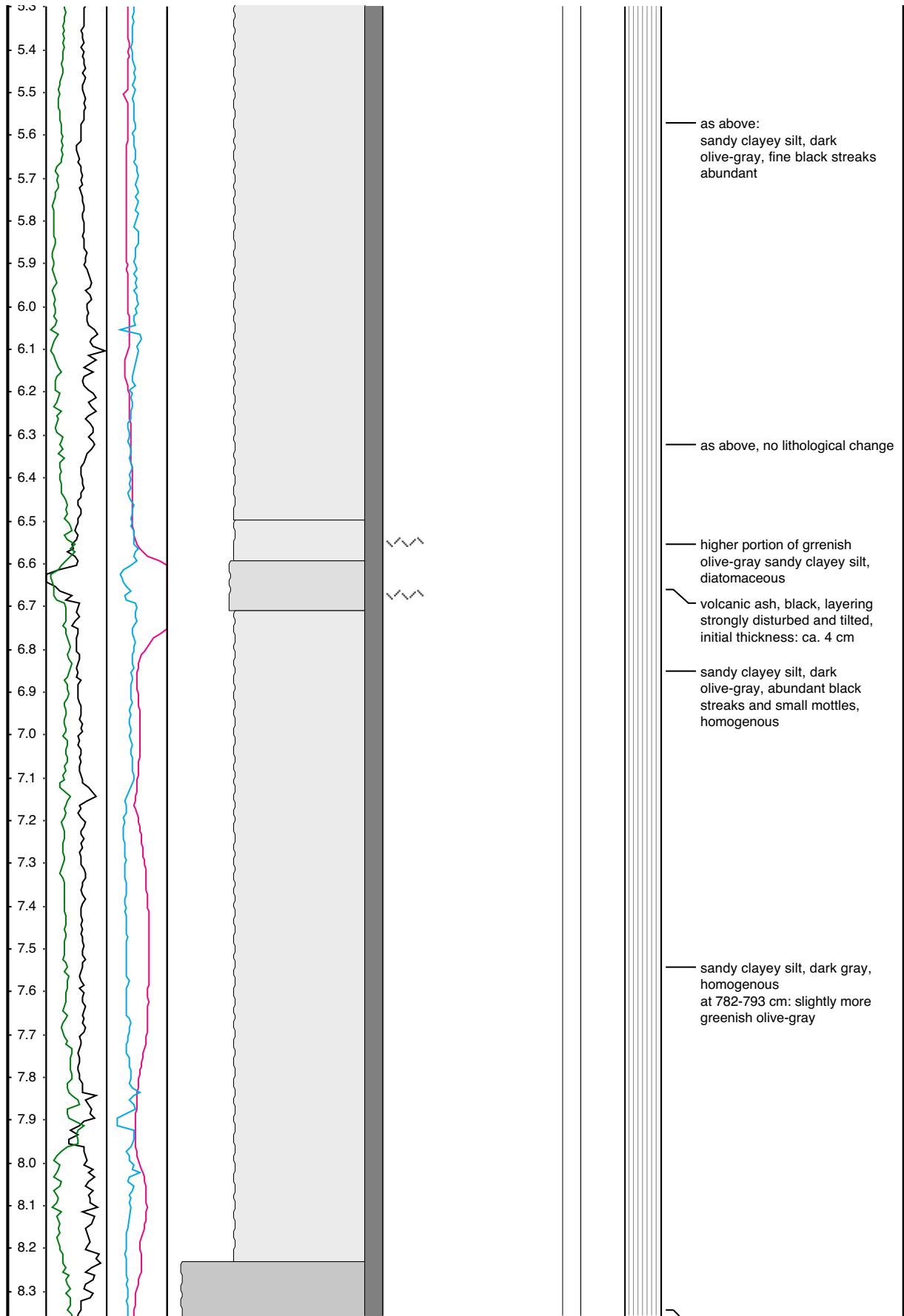
Appendix VI



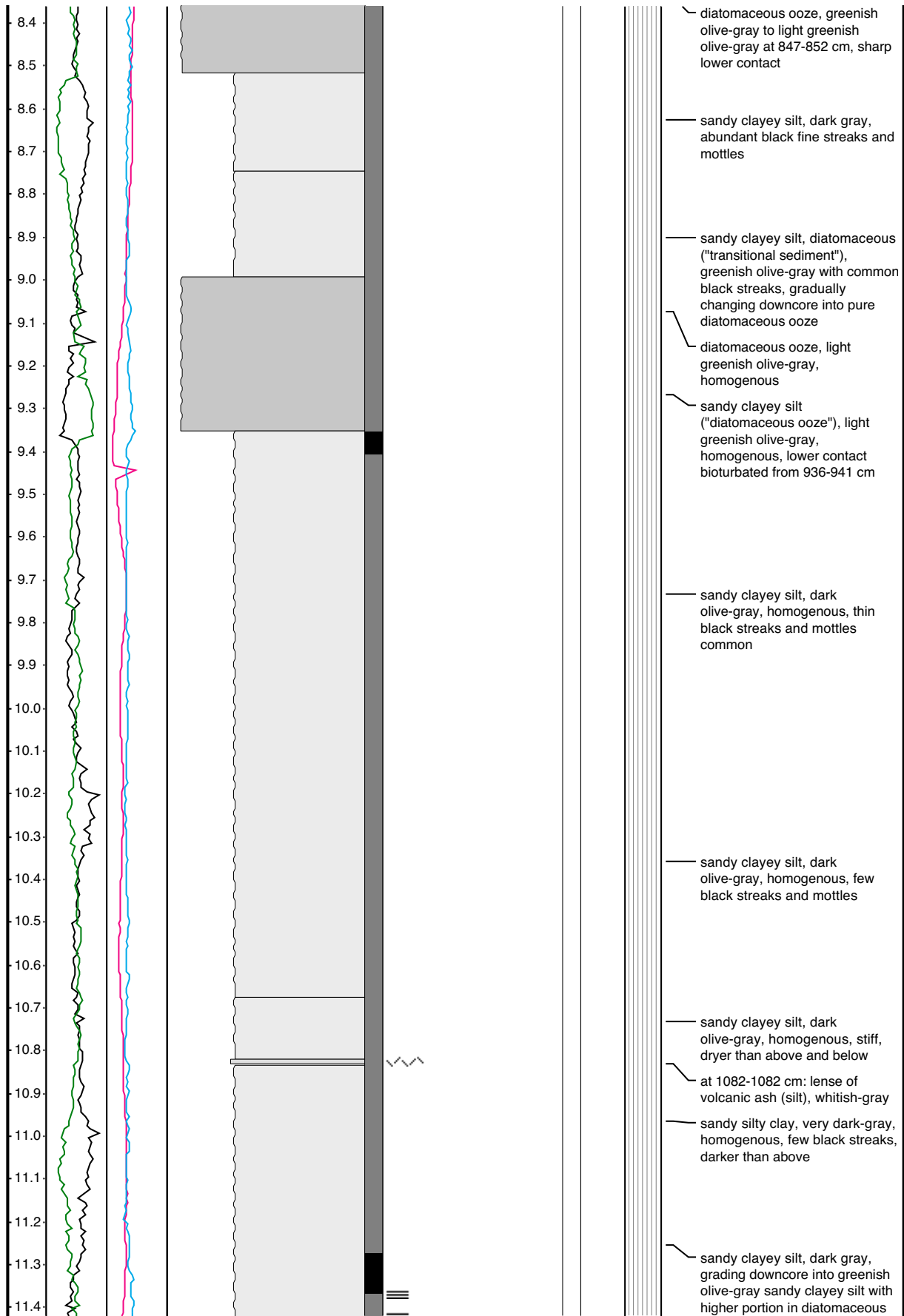
Appendix VI



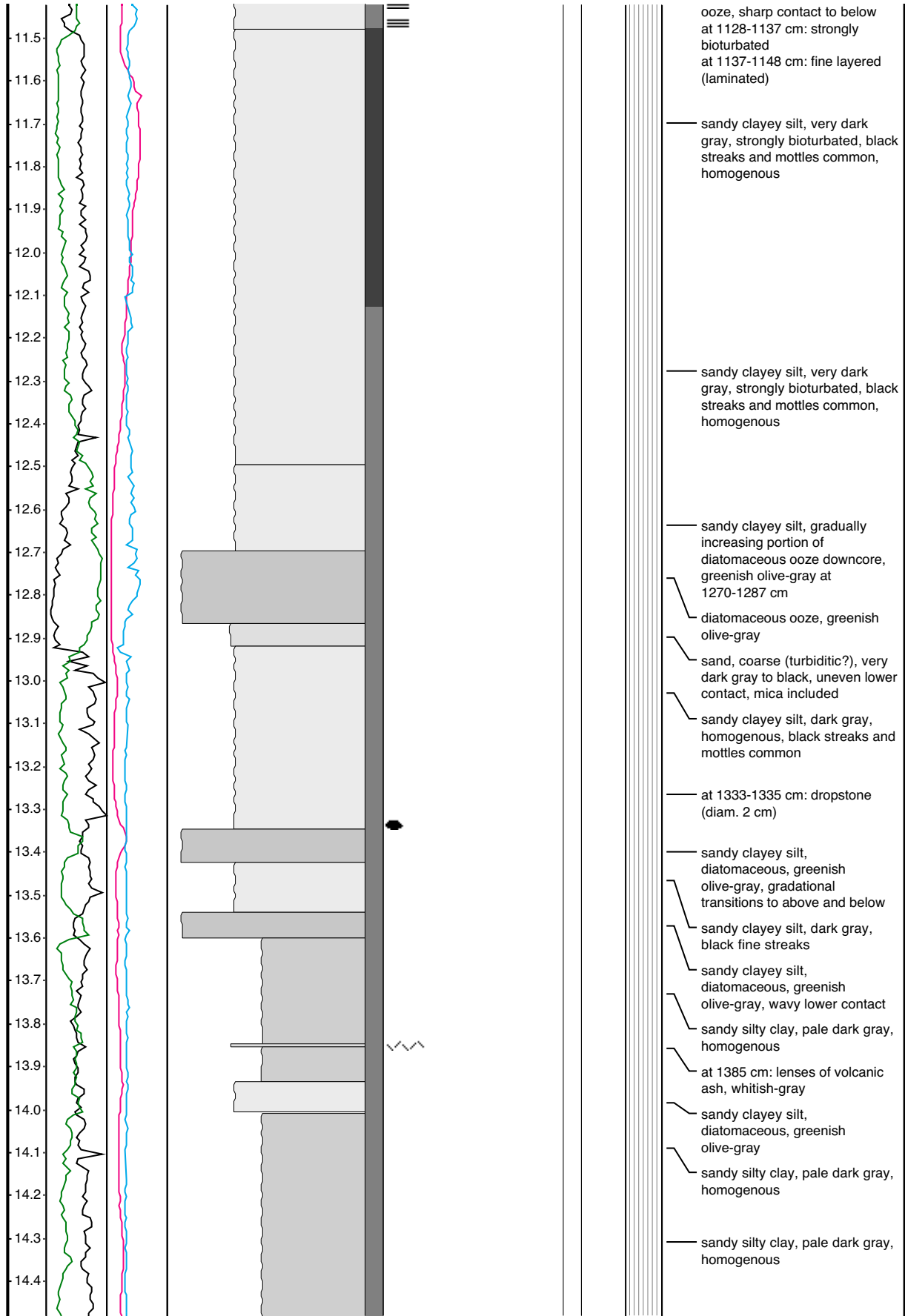
Appendix VI



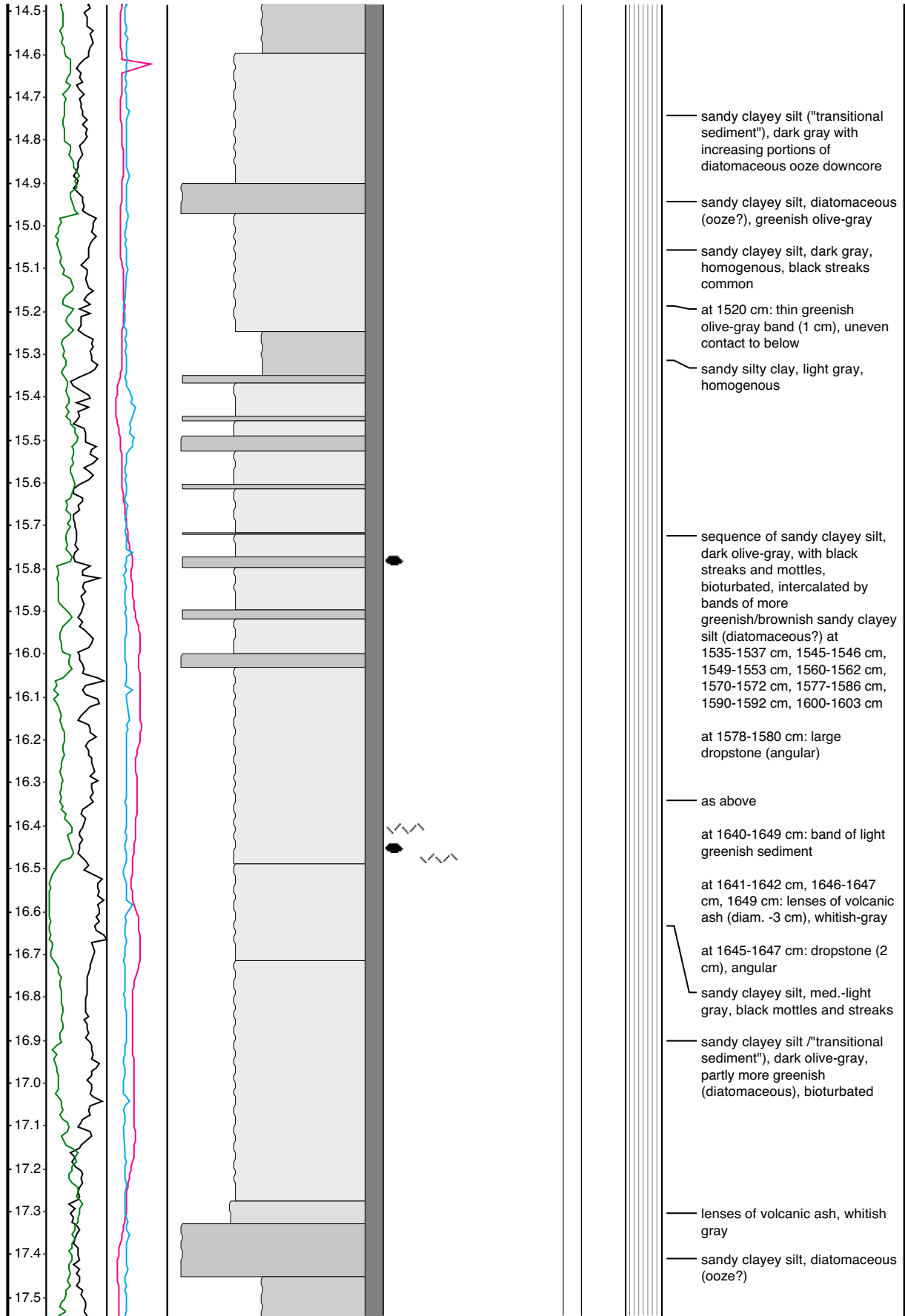
Appendix VI



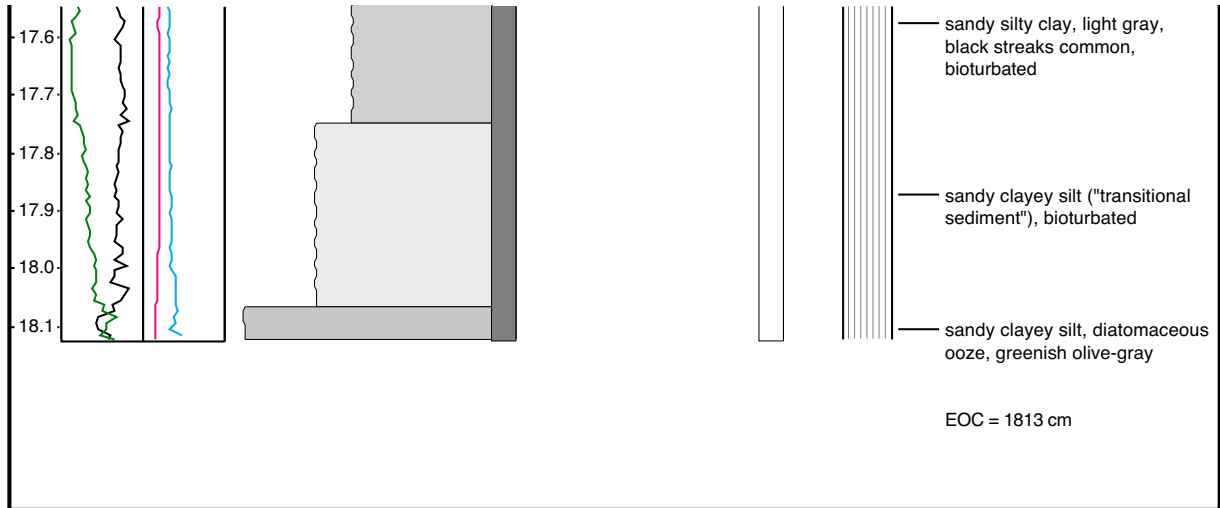
Appendix VI



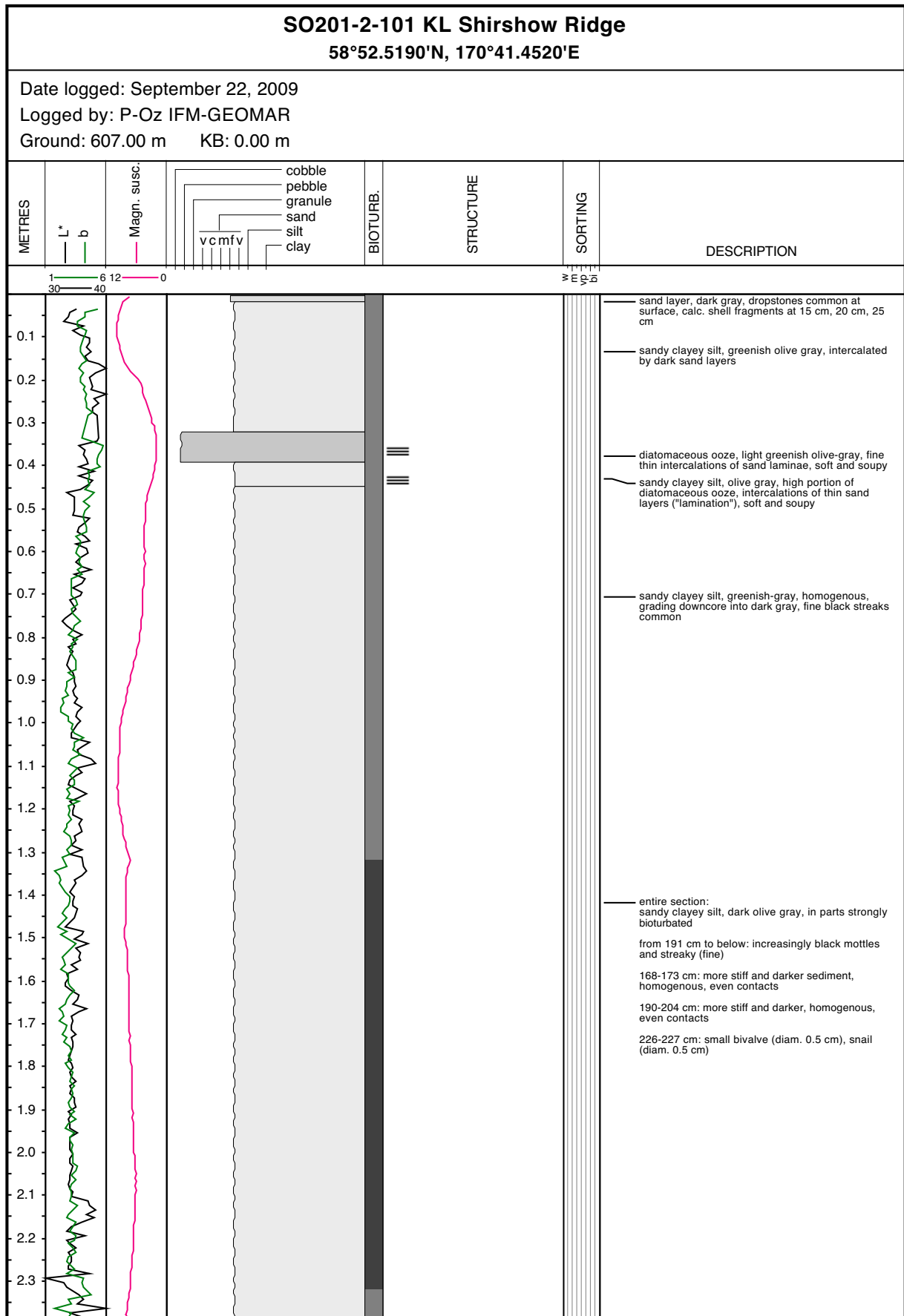
Appendix VI



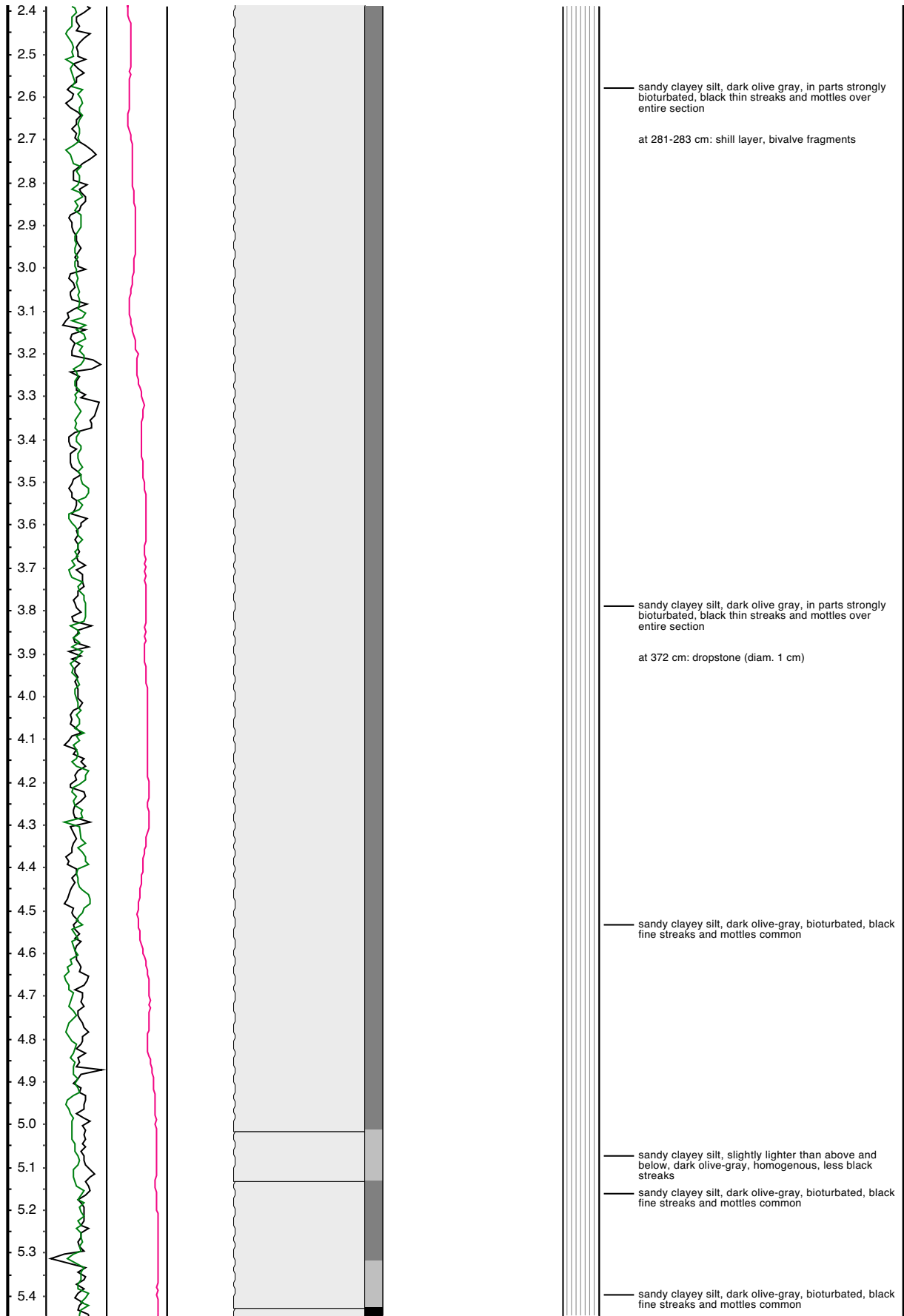
Appendix VI



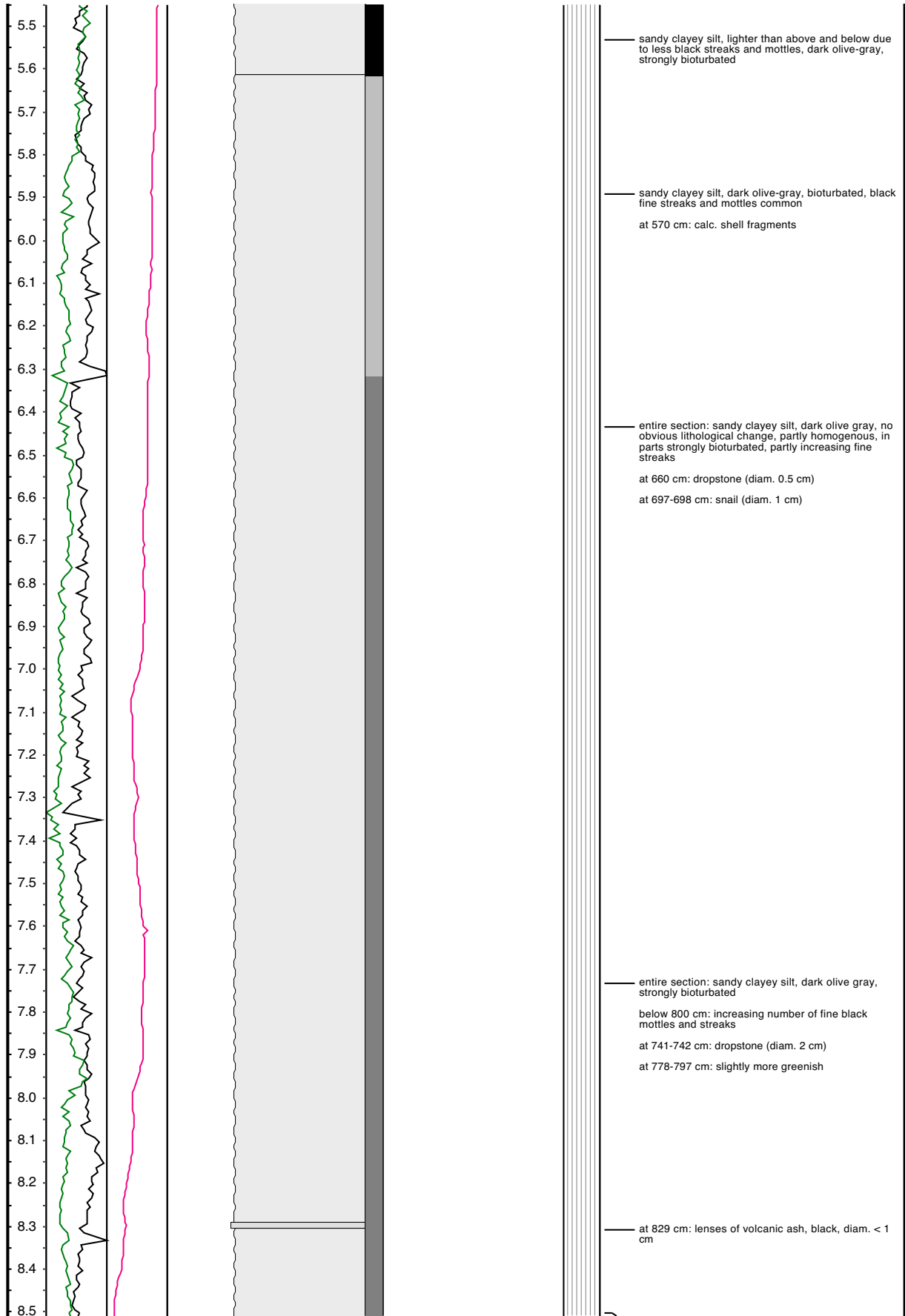
Appendix VI



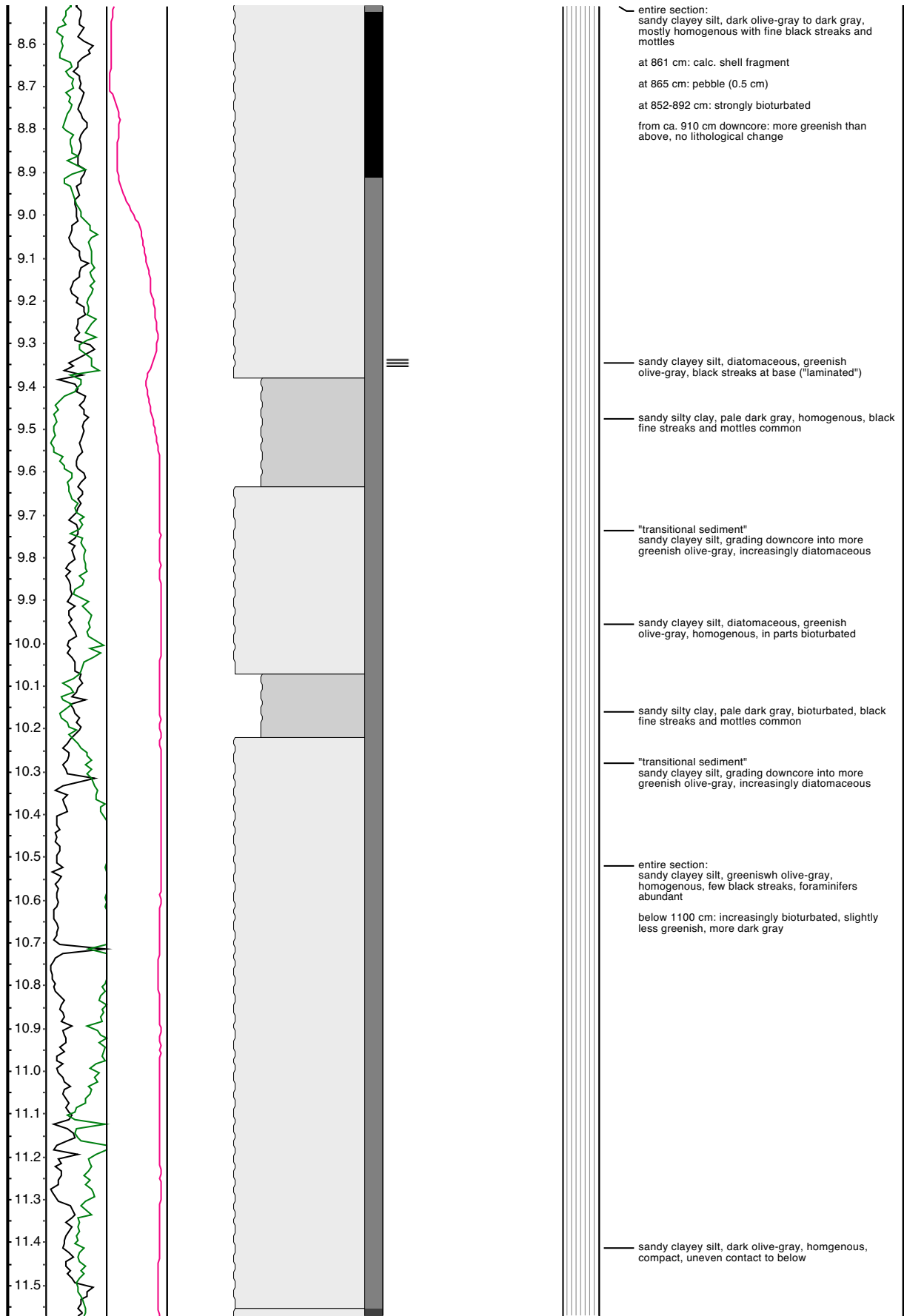
Appendix VI



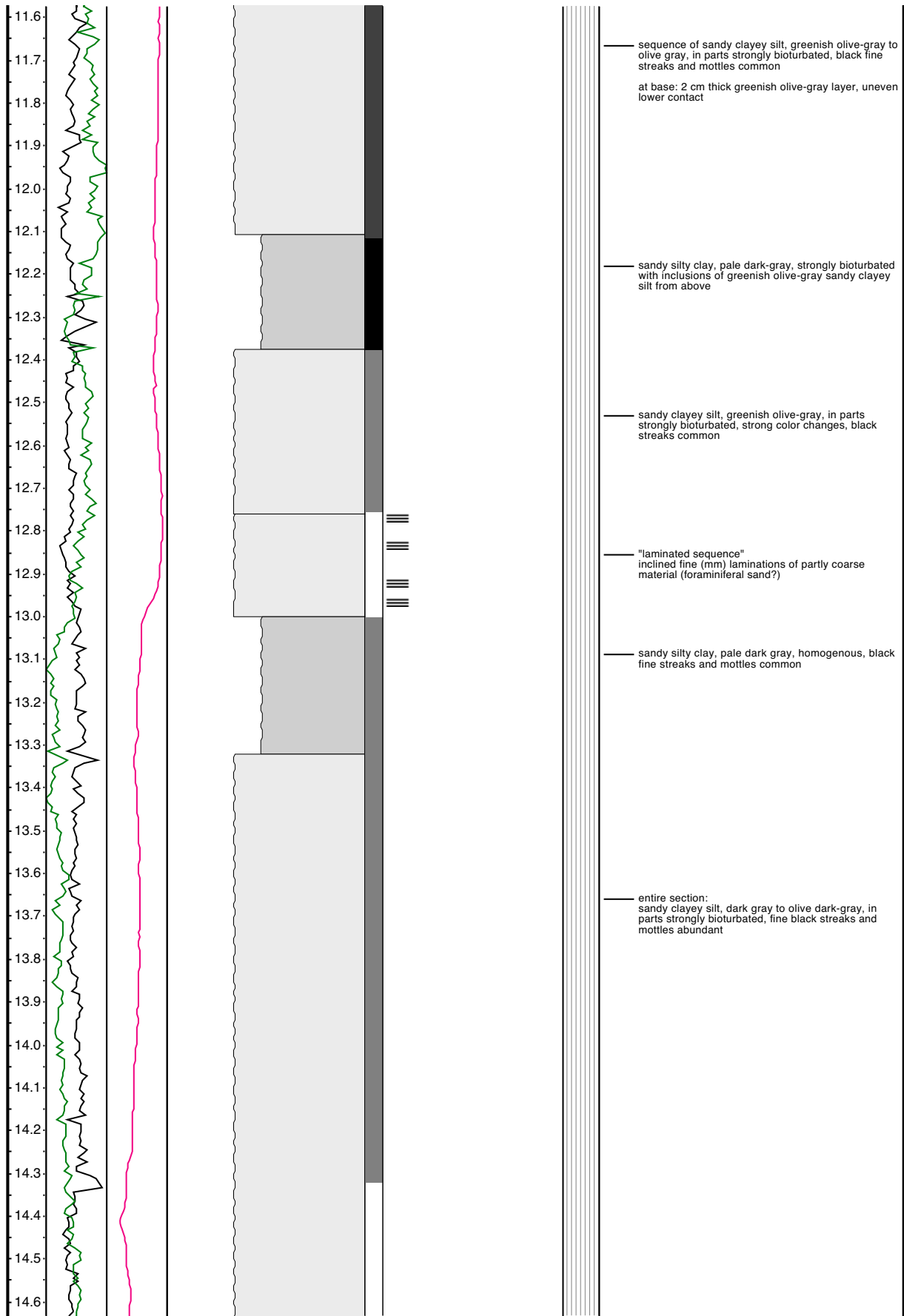
Appendix VI



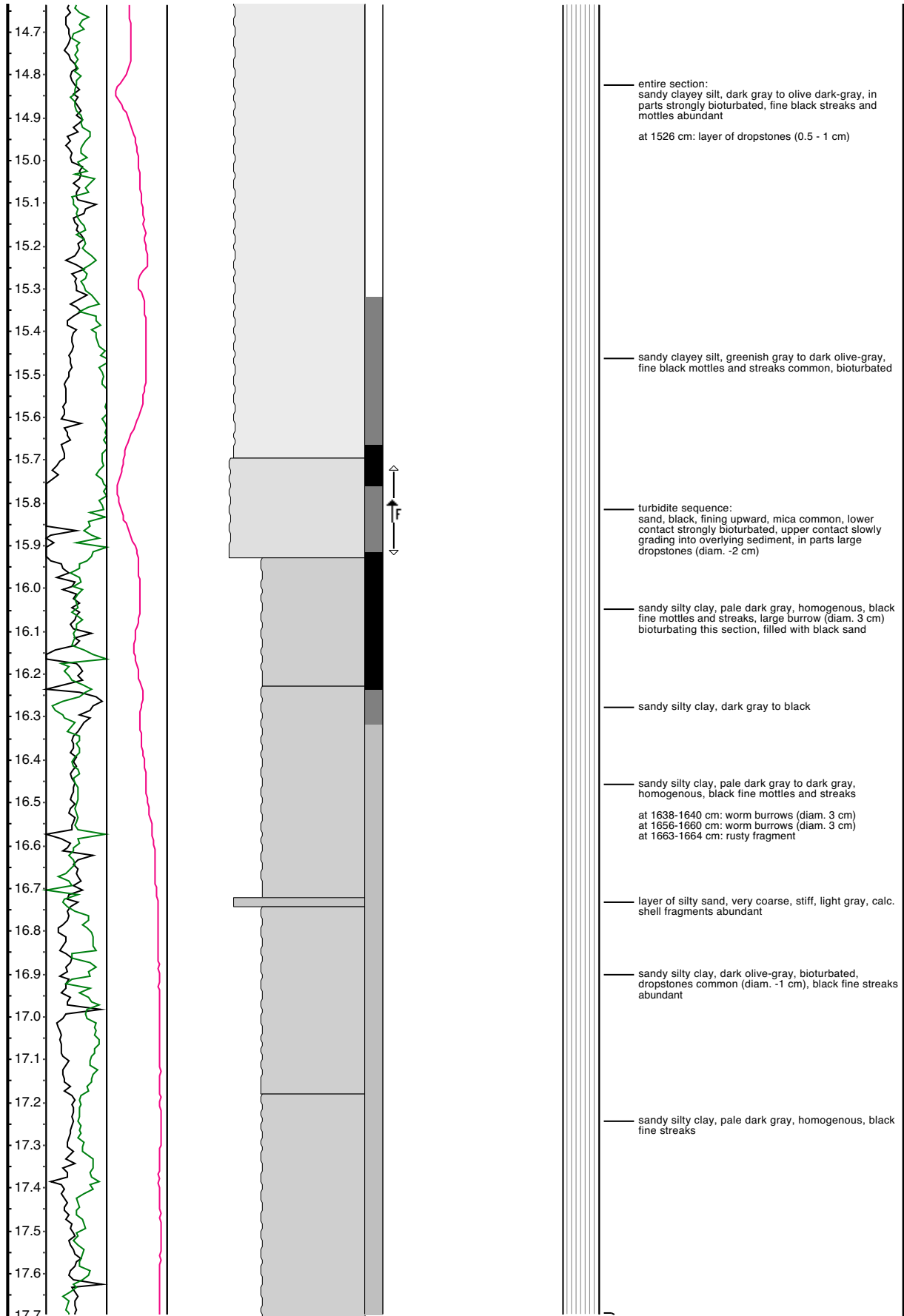
Appendix VI



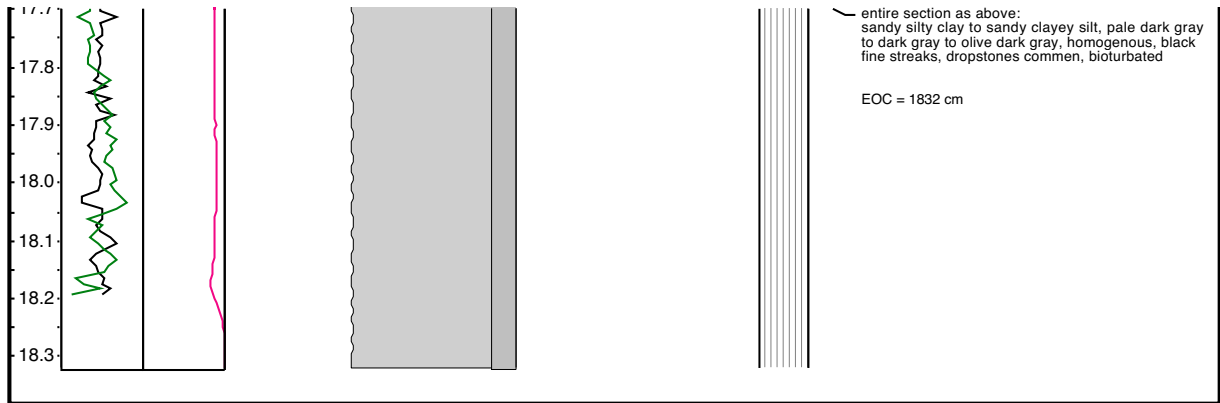
Appendix VI



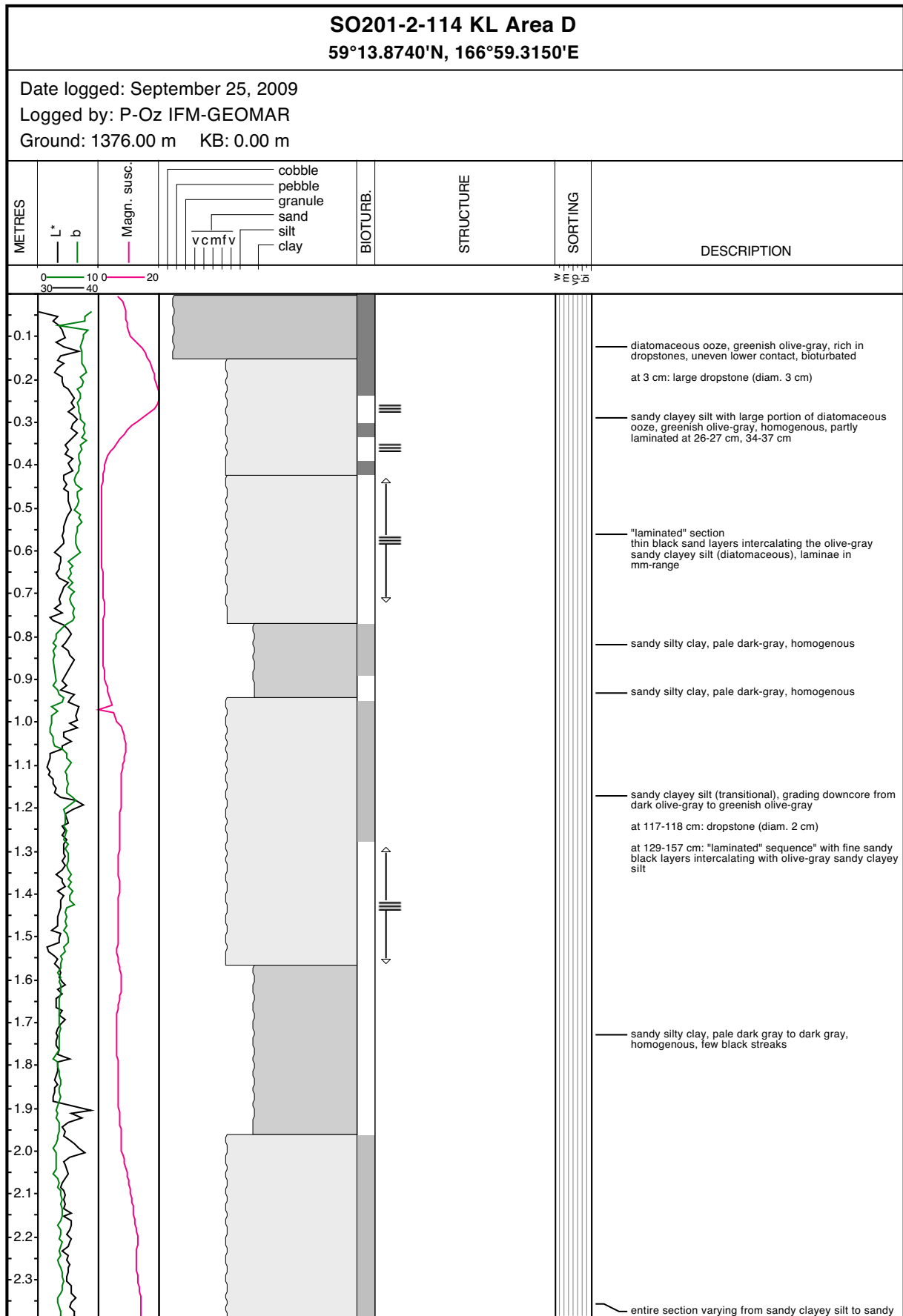
Appendix VI



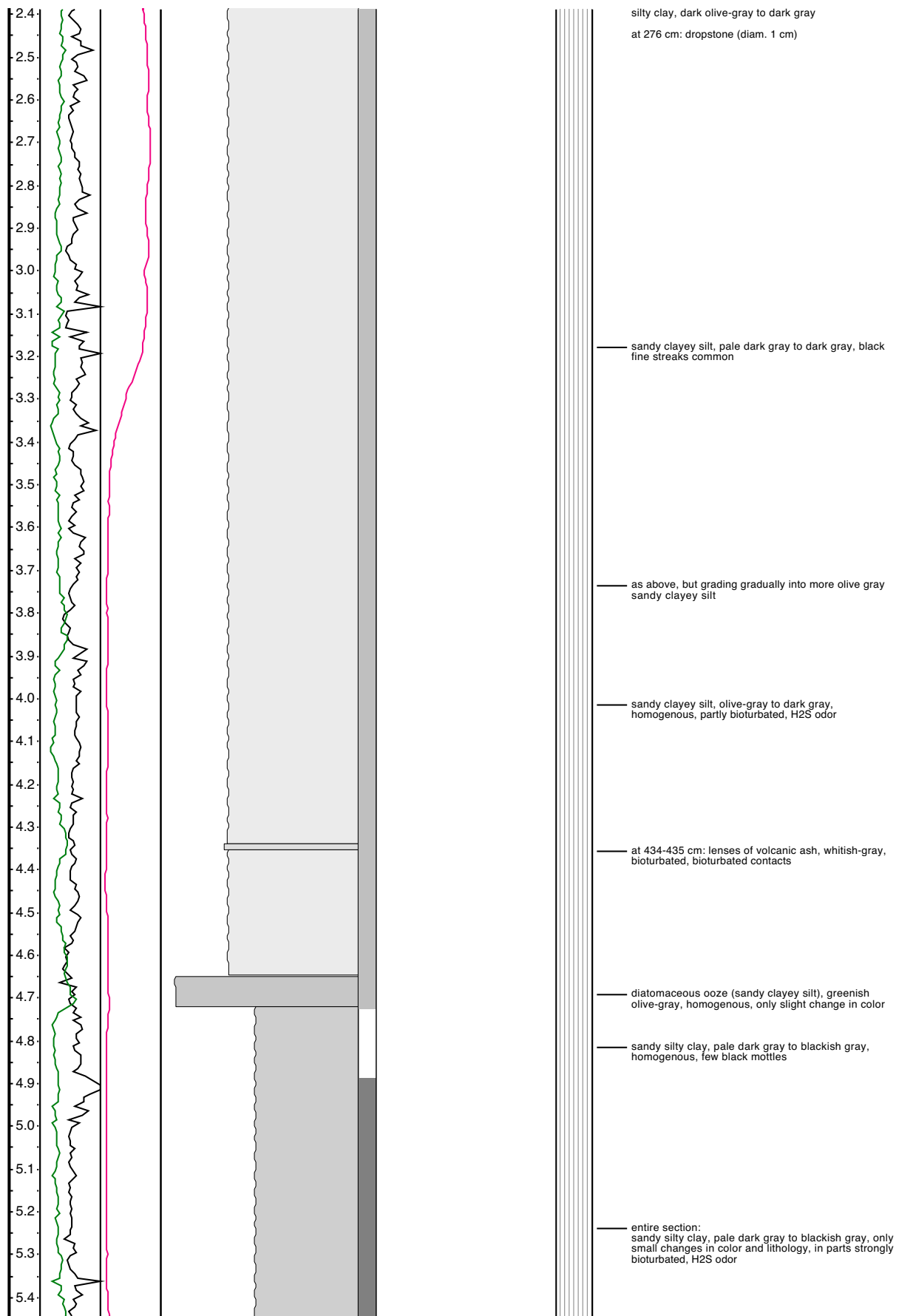
Appendix VI



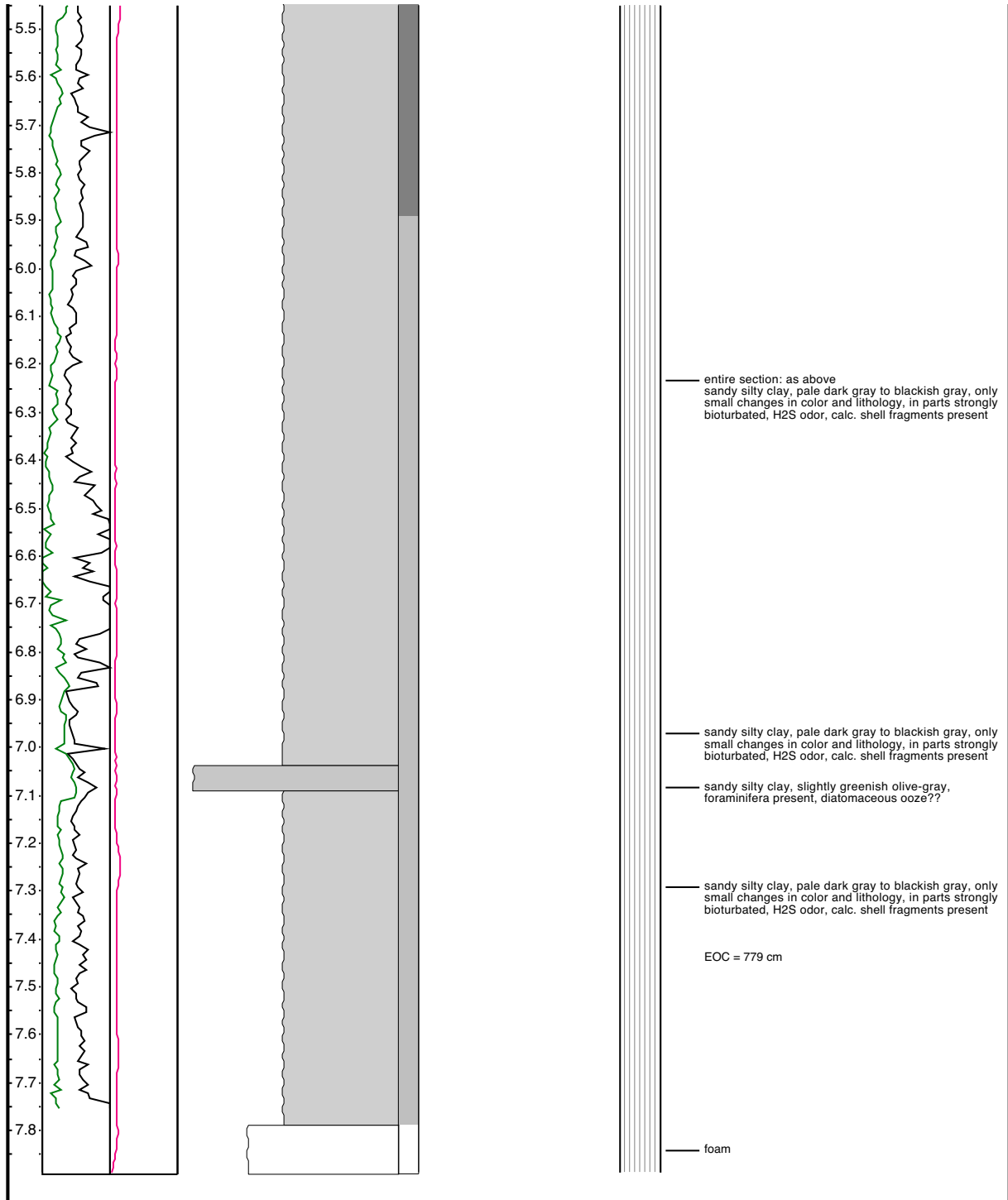
Appendix VI



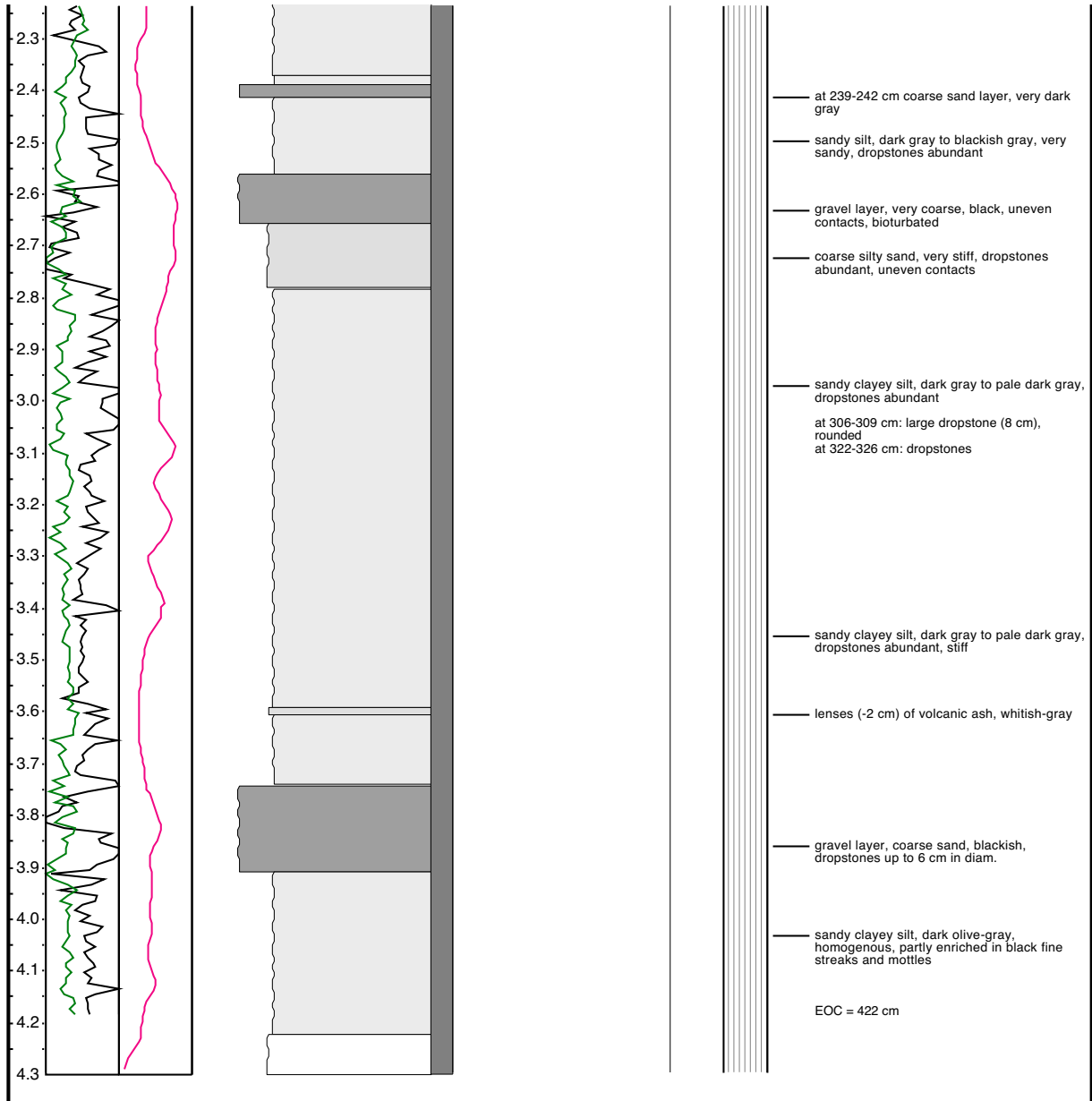
Appendix VI



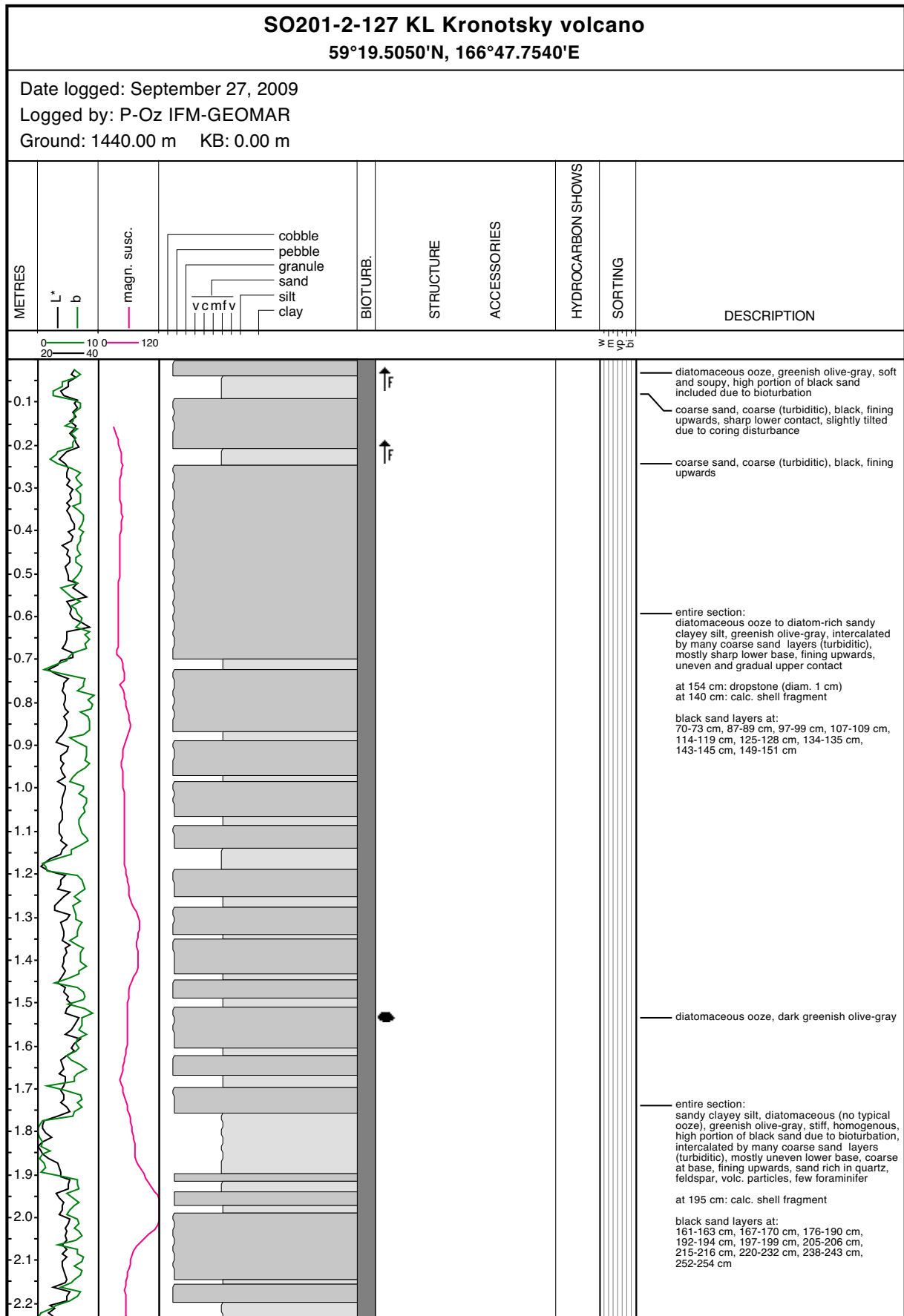
Appendix VI



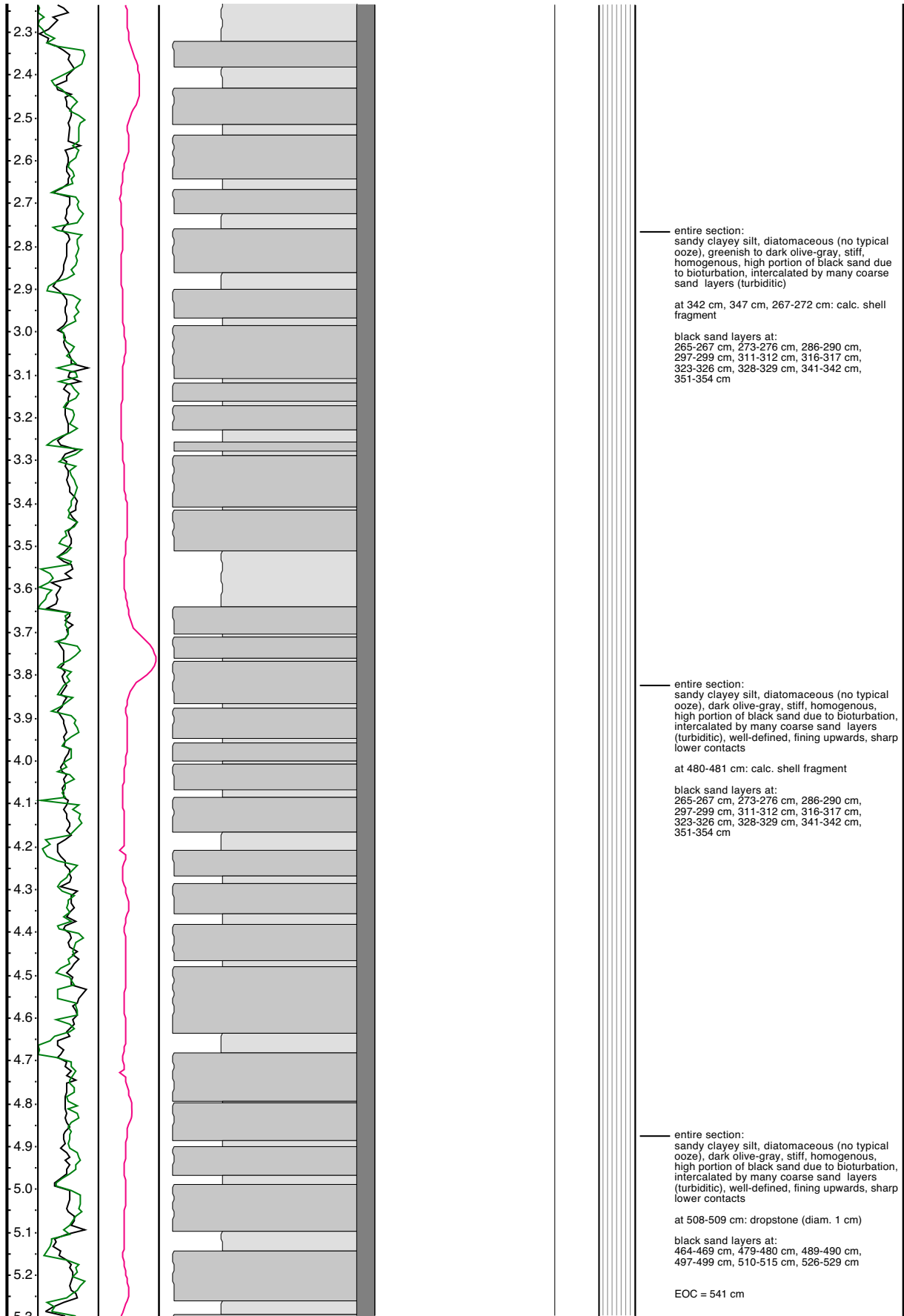
Appendix VI



Appendix VI



Appendix VI

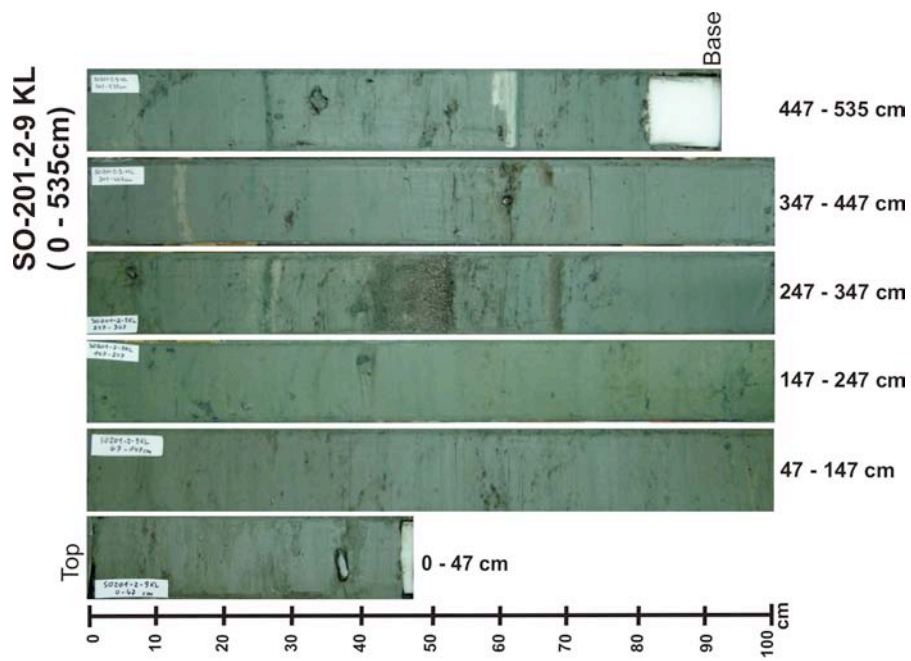
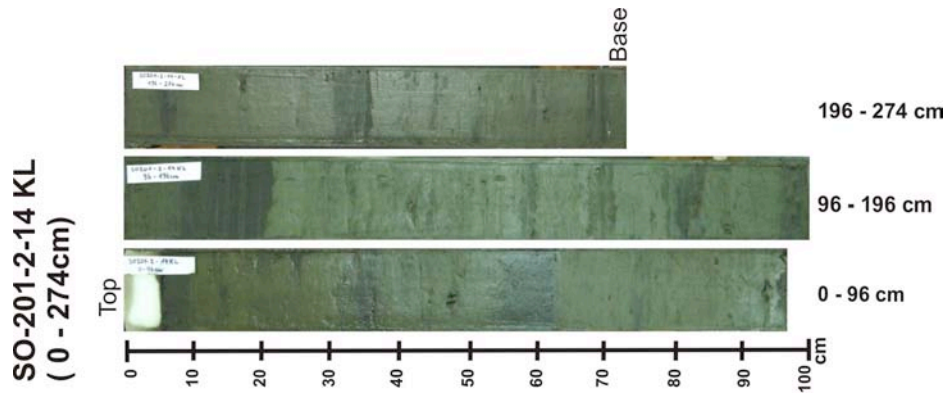


Appendix VI

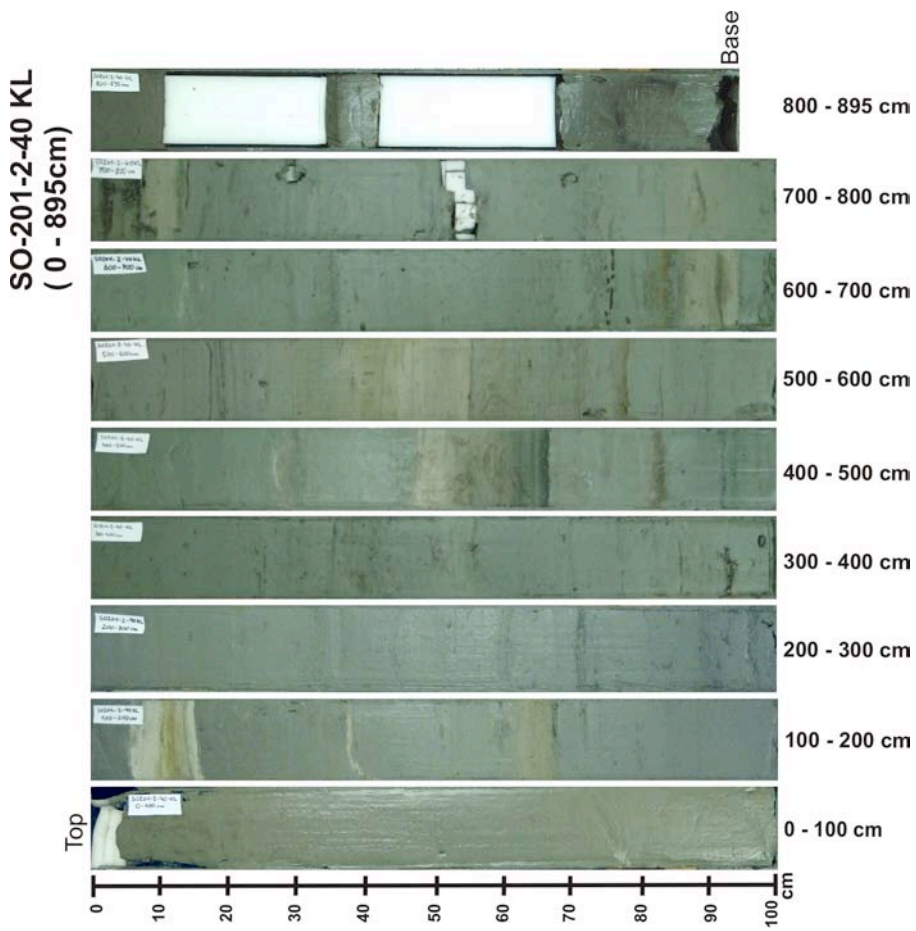
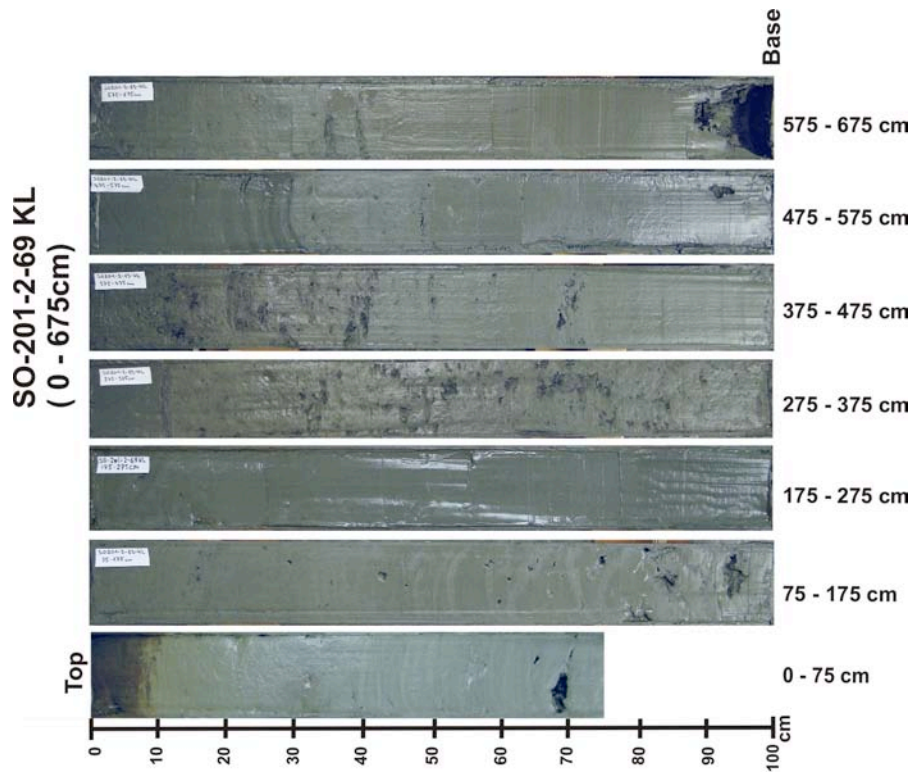


Appendix VII
Core Photography

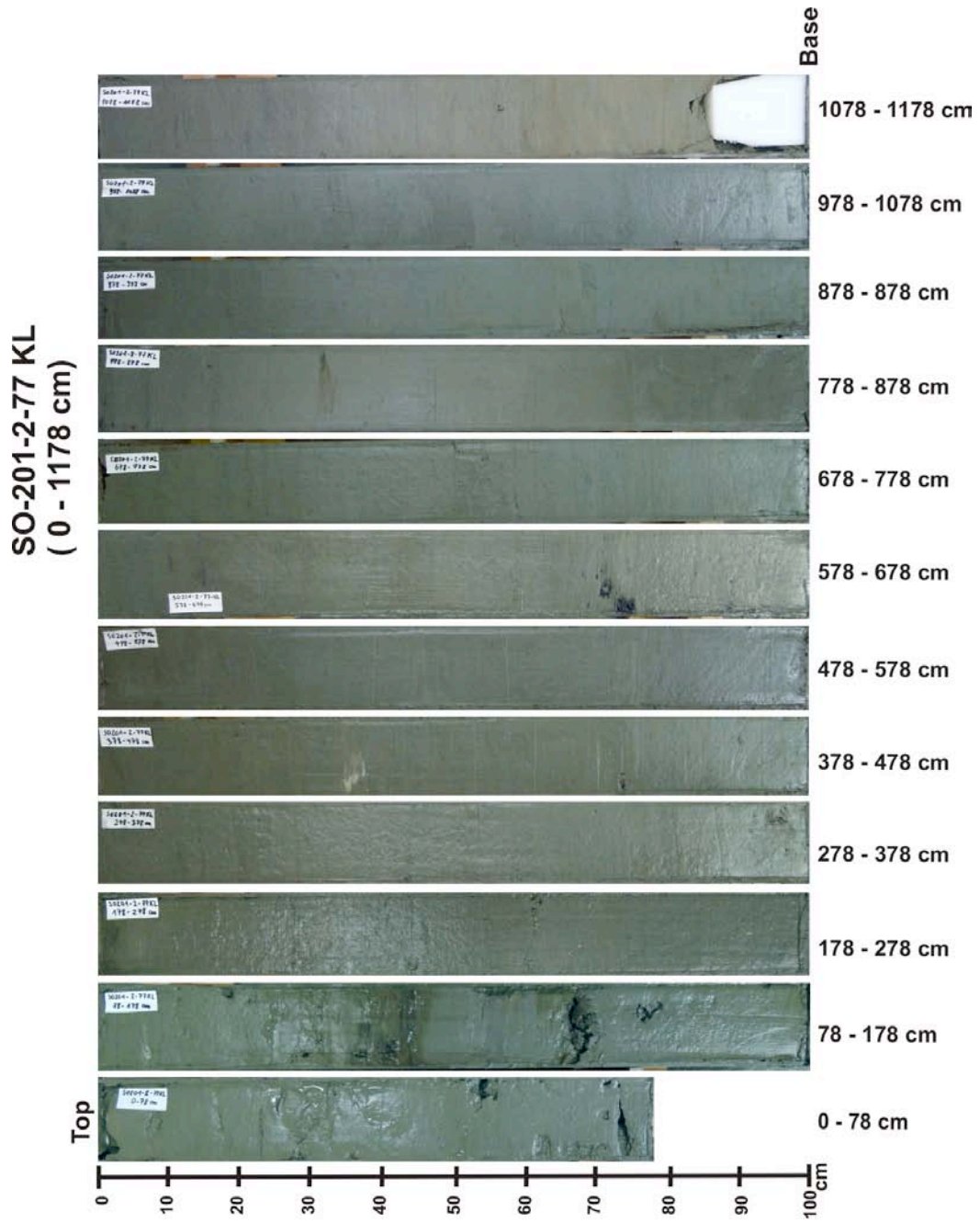
Appendix VII



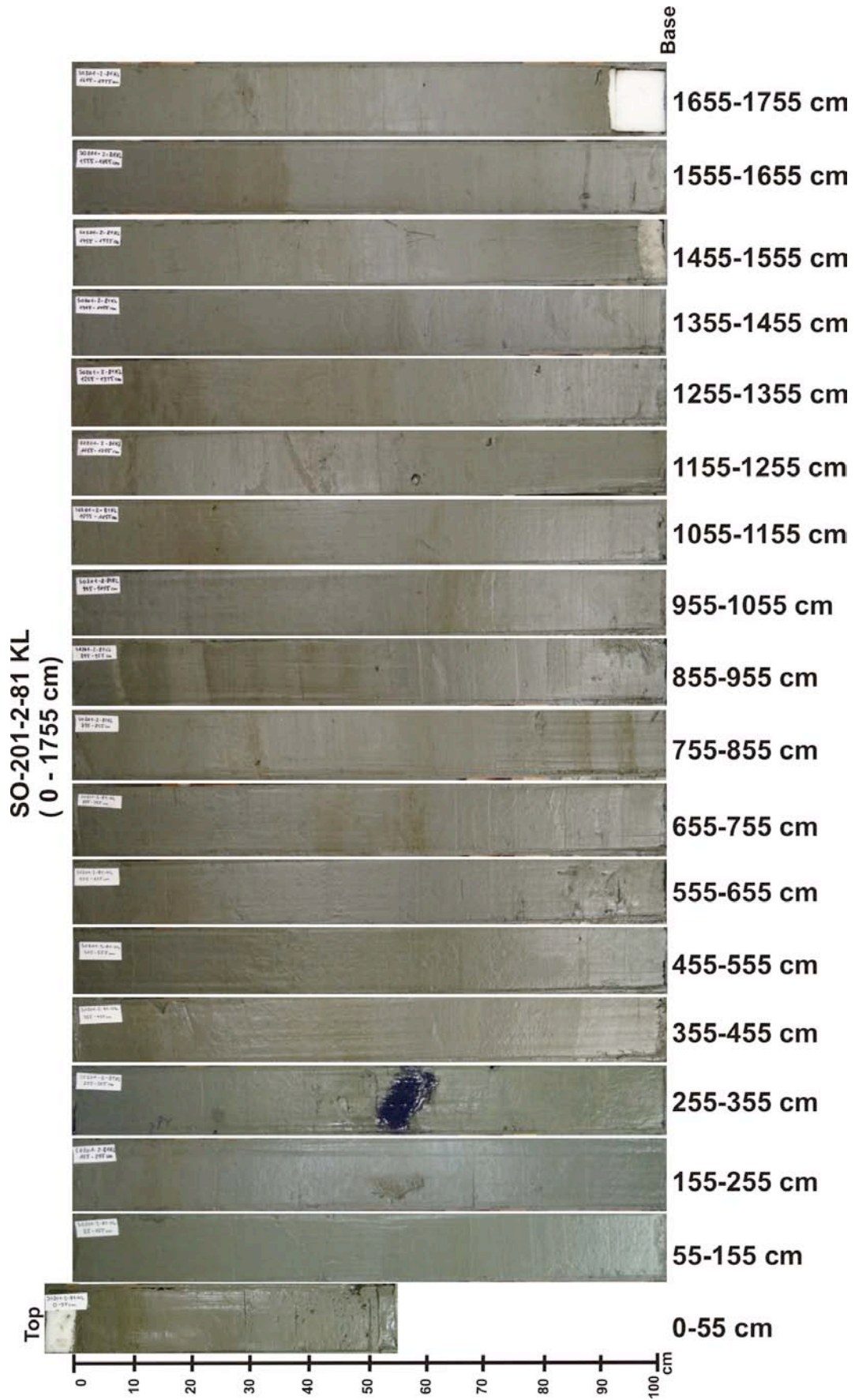
Appendix VII



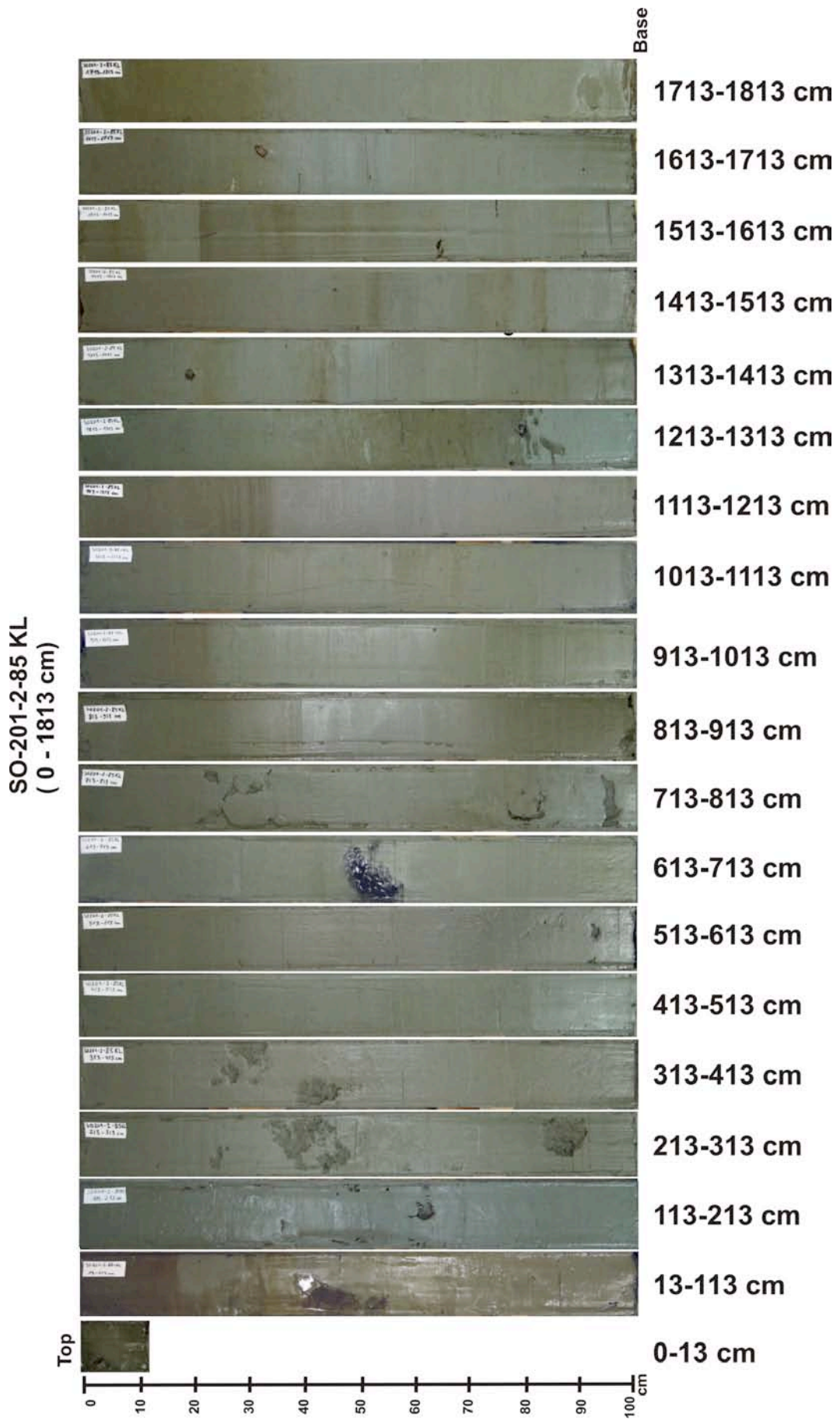
Appendix VII



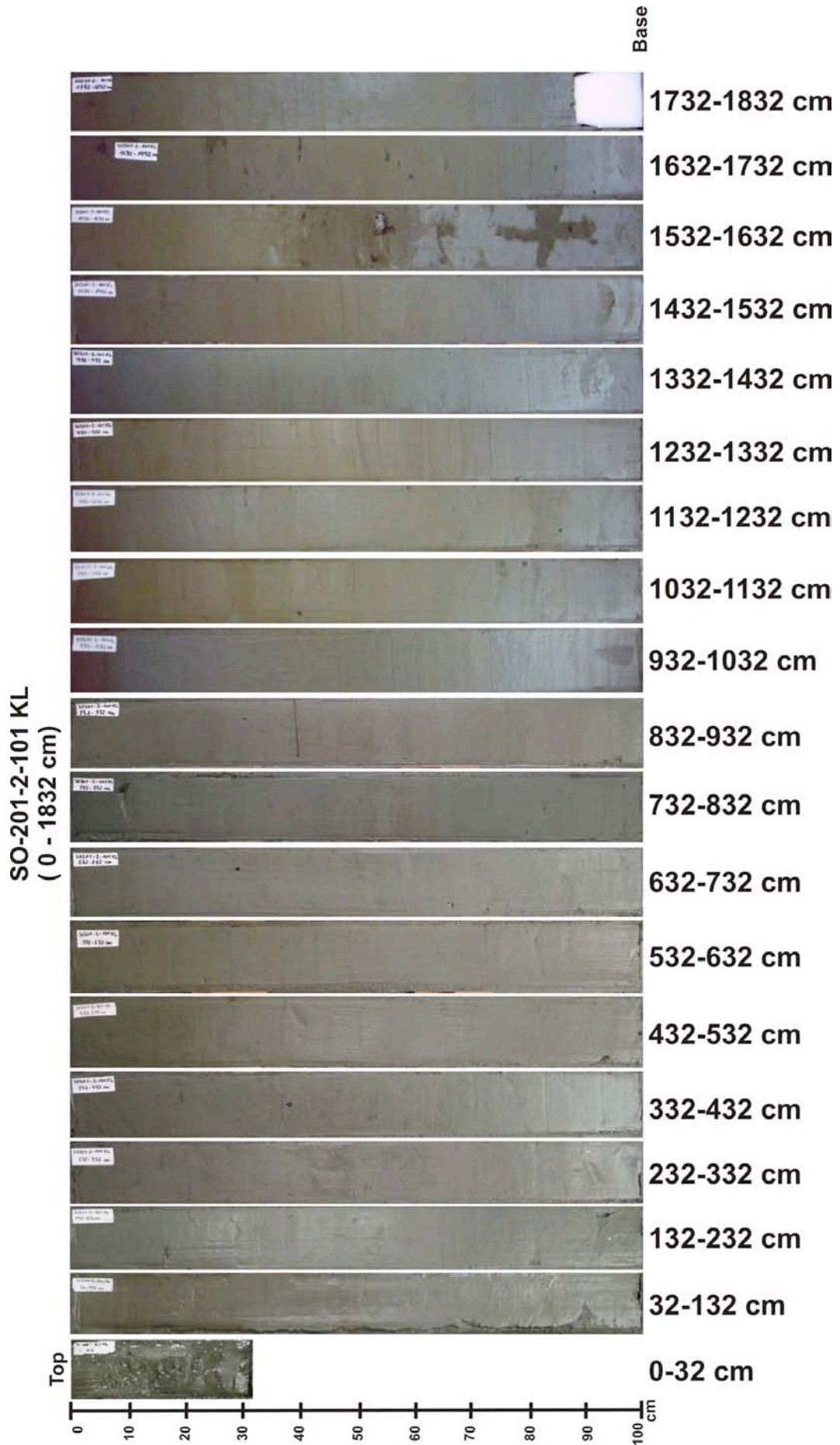
Appendix VII



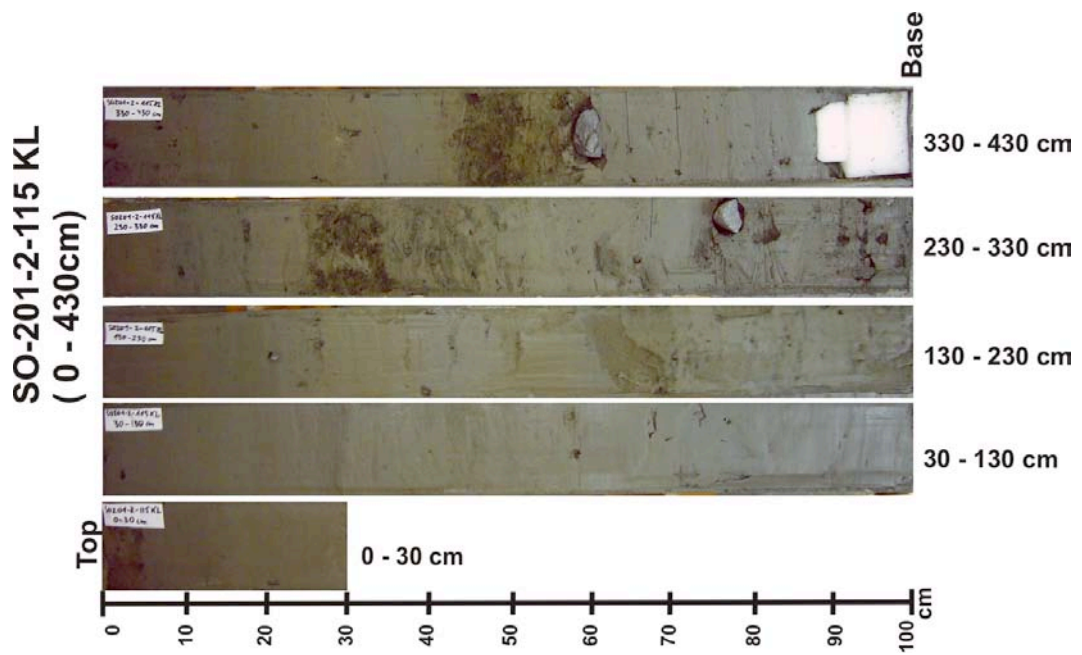
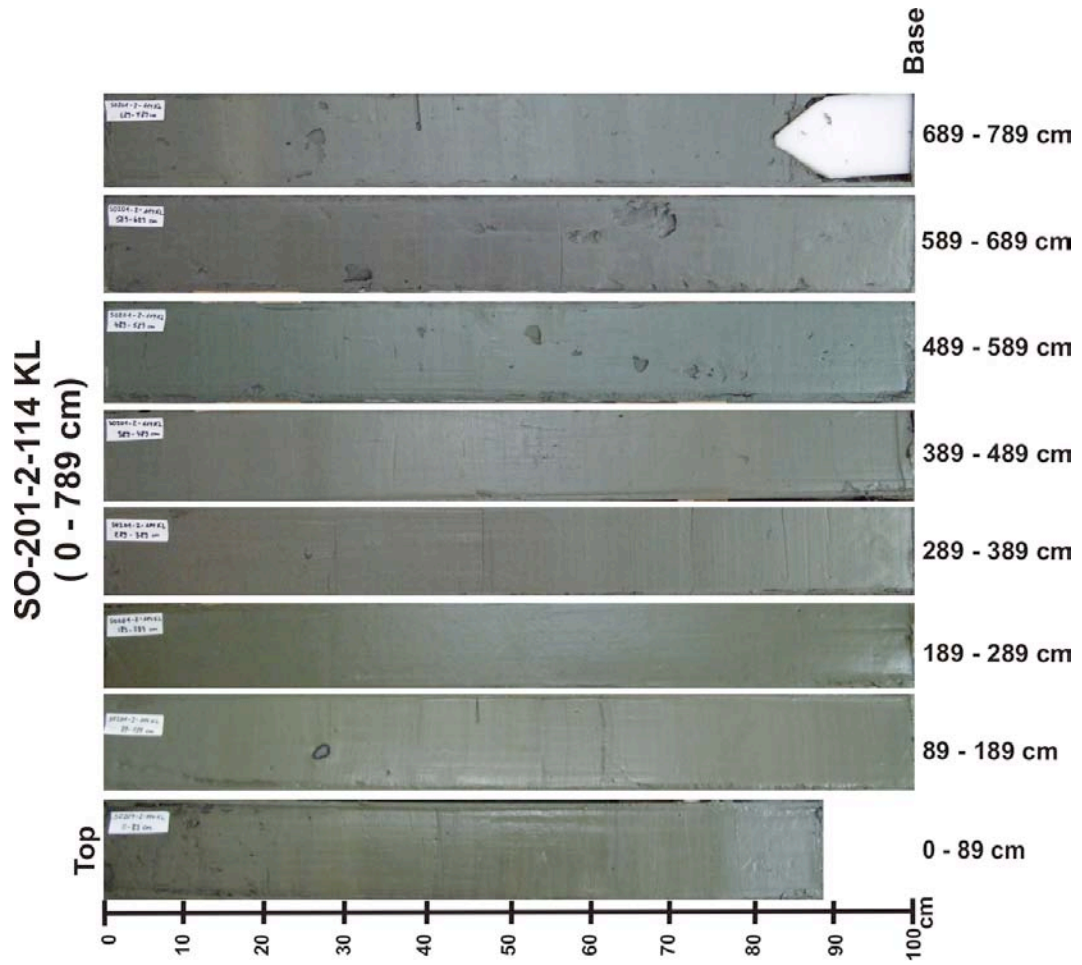
Appendix VII



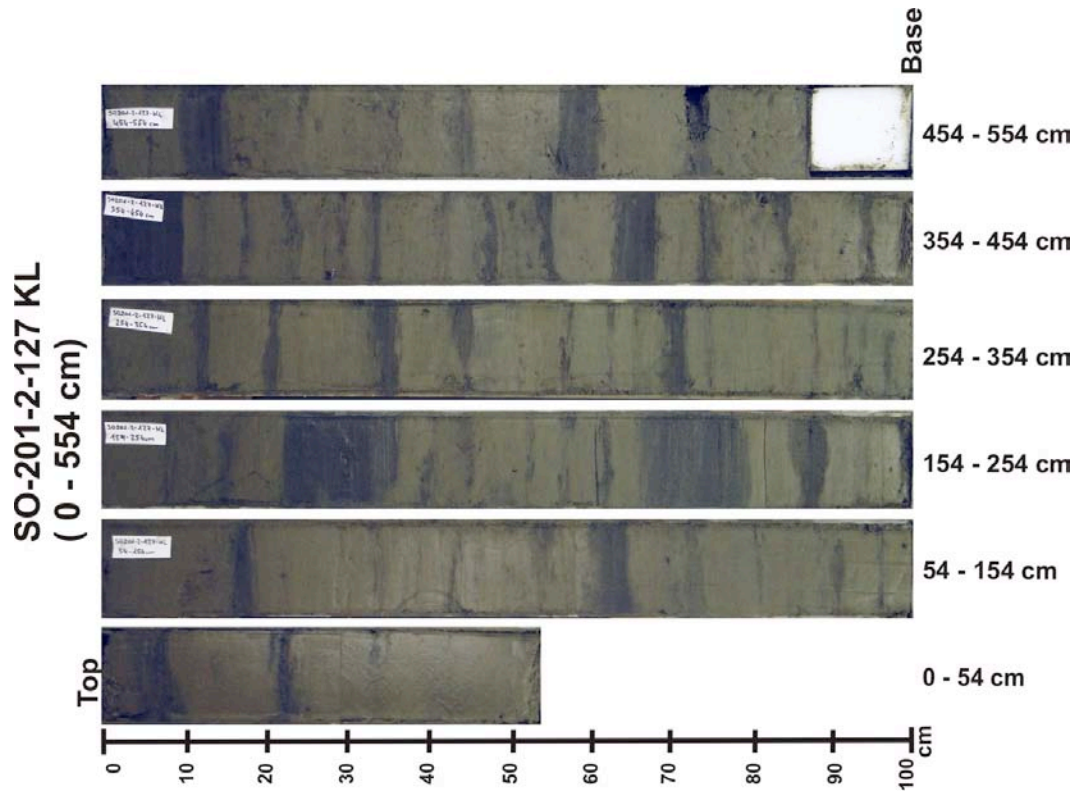
Appendix VII



Appendix VII

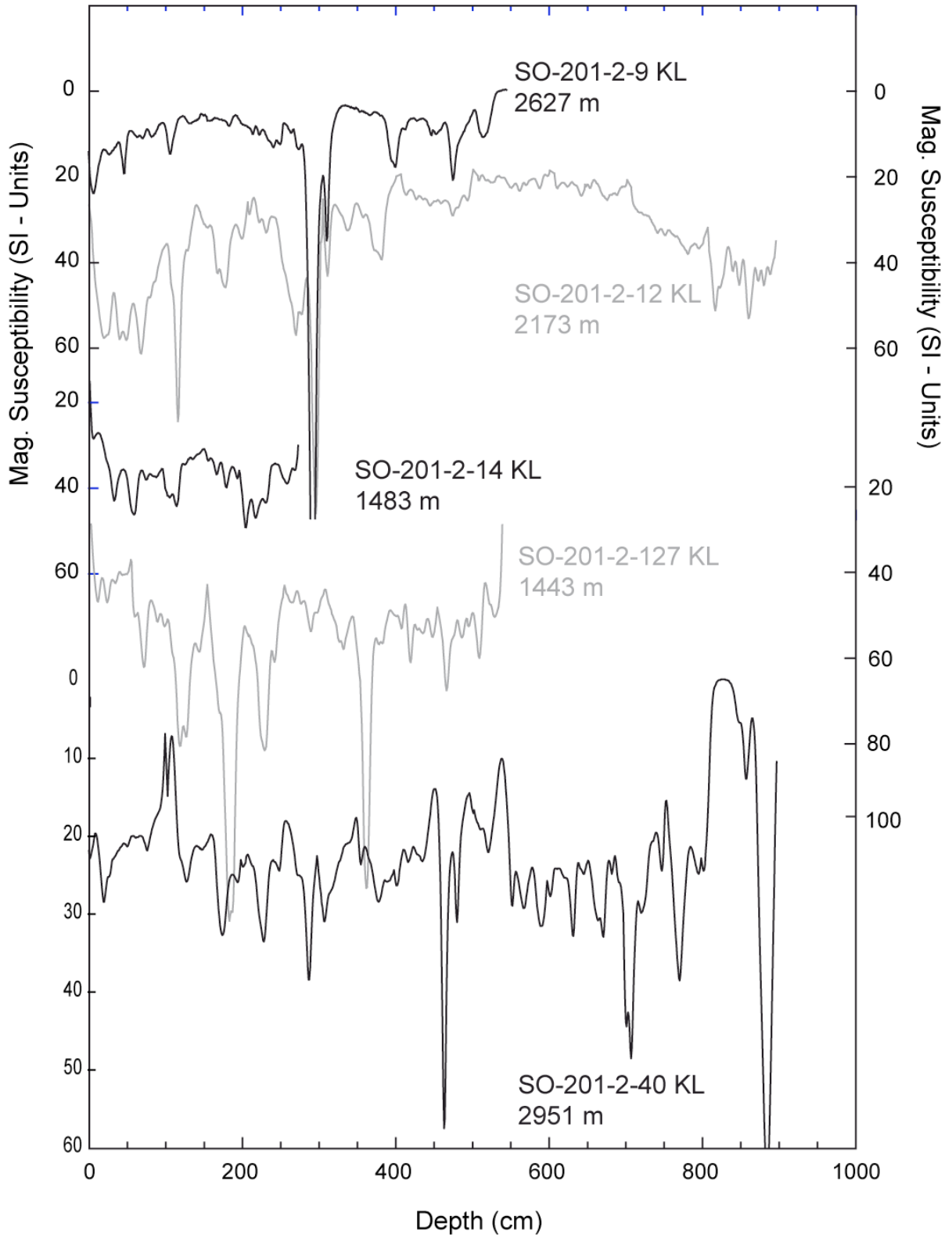


Appendix VII



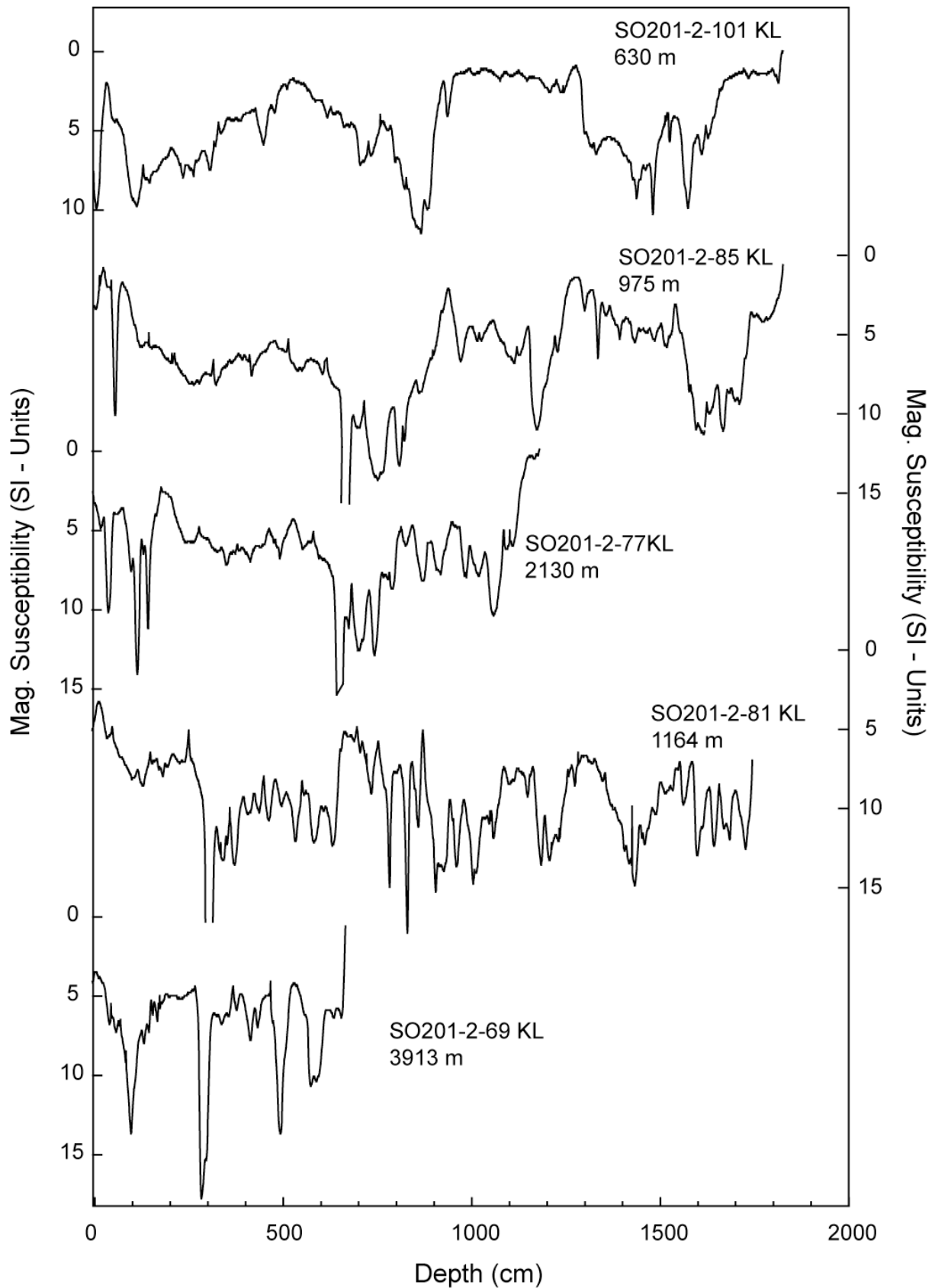
Appendix VIII
Magnetic Susceptibility Records

NW-Pacific continental margin offshore Kamtchatka and Meiji Seamount (Area B):
magnetic susceptibility records



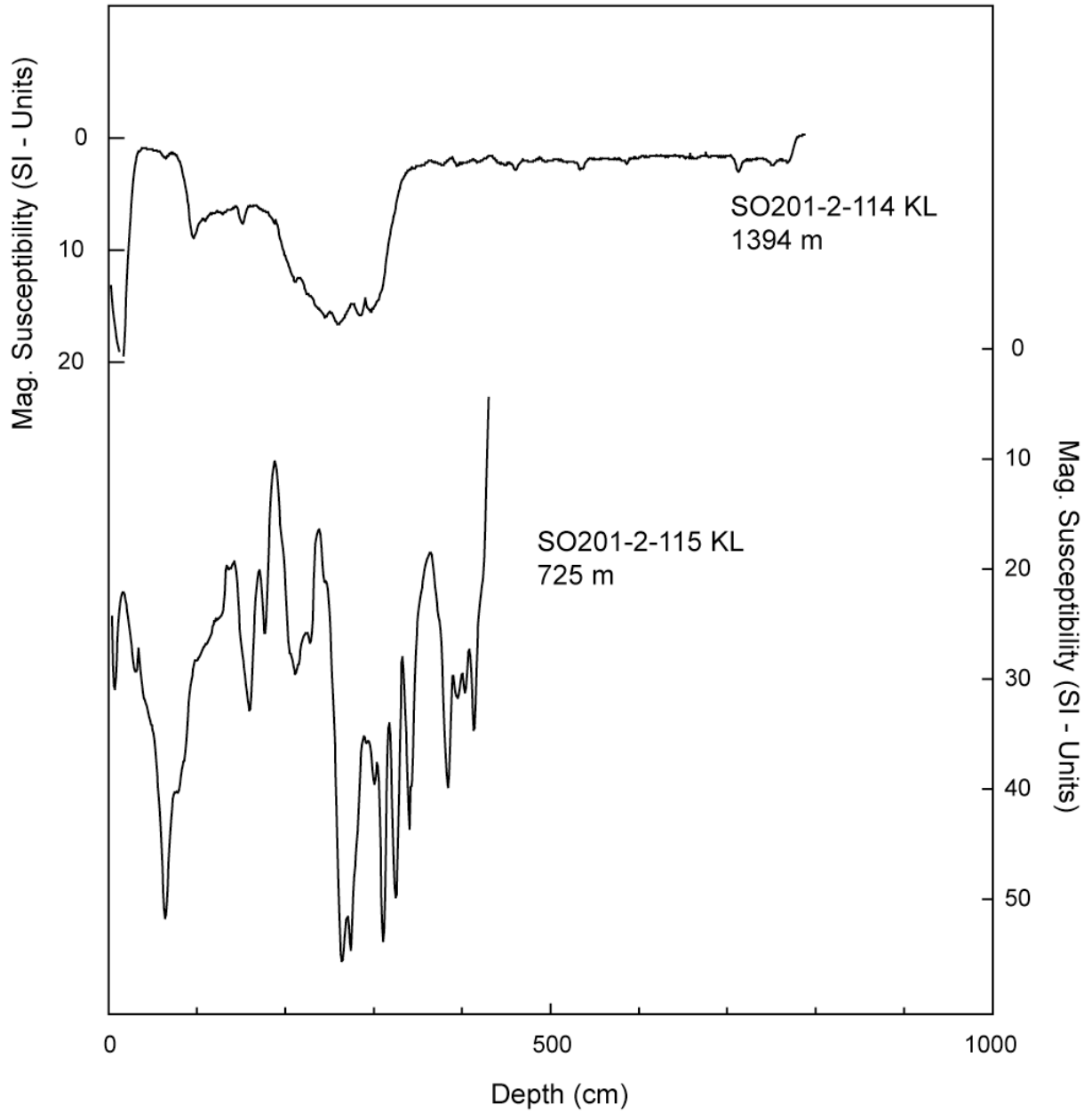
Magnetic susceptibility values versus core depth for sediment records from Area B (Kronotsky continental margin).

Shirshov Ridge (Area E): Magnetic susceptibility records



Magnetic susceptibility values versus core depth for sediment records from Area E (Shirshov Ridge).

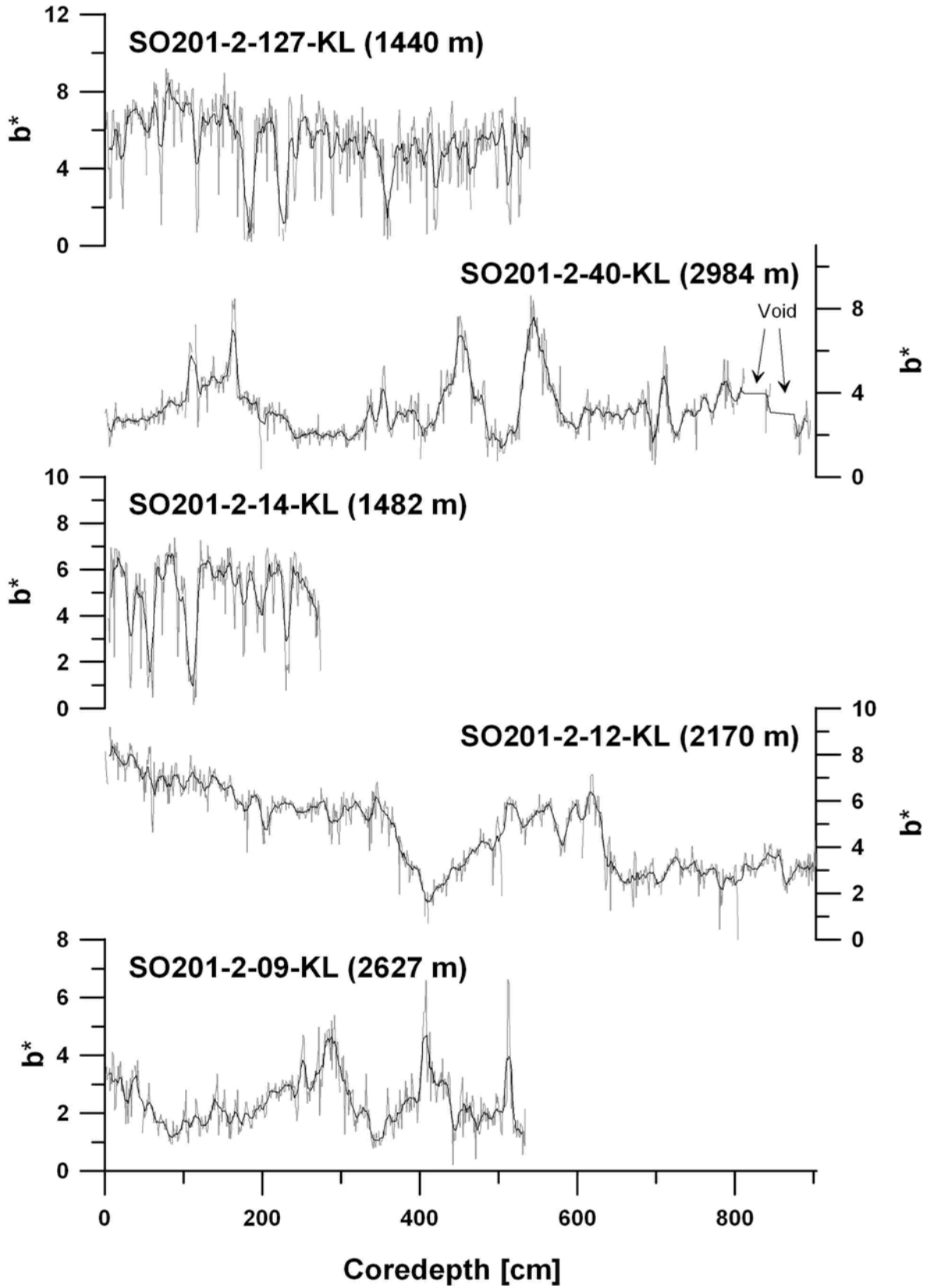
NW-Bering Sea continental margin offshore Kamtchatka (Area D):
magnetic susceptibility records



Magnetic susceptibility values versus core depth for sediment records from Area D

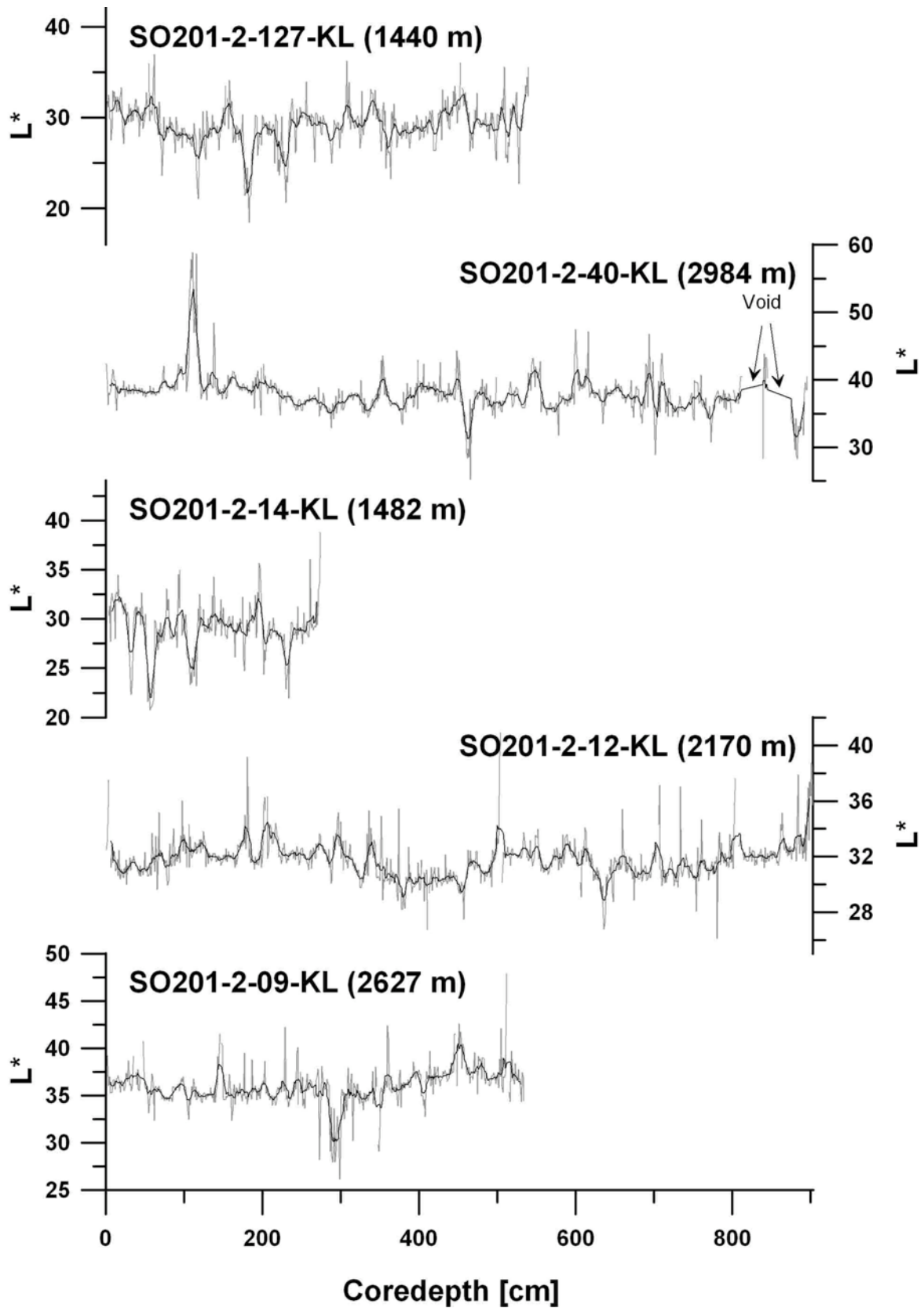
Appendix IX
Color Reflectance Values

Appendix IX



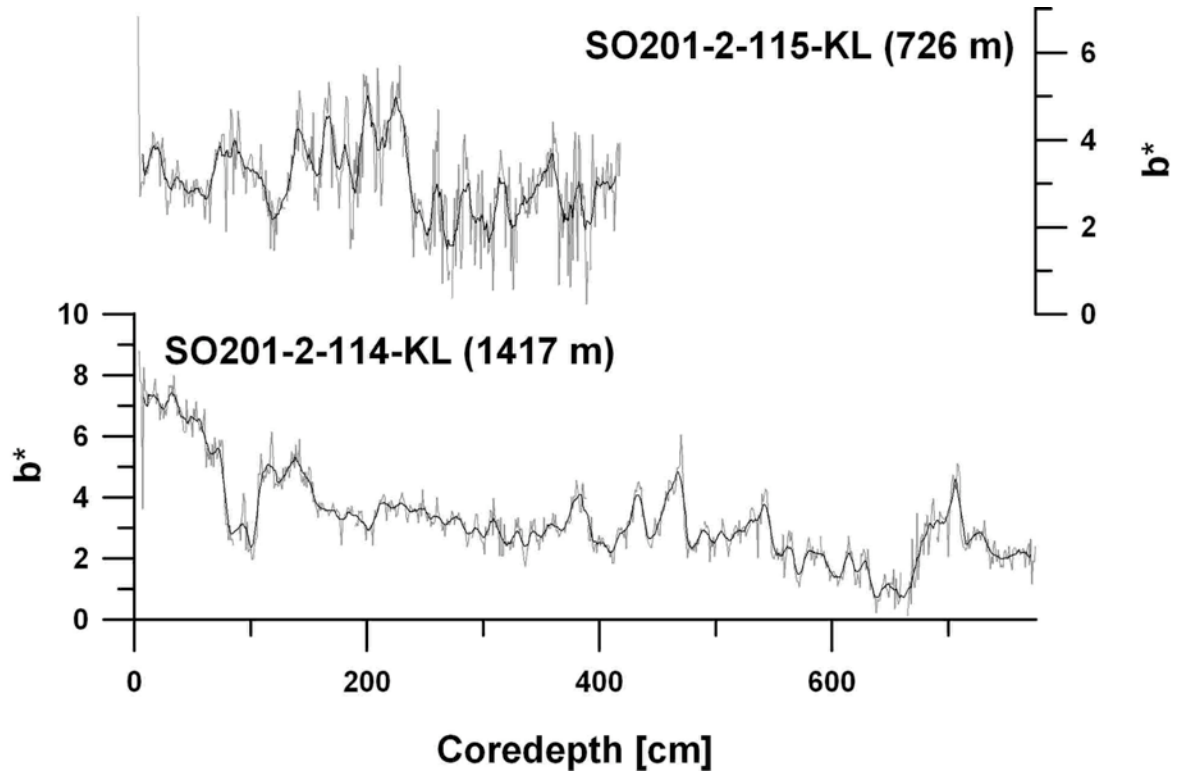
Color b^ values versus core depth for sediment records from Area B (Kronotsky continental margin). The raw data are overlain by a 9 point running average.*

Appendix IX

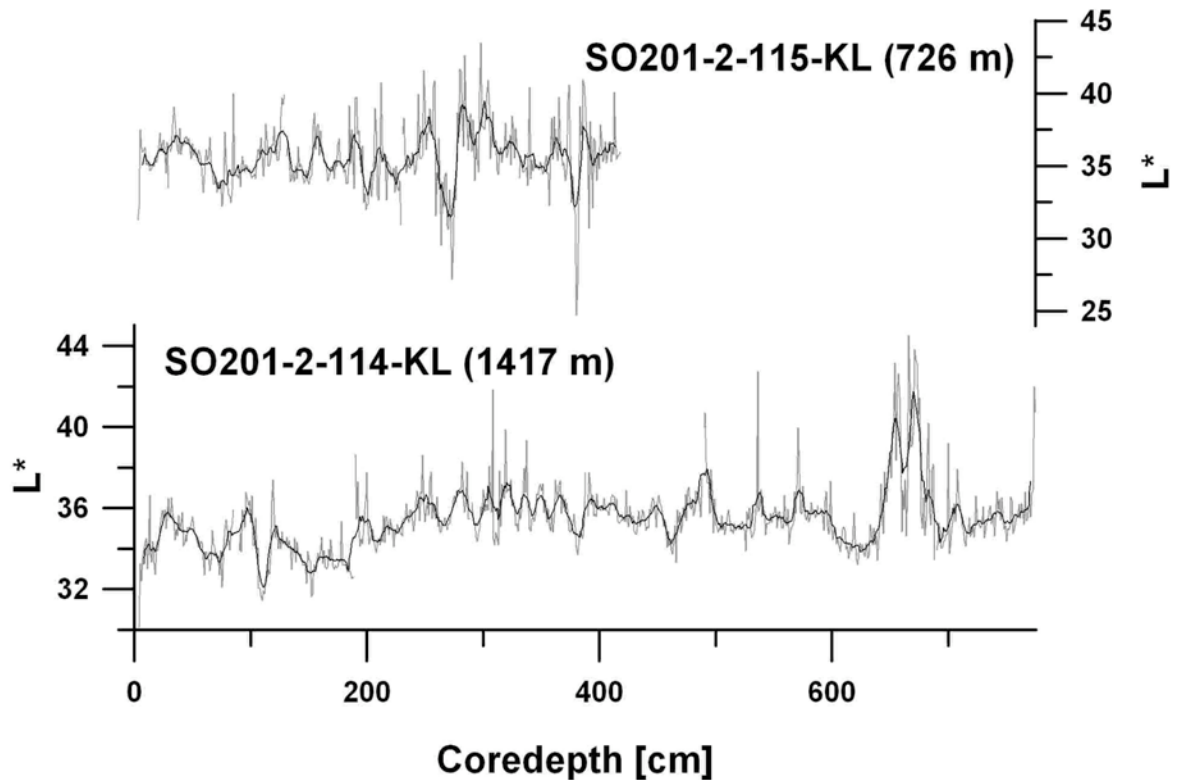


Color reflectance values (L^*) versus core depth for sediment records from Area B (Kronotsky continental margin). The raw data are overlain by a 9 point running average.

Appendix IX

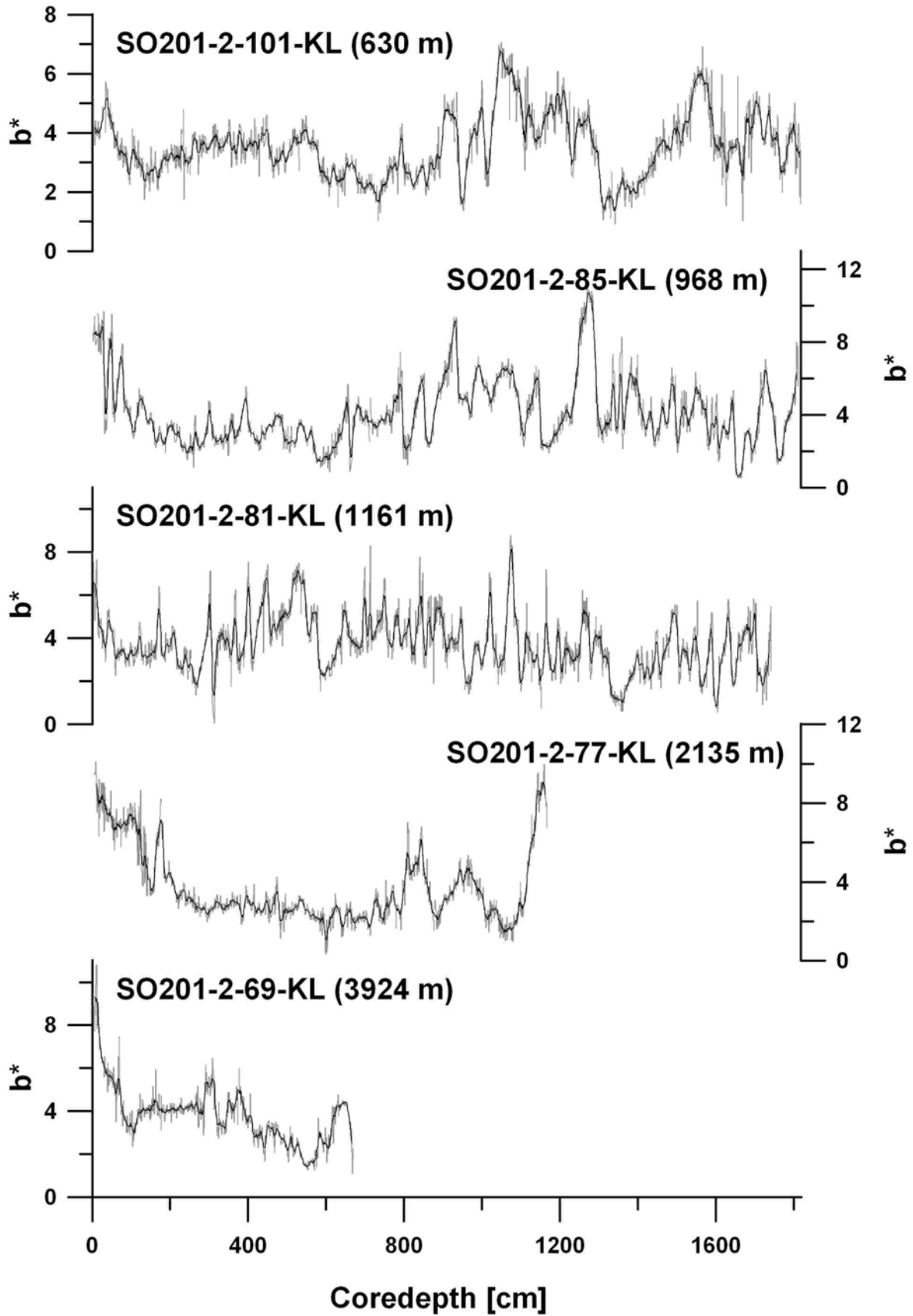


Color b^* values versus core depth for sediment records from Area D. The raw data are overlain by a 9 point running average.



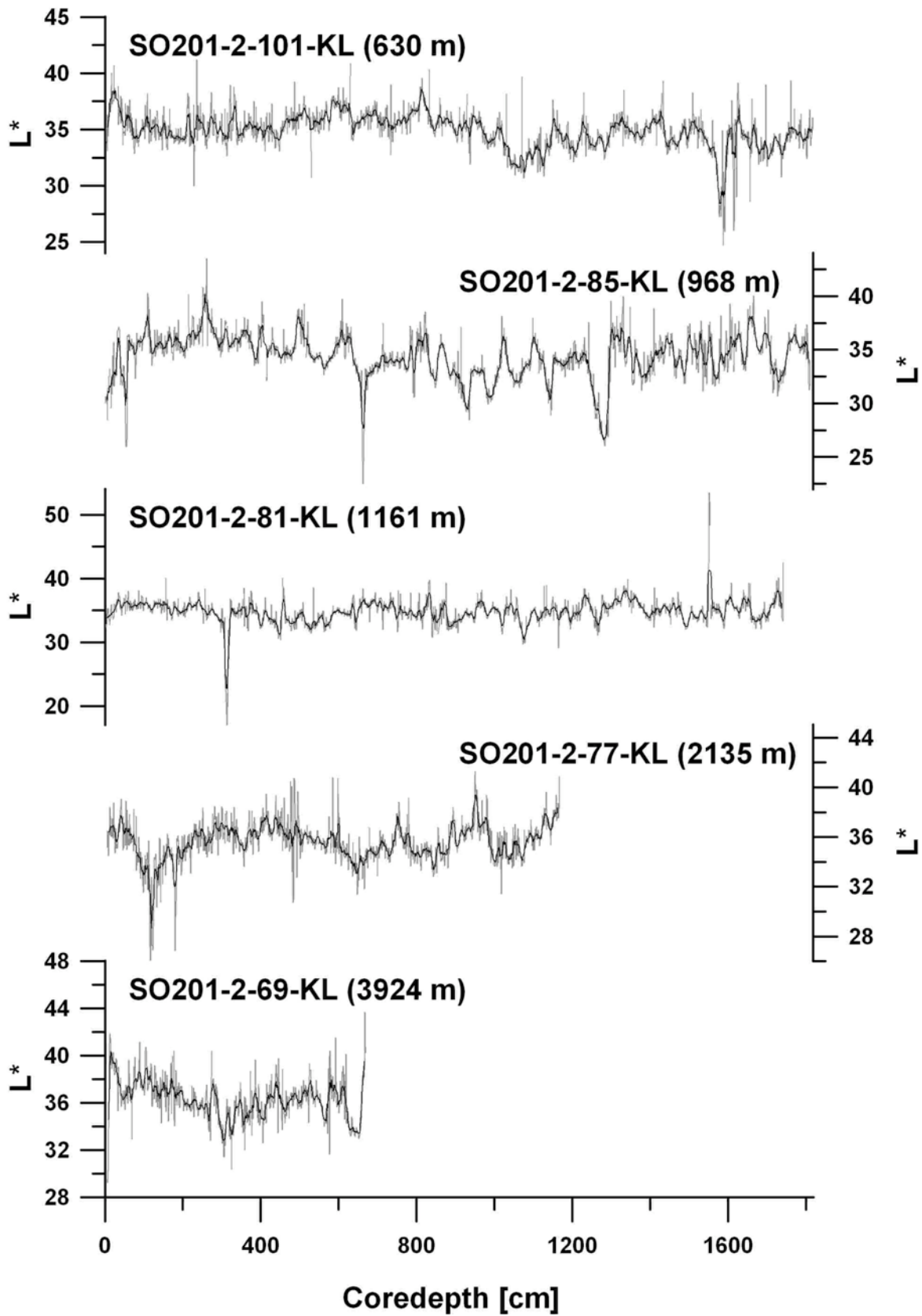
Color reflectance values (L^*) versus core depth for sediment records from Area D. The raw data are overlain by a 9 point running average.

Appendix IX



Color b^* values versus core depth for sediment records from Area E (Shirshow Ridge). The raw data are overlain by a 9 point running average.

Appendix IX



Color reflectance values (L^*) versus core depth for sediment records from Area E (Shirshow Ridge). The raw data are overlain by a 9 point running average.

IFM-GEOMAR Reports

- | No. | Title |
|-----|--|
| 1 | RV Sonne Fahrtbericht / Cruise Report SO 176 & 179 MERAMEX I & II (Merapi Amphibious Experiment) 18.05.-01.06.04 & 16.09.-07.10.04. Ed. by Heidrun Kopp & Ernst R. Flueh, 2004, 206 pp.
In English |
| 2 | RV Sonne Fahrtbericht / Cruise Report SO 181 TIPTEQ (from The Incoming Plate to mega Thrust EarthQuakes) 06.12.2004.-26.02.2005. Ed. by Ernst R. Flueh & Ingo Grevemeyer, 2005, 533 pp.
In English |
| 3 | RV Poseidon Fahrtbericht / Cruise Report POS 316 Carbonate Mounds and Aphotic Corals in the NE-Atlantic 03.08.-17.08.2004. Ed. by Olaf Pfannkuche & Christine Utecht, 2005, 64 pp.
In English |
| 4 | RV Sonne Fahrtbericht / Cruise Report SO 177 - (Sino-German Cooperative Project, South China Sea: Distribution, Formation and Effect of Methane & Gas Hydrate on the Environment) 02.06.-20.07.2004. Ed. by Erwin Suess, Yongyang Huang, Nengyou Wu, Xiqiu Han & Xin Su, 2005, 154 pp.
In English and Chinese |
| 5 | RV Sonne Fahrtbericht / Cruise Report SO 186 – GITEWS (German Indonesian Tsunami Early Warning System 28.10.-13.1.2005 & 15.11.-28.11.2005 & 07.01.-20.01.2006. Ed. by Ernst R. Flueh, Tilo Schoene & Wilhelm Weinrebe, 2006, 169 pp.
In English |
| 6 | RV Sonne Fahrtbericht / Cruise Report SO 186 -3 – SeaCause II, 26.02.-16.03.2006. Ed. by Heidrun Kopp & Ernst R. Flueh, 2006, 174 pp.
In English |
| 7 | RV Meteor, Fahrtbericht / Cruise Report M67/1 CHILE-MARGIN-SURVEY 20.02.-13.03.2006. Ed. by Wilhelm Weinrebe und Silke Schenk, 2006, 112 pp.
In English |
| 8 | RV Sonne Fahrtbericht / Cruise Report SO 190 - SINDBAD (Seismic and Geoacoustic Investigations Along The Sunda-Banda Arc Transition) 10.11.2006 - 24.12.2006. Ed. by Heidrun Kopp & Ernst R. Flueh, 2006, 193 pp.
In English |
| 9 | RV Sonne Fahrtbericht / Cruise Report SO 191 - New Vents "Puaretanga Hou" 11.01. - 23.03.2007. Ed. by Jörg Bialas, Jens Greinert, Peter Linke, Olaf Pfannkuche, 2007, 190 pp.
In English |
| 10 | FS ALKOR Fahrtbericht / Cruise Report AL 275 - Geobiological investigations and sampling of aphotic coral reef ecosystems in the NE-Skagerrak, 24.03. - 30.03.2006, Eds.: Andres Rüggeberg & Armin Form, 39 pp. In English |

No.	Title
11	FS Sonne / Fahrtbericht / Cruise Report SO 192-1: MANGO: Marine Geoscientific Investigations on the Input and Output of the Kermadec Subduction Zone, 24.03. - 22.04.2007, Ernst Flüh & Heidrun Kopp, 127 pp. In English
12	FS Maria S. Merian / Fahrtbericht / Cruise Report MSM 04-2: Seismic Wide-Angle Profiles, Fort-de-France – Fort-de-France, 03.01. - 19.01.2007, Ed.: Ernst Flüh, 45 pp. In English
13	FS Sonne / Fahrtbericht / Cruise Report SO 193: MANIHIKI Temporal, Spatial, and Tectonic Evolution of Oceanic Plateaus, Suva/Fiji – Apia/Samoa 19.05. - 30.06.2007, Eds.: Reinhard Werner and Folkmar Hauff, 201 pp. In English
14	FS Sonne / Fahrtbericht / Cruise Report SO195: TOTAL TONGA Thrust earthquake Asperity at Louisville Ridge, Suva/Fiji – Suva/Fiji 07.01. - 16.02.2008, Eds.: Ingo Grevemeyer & Ernst R. Flüh, 106 pp. In English
15	RV Poseidon Fahrtbericht / Cruise Report P362-2: West Nile Delta Mud Volcanoes, Piräus – Heraklion 09.02. - 25.02.2008, Ed.: Thomas Feseker, 63 pp. In English
16	RV Poseidon Fahrtbericht / Cruise Report P347: Mauritanian Upwelling and Mixing Process Study (MUMP), Las-Palmas - Las Palmas, 18.01. - 05.02.2007, Ed.: Marcus Dengler et al., 34 pp. In English
17	FS Maria S. Merian Fahrtbericht / Cruise Report MSM 04-1: Meridional Overturning Variability Experiment (MOVE 2006), Fort de France – Fort de France, 02.12. - 21.12.2006, Ed.: Thomas J. Müller, 41 pp. In English
18	FS Poseidon Fahrtbericht /Cruise Report P348: SOPRAN: Mauritanian Upwelling Study 2007, Las Palmas - Las Palmas, 08.02. - 26.02.2007, Ed.: Hermann W. Bange, 42 pp. In English
19	R/V L'ATALANTE Fahrtbericht / Cruise Report IFM-GEOMAR-4: Circulation and Oxygen Distribution in the Tropical Atlantic, Mindelo/Cape Verde - Mindelo/Cape Verde, 23.02. - 15. 03.2008, Ed.: Peter Brandt, 65 pp. In English
20	RRS JAMES COOK Fahrtbericht / Cruise Report JC23-A & B: CHILE-MARGIN-SURVEY, OFEG Barter Cruise with SFB 574, 03.03.-25.03. 2008 Valparaiso – Valparaiso, 26.03.-18.04.2008 Valparaiso - Valparaiso, Eds.: Ernst Flüh & Jörg Bialas, 242 pp. In English
21	FS Poseidon Fahrtbericht / Cruise Report P340 – TYMAS "Tyrrhenische Massivsulfide", Messina – Messina, 06.07.-17.07.2006, Eds.: Sven Petersen and Thomas Monecke, 77 pp. In English

No.	Title
22	RV Atalante Fahrtbericht / Cruise Report HYDROMAR V (replacement of cruise MSM06/2), Toulon, France - Recife, Brazil, 04.12.2007 - 02.01.2008, Ed.: Sven Petersen, 103 pp. In English
23	RV Atalante Fahrtbericht / Cruise Report MARSUED IV (replacement of MSM06/3), Recife, Brazil - Dakar, Senegal, 07.01. - 31.01.2008, Ed.: Colin Devey, 126 pp. In English
24	RV Poseidon Fahrtbericht / Cruise Report P376 ABYSS Test, Las Palmas - Las Palmas, 10.11. - 03.12.2008, Eds.: Colin Devey and Sven Petersen, 36 pp, In English
25	RV SONNE Fahrtbericht / Cruise Report SO 199 CHRISP Christmas Island Seamount Province and the Investigator Ridge: Age and Causes of Intraplate Volcanism and Geodynamic Evolution of the south-eastern Indian Ocean, Merak/Indonesia – Singapore, 02.08.2008 - 22.09.2008, Eds.: Reinhard Werner, Folkmar Hauff and Kaj Hoernle, 210 pp. In English
26	RV POSEIDON Fahrtbericht / Cruise Report P350: Internal wave and mixing processes studied by contemporaneous hydrographic, current, and seismic measurements, Funchal – Lissabon, 26.04.-10.05.2007 Ed.: Gerd Krahnemann, 32 pp. In English
27	RV PELAGIA Fahrtbericht / Cruise Report Cruise 64PE298: West Nile Delta Project Cruise - WND-3, Heraklion - Port Said, 07.11.-25.11.2008, Eds.: Jörg Bialas & Warner Brueckmann, 64 pp. In English
28	FS POSEIDON Fahrtbericht / Cruise Report P379/1: Vulkanismus im Karibik-Kanaren-Korridor (ViKKi), Las Palmas – Mindelo, 25.01.-12.02.2009, Ed.: Svend Duggen, 74 pp. In English
29	FS POSEIDON Fahrtbericht / Cruise Report P379/2: Mid-Atlantic-Researcher Ridge Volcanism (MARRVi), Mindelo- Fort-de-France, 15.02.-08.03.2009, Ed.: Svend Duggen, 80 pp. In English
30	FS METEOR Fahrtbericht / Cruise Report M73/2: Shallow drilling of hydrothermal sites in the Tyrrhenian Sea (PALINDRILL), Genoa – Heraklion, 14.08.2007 – 30.08.2007, Eds.: Sven Petersen & Thomas Monecke, 235 pp. In English
31	FS POSEIDON Fahrtbericht / Cruise Report P388: West Nile Delta Project - WND-4, Valetta – Valetta, 13.07. - 04.08.2009, Eds.: Jörg Bialas & Warner Brückmann, 65 pp. In English
32	FS SONNE Fahrtbericht / Cruise Report SO201-1b: KALMAR (Kurile-Kamchatka and ALeutian MARGinal Sea-Island Arc Systems): Geodynamic and Climate Interaction in Space and Time, Yokohama, Japan - Tomakomai, Japan, 10.06. - 06.07.2009, Eds.: Reinhard Werner & Folkmar Hauff, 105 pp. In English
33	FS SONNE Fahrtbericht / Cruise Report SO203: WOODLARK Magma genesis, tectonics and hydrothermalism in the Woodlark Basin, Townsville, Australia - Auckland, New Zealand 27.10. - 06.12.2009, Ed.: Colin Devey, 177 pp. In English

No.	Title
34	FS Maria S. Merian Fahrtbericht / Cruise Report MSM 03-2: HYDROMAR IV: The 3rd dimension of the Logatchev hydrothermal field, Fort-de-France - Fort-de-France, 08.11. - 30.11.2006, Ed.: Sven Petersen, 98 pp. In English



Das Leibniz-Institut für Meereswissenschaften
ist ein Institut der Wissenschaftsgemeinschaft
Gottfried Wilhelm Leibniz (WGL)

The Leibniz-Institute of Marine Sciences is a
member of the Leibniz Association
(Wissenschaftsgemeinschaft Gottfried
Wilhelm Leibniz).

Leibniz-Institut für Meereswissenschaften / Leibniz-Institute of Marine Sciences

IFM-GEOMAR
Dienstgebäude Westufer / West Shore Building
Düsternbrooker Weg 20
D-24105 Kiel
Germany

Leibniz-Institut für Meereswissenschaften / Leibniz-Institute of Marine Sciences

IFM-GEOMAR
Dienstgebäude Ostufer / East Shore Building
Wischhofstr. 1-3
D-24148 Kiel
Germany

Tel.: ++49 431 600-0
Fax: ++49 431 600-2805
www.ifm-geomar.de